Methods in Molecular Biology 1379

Springer Protocols

Sabrina Strano *Editor*

Cancer Chemo-prevention

Methods and Protocols

Humana Press

METHODS IN MOLECULAR BIOLOGY

Series Editor
John M. Walker
School of Life and Medical Sciences
University of Hertfordshire
Hatfield, Hertfordshire, AL10 9AB, UK

For further volumes:
http://www.springer.com/series/7651

Cancer Chemoprevention

Methods and Protocols

Edited by

Sabrina Strano

Molecular Cancer Chemoprevention Unit, Molecular Medicine Department, Regina Elena National Cancer Institute, Rome, Italy

Department of Oncology, Juravinski Cancer Center-McMaster University Hamilton, Hamilton, ON L8V 5C2, ON, Canada

Humana Press

Editor
Sabrina Strano
Molecular Cancer Chemoprevention Unit
Molecular Medicine Department
Regina Elena National Cancer Institute
Rome, Italy

Department of Oncology
Juravinski Cancer Center-McMaster
University Hamilton
Hamilton, Ontario, Canada

ISSN 1064-3745 ISSN 1940-6029 (electronic)
Methods in Molecular Biology
ISBN 978-1-4939-3190-3 ISBN 978-1-4939-3191-0 (eBook)
DOI 10.1007/978-1-4939-3191-0

Library of Congress Control Number: 2015957808

Springer New York Heidelberg Dordrecht London

Printed on acid-free paper

Humana Press is a brand of Springer
Springer Science+Business Media LLC New York is part of Springer Science+Business Media (www.springer.com)

Preface

Despite the advent of personalized therapies, cancer still remains a leading cause of death worldwide. The number of cancer cases is rising yearly and is expected to double in the next 20 years. The largest increase of new cases will occur mainly in lower income countries, where the access to cancer care is still inadequate. Thus, there is a strong and urgent need of additional and complementary therapies. The increasing healthcare costs of novel anticancer therapeutic agents and their toxic side effects in high-income countries pave the way for cancer chemoprevention strategies. Natural compounds and dietary supplement phytochemicals appear to be efficacious arms of intervention in cancer chemoprevention. The potential value of these agents has been demonstrated in preclinical and observational studies. Large-scale clinical trials of primary and secondary cancer chemoprevention are still in progress. As for any type of clinical trials, the monitoring of the endpoints through the evaluation of proper biomarkers is still the challenge to pursue. With the present book for Cancer Chemoprevention Protocols, we depict along the 18 chapters the state of the art of methods that can be useful for both basic and translational researchers to conduct chemoprevention preclinical studies. Each chapter includes an introduction to the specific technology and a detailed method section. Published and unpublished observations of the contributing authors are also included.

I take the occasion to thank all the authors for their great contributions and for the enjoyable scientific interaction.

Rome, Italy *Sabrina Strano*

Contents

Preface . . . . . *v*
Contributors . . . . . *ix*

1 Controlled Delivery of Chemopreventive Agents by Polymeric Implants 1
Farrukh Aqil and Ramesh C. Gupta

2 Use of Buffy Coat miRNA Profiling for Breast Cancer Prediction in Healthy Women 13
Sara Donzelli, Giovanni Blandino, and Paola Muti

3 microRNAs in Cancer Chemoprevention: Method to Isolate Them from Fresh Tissues 21
Federica Ganci and Giovanni Blandino

4 Application of RNA-Seq Technology in Cancer Chemoprevention 31
Frauke Goeman and Maurizio Fanciulli

5 Detection of Circulating Tumor DNA in the Blood of Cancer Patients: An Important Tool in Cancer Chemoprevention 45
Peter Ulz, Martina Auer, and Ellen Heitzer

6 The Methylated DNA Immunoprecipitation [MeDIP] to Investigate the Epigenetic Remodeling in Cell Fate Determination and Cancer Development 69
Silvia Masciarelli, Teresa Bellissimo, Ilaria Iosue, and Francesco Fazi

7 LC-MS-Based Metabolomic Investigation of Chemopreventive Phytochemical-Elicited Metabolic Events 77
Lei Wang, Dan Yao, and Chi Chen

8 ^{1}H NMR Metabolomic Footprinting Analysis for the In Vitro Screening of Potential Chemopreventive Agents 89
Luca Casadei and Mariacristina Valerio

9 Comet Assay in Cancer Chemoprevention 99
Raffaela Santoro, Maria Ferraiuolo, Gian Paolo Morgano, Paola Muti, and Sabrina Strano

10 Angiogenesis Assays 107
Dhanya K. Nambiar, Praveen K. Kujur, and Rana P. Singh

11 AlgiMatrix™-Based 3D Cell Culture System as an In Vitro Tumor Model: An Important Tool in Cancer Research 117
Chandraiah Godugu and Mandip Singh

12 Cancer Gastric Chemoprevention: Isolation of Gastric Tumor-Initiating Cells 129
Federica Mori, Valeria Canu, Laura Lorenzon, Alfredo Garofalo, Giovanni Blandino, and Sabrina Strano

13 Isolation of Chemoresistant Cell Subpopulations 139
Claudia Canino and Mario Cioce

14 Autophagy in Cancer Chemoprevention: Identification of Novel Autophagy Modulators with Anticancer Potential 151
Yuanzhi Lao and Naihan Xu

15 Protocol for a Steady-State FRET Assay in Cancer Chemoprevention 165
Marjolein C.A. Schaap, Andreia M.R. Guimarães, Andrew F. Wilderspin, and Geoffrey Wells

16 3D Tumor Models and Time-Lapse Analysis by Multidimensional Microscopy 181
Dimitri Scholz and Nobue Itasaki

17 Antibody Array as a Tool for Screening of Natural Agents in Cancer Chemoprevention 189
Claudio Pulito, Andrea Sacconi, Etleva Korita, Anna Maidecchi, and Sabrina Strano

18 South African Herbal Extracts as Potential Chemopreventive Agents: Screening for Anticancer Splicing Activity 201
Zodwa Dlamini, Zukile Mbita, and David Bates

Erratum *E1*

Index *213*

Contributors

Farrukh Aqil • *James Graham Brown Cancer Center, University of Louisville, Louisville, KY, USA; Department of Medicine, University of Louisville, Louisville, KY, USA*

Martina Auer • *Institute of Human Genetics, Medical University of Graz, Graz, Austria*

David Bates • *Faculty of Medicine and Health Sciences, Division of Pre-clinical Oncology, University of Nottingham, Nottingham, UK*

Teresa Bellissimo • *Section of Histology and Medical Embryology, Department of Anatomical, Histological, Forensic and Orthopaedic Sciences, Sapienza University of Rome, Rome, Italy*

Giovanni Blandino • *Laboratory of Translational Oncogenomics, Molecular Medicine Department, Regina Elena National Cancer Institute, Rome, Italy*

Claudia Canino • *Division of Thoracic Surgery, Department of Cardiothoracic Surgery, Langone Medical Center, New York University, New York, NY, USA*

Valeria Canu • *Translational Oncogenomic Unit, Molecular Medicine Department, Regina Elena National Cancer Institute, Rome, Italy*

Luca Casadei • *Department of Chemistry, "Sapienza" University of Rome, Rome, Italy*

Chi Chen • *Department of Food Science and Nutrition, University of Minnesota, St. Paul, MN, USA*

Mario Cioce • *Division of Thoracic Surgery, Department of Cardiothoracic Surgery, Langone Medical Center, New York University, New York, NY, USA*

Zodwa Diamini • *Research, Innovation & Engagements, Mangosuthu University of Technology, Durban, South Africa*

Sara Donzelli • *Translational Oncogenomics Unit, Regina Elena Italian National Cancer Institute, Rome, Italy*

Maurizio Fanciulli • *Laboratory of Epigenetic, Molecular Medicine Area, Italian National Cancer Institute "Regina Elena", Rome, Italy*

Francesco Fazi • *Section of Histology and Medical Embryology, Department of Anatomical, Histological, Forensic and Orthopaedic Sciences, "Sapienza" University of Rome, Rome, Italy*

Maria Ferraiuolo • *Molecular Chemoprevention Unit, Molecular Medicine Area, Regina Elena National Cancer Institute, Rome, Italy*

Federica Ganci • *Translational Oncogenomics Unit, Italian National Cancer Institute "Regina Elena", Rome, Italy*

Alfredo Garofalo • *Department of GI Surgery, Regina Elena National Cancer Institute, Rome, Italy*

Chandraiah Godugu • *Department of Regulatory Toxicology, National Institute of Pharmaceutical Education and Research (NIPER), Hyderabad, Telangana, India*

Frauke Goeman • *Translational Oncogenomics Unit, Italian National Cancer Institute "Regina Elena", Rome, Italy*

Andreia M.R. Guimarães • *UCL School of Pharmacy, University College London, London, UK*

Ramesh C. Gupta • *James Graham Brown Cancer Center, University of Louisville, Louisville, KY, USA; Department of Pharmacology and Toxicology, University of Louisville, Louisville, KY, USA*

Ellen Heitzer • *Institute of Human Genetics, Medical University of Graz, Graz, Austria*
Ilaria Iosue • *Section of Histology and Medical Embryology, Department of Anatomical, Histological, Forensic and Orthopaedic Sciences, "Sapienza" University of Rome, Rome, Italy*
Nobue Itasaki • *School of Medicine and Medical Science, University College Dublin, Dublin, Ireland; Faculty of Health Sciences, University of Bristol, Bristol, UK*
Etleva Korita • *Molecular Chemoprevention Unit, Molecular Medicine Area, Italian National Cancer Institute "Regina Elena", Rome, Italy*
Praveen K. Kujur • *Cancer Biology Laboratory, School of Life Sciences, Jawaharlal Nehru University, New Delhi, India*
Yuanzhi Lao • *School of Pharmacy, Shanghai University of Traditional Chinese Medicine, Shanghai, China*
Laura Lorenzon • *Surgical and Medical Department of Translational Medicine, Faculty of Medicine and Psychology, Sant'Andrea Hospital, University of Rome "La Sapienza", Rome, Italy*
Anna Maidecchi • *Aboca SpA Società Agricola, Sansepolcro, Italy*
Silvia Masciarelli • *Section of Histology and Medical Embryology, Department of Anatomical, Histological, Forensic and Orthopaedic Sciences, Sapienza University of Rome, Rome, Italy*
Zukile Mbita • *Mangosuthu University of Technology Research, Innovation and Engagements Portfolio, Durban, South Africa*
Gian Paolo Morgano • *Department of Clinical Epidemiology and Biostatistics, McMaster University, Hamilton, ON, Canada*
Federica Mori • *Molecular Chemoprevention Unit, Molecular Medicine Department, Regina Elena National Cancer Institute, Rome, Italy*
Paola Muti • *Department of Oncology, Juravinski Cancer Center, McMaster University, Hamilton, ON, Canada*
Dhanya K. Nambiar • *Cancer Biology Laboratory, School of Life Sciences, Jawaharlal Nehru University, New Delhi, India*
Claudio Pulito • *Molecular Chemoprevention Unit, Molecular Medicine Area, Italian National Cancer Institute "Regina Elena", Rome, Italy*
Andrea Sacconi • *Molecular Medicine Area, Regina Elena National Cancer Institute, Rome, Italy*
Raffaela Santoro • *Molecular Chemoprevention Unit, Molecular Medicine Area, Regina Elena National Cancer Institute, Rome, Italy*
Marjolein C.A. Schaap • *UCL School of Pharmacy, University College London, London, UK*
Dimitri Scholz • *Conway Institute, University College Dublin, Dublin, Ireland*
Rana P. Singh • *Cancer Biology Laboratory, School of Life Sciences, Jawaharlal Nehru University, New Delhi, India; School of Life Sciences, Central University of Gujarat, Gandhinagar, Gujarat, India*
Mandip Singh • *College of Pharmacy and Pharmaceutical Sciences, Florida A & M University, Tallahassee, FL, USA*
Sabrina Strano • *Molecular Cancer Chemoprevention Unit, Molecular Medicine Department, Regina Elena National Cancer Institute, Rome, Italy; Department of Oncology, Juravinski Cancer Center-McMaster University Hamilton, Hamilton, ON, Canada*
Peter Ulz • *Institute of Human Genetics, Medical University of Graz, Graz, Austria*
Mariacristina Valerio • *Department of Chemistry, "Sapienza" University of Rome, Rome, Italy*

Lei Wang • *Department of Food Science and Nutrition, University of Minnesota, St. Paul, MN, USA*
Geoffrey Wells • *UCL School of Pharmacy, University College London, London, UK*
Andrew F. Wilderspin • *UCL School of Pharmacy, University College London, London, UK*
Naihan Xu • *Key Lab in Healthy Science and Technology, Division of Life Science, Graduate School at Shenzhen, Tsinghua University, Shenzhen, China*
Dan Yao • *Department of Food Science and Nutrition, University of Minnesota, St. Paul, MN, USA*

Chapter 1

Controlled Delivery of Chemopreventive Agents by Polymeric Implants

Farrukh Aqil and Ramesh C. Gupta

Abstract

The clinical development of cancer chemopreventive agents has been hampered by poor oral bioavailability issue. Several compounds have low aqueous solubility and undergo extensive first pass metabolism following oral dosing. To overcome this limitation, we developed polymeric implants from biodegradable ε-polycaprolactone (PCL) that can deliver both lipophilic as well as hydrophilic compounds. Implants furnish controlled release of compounds for long duration and provide dose-dependent release. The rate of release in vitro correlated well with the in vivo release. The polymeric implant technology thus overcomes the oral bioavailability issues, lowers the total required dose and minimizes or eliminates toxicity generally associated with high doses.

Key words Drug delivery, Polycaprolactone, Polymeric implants, Controlled release, Bioavailability

1 Introduction

Issues of poor oral bioavailability of chemopreventive and therapeutic agents have hindered the progress in cancer prevention and treatment. Drug delivery systems are engineered technologies for the targeted delivery and/or controlled release of chemopreventive and therapeutic agents. The practice of drug delivery has changed dramatically in the last few decades and even greater changes are anticipated in the near future. The development of new approaches in cancer prevention and treatment could encompass new delivery systems for approved and newly investigated compounds [1, 2]. Moreover, targeted drug delivery is intended to reduce the side effects of drugs with concomitant decreases in drug amount and treatment expenses. It is generally expected that most applicable drug delivery systems be biodegradable, biocompatible, and with minimal adverse effects. The major emphasis of an effective delivery system is to deliver the compound in minimum therapeutic doses with minimal or no toxicity.

Sabrina Strano (ed.), *Cancer Chemoprevention: Methods and Protocols*, Methods in Molecular Biology, vol. 1379,
DOI 10.1007/978-1-4939-3191-0_1,

Bioavailability of the drugs and chemopreventive agents can be increased by encapsulation or systemic delivery by various means, including nanoparticles, liposomes, microparticles, micelles, and implants (reviewed in [3]). Encapsulation of agents using polymeric nanoparticles or nanocarriers has emerged as the workhorse solution to manage poor biodistribution and stability of chemopreventives and therapeutics [4]. However, subchronic and chronic toxicity studies with nanoparticle formations are elusive, and could potentially pose problems for toxicity of the carrier over long durations. Incredible choices in the polymeric designs offer a direct route to optimal carrier design. Polymeric implants offer controlled delivery as shown by us [3, 5–8] and others [9, 10]. Unlike oral nanoparticles, polymeric implants provide continuous delivery for long durations (months to >1 year) circumventing repeated dosing thereby eliminating polymer toxicity [3, 6].

Different types of implantable devices have been used, such as poly(lactide-co-glycolide) (PLGA)-based implants and implants of high-melting-point polymers. However, their uses are limited due to development of fibrous encapsulation around PLGA implants [11]; and use of compounds with high thermal stability in the later [12]. We have initially demonstrated the use of silastic tubing implants which, due to their non-biodegradable nature, have encountered issues with their removal after the end of treatment [13].

We recently developed biodegradable polymeric implants using ε-polycaprolactone (PCL):F-68 embedded with chemopreventive agents. These implants provided sustained release for long durations in vivo [3, 14]. This concept has been tested successfully for various agents. A simple procedure has been used to develop the polymeric "extrusion" implants. Polymeric implants are prepared by homogenous entrapment of agents in a polymeric matrix. The implants provide slow-release kinetics with a continuous drug release for long durations (months to >1 year) [14]. The implants can be grafted at various sites and elicit a sustained systemic or localized delivery of agents with complete bioavailability with no observable toxicity. These advantageous attributes of polymeric implants not only improve bioavailability, but can also improve patient compliance by eliminating the need for frequent parenteral dosing [3]. However, implants developed using this formulation ("extrusion" method) generally results in an initial high burst release followed by a gradual decline and also do not apply to heat-labile compounds.

More recently, we have improvised the method and developed multi-layer coated implants that can accommodate almost all types of compounds including compounds of different physicochemical properties. This method involves (1) preparation of blank PCL:F-68 implants (1.4 mm dia), and (2) coating of 20–40 layers

by dipping blank implants, with intermittent drying, in 10–20 % PCL solution in dichloromethane (DCM) containing 0.5–2 % of test agent in DCM or another appropriate solvent. The coated implants of various chemopreventive agents when tested for in vitro release showed that the burst release was substantially reduced, and the release was largely sustained for 3 weeks. The details of the two types of implant technologies (extrusion and multilayer) are provided below.

2 Materials

Prepare all solutions using ultrapure water and analytical grade reagents. Prepare and store all reagents at room temperature, except wherever indicated. Diligently follow all waste disposal regulations when disposing waste materials. All the solvents used in the preparation were of HPLC grate unless otherwise specified. Take all other precautions as required.

2.1 Supplies for Implant Formulation

1. The polymers and other materials used were obtained from these sources: PCL mol. wt. 80,000 (P-80), PCL mol. wt. 65,000 (P-65), and PCL mol. wt. 15,000 (P-15) were from Sigma–Aldrich (St. Louis, MO, USA), and polyethylene glycol, mol. wt. 8000 (PEG-8) from Fisher Scientific (Fair Lawn, NJ, USA). Pluronic^{R} F68 (F-68) was a gift from BASF Corporation (Florham Park, NJ, USA). Silastic tubing of different diameters (1.4, 2.0, and 3.2 mm internal diameter) were purchased from Allied Biomedical (Ventura, CA, USA). Test agents used for the implant preparation were purchased from different sources. DCM, tetrahydrofurane (THF) and absolute ethanol were from BDH chemicals (VWR, West Chester, PA), Sigma-Aldrich (St. Louis, MO), and Pharmco-AAPER (Louisville, KY, USA), respectively. All other chemicals were of analytical grade.

2.2 Supplies for Release Media

1. Release of the agents from polymeric implants was done in the release medium containing phosphate-buffered-saline (PBS), pH 7.4 containing 10 % calf serum. We also used 1 % of penicillin-streptomycin solution to suppress any bacterial growth. PBS tablets were from Sigma–Aldrich (St. Louis, MO, USA). Bovine calf serum was from Hyclone (Logan, UT, USA) and stored in aliquots at −20 °C for long durations. Penicillin/streptomycin solution was purchased from Life Technologies (Invitrogen, Carlsbad, CA). Scintillation vials (clear and amber) (20 and 40 ml) were purchased from National Scientific (Rockwood, TN, USA).

3 Methods

3.1 Formulation of "Extrusion" Polymeric Implants

1. Add 4.05 g P-80 (or P-65) and 0.45 g F-68 or polyethylene glycol mol. wt. 8000 (PEG-8K) to 10 ml DCM in a 50 ml glass beaker (*see* **Note 1**) (Fig. 1a).
2. Keep the beaker at room temperature and stir the solution with a glass rod occasionally until polymers solubilize.
3. Dissolve 0.5 g curcumin (or other agent) in 2–3 ml of solvent (ethanol, DCM, or THF) in a glass tube or scintillation vial. Vortex to solubilize the compound (*see* **Notes 2** and **3**) (Fig. 1a).
4. Add drug solution to the polymer solution slowly (*see* **Note 4**).
5. Place a water bath under fume hood, and set it at 70 °C. Transfer the formulation to the water bath. Stir the solution with a glass rod occasionally (*see* **Note 5**). Alternatively, transfer the solution to a glass Petri dish and the solution is evaporated under hood (Fig. 1b, c).
6. Once the solvent is almost completely evaporated, place the beaker/Petri dish in a Savant Speed-Vac (Thermo-Savant, Holbrook, NY) for complete removal of the solvents under reduced pressure (*see* **Note 6**). Formulation should be left in Savant at 65 °C for 6–8 h or overnight for complete removal of residual solvents.
7. Collect the material from the Savant Speed-Vac, and excise into small pieces using a scissor.
8. Take 5 ml plastic syringe (BD, Franklin Lakes, NJ), and attach it to a silastic tubing of desired internal diameter (Fig. 1d) (*see* **Note 7**).

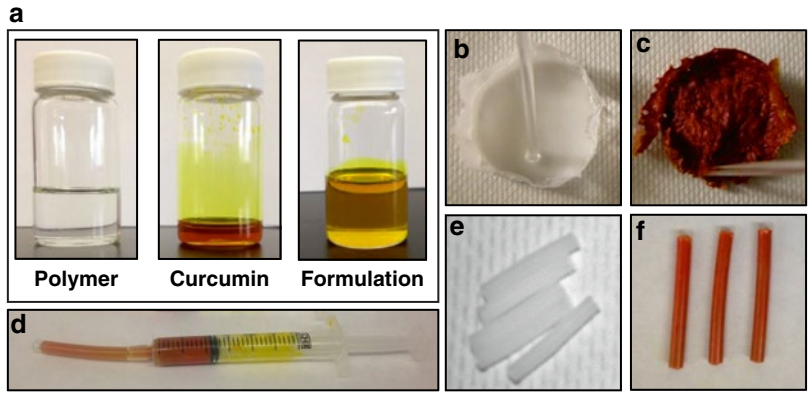

Fig. 1 Solution of ε-polycaprolactone (P-65) and F-68 in dichloromethane, curcumin in tetrahydrofuran, mixture of P-65/F-68 solution and curcumin solution (**a**). Dried sham. (**b**) Polymer-drug formulation (**c**). Dried polymer was exercised into small pieces and heated in syringe attached with a silastic tube (**d**). Photographs of representative sham (**e**) and curcumin (**f**) implants prepared by extrusion method

9. Fill the syringe with dried pieces of polymer-drug formulation.
10. Keep the assembly of syringe attached with silastic tubing (Fig. 1d) at 70 °C in an incubator for 30 min.
11. Remove the assembly from the incubator, and extrude the material immediately but slowly (*see* **Note 8**).
12. After cooling the assembly at room temperature, remove the implant by cutting the silastic tubing mold longitudinally with a scalpel or blade and excise implants into desired sizes (Fig. 1e, f).
13. Store implants in amber vials under argon at 4 °C.

3.2 Formulation of "Coated" Polymeric Implants

To overcome the issues related to burst release and use of heat-labile compounds, we improvised the methodology as "coated implants" as described below.

1. Prepare extruded implants in the absence of any drug as described above using silastic tubing mold of internal diameter 1.4 mm. These are thin implants and referred as inserts (Fig. 2a).

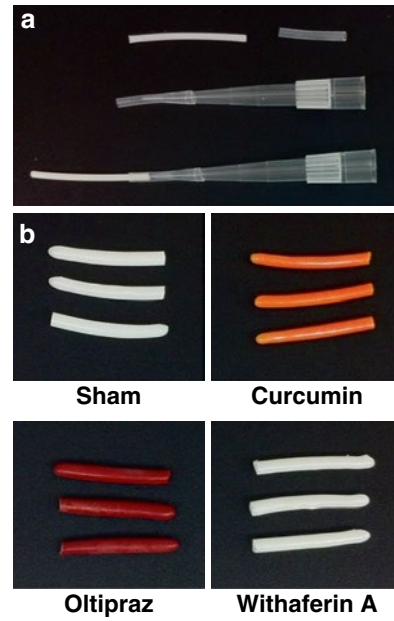

Fig. 2 Assembly of sham insert assembled with pipet tip using silastic tubing for coating (**a**), and photographs of representative coated polymeric implants (**b**). Implants were prepared by coating indicated compounds mixed with P-80 as described in Subheading 3.2. Implant size: 2 cm length, 2.6 mm diameter. Reprinted from Cancer Letters, 326 (1), Aqil et al., Multilayer polymeric implants for sustained release of chemopreventives, 33–40. Copyright (2012), with permission from Elsevier

2. Excise inserts into 2.5–3.5 cm pieces.
3. Cut silastic tubing (1.4 mm internal diameter) in about 6 mm pieces.
4. Attach one end of the silastic tubing plug to a pipet tip while the other end to blank insert (Fig. 2a) (*see* **Note 13**).
5. Polymer-drug solution: Dissolve 4.5 g P-80 in 20 ml DCM in a 50 ml glass beaker (*see* **Note 1**).
6. Dissolve curcumin (or other test agent) in 2–3 ml solvent (ethanol, DCM, or THF) in a glass tube or scintillation vial (*see* **Notes 2**, **3**, and **14**).
7. Add drug solution to the polymer solution slowly and mix the two solutions thoroughly, stirring with a glass rod (*see* **Note 4**). This solution is referred to as coating solution.
8. Set up clamp under the hood and attach a commercial hair dryer with cool air setting.
9. For coating, hold the implant assembly and dip quickly into the coating solution (*see* **Note 15**).
10. Place the coated implants into a rack and place under the hair dryer for drying for 2–3 min (*see* **Note 16**).
11. Repeat the coating process 25–30 times. These coatings generally increase the size of coated implants from 1.4 to 2.6 mm diameter as measured by a digital caliper (Fig. 2b).
12. Place the assembly under hood overnight to remove the residual DCM.
13. Excise the implants in 1 or 2 cm lengths and store in amber vials under argon at −20 °C until use (*see* **Note 17**).

3.3 In Vitro Release

1. Release media: Add 8.9 ml PBS in amber color 20 ml glass scintillation vial. Add 0.1 ml of penicillin–streptomycin solution (Invitrogen, Carlsbad, CA) (1 %, v/v) to minimize the growth of microorganisms. Finally, add 1 ml (10 %, v/v) of bovine calf serum to simulate the in vivo scenario.
2. Release study: Place 1 or 2 cm implants in media placed in 20 ml amber vials to determine the rate of release of test agents.
3. Incubate vials containing the media and implant at 37 °C with constant agitation in a water bath (Julabo SW 23, Seelback, Germany) for 24 h.
4. Transfer the media from the vial to a fresh scintillation vial and add 1 ml ethanol (10 % final concentration) to the release medium to completely solubilize the compound. Add fresh release media and continue incubation.

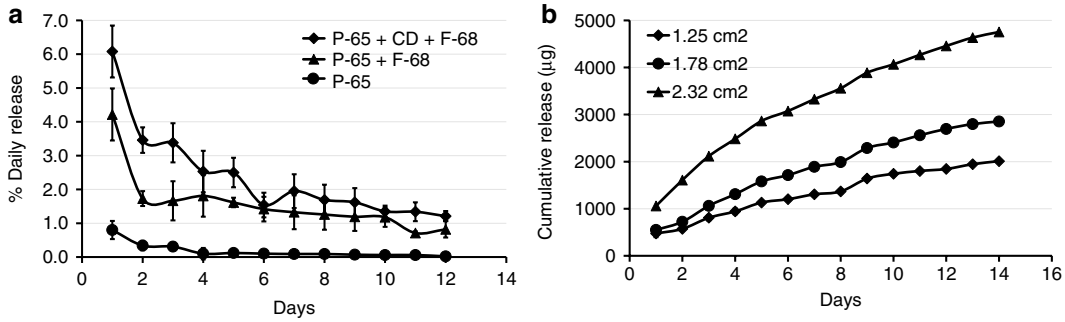

Fig. 3 Effect of water-soluble polymer on the percent daily release of punicalagins. Addition of water-soluble polymers [cyclodextrin (CD) and F-68] increase the release as it facilitates entry of release media in the polymer matrix and allows drug to dissolve and come out (**a**). In vitro cumulative release of punicalagins from different size (1 cm, 1.5 cm and 2 cm) implants providing total surface area of 1.25 cm^2, 1.78 cm^2, and 2.32 cm^2, respectively. As expected the release was found directly proportional to the surface area. The release was measured by incubating implants in a shaker incubator in PBS supplemented with 10 % bovine serum as described in Subheading 3.3. SD was generally 5–10 % (**b**)

5. To measure the compound released, transfer 1 ml of the solution to an Eppendorf tube, centrifuge at 10,000 × *g* for 10 min.
6. Collect the supernatant and measure the release spectrophotometrically at 430 nm, the absorbance maxima for curcumin.
7. Generate a standard curve using curcumin and calculate the concentration against the standard curve.
8. Rate of release (extrusion implants): We observed that (1) the inclusion of the water-soluble polymer(s) facilitates the release from the implants (Fig. 3a), (2) the release is proportionately increased with the increase of surface area (Fig. 3b), and (3) the release is largely sustained for long duration when tested for various compounds (Table 1) including chemopreventive agents [3, 6, 8, 15], carcinogens [16, 17], and chemotherapeutic drug.
9. Rate of release (coated implants): Multi-layer coated implants generally provide sustained release as shown for oltipraz, curcumin, and withaferin A [6] for long durations. When withaferin A implants coated with 6 and 10 times with blank polymer, it minimize the burst release and provided sustained release (Fig. 4). The effect was even more pronounced with eight coatings and release was almost sustained as tested for curcumin.

Table 1
Compounds successfully tested for release

(1) Chemopreventive agents		
Curcumin	Curcumin I	Demethoxycurcumin
Bisdemethoxycurcumin	Green tea polyphenols	Punicalagins
Resveratrol	Withaferin A	Tanshinone II
Cucurbitacin B	Luteolin	Oltipraz
Diindolylmethane	Ellagic acid	Anacardic acid
(2) Carcinogenic agents		
PCB-126	PCB-153	Benzo[*a*]pyrene
Dibenzo[*a*,*l*]pyrene		
(3) Chemotherapeutic agents		
Paclitaxel		

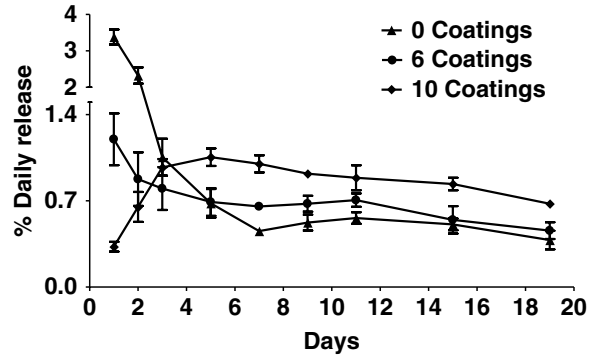

Fig. 4 Effect of coatings with blank P-80 on withaferin A polymeric implants to minimize the burst release. Withaferin A implants were coated 6 and 10 times with 10 % solution of P-80 in dichloromethane with intermittent drying. The in vitro release was measured as described in Subheading 3.3. Data represent average of 3 implants ± SD

4 Notes

1. P-80 or P-65 or P-15 provides almost similar release from the implants. However, the release rate changes if PCL material is of higher or lower mol. wts.
2. Solvents to dissolve test agents should be chosen based on miscibility with DCM. Curcumin is used here as a model compound which has high solubility in THF. The volume of the drug

solvent can vary based on drug's solubility. In our experience the drug solvent to DCM ratio is about 1:3 to avoid crystallization of drug or polymer.

3. There are three major components of the implant formulation: First, drug percent should be calculated based on drug and polymer weight. Second, ratio of two polymers (PCL and F-68) can vary based on the use. Usually we use 10 % F-68 or 10–30 % PEG-8K. The ratio of polymer weight should be calculated based on total weight minus drug weight.
4. While adding drug to the polymer solution, continuous stirring helps to obtain uniform drug distribution into matrix.
5. Alternatively, formulation can be dried by pouring the material in a Petri dish and leaving it under the hood. Once solvent is evaporated, the Petri dish is transferred to Savant Speed-Vac for more complete removal of residual solvents. All precautions like wearing gloves should be exercised.
6. High drying rate should be selected as it provides around 65 °C temperature and keep formulation in molten form for more complete removal of residual solvents. Use lower temperature for heat-labile compounds but increase evaporation time.
7. Size of silastic tubing should be chosen based on the requirement of implant size. The release of compounds from the implants is based on the surface area. We observed that a diameter of 3.2 mm is desirable for rat studies and 1.4–2.6 mm for mice.
8. Slow and steady extrusion is needed as rapid extrusion sometimes leaves air bubbles in implants. Long processing time may result in solidification of formulation; in the event the matrix solidifies, the assembly is heated again for 20–30 min.
9. In our experience, we observed 120 RPM is optimum for shaking the implants in release media. At this speed we do not observe any adverse effect on implants.
10. Centrifugation step is included to remove any precipitate due to the addition of ethanol.
11. Curcumin is a mixture of three curcuminoids. These curcuminoids are structural analogs and absorb at similar wavelength (430 nm). Wavelength should be selected based on the compounds used.
12. Calibration curves for each compound should be generated by spiking PBS containing 10 % bovine serum, 1 % penicillin-streptomycin solution and 10 % ethanol with known concentrations of test compound.
13. Make sure that silastic tubing holds both insert and pipette tip tightly. Implants can fall off from the loose assembly.

14. Polymer and drug ratio can be selected based on the requirement. For example 20 % drug loading can be achieved by mixing 4 g of polymer with 1 g of drug (w/w).
15. Implant assembly should be rotated after dipping to provide uniform coating.
16. A single coat usually takes 2–3 min for complete drying. However, time can be increased to confirm the drying. Do not dry implants under hot air as it can melt the polymeric coating.
17. Implants thus formulated will have a 10 % drug load of the test agents.

Acknowledgements

This work was supported from the USPHS grants CA-118114 and CA-125152, Kentucky Lung Cancer Research Program Cycles 7 and 10, and the Agnes Brown Duggan Endowment. R.C.G. holds the Agnes Brown Duggan Chair in Oncological Research. We thank Drs. Manicka V. Vadhanam, Dr. Shyam S. Bansal, Mr. Jeyaprakash Jeyabalam, Dr. Pengxiao Cao, Dr. Hina Kausar, Dr. Gilandra K. Russell, Dr. Radha Munagala, and Dr. Srivani Ravoori for their contributions in the development of this technology.

References

1. Aqil F, Munagala R, Jeyabalan J et al (2013) Bioavailability of phytochemicals and its enhancement by drug delivery systems. Cancer Lett 334:133–141
2. Jabir NR, Tabrez S, Ashraf GM et al (2012) Nanotechnology-based approaches in anticancer research. Int J Nanomedicine 7:4391–4408
3. Bansal S, Kausar H, Aqil F et al (2011) Curcumin implants for continuous systemic delivery: safety and biocompatibility. Drug Deliv Transl Res 1:332–341
4. Hoffman AS (2008) The origins and evolution of "controlled" drug delivery systems. J Control Release 132:153–163
5. Aqil F, Vadhanam MV, Gupta RC (2012) Enhanced activity of punicalagin delivered via polymeric implants against benzo[a]pyrene-induced DNA adducts. Mutat Res 743: 59–66
6. Aqil F, Jeyabalan J, Kausar H et al (2012) Multi-layer polymeric implants for sustained release of chemopreventives. Cancer Lett 326:33–40
7. Cao PX, Vadhanam MV, Spencer WA et al (2011) Sustained systemic delivery of green tea polyphenols by polymeric implants significantly diminishes Benzo[a]pyrene-induced DNA adducts. Chem Res Toxicol 24:877–886
8. Cao P, Jeyabalan J, Aqil F et al (2014) Polymeric implants for the delivery of green tea polyphenols. J Pharm Sci 103:945–951
9. Hafeman AE, Li B, Yoshii T et al (2008) Injectable biodegradable polyurethane scaffolds with release of platelet-derived growth factor for tissue repair and regeneration. Pharm Res 25:2387–2399
10. Ghalanbor Z, Korber M, Bodmeier R (2010) Improved lysozyme stability and release properties of poly(lactide-co-glycolide) implants prepared by hot-melt extrusion. Pharm Res 27:371–379
11. Fulzele SV, Satturwar PM, Dorle AK (2003) Study of the biodegradation and in vivo biocompatibility of novel biomaterials. Eur J Pharm Sci 20:53–61
12. Dickers KJ, Huatan H, Cameron RE (2003) Polyglycolide-based blends for drug delivery: a differential scanning calorimetry study of the melting behavior. J Appl Polym Sci 89: 2937–2939
13. Klitsch M (1983) Hormonal implants: the next wave of contraceptives. Fam Plann Perspect 15(239):241–243

14. Bansal SS, Vadhanam MV, Gupta RC (2011) Development and in vitro-in vivo evaluation of polymeric implants for continuous systemic delivery of curcumin. Pharm Res 28:1121–1130
15. Gupta RC, Bansal SS, Aqil F et al (2012) Controlled-release systemic delivery - a new concept in cancer chemoprevention. Carcinogenesis 33:1608–1615
16. Jeyabalan J, Vadhanam MV, Ravoori S et al (2011) Sustained overexpression of CYP1A1 and 1B1 and steady accumulation of DNA adducts by low-dose, continuous exposure to benzo[a]pyrene by polymeric implants. Chem Res Toxicol 24:1937–1943
17. Aqil F, Shen H, Jeyabalan J et al (2014) Sustained expression of CYPs and DNA adduct accumulation with continuous exposure to PCB126 and PCB153 through a new delivery method: polymeric implants. Toxicol Rep 1:820–833

Chapter 2

Use of Buffy Coat miRNA Profiling for Breast Cancer Prediction in Healthy Women

Sara Donzelli, Giovanni Blandino, and Paola Muti

Abstract

MicroRNAs are key regulators of different biological processes and their deregulation is associated with the occurrence of many diseases among which cancer. Due to the higher stability of microRNAs and to the easiness in their detection both in organs than in biological fluids, many studies are turned toward potential use of this small molecules as biomarkers for the prediction and diagnosis of different types of cancer. Here we describe the experiment protocol that we have used for microRNA profiling analysis in buffy coat samples of women who developed breast cancer versus women who remained healthy during a 20 year follow-up period, with the aim to identify predictive microRNAs of breast cancer occurrence.

Key words microRNA, microRNA profiling, Buffy coat, Breast cancer, RNA extraction

1 Introduction

MicroRNAs (miRNAs) are a class of small noncoding RNAs able to modulate gene expression at posttranscriptional level degrading mRNA and/or impairing translation [1]. miRNAs constitute about 3 % of the human genome, indicating that thousands of human genes can be target of miRNA-mediated regulation.

MiRNA activity has been correlated to the pathogenesis of cancer, since miRNAs were identified as a new class of genes with tumor-suppressor and oncogenic functions [2–7]. Moreover, the localization of nonrandom chromosomal abnormalities and other types of genetic alterations at miRNA genomic regions observed in several types of cancer cells furthermore underline the contribution of the deregulation of miRNA expression to malignancies process [8].

Advance in expression technologies has facilitated the high-throughput analysis of small RNAs, showing that these genes may be aberrantly expressed in various human tumors. MiRNA profiling is emerging as a useful tool in the characterization of a variety of human cancers, potentially being of even greater predictive/

Sabrina Strano (ed.), *Cancer Chemoprevention: Methods and Protocols*, Methods in Molecular Biology, vol. 1379,
DOI 10.1007/978-1-4939-3191-0_2,

prognostic value than the analysis of the expression of messenger RNAs [9–11].

The higher stability of miRNAs is clearly in contrast to the distinctly lower stability of mRNAs. This difference is due principally to the dissimilarity in their length: miRNAs are only 20–22 nucleotides in length, so also in degraded RNA preparation from human tissue they maintain their stability [12, 13]. This feature makes miRNAs excellent potential biomarkers; for this reason many studies are designed to identify differences in the expression of miRNAs between normal tissue and tumoral tissue.

In our study, we aimed to test the hypothesis that miRNAs may represent early indicators of future breast cancer incidence. In particular we compared leucocyte miRNA profiles of healthy women who subsequently became affected with breast cancer, versus women who remained healthy. This was performed using a case–control study design nested in the ORDET (h*OR*mones and *D*iet in the *ET*iology of Breast Cancer) prospective cohort over a follow-up period of 20 years [14].

The analysis identified 20 differentially expressed miRNAs, 15 of them were down-regulated. Among the 20 miRNAs, miRNA-145-5p and miRNA-145-3p, each derived from another arm of the respective pre-miRNA, were consistently and significantly down-regulated in all databases we surveyed. For example, analysis of more than 1500 patients (the UK Metabric cohort) indicated that high abundance of miRNA 145-3p and miRNA-145-5p was associated with longer, and for miRNA-145-3p also statistically significant, survival. The experimental data attributed different roles to the identified microRNAs: while the 5p isoform was associated with invasion and metastasis the other isoform appears related to cell proliferation [15].

Here we describe how to obtain good-quality RNA from leucocytes preserved at −80 °C for 20 years that can be used for miRNA profiling on Agilent Platform.

2 Materials

2.1 RNA Extraction

1. TRIzol Reagent (Life Tec Rockville, MD) Chloroform.
2. Isopropyl alcohol.
3. 475 % ethanol (in DEPC-treated water).
4. RNase-free water (to prepare RNase-free water, draw water into RNase-free glass bottles). Add diethylpyrocarbonate (DEPC) to 0.01 % (v/v). Let stand overnight and autoclave.)

2.2 RNA Quality Control

1. Spectrophotometers (NanoDrop ND-1000, Thermo Fisher Scientific, Waltham, MA, or similar).
2. Agilent 2100 bioanalyzer.

2.3 RNA Hybridization

1. Human microRNA Microarray (Agilent).
2. miRNA Labeling and Hybridization Kit (Agilent).
3. Agilent DNA Microarray Scanner (P/N G2565BA).

3 Methods

3.1 Buffy Coat Collection

1. Blood samples were drawn after overnight fasting between 7:30 and 9:00 AM in the morning from each woman and stored at −80 °C.
2. Samples from each case and related control were handled identically and assayed together on the same laboratory session. Laboratory personnel were blinded to case–control status.
3. A total of 20 mL of blood was collected in two 10 mL heparin vacutainers:
   (a) 1–10 mL vacutainer, containing sodium heparin as anticoagulant.
   (b) 1–10 mL vacutainers, containing no additives.
4. Each vacutainer was identified by a different color.
5. The filled vacutainers were immediately protected from direct light using aluminum foil, then kept on ice at −4 °C until the samples were transferred to the central laboratory for processing and aliquoting. The time of the blood drawing was recorded.
6. From the heparin vacutainer, the buffy coat (0.8 mL) was collected from the most superficial part of the tube's corpuscular portion by moving the top of the pipette gently around the surface of the clot.

3.2 RNA Isolation

RNA isolation from buffy coat was performed by using TRIzol Reagent.

TRIzol Reagent is based on RNA separation from DNA after extraction with an acidic solution containing guanidinium thiocyanate, sodium acetate, phenol, and chloroform, followed by centrifugation [16]. Under acidic conditions, total RNA remains in the upper aqueous phase, while most of DNA and proteins remain either in the interphase or in the lower organic phase. Total RNA is then recovered by precipitation with isopropanol.

Here is the procedure that we have used for buffy coat samples that is quite similar to the original protocol but with some changes to enhance RNA yield:

1. Lyse buffy coat cells by adding 3 mL of TRIzol Reagent to 1.5 mL of buffy coat. Vortex vigorously and incubate samples for 15 min at room temperature to permit the complete dissociation of nucleoprotein complexes.

2. Add 0.6 mL of chloroform. Vortex vigorously and incubate samples for 5 min at room temperature. Centrifuge at 12,000 × *g* for 20 min at 4 °C (*see* **Note 1**).
3. Remove the aqueous phase of the sample by angling the tube at 45° and pipetting the solution out. Avoid drawing any of the interphase or organic layer into the pipette when removing the aqueous phase.
   The volume amount should be ~2.5 mL to be divided into two 2 mL tubes (~1250 mL each) (*see* **Note 2**).
4. Add 0.75 mL of 100 % isopropanol to the aqueous phase, shake tubes by hand and incubate at room temperature for 30 min. Centrifuge at 12,000 × *g* for 30 min at 4 °C (*see* **Note 3**).
5. Remove the supernatant from the tube, leaving only the RNA pellet.
6. Wash the pellet with 0.5 mL of 75 % ethanol. Vortex the sample briefly, and then centrifuge the tube at 7500 × *g* for 10 min at 4 °C. Discard the wash.
7. Air-dry the RNA pellet for 10–20 min (*see* **Note 4**).
8. Resuspend the RNA pellet in RNase-free water or (20–50 μL) by vortexing in heat block set at 55–60 °C for 15 min.
9. Proceed to downstream application, or store at –80 °C.

To preserve RNA integrity avoid frequent freeze and thaw. It is suggested to aliquot RNA.

3.3 RNA Quality Control

The long-term effect of cryopreservation may be a factor which affects the miRNA arrays. We matched cases and controls on the date of sample collection to allow for potential cryopreservation effect. Furthermore, the fact that samples may have been exposed to the long term effects of cryopreservation means that the quality of total RNA derived from samples makes it difficult to carry out gene expression analyses. This was one of the reasons for us to focus on miRNA because this RNA population is less sensitive to degradation and, as analyzed by Agilent bioanalyzer and Northern blot analysis, miRNA population resulted suitable for further experimental evaluation.

To proceed with miRNA expression profile analysis it is important to check the quantity and quality of the RNA.

To assess the concentration and purity of total RNA use a NanodropTM 1000 spectrophotometer (Nanodrop Technologies, Wilmington, DE, USA) or similar. The amount of RNA yield from 1.5 mL of buffy coat sample should be between 25 and 120 μg.

It is also suggested to check the amount of small RNA fraction (<200 nucleotides, including microRNAs) in the total RNA isolated from buffy coat samples.

We analyzed the small nucleic acids ranging in size from 6 to 150 nucleotides running the small RNA assay on the Agilent 2100 bioanalyzer.

The small RNA assay can (a) visualize miRNA, small RNA, oligo nucleotides from 6 to 150 nt for verifying sample integrity; (b) quantify miRNA component (in the concentration range of 50–2000 pg/μL) among all small RNAs (pre-miRNA, 5S, ribosomal RNA, etc.) relative to an external standard, for verifying sample enrichment and purity; and (c) automate sample quantization, sizing, and purity determination.

The resulting miRNA component in our samples was about 20–30 % (Fig. 1).

To verify the hybridization ability of the miRNAs present in the preparations we also performed a northern blot assay on a pull of samples (Fig. 1). The blot filter was hybridized with a [32P] γATP radiolabeled LNA oligonucleotide complementary to miRNA-223 sequence. miR-223 is highly specific for hematopoietic cells and constitutes a regulator of myelopoiesis [15, 16].

The RNA samples displayed a good hybridization ability, where human promyelocytic HL60 cells treated with retinoic acid 10–6 M, a known inducer of miR-223, were included as positive control.

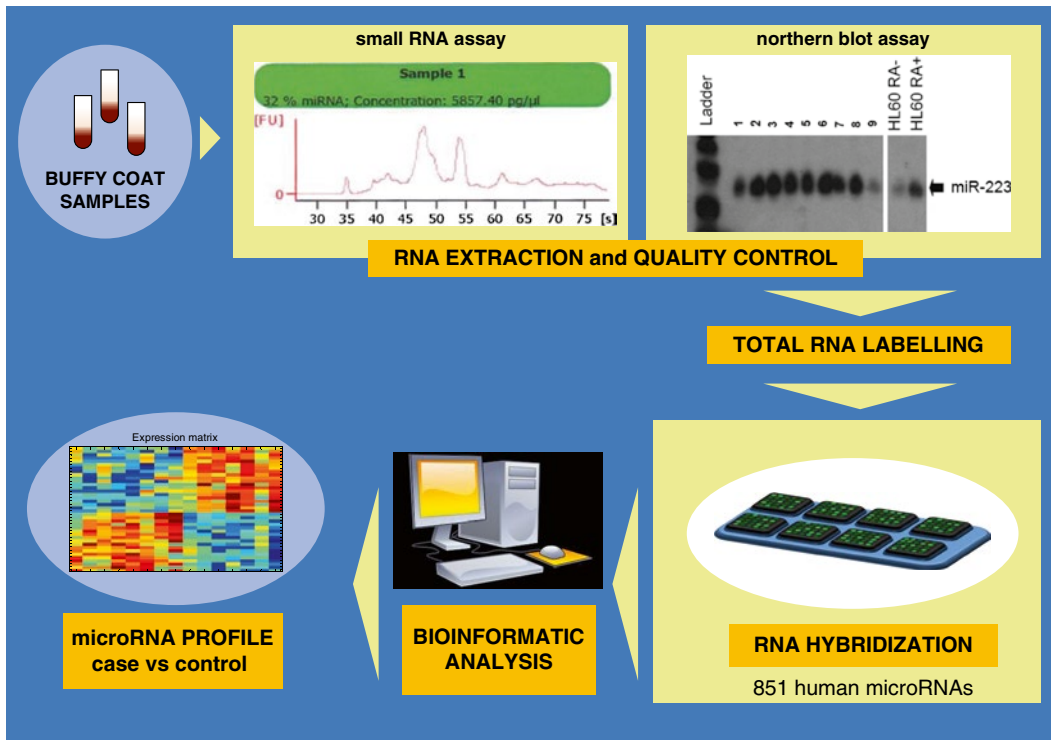

Fig. 1 Schematic representation of the experimental workflow

3.4 RNA Hybridization

Total RNA (100 ng) was labeled and hybridized to human microRNA Microarray V.3 (Agilent) containing probes for 866 human and 89 human viral miRNAs from the Sanger database release 12.0.

Each slide is an 8×15K format (~15,000 features printed in an 8-plex format, eight individual microarrays on a 1″×3″ glass slide) printed using Agilent's 60-mer Inkjet Technology, which, unlike competitive platforms, synthesizes 40–60-mer oligonucleotide probes directly on the array, resulting in high-purity, high-fidelity probes.

This miRNA platform requires small input amounts of total RNA—in the 100 nanogram range—because it uses a high-yield labeling method, and does not require size fractionation or amplification steps that may introduce undesired bias during miRNA profiling.

Scanning and image analysis were performed using the Agilent DNA Microarray Scanner (P/N G2565BA) equipped with extended dynamic range (XDR) software according to the Agilent miRNA Microarray System with miRNA Complete Labeling and Hybridization Kit Protocol manual.

Feature Extraction Software (Version 10.5) was used for data extraction from raw microarray image files using the miRNA_105_Dec08 FE protocol.

3.5 Microarray Data Analysis

Data were verified and extracted by Agilent Extraction 10.7.3.1 software and analyzed using an in-house built routines by Matlab (The MathWorks Inc.).

All arrays were quantile-normalized, assuming that all samples were measured and analyzed under the same condition, enforcing all the arrays to assume the same mean distribution. Pearson's coefficient was calculated to assess correlation between technical replicates of some randomly chosen samples.

We fitted a linear model to the expression values for each miRNA, to assess the significance of differential expression between case and control. In addition, we used empirical Bayes methods implemented in the LIMMA package to construct moderated-t statistics and incorporated the statistical tools to adjust for the multiplicity of the tests. The Benjamini and Hochberg's method (1995) was used to control for false discovery [17].

We considered the liner model including the matched case–control study design, the case–control status and the error term.

4 Notes

1. The mixture separates into a lower red phenol chloroform phase, an interphase, and a colorless upper aqueous phase. RNA remains exclusively in the aqueous phase. The upper aqueous phase is ~50 % of the total volume.

2. Save the interphase and organic phenol chloroform phase if isolation of DNA or protein is desired. The organic phase can be stored at 4 °C overnight.
3. The RNA is often invisible prior to centrifugation, and forms a gel-like pellet on the side and bottom of the tube.
4. Do not allow the RNA to dry completely, because the pellet can lose solubility. Partially dissolved RNA samples have an A 260/280 ratio <1.6.

Acknowledgment

We are indebted to the 10,786 ORDET participants. We also thank Dr. Paolo Contiero and the staff of the Lombardy Cancer Registry for technical assistance. This work was supported by Department of Defense grant W81 XWH 04 1 0195 and by the Veronesi Foundation.

References

1. Calin GA, Croce CM (2006) MicroRNA signatures in human cancers. Nat Rev Cancer 6:857–866
2. Martello G, Rosato A, Ferrari F et al (2010) A MicroRNA targeting dicer for metastasis control. Cell 141:1195–1207
3. Biagioni F, Bossel Ben-Moshe N, Fontemaggi G et al (2012) miR-10b*, a master inhibitor of the cell cycle, is down-regulated in human breast tumours. EMBO Mol Med 4:1214–1229
4. Cioce M, Ganci F, Canu V et al (2014) Protumorigenic effects of mir-145 loss in malignant pleural mesothelioma. Oncogene 33:5319
5. Kent OA, Mendell JT (2006) A small piece in the cancer puzzle: microRNAs as tumor suppressors and oncogenes. Oncogene 25:6188–6196
6. Blandino G, Fazi F, Donzelli S et al (2014) Tumor suppressor microRNAs: a novel noncoding alliance against cancer. FEBS Lett 588:2639–2652
7. Esquela-Kerscher A, Slack FJ (2006) Oncomirs - microRNAs with a role in cancer. Nat Rev Cancer 6:259–269
8. Calin GA, Croce CM (2006) MicroRNAs and chromosomal abnormalities in cancer cells. Oncogene 25:6202–6210
9. Lu J, Getz G, Miska EA et al (2005) MicroRNA expression profiles classify human cancers. Nature 435:834–838
10. Calin GA, Ferracin M, Cimmino A et al (2005) A MicroRNA signature associated with prognosis and progression in chronic lymphocytic leukemia. N Engl J Med 353:1793–1801
11. Chen PS, Su JL, Hung MC (2012) Dysregulation of microRNAs in cancer. J Biomed Sci 19:90
12. Jung M, Schaefer A, Steiner I et al (2010) Robust microRNA stability in degraded RNA preparations from human tissue and cell samples. Clin Chem 56:998–1006
13. Mraz M, Malinova K, Mayer J et al (2009) MicroRNA isolation and stability in stored RNA samples. Biochem Biophys Res Commun 390:1–4
14. Muti P, Pisani P, Crosignani P et al (1988) ORDET--prospective study on hormones, diet and breast cancer: feasibility studies and long-term quality control. Steroids 52:395–396
15. Muti P, Sacconi A, Hossain A et al (2014) Downregulation of microRNAs 145-3p and 145-5p is a long-term predictor of postmenopausal breast cancer risk: the ORDET prospective study. Cancer Epidemiol Biomarkers Prev 23:2471–2481
16. Chomczynski P, Sacchi N (2006) The single-step method of RNA isolation by acid guanidinium thiocyanate-phenol-chloroform extraction: twenty-something years on. Nat Protoc 1:581–58517
17. Benjamini Y, Hochberg Y (1995) Controlling the false discovery rate: A practical and powerful approach to multiple testing. Journal of the Royal Statistical Society Series B. Methodological, 57:289–300

Chapter 3

microRNAs in Cancer Chemoprevention: Method to Isolate Them from Fresh Tissues

Federica Ganci and Giovanni Blandino

Abstract

microRNAs are 22-nucleotide-long double-strand small RNAs, able to modulate gene expression at posttranscriptional level, degrading mRNA and/or impairing translation. They have been shown to regulate mRNA and protein abundance and to participate in many regulatory circuits controlling developmental timing, cell proliferation and differentiation, apoptosis and stress response. Notably, microRNA activity has been correlated to the pathogenesis of cancer; they are aberrantly expressed in solid and hematological tumors, suggesting that they could function as oncogenes or tumor suppressors. The emerging role of miRNAs in the carcinogenesis and tumor progression has provided opportunities for their clinical application in the capacity of cancer detection, diagnosis, and prognosis prediction. Here, we describe the experimental protocol used to isolate microRNAs from human tissues coming from head and neck, mesothelioma, and thymoma tumors in order to perform microarray and RT-qPCR experiments.

Key words microRNA, Fresh tissues, RNA extraction, HNSCC, Mesothelioma, Thymoma

1 Introduction

microRNAs (miRNAs) are highly conserved small noncoding RNAs (20–22 nucleotides long) that modulate negatively the gene expression by binding to the 3′UTR of multiple target mRNAs [1, 2]. miRNAs play an essential role in many biological processes such as cell proliferation and maturation, cell death, apoptosis, and regulation of chronic inflammation [3, 4]. Based on computational prediction, it has been estimated that more than 60 % of human mRNAs are targeted by at least one miRNA [5]. Many recent studies have shown that miRNAs have specific expression patterns in each cell type and tissues [6] and their aberrantly expression was observed in a wide range of pathologies, including cancer [7, 8]. Moreover, it was recently found that miRNA profiles are more informative than messenger RNA profiles and could classify poorly differentiated tumors since they better reflect the developmental lineage and differentiation state of cancer [9].

Sabrina Strano (ed.), *Cancer Chemoprevention: Methods and Protocols*, Methods in Molecular Biology, vol. 1379,
DOI 10.1007/978-1-4939-3191-0_3,

Therefore, miRNAs' expression profile is emerging among the best markers for diagnosis, staging, and treatment of cancer. Given the significance of miRNAs in modulating gene expression, they could also be used as biomarkers for assessing antineoplastic activity of cancer chemopreventive agents. A key advantage respect to their potential role as biomarkers is their stability due especially to their short length [10]. This stability offers an important privilege in the use of miRNA over mRNA because they are also well preserved in formalin- or paraffin-fixed (FFPE) tissue or fresh tissue with no good quality of RNA and these sample types may be often the only available in a clinical study [10, 11].

The quality of the miRNA expression profiles might depend on the starting RNA material and a robust RNA isolation method is essential for reproducible results. In this chapter, we aim to describe the protocol to isolate total RNA, including miRNA fraction, from head and neck, mesothelioma, and thymoma fresh frozen tissue samples in order to perform miRNA expression analyses by RT-qPCR and/or microarray experiments using Agilent and Affymetrix platforms [12–14].

2 Materials

2.1 RNA Extraction

1. RNaseZapRNase Decontamination Solution (Ambion, Foster City, CA) or similar.
2. RNA later solution (Life Tec Rockville, MD).
3. Phosphate-buffered saline (PBS).
4. Homogenizer for tissues; gentleMACS dissociator (Miltenyi Biotec, Bergisch Gladbach, GE) or similar.
5. miRNeasy Mini kit (Qiagen, Hilden, Germany).
6. Chloroform.
7. Ethanol.
8. DNAse-, RNAse-free set (Qiagen, Hilden, Germany).
9. RNase-free water for molecular biology.

2.2 RNA Quality Control

1. Spectrophotometer (NanoDrop ND-1000, Thermo Fisher Scientific, Waltham, MA).
2. Agilent 2100 Bioanalyzer; Total RNA 6000 Nano Kit; Small RNA kit.

3 Methods

3.1 Tissue Sample Collection

The fresh tissue coming from tumor and normal controls may be immediately placed in RNA later stabilization solution (Ambion, Foster City, CA) after tumor removal by surgery (*see* **Note 1**).

This reagent is an aqueous tissue storage solution that rapidly permeates tissue to protect and stabilize its RNA (proteins are also preserved in RNA later solution). The specimen was stored at 4 °C overnight (to allow the solution to thoroughly penetrate the tissue) before to process it. Next the tissue was washed in PBS solution, placed in a cryovial and moved to −80 °C for long-term storage (*see* **Note 2**).

Samples from each case and related control were handled identically and assayed together on the same laboratory session.

3.2 RNA Isolation

The quality of the miRNA expression profiles largely depends on the starting RNA material and a robust RNA isolation method is essential for reproducible results. Before starting, it is important to consider the potential for infection or disease transmission by materials used that contact the sample and/or the homogenate. Wear a lab coat and gloves, RNA extraction may be performed under a chemical hood. In addition, the RNA extraction is complicated by the ubiquitous presence of ribonuclease enzymes which can rapidly degrade RNA. Therefore, the RNase decontamination solution can be applied directly to surfaces and pipettes which will be used during the RNA extraction.

RNA isolation from human tissues was performed by miRNeasy mini kit (Qiagen, Hilden, Germany) according to the manufacturer's instructions with the addition of simple modifications to improve essentially the purity of RNA and to enhance RNA yeld.

The miRNeasy mini kit is based on the phenol/guanidine lysis of samples and their purification by the binding of total RNA in silica membrane. Lysis was performed by QIAzol Lysis reagent (included in the miRNeasy mini kit), containing phenol and guanidine thiocyanate which in addition to lysing action prevent the activity of RNase and DNase enzymes to ensure purification of intact RNA. Subsequently, by adding chloroform solution and centrifuging, the homogenate was separated into an upper aqueous phase, containing RNA, a lower interphase and organic phase, containing DNA and proteins. After the addition of absolute ethanol to provide appropriate binding conditions, total RNA from aqueous phase was moved into spin column where RNA binds to the membrane and phenol contaminants are efficiently washed away. Finally, RNA is then eluted in RNase-free water.

With the miRNeasy protocol, all RNA molecules longer than 18 nucleotides are purified.

Carry out all steps at room temperature (15–25 °C) and under chemical hood unless otherwise specified.

1. Homogenize frozen tissue directly in at least 0.7 mL of QIAzol solution and incubate sample for 20 min at room temperature to allow the complete dissociation of nucleoprotein complexes (*see* **Note 3**).

2. Add 140 μL of chloroform. Shake vigorously for 25 s and incubate sample for 3–5 min at room temperature. Centrifuge at 15,700 rcf for 20 min at 4 °C.
3. Draw up carefully the upper aqueous phase of the sample (about 350 μL) by P-200 pipette and transfer it to a new 1.5 mL tube. Be certain that you do not take any of the lower phases when removing the aqueous phase (*see* **Note 4**).
4. Add 1.5 volumes (about 0.525 mL) of absolute ethanol solution and mix by pipetting up and down 8–10 times.
5. Move the obtained solution (about 0.7 mL) into the RNEasy mini spin column in a 2 mL tube. Be certain that the sample does not touch the lid during its closing. Centrifuge the tube at 9300 rcf for 20 s. Discard the flow-through (the 2 mL tube can be used again for next step).
6. Repeat the **step 5** if the solution was more than 0.7 mL.
7. Wash the membrane with the adding of 350 μL of RWT buffer into RNEasy mini spin column and centrifuge for 20 s at 9300 rcf.
8. Use the DNAse-, RNAse-free set (Qiagen, Hilden, Germany) and prepare the DNase mix solution in a 1.5 tube (add 10 μL of DNase stock solution to 70 μL of buffer RDD). Mix gently by inverting the tube (not vortex) and put it in ice before and during the use.
9. Add the DNase mix solution (80 μL) into the RNEasy mini spin column membrane and incubate it at room temperature for 15 min. Do not leave the DNase mix solution into the membrane for more 20 min, the quality of RNA might be compromise.
10. Add 350 μL of RWT wash buffer to the RNEasy mini spin column and centrifuge for 20 s at 9300 rcf. Discard the flow-through; the 2 mL tube can be used again for next step (*see* **Note 5**).
11. Pipette 0.5 mL of the second wash buffer RPE into to the RNEasy mini spin column and close the lid. Wash the column by centrifuging for 20 s at 9300 rcf. Discard the flow-through and use again the 2 mL tube for the next step.
12. Add again 0.5 mL of RPE buffer, close the lid and gently invert the tube 1–2 times to efficiently wash away all contaminants from the lid (*see* **Note 6**). Centrifuge for 2 min the spin column at 9300 rcf to dry the membrane.
13. Move the spin column into a new 2 mL tube and centrifuge for 1 min at full speed to remove any residual of flow-through.
14. Optional: Open the lid of spin column and leave it on the bench for 5 min to be sure to dry any residual of wash buffer.

15. Move the RNEasy mini spin column into a new 1.5 mL tube, elute RNA by pipetting 30–50 μL of RNase-free water directly the membrane without touch it. Close the lid and leave the tube 1 min at room temperature to obtain a higher amount of total RNA. Centrifuge for 1 min at 9300 rcf.
16. Move the RNA sample in ice and quantify its concentration by NanoDrop 2000 Spectrophotometer (Thermo Fisher Scientific Inc, Asheville, NC). Do not discard immediately the RNEasy spin column, but move it in a new 1.5 mL tube and leave at room temperature waiting the quantification of RNA.
17. If the concentration of RNA is >about 500 ng/μL, again add water (30 μL) to membrane of spin column and centrifuge for 1 min at 9300 rcf. Move the second aliquot of RNA sample in ice and quantify; you can add the second elute of RNA to the first one, but if the concentration of the second one is too low we suggest you maintain separately the two RNA elutes obtained.
18. Proceed to downstream application, or store at −80 °C (*see* **Note 7**).

To preserve RNA integrity, subdivide the first elute of RNA in at least two sub-aliquots in order to avoid frequent freeze and thaw.

3.3 RNA Quality Control

The expression profiling data can be potentially influenced not only by the method used to isolate the miRNAs, but also by the RNA storage conditions and handling [15]. Studies correlating the RNA quality with the outcome of the microRNA expression experiments have shown contradictory results [16]; several works have reported that a good quality of starting RNA material was essential to obtain reproducible and robust data [17–19], others showed that RNA degradation did not significantly influence the miRNA expression results [20, 21] probably because for their small size, microRNAs are less susceptible to degradation in comparison with mRNAs [22]. In our experience, data obtained by the analysis of microRNAs expression in RNA degraded samples were comparable with the results coming from analysis of intact RNA. However, a good quality of total RNA gives the further advantage to perform expression profile of both mRNAs and miRNAs using the same sample.

Assessment of the purity and quantity of extracted total RNA can be determined by a NanoDrop 2000 Spectrophotometer or similar. Instead, RNA integrity can be assessed by Bioanalyzer 2100 (Agilent Technologies, USA), where total RNA are electrophoretical separated on a chip and detected via laser induced fluorescence detection. Integrity of the RNA may be assessed by visualization of the 18S and 28S ribosomal RNA bands. In order to standardize the RNA integrity interpretation, Agilent technology

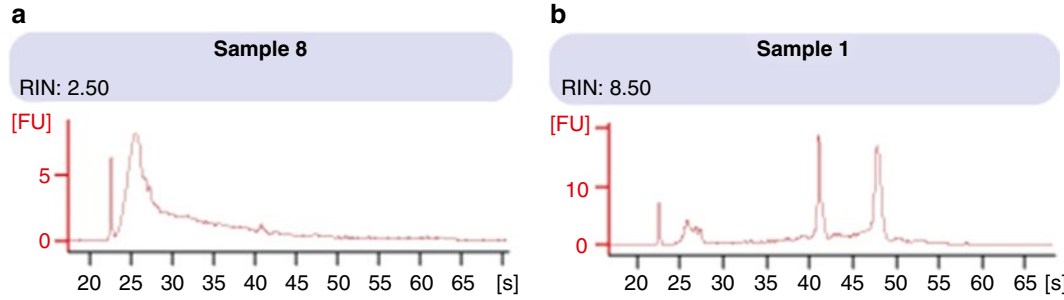

Fig. 1 Example of Agilent Bioanalyzer results. (**a**) Profile of a sample having a completely degraded RNA. (**b**) Profile of a sample with an intact RNA

has developed the RNA Integrity Number (RIN) software algorithm by which total RNA is classified based on numbering system from 1 to 10, according to its integrity; RIN 1 represents the most degraded RNA profile, while RIN 10 represents the most intact RNA (Fig. 1). Typically, values over 7 are good enough for transcriptome analysis using Affymetrix and Agilent platforms. This methodology requires a very small amount of RNA sample (>200 pg). In addition, by Bioanalyzer 2100 instrument can be estimate miRNA abundance expressed as the proportion of RNA in the 15–40 nt window relative to total small RNA abundance (6–150 nt). This information can be useful to evaluate if tissues analyzed have or not similar miRNAs abundance. However, the estimation of miRNA abundance by this method may only be accurate when overall RNA integrity is very high.

The basic workflow of the entire protocol is shown in Fig. 2.

4 Notes

1. This step is critical to obtain an intact RNA from specimen. The piece of tissue may be place immediately into RNA stabilization solution after surgery removal, a delay of a few minutes might cause a rapidly and significant degradation of RNA. The size of tissue should be <0.5 cm and the amount of RNAlater solution may be 8–10 volumes respect to the size of tissue. An incorrect ratio of solution volume on tissue size might be not to ensure the preservation of RNA in all parts of tissue. Usually, we place 1.8 mL of solution in a cryovial where then the surgeon will put the piece of tissue.
2. Do not freeze sample in RNAlater solution immediately, the sample in RNA later solution can be stored at room temperature until 1 week or at 4 °C until 1 month without compromising the quality of RNA. The sample can be freeze at −20 or −80 °C indefinitely also directly in RNA later solution.

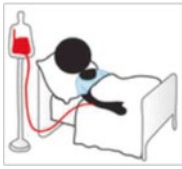

Put frozen tissue in RNA later solution and storage at 4° C overnight

Homogenize and lyse frozen tissue in Qlazol solution

Transfer homogenate to an eppendorf, add chloroform solution and shake

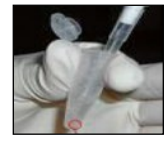

Separate the phases

Move upper aqueous phase to new tube and add ethanol

Bind total RNA including small RNA by moving the solution into the column

Wash the column

Elute to obtain total RNA including small RNAs

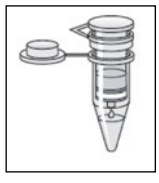

Total and small RNAs are ready to perform miRNA and gene expression analysis

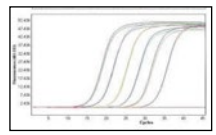

Expression matrix

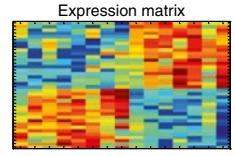

Quantify and check the quality of total and small RNAs

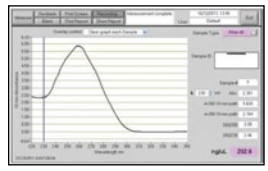

RNA quality control

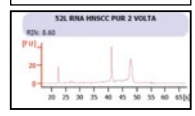

Small RNAs control

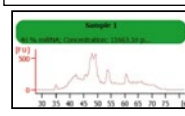

Fig. 2 The basic workflow of the entire protocol of miRNA extraction from tissue

3. To homogenize by gentleMACS Dissociator, transfer the frozen piece into gentleMACS M tube containing QIAzol solution, and set up the program RNA_02 by which the piece will be homogenize in 84 s. If the piece is not completely homogenized, the homogenization can be repeated by adding other 0.7 mL of QIAzol to M tube containing the partially homogenate specimen. After the homogenization, transfer the homogenized sample into to new 1.5 mL tube and proceed with the RNA extraction. Alternatively, the sample in QIAzol solution can be stored at −80 °C for several months without compromising the quality of RNA.
4. If you draw up residuals of lower phase, pull down the aqueous phase contained in the tip of pipette into the 1.5 mL tube, centrifuge it for 5 min at 13,400 rcf in order to separate again the phases and repeat the passage 3. If isolation of DNA or protein is desired, save the interphase and organic phenol chloroform phase. The organic phase can be stored at 4 °C overnight. Follow the protocol of Trizol to proceed with DNA and protein extraction.
5. The necessary to digest sample with DNase enzyme depends on the use that it will be done of RNA. For instance, RNA-seq or other types of gene expression experiments, usually require the removal of DNA from RNA sample. If the treatment of DNase is not necessary, after the passage 7, do not proceed with **steps 8–10**, but add 0.7 mL of RWT wash buffer into the column and centrifuge for 20 s at 9300 rcf. Discard the flow-through, and proceed with the **step 11**.
6. The inversion of tube can increase significantly the purity of RNA, consequently the ratio 260/230 results will be >1.8.
7. Before to freeze the RNA, prepare a small aliquot containing few microliters of sample to perform the quality control by Bionalyzer 2100 (in case of impossibility to check the quality immediately after extraction).

References

1. Lagos-Quintana M, Rauhut R, Lendeckel W et al (2001) Identification of novel genes coding for small expressed RNAs. Science 294:853–858
2. Tang G, Tang X, Mendu V et al (2008) The art of microRNA: various strategies leading to gene silencing via an ancient pathway. Biochim Biophys Acta 1779:655–662
3. Ambros V (2004) The functions of animal microRNAs. Nature 431:350–355
4. Bartel DP (2004) MicroRNAs: genomics, biogenesis, mechanism, and function. Cell 116:281–297
5. Friedman RC, Farh KK, Burge CB et al (2009) Most mammalian mRNAs are conserved targets of microRNAs. Genome Res 19:92–105
6. Landgraf P, Rusu M, Sheridan R et al (2007) A mammalian microRNA expression atlas based on small RNA library sequencing. Cell 129: 1401–1414

7. Ross JS, Carlson JA, Brock G (2007) miRNA: the new gene silencer. Am J Clin Pathol 128: 830–836
8. Visone R, Croce CM (2009) MiRNAs and cancer. Am J Pathol 174:1131–1138
9. Lu J, Getz G, Miska EA et al (2005) MicroRNA expression profiles classify human cancers. Nature 435:834–838
10. Pritchard CC, Cheng HH, Tewari M (2012) MicroRNA profiling: approaches and considerations. Nat Rev Genet 13:358–369
11. Li J, Smyth P, Flavin R et al (2007) Comparison of miRNA expression patterns using total RNA extracted from matched samples of formalin-fixed paraffin-embedded (FFPE) cells and snap frozen cells. BMC Biotechnol 7:36
12. Cioce M, Ganci F, Canu V et al (2014) Protumorigenic effects of mir-145 loss in malignant pleural mesothelioma. Oncogene 33:5319
13. Ganci F, Sacconi A, Bossel Ben-Moshe N et al (2013) Expression of TP53 mutation-associated microRNAs predicts clinical outcome in head and neck squamous cell carcinoma patients. Ann Oncol 24: 3082–3088
14. Ganci F, Vico C, Korita E et al (2014) MicroRNA expression profiling of thymic epithelial tumors. Lung Cancer 85:197–204
15. Mraz M, Malinova K, Mayer J et al (2009) MicroRNA isolation and stability in stored RNA samples. Biochem Biophys Res Commun 390:1–4
16. Podolska A, Kaczkowski B, Litman T et al (2011) How the RNA isolation method can affect microRNA microarray results. Acta Biochim Pol 58:535–540
17. Hammerle-Fickinger A, Riedmaier I, Becker C et al (2010) Validation of extraction methods for total RNA and miRNA from bovine blood prior to quantitative gene expression analyses. Biotechnol Lett 32:35–44
18. Ibberson D, Benes V, Muckenthaler MU et al (2009) RNA degradation compromises the reliability of microRNA expression profiling. BMC Biotechnol 9:102
19. Wang WX, Wilfred BR, Baldwin DA et al (2008) Focus on RNA isolation: obtaining RNA for microRNA (miRNA) expression profiling analyses of neural tissue. Biochim Biophys Acta 1779:749–757
20. Liu A, Tetzlaff MT, Vanbelle P et al (2009) MicroRNA expression profiling outperforms mRNA expression profiling in formalin-fixed paraffin-embedded tissues. Int J Clin Exp Pathol 2:519–527
21. Zhang X, Chen J, Radcliffe T et al (2008) An array-based analysis of microRNA expression comparing matched frozen and formalin-fixed paraffin-embedded human tissue samples. J Mol Diagn 10:513–519
22. Doleshal M, Magotra AA, Choudhury B et al (2008) Evaluation and validation of total RNA extraction methods for microRNA expression analyses in formalin-fixed, paraffin-embedded tissues. J Mol Diagn 10:203–211

Chapter 4

Application of RNA-Seq Technology in Cancer Chemoprevention

Frauke Goeman and Maurizio Fanciulli

Abstract

RNA-sequencing is a revolutionary tool to follow differential expression after treatment with cancer chemopreventive agents. It allows a real genome-wide screening independent of prior assumptions and is well suited for analyzing coding but also long noncoding RNAs. It still consents the discovery of new genes and isoforms and increased our knowledge of antisense and other noncoding RNAs in a tremendous manner. Moreover, it permits to detect low-abundance and biologically critical isoforms and reveals genetic variants and gene fusions in one single assay. Here, we provide a detailed protocol for stranded RNA-sequencing.

Key words RNA-Seq, Deep-sequencing, Chemoprevention, Transcriptome profiling, Long noncoding RNA, Stranded RNA-Seq, Transcriptional signature, Novel transcript and isoform discovery

1 Introduction

The development of RNA-sequencing (RNA-Seq)has allowed many advances in the genome-wide transcriptional profiling [1]. RNA-Seq is based on next generation sequencing and consents the quantification of all transcripts longer than 200 nucleotides, including those that are not annotated yet, and therefore still gives rise to the discovery of new genes and transcripts. It revolutionized our understanding of the complexity of transcription. There is no limit of the dynamic range of transcript detection due to the technique, permitting therefore also the detection of rare RNA transcripts and of more differentially expressed genes with a higher fold change [2]. Furthermore, it allows the identification of alternative splicing, allelic-specific expression, and posttranscriptional RNA editing events. But also gene fusions or genetic variants can be reliably detected.

Despite the classical RNA-Seq, there are also several alternative methodologies described in literature. RNA immunoprecipitation sequencing (RIP-Seq) allows mapping RNA-protein interactions [3]. Argonaute HITS-CLIP decodes microRNA-mRNA interac-

Sabrina Strano (ed.), *Cancer Chemoprevention: Methods and Protocols*, Methods in Molecular Biology, vol. 1379,
DOI 10.1007/978-1-4939-3191-0_4,

tion maps [4]. Ribo-Seq identifies those mRNAs that are actively translated [5] whereas global run-on sequencing (GRO-Seq) is quantifying transcription by directly measuring nascent RNA production [6].

To perform a classical RNA-sequencing, there are two decisions to make. The first one involves the rRNA removal that can be done either by poly(A) purification of the RNA or by ribosomal depletion. The latter retains the whole spectrum of RNA transcripts and therefore also transcripts that do not contain a poly(A) tail. The second decision to take is whether the RNA-Seq should be stranded or not. A stranded RNA-Seq allows us to know immediately from which DNA strand a given RNA transcript is deriving from which is helpful for newly discovered transcripts but really indispensable for antisense transcript detection. Additionally it is thought to enhance alignment and transcript annotation.

Here, we describe the protocol for a stranded RNA-sequencing with previous ribosomal depletion, starting from the RNA extraction to the library preparation and the final setting up of the sequencing reaction including all necessary quality control and quantification steps (Fig. 1).

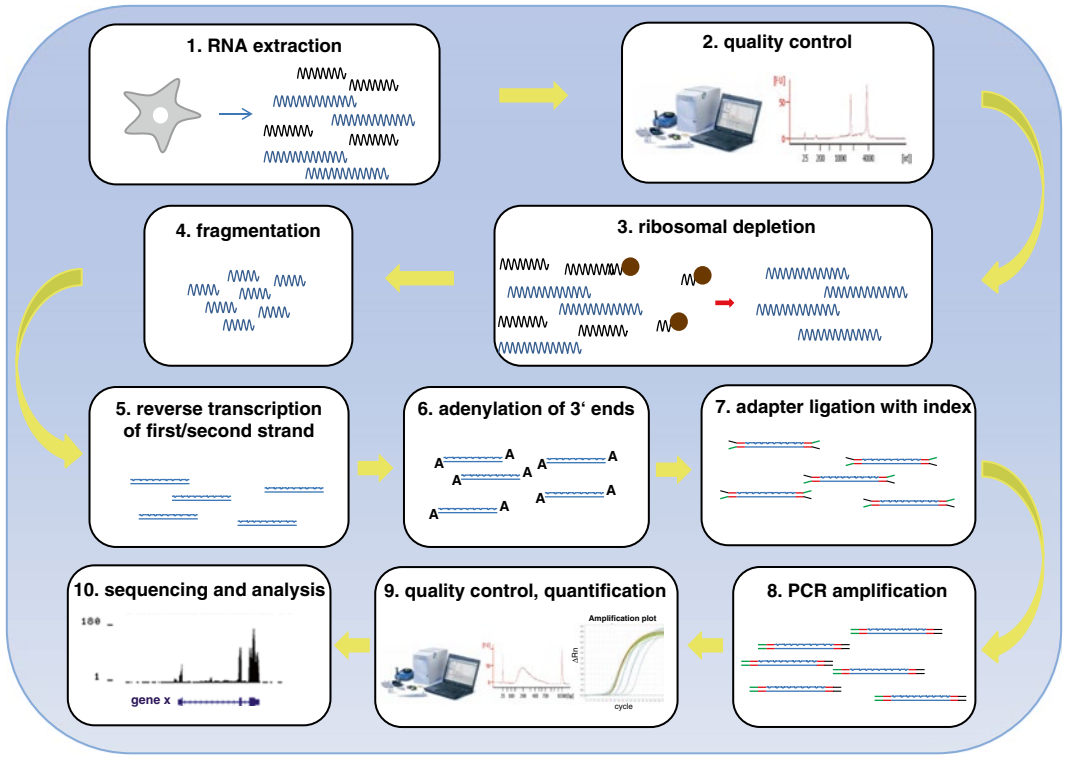

Fig. 1 Schematic overview of the library preparation steps for stranded RNA-sequencing

2 Materials

2.1 RNA-Extraction

1. miRNeasy Kit (Qiagen, Valencia, CA, USA).
2. RNase Zapper (Life Technologies, Carlsbad, CA, USA).
3. RNase-free ultrapure water.
4. Phosphate-buffered saline (PBS): To obtain a 10× stock solution add 80 g NaCl, 2 g KCL, 14.4 g Na_2HPO_4 (dibasic anhydrous), and 2.4 g KH_2PO_4 (monobasic anhydrous), fill up to 1 L with ultrapure water, and autoclave. The pH should be 7.4. The final 1× working concentration is 137 mM NaCl, 2.7 mM KCl, 10 mM Na_2HPO_4, and 1.8 mM KH_2PO_4.
5. Ethanol (100 %).
6. QIAzol Lysis Reagent and RPE Buffer make part of the miRNeasy Kit (Qiagen, Valencia, CA, USA).
7. Chloroform.
8. RNase-Free DNase Set (cat. no. 79254, Qiagen, Valencia, CA, USA).
9. NanoDrop® spectrophotometer (NanoDrop Technologies, Wilmington, DE, USA).
10. Agilent RNA 6000 Nano Kit (Agilent Technologies, Santa Clara, CA, USA).
11. Agilent Bioanalyzer (Agilent Technologies, Santa Clara, CA, USA).

2.2 Library Preparation and Quality Control

1. TruSeq Stranded Total RNA LT Sample Prep Kit with Ribo-Zero Gold (Illumina Inc., San Diego, CA, USA; part # RS-122-2301).
2. Magnetic stand-96 (Life Technologies, Carlsbad, CA, USA; part # AM10027).
3. Agencourt RNAClean XP 40 mL (Beckman Coulter Genomics, Fullerton, CA, USA).
4. Agencourt AMPure XP 60 mL (Beckman Coulter Genomics, Fullerton, CA, USA).
5. Agilent High Sensitivity DNA Kit (Agilent Technologies, Santa Clara, CA, USA).
6. SuperScript II Reverse Transcriptase (Invitrogen, Carlsbad, CA, USA).
7. 80 % Ethanol: Prepare always fresh by adding 2 mL of ultrapure water to 8 mL 100 % ethanol.
8. 1 M Tris–HCl pH 8.5: Weigh 60.57 g Tris [Tris (hydroxymethyl) aminomethane] into 450 mL of ultrapure water. Adjust the pH with HCl, make up to 500 mL with ultrapure water, and filter through a 0.2 μM cellulose acetate filter.

9. 10 mM Tris–HCl pH 8.5 with 0.1 % Tween 20: Dilute 1 mL of 1 M Tris–HCl pH 8.5 into 50 mL of ultrapure water and add 100µL of Tween 20. Finally, the solution has to be filled up with ultrapure water to 100 mL.
10. Agilent DNA 1000 Kit or Agilent High Sensitivity DNA Kit (Agilent Technologies, Santa Clara, CA, USA).
11. Real-time PCR instrument like Applied Biosystems StepOne™.
12. KAPA SYBR FAST ABI PRISM Readymix, part # KK4604 (Kapa Biosystems, Wilmington, MA, USA).
13. qPCR primer 1.1: 5′ AATGATACGGCGACCACCGAGAT 3′ HPLC purified; qPCR primer 2.1: 5′ CAAGCAGAAGAC GGCATACGA 3′ HPLC purified.
14. Optional: KAPA Library Quantification Kit (Kapa Biosystems, Wilmington, MA, USA) (*see* **Note 21**).
15. cBot or Cluster Station (Illumina Inc., San Diego, CA, USA).
16. Genome Analyzer, NextSeq or HiSeq (Illumina Inc., San Diego, CA, USA).

3 Methods

3.1 RNA-Extraction

To extract sufficient material to perform an RNA-Seq experiment we usually start with 60 mm dishes containing cells being ca. 80 % confluent (*see* **Notes 1** and **2**). Perform the experiments in triplicate.

1. You can lyse the cells directly on the plate after two washes with ice-cold PBS by adding 700 µL of QIAzol Lysis Reagents (*see* **Note 3**). The solution is pipetted up and down onto the plate until the cells are getting lysed (*see* **Note 4**). Transfer the homogenate into a 1.5 mL tube and vortex for 1 min. Incubate at room temperature (RT) for 5 min. Add 140 µL of chloroform and shake vigorously for exactly 15 s. Incubate again at RT for 2–3 min. Centrifuge the tubes for 15 min at 12,000 × *g* at 4 °C (*see* **Note 5**).
2. Collect the upper aqueous phase and transfer it into a new tube. Add 1.5 volumes of ethanol 100 %, mix thoroughly (*see* **Note 6**), and transfer up to 750 µL into an RNeasy spin column. Centrifuge at room temperature for 30 s at 8000 × *g*. Remove and discard the flow-through. Repeat this step until all liquid was loaded onto the column.
3. Perform an on-column DNase digestion (*see* **Note 7**). The buffers and DNase enzymes are supplied in the RNase-free DNase Set. Wash the column with 350 µL buffer RWT by adding it on top of the column and centrifuge at 8000 × *g* for 30 s at RT. Discard the flow-through. Mix 10 µL of the DNase I

stock with 70 µL RDD and add all to the column. Incubate for 15 min at 20–30 °C. Subsequently wash again with 350 µL buffer RWT like described above.

4. Wash with 500 µL RPE buffer by adding it on top of the column and centrifuging at 8000 × *g* for 30 s at RT, and discard the flow-through. Repeat the washing with 500 µL RPE buffer and centrifuge for 2 min. Place the column in a new collection tube and centrifuge again for 1 min at 8000 × *g* to dry completely the column membrane. Place the column into a new 1.5 mL tube; add 30 µL RNase-free ultrapure water and centrifuge at 8000 × *g* for 1 min to elute the RNA.

3.2 RNA Quality Control

1. The quality of the extracted RNA should be evaluated to adjust later on the protocol for the library preparation. The quality can be determined using the Agilent RNA 6000 Nano Kit together with the Agilent Bioanalyzer. The quality of the RNA will be expressed as RIN (RNA integrity number) ranging from 1 to 10.
2. The RNA should be tested by qPCR with target genes that are known to be differentially expressed after chemopreventive treatment. Design the amplicons in the 50–150 bp range to be able to use them again after the library preparation.

3.3 Library Preparation

We usually start with 500 ng RNA for the library preparation (*see* **Note 8**). The steps to be performed are: removal of ribosomal RNA, fragmentation of the RNA, reverse transcription of the first strand with random hexamers, reverse transcription of the second strand, adenylation of the 3′end, ligation of Illumina adapters with indices, and finally PCR amplification (*see* **Note 9**).

3.4 Removal of Ribosomal RNA

1. Dilute 500 ng RNA in 10 µL ultrapure water in a 96-well 0.3 mL PCR plate (*see* **Note 10**) and add 5 µL of rRNA Binding Buffer. Add 5 µL of rRNA Removal Mix-Gold and mix well by pipetting up and down.
2. Seal the plate and denaturate the RNA in a thermal cycler for 5 min at 68 °C. Take the plate out of the thermal cycler and leave it at RT for 1 min.
3. Vortex the rRNA Removal Beads well and transfer 35 µL into each well of a *new* PCR plate. Add the denatured RNA mix by pipetting immediately quickly up and down (*see* **Note 11**) and incubate them for 1 min at RT. Place the plate on the magnetic stand and incubate for 1 min. Remove the supernatant and transfer it into a new 0.3 mL PCR plate. Control if no beads were carried over by placing the plate for 1 min on the magnetic stand.
4. Mix the RNAClean XP beads well by vortexing. Add 99 µL into each well of the 0.3 mL PCR plate containing ribosomal

depleted RNA and mix well by pipetting. If the RNA was degraded (below RIN 6–7), use instead 193 μL of beads. Incubate at RT for 15 min. Place the plate on the magnetic stand for 5 min and eliminate the supernatant. Add 200 μL of freshly prepared 70 % ethanol to the beads without disturbing them on the magnet, wait for 30 s and remove again the supernatant. Let the beads dry at RT for 15 min.

5. Remove the plate from the magnetic stand and elute the RNA from the beads by adding 11 μL of Elution Buffer and pipetting the beads up and down. Let them incubate for 2 min at RT and separate subsequently the RNA from the beads by placing the plate on the magnetic stand for 5 min. The supernatant contains the ribosomal depleted RNA.

3.5 RNA Fragmentation

1. Transfer 8.5 μL of the eluted ribosomal depleted RNA into a new 96-well 0.3 mL PCR plate and add 8.5 μL Elute, Prime, Fragment High Mix. Mix well by pipetting.
2. Seal the plate and fragment the RNA in a thermal cycler. Program setting: 94 °C for 8 min if the RNA was not degraded; hold at 4 °C (*see* **Note 12**). Briefly centrifuge the plate after the incubation.

3.6 Reverse Transcription of the First Strand

1. Transfer 50 μL of SuperScript II Reverse Transcriptase into the First Strand Synthesis Act D Mix and mix by pipetting (*see* **Notes 13** and **14**). Add 8 μL of it into each well of the 96-well PCR plate containing the fragmented ribosomal depleted RNA and mix by pipetting. Seal the plate with an adhesive seal and incubate the samples for the reverse transcription on the thermal cycler like following: 10 min 25 °C, 15 min 42 °C, 15 min 70 °C, hold at 4 °C. Perform immediately the second-strand synthesis.

3.7 Reverse Transcription of the Second Strand

The second cDNA strand will be generated by incorporating dUTP instead of dTTP. It will give rise to a double-stranded cDNA that is required for the subsequent Illumina Adapter ligation that permits PCR amplification, sequencing, and indexing. The dUTP ensures the strandedness because in the subsequent PCR amplification the polymerase will amplify only the strands that do not contain dUTP.

1. Add 5 μL of Resuspension Buffer to each well of the 96-well PCR plate. Add 20 μL Second Strand Marking Master Mix to each sample and mix by pipetting. Seal the plate with an adhesive seal and incubate for 1 h at 16 °C in a thermal cycler.
2. Purify the double stranded cDNA with 90 μL AMPure XP beads equilibrated to room temperature. Mix well and incubate for 15 min at RT. Place the plate on the magnetic stand for 5 min. Remove the supernatant and wash the beads still attached

to the magnet with 200 μL freshly prepared 80 % Ethanol. After 30-s incubation remove the supernatant and wash again with 200 μL 80 % ethanol like described before. Discard again the supernatant and let the beads air-dry at RT for 15 min. Remove the plate from the magnet and add 17.5 μL of Resuspension Buffer (equilibrated to RT) to the beads. Mix well by pipetting. Incubate for 2 min and subsequently place the plate on the magnet for 5 min. Transfer 15 μL of the supernatant into a new 96-well 0.3 mL PCR plate (*see* **Note 15**).

3.8 Adenylation of the 3′ End

In the subsequent step, the 3′ ends of the cDNA fragments will be adenylated. The attachment of a single A nucleotide will increase the efficiency to ligate the Illumina Adapters that contain a corresponding T'overhang. Furthermore, it will help avoiding a ligation between the cDNA fragments.

1. Add 2.5 μL of Resuspension Buffer and 12.5 μL of A-Tailing Mix to each well of the 0.3 mL PCR plate containing the cDNA. Mix well by pipetting, seal the plate with an adhesive seal and place the plate into a thermal cycler. Incubate for 30 min at 37 °C, followed by 5 min at 70 °C and a hold at 4 °C.
2. Proceed immediately to the adapter ligation.

3.9 Adapter Ligation

Illumina uses two color channels for sequencing, a red one for A/C and a green one for G/T. The adapters have to be chosen in a way that the samples that will be pooled and therefore sequenced together in one lane contain in each base position nucleotides from both channels. Please check the Illumina guidelines for pooling samples in the original "TruSeq Stranded Total RNA Sample Prep Guide."

1. Add 2.5 μL of Resuspension Buffer and 2.5 μL of Ligation Mix to each well of the adenylated cDNA and mix well by pipetting (*see* **Note 16**). Add 2.5 μL of the appropriate Adapter and mix well. Seal the plate and incubate in a thermal cycler for 10 min at 30 °C.
2. Add 5 μL of Stop Ligation Buffer to each well.
3. Purify the samples with AMPure XP Beads equilibrated to room temperature. Add 42 μL of beads to each sample and mix well by pipetting. Incubate at RT for 15 min. Separate the beads from the solution by incubating the plate on the magnet for 5 min. Discard the supernatant and wash the beads with 200 μL freshly prepared 80 % ethanol without disturbing the beads attached to the magnet. Wait for 30 s, remove the ethanol and wash again with 200 μL of 80 % ethanol. Air-dry the pellet for 15 min while still being attached to the magnet. Remove the plate from the magnet and resuspend the beads with 52.5 μL of Resuspension Buffer. After 2-min incubation

at RT place the plate on the magnet for 5 min. Transfer 50 μL of the supernatant into a new 0.3 mL PCR tube.

4. Purify again with AMPure XP Beads by adding 50 μL of beads to the samples. Mix well by pipetting and incubate for 15 min at RT. Place the plate on the magnetic stand and incubate for 5 min. Discard the supernatant and wash the beads by adding 200 μL of freshly prepared 80 % ethanol without disturbing the beads. Incubate for 30 s, remove the supernatant, and wash again with 200 μL of 80 % ethanol like described before. Remove completely the supernatant and allow the beads to air dry for 15 min while still being attached to the magnet. Remove the plate from the magnet and resuspend the beads with 22.5 μL of Resuspension Buffer. Incubate for 2 min and separate the beads from the supernatant by 5 min incubation of the plate on the magnetic stand. Transfer 20 μL of the supernatant into a new 0.3 mL PCR plate (*see* **Note 17**).

3.10 PCR Amplification

Here, all cDNA fragments will be amplified via the adapter attached before. The PCR amplification will enable you to perform the subsequent quality control steps but also ensure the enrichment of those cDNAs that have linkers on both sides. The adapters are necessary for (1) the binding to the flow cell, (2) the cluster formation, and (3) the sequencing reaction.

1. Add 5 μL of PCR primers and 25 μL of PCR master mix to each well of the PCR plate. Mix well by pipetting. Seal the plate and incubate in a thermal cycler at 98 °C for 30 s followed by 15 cycles of 98 °C for 10 s, 60 °C for 30 s, and 72 °C for 30 s and a subsequent elongation at 72 °C for 5 min and a hold at 4 °C (*see* **Note 18**).
2. Purify the PCR products with AMPure XP Beads. Centrifuge briefly the plate and add 50 μL of well dispersed beads slurry to each well of the PCR plate. Mix well by pipetting and incubate for 15 min. Separate the beads from the supernatant by placing the plate on the magnetic stand for 5 min. Discard the supernatant and wash the beads with 200 μL of freshly prepared 80 % Ethanol with the plate remaining on the magnet. Wait for 30 s and then remove the supernatant and wash again with 200 μL of 80 % Ethanol like described before. Eliminate all supernatant and allow the beads to air dry for 15 min. Remove the plate from the magnet and resuspend the beads in 32.5 μL of Resuspension Buffer. Incubate for 2 min and place subsequently the plate on the magnet for 5 min. Transfer 30 μL of the supernatant that contains the final library to a new 0.3 mL PCR plate.

3.11 Validation of the Library

The final library has to be well controlled before sequencing.

3.12 Quality Control

1. The quality will be verified with the Agilent Bioanalyzer using an Agilent DNA 1000 Kit or an Agilent High Sensitivity DNA Kit (*see* **Note 19**). The library should give a peak around 260–290 bp (Fig. 3a and *see* **Note 20**).
2. A second quality control could include a qPCR using the same primers that were employed before to validate the differential expression after chemopreventive treatment [7].

3.13 Quantification of the Library

The quantity will be assessed via qPCR using primers specific for the adapter regions (qPCR primer 1.1 and qPCR primer 2.1.).

1. Measure your library with a NanoDrop® spectrophotometer and dilute your library to ca. 5 ng/μL in Resuspension Buffer. Transfer 1 μL of this dilution into 500 μL of 10 mM Tris–HCl pH 8.5 with 0.1 % Tween 20.
2. Use a library with known concentration to prepare 2× serial dilutions for the standard. The standards should be in the range of 100, 50, 25, 12.5, and 6.25 pM. Dilute the DNA standard library in 200 μL 10 mM Tris–HCl pH 8.5 with 0.1 % Tween 20 (*see* **Note 21**).
3. Perform the qPCR in 20 μL reaction volume, using in each well of an optical 0.3 mL PCR plate 10 μL KAPA SYBR Fast Master Mix, 0.2 μL qPCR primer 1.1, 0.2 μL qPCR primer 2.1, 7.6 μL ultrapure water, and 2 μL of the standard or the new library. Conduct the qPCR at least in duplicate. Use the following thermal profile: 95 °C for 5 min, 40 cycles with 95 °C 3 s, 60 °C 30 s plus melting curve.

Calculate the concentration of your libraries with the following formula:

$$\frac{\text{quantity} \times \text{bp length of standard}}{\text{bp length of new library}} \times \text{dilution factor } 500 = \text{concentration (pM)}$$

3.14 Performing a Sequencing Run

The libraries have to be diluted to 10 nM and denatured with NaOH. Dilute the libraries in 10 mM Tris–HCl pH 8.5 to 10 nM (*see* **Note 22**). Add 2 μL of the 10 nM DNA library to 17 μL of 10 mM Tris–HCl pH 8.5 and denature for 5 min at RT with 1 μL 2 N NaOH. For setting up the instruments follow the manufacturer's instructions. The sequencing is divided into two steps. The first one comprises the binding of the DNA library to the flow cell and the cluster formation via bridge amplification which is the prerequisite

for the subsequent visualization of the sequencing reaction. The second step comprehends the sequencing itself.

3.15 Sequence Analysis

The sequence analysis comprises alignment and quality control of the reads, transcript assembly and quantification of the transcripts, and finally differential expression analysis. RNA-Seq is also well suited to analyze differential exon usage, gene fusions, and RNA editing. There are several commercial but also free RNA-Seq software packages available. TopHat and Cufflinks for instance are free, open-source software tools that perform the mapping, and transcript assembly and quantification, respectively. The differential expression can be analyzed via Cuffdiff [8, 9].

4 Notes

1. Take care that the cells are free of mycoplasms. The Ribominus protocol removes only ribosomal RNA and retains the whole spectrum of RNA molecules, including RNA from mycoplasms!
2. RNA is easily degraded by RNase enzymes. These enzymes are located within the cells but also on hands and labware. There are stable to heat and detergents. It is therefore essential to wear gloves and it is suggested to use RNA-zapper to decontaminate the pipettes and if necessary the work surfaces. Use RNase-free certified plasticware and ultrapure water. Use RNase-free barrier filter tips.
3. It is important to process cells immediately as soon as harvested to avoid changes in gene expression or RNA degradation. Solutions like QIAzol Lysis Reagents are phenol/guanidine based and function to lyse the cells but also contemporaneously to prevent RNA degradation due to its protein denaturing activity.
4. The solution is getting viscous.
5. The centrifugation results in the separation of an upper aqueous phase containing the RNA and an interphase and lower organic phase encompassing the DNA and proteins.
6. Do not centrifuge to avoid losing a precipitate that might have been formed.
7. It is highly recommended to remove all genomic DNA to avoid high background noise and the loss of strandedness in the RNA-sequencing (*see* Fig. 2).
8. The official protocol from Illumina recommends 0.1–1 μg RNA as starting material. Here, we describe the library preparation using the TruSeq Stranded Total RNA LT Sample Prep Kit from Illumina. But there are also stranded library prep kits from other

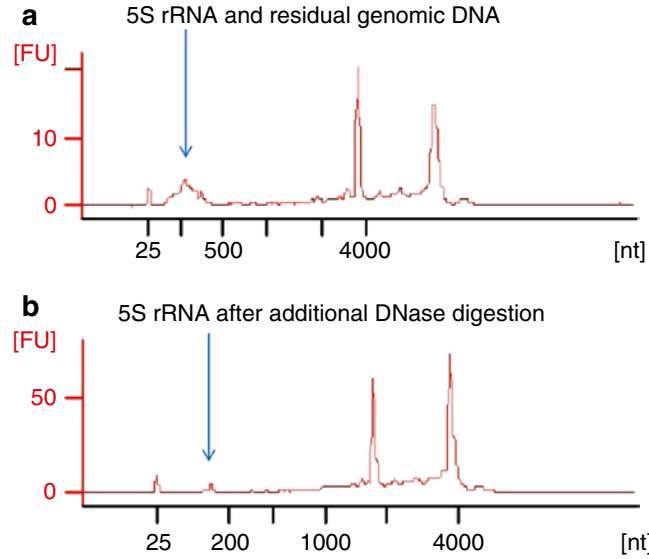

Fig. 2 Examples of human total RNAs on a Bioanalyzer electropherogram. (**a**) Total RNA without DNase treatment. (**b**) The same total RNA as in (**a**) after DNase digestion

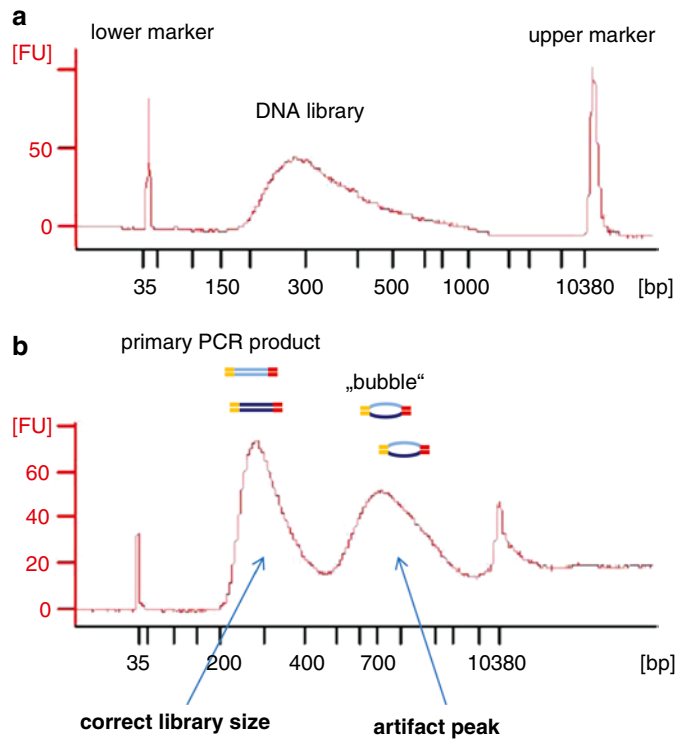

Fig. 3 Typical profiles from the Bioanalyzer representing stranded cDNA libraries. (**a**) Stranded cDNA library showing a peak in the expected size range. (**b**) Stranded cDNA library displaying a secondary artifact peak in the higher bp range

companies available like Epicentre (Illumina), Bio Scientific, Clontech, KAPA Biosystems, NuGen, Lexogenor, NEB.

9. Let all beads used in this protocol come to room temperature for 30 min before usage.
10. Later on the nucleic acids (RNA and after the reverse transcription DNA) will be purified by magnetic beads. The separation works best with 96-well PCR plates and a 96-well magnetic stand. The use of 1.5 mL microcentrifuge tubes with a corresponding magnet is possible but results sometimes in difficulties removing the supernatant from the beads. Therefore, it is recommended to use in each step directly the 96-well PCR plates, even with low-throughput samples.
11. Do not add the beads directly to the denatured RNA mix to ensure proper rRNA removal! Avoid foaming. The rRNA targeting oligos are biotinylated and can therefore be easily removed with streptavidin containing beads.
12. The time of incubation at 94 °C has to be modified if one is interested in increasing the insert size of the library or if the starting RNA material was degraded. Please consult the Appendix of the original Illumina protocol "TruSeq Stranded mRNA Sample Prep Guide."
13. Actinomycin D is toxic. It is included in the first strand buffer to inhibit DNA dependent DNA-synthesis that could occur after reverse transcription by using the newly generated cDNA strand as template again. As a consequence, the strandedness is improved and antisense artifacts due to spurious second-strand cDNA synthesis should be avoided [10].
14. To avoid multiple freeze and thaw cycles (not more than 6×) aliquot the first-strand synthesis mix into small aliquots. Immediately after use return them to −20 °C.
15. The protocol can be paused here. Store the plate at −20 °C.
16. Return the ligation mix immediately to −20 °C after use.
17. The protocol can be paused here. Store the plate at −20 °C.
18. The number of cycles might be decreased to reduce the possibility to introduce biases.
19. If using the Agilent High Sensitivity DNA Kit load around 5 ng onto a chip (the concentration can be determined by the NanoDrop® spectrophotometer).
20. If in the Bioanalyzer profile a second, bigger peak like in Fig. 3b is showing up, an over-amplification of the library occurred. The primers were used up and the different fragments hybridized with each other via the linker region forming a kind of bubble. You can still proceed to sequencing. Using the AMPure XP Beads for purification there should be no peak below 150 bp that could arise from primer dimers or adapter dimers.

21. If no DNA library with known concentration is available, one can use the "KAPA Library Quantification Kit" for the first library quantification which contains a set of standards.
22. Avoid repeated freeze and thaw of the 10 nM diluted library.

Acknowledgements

We greatly appreciate the support given by the Progetto Finalizzato Ministero della Salute "Tumori Femminili."

References

1. Ozsolak F, Milos PM (2011) RNA sequencing: advances, challenges and opportunities. Nat Rev Genet 12:87–98
2. Zhao S, Fung-Leung WP, Bittner A et al (2014) Comparison of RNA-Seq and microarray in transcriptome profiling of activated T cells. PLoS One 9:e78644
3. Zhao J, Ohsumi TK, Kung JT et al (2010) Genome-wide identification of polycomb-associated RNAs by RIP-seq. Mol Cell 40:939–953
4. Chi SW, Zang JB, Mele A et al (2009) Argonaute HITS-CLIP decodes microRNA-mRNA interaction maps. Nature 460:479–486
5. Ingolia NT, Brar GA, Rouskin S et al (2012) The ribosome profiling strategy for monitoring translation in vivo by deep sequencing of ribosome-protected mRNA fragments. Nat Protoc 7:1534–1550
6. Core LJ, Waterfall JJ, Lis JT (2008) Nascent RNA sequencing reveals widespread pausing and divergent initiation at human promoters. Science 322:1845–1848
7. Goeman F, De Nicola F, D'Onorio De Meo P et al (2014) VDR primary targets by genome-wide transcriptional profiling. J Steroid Biochem Mol Biol 143C:348–356
8. Roberts A, Pimentel H, Trapnell C et al (2011) Identification of novel transcripts in annotated genomes using RNA-Seq. Bioinformatics 27:2325–2329
9. Trapnell C, Roberts A, Goff L et al (2012) Differential gene and transcript expression analysis of RNA-seq experiments with TopHat and Cufflinks. Nat Protoc 7:562–578
10. Perocchi F, Xu Z, Clauder-Munster S et al (2007) Antisense artifacts in transcriptome microarray experiments are resolved by actinomycin D. Nucleic Acids Res 35:e128

Chapter 5

Detection of Circulating Tumor DNA in the Blood of Cancer Patients: An Important Tool in Cancer Chemoprevention

Peter Ulz, Martina Auer, and Ellen Heitzer

Abstract

Liquid biopsies represent novel promising tools to determine the impact of clonal heterogeneity on clinical outcomes with the potential to identify novel therapeutic targets in cancer patients. We developed a low-coverage whole-genome sequencing approach in order to noninvasively establish copy number aberrations in plasma DNA from metastasized cancer patients. Using plasma-Seq we were able to monitor genetic evolution including the acquirement of novel copy number changes, such as focal amplifications and chromosomal polysomies. The big advantage of our approach is that it can be performed on a benchtop sequencer, speed, and cost-effectiveness. Therefore, plasma-Seq represents an easy, fast, and affordable tool to provide the urgently needed genetic follow-up data. Here we describe our method including plasma DNA extraction, library preparation, and bioinformatic analyses.

Key words Cell-free DNA, Circulating tumor DNA, Plasma DNA, Copy number aberrations, Low-coverage whole-genome sequencing, Plasma-Seq

1 Introduction

The analysis of cell-free circulating tumor DNA from plasma, often referred to as "liquid biopsy" has recently gained considerable interest. Cell-free DNA is released from tumor and normal cells by different mechanisms including necrosis and apoptosis making it a challenging analyte owing to its high degree of fragmentation [1, 2]. Nevertheless, ctDNA is released from multiple tumor locations and therefore it reflects the entire tumor genome. Many recent studies have shown the feasibility of ctDNA analysis using next-generation sequencing based methods, thereby allowing the monitoring of tumor genomes by noninvasive means [3–14]. As the trend of optimal therapy management is towards decisions based on the current status of the entire tumor genome, the use of ctDNA as a liquid biopsy may help to obtain the urgently needed genetic follow-up data.

Sabrina Strano (ed.), *Cancer Chemoprevention: Methods and Protocols*, Methods in Molecular Biology, vol. 1379,
DOI 10.1007/978-1-4939-3191-0_5,

Generally, there are two approaches for the analysis of plasma DNA, (1) targeted approaches, which include the analysis of known genetic changes from the primary tumor or frequently occurring driver mutations, and (2) untargeted approaches like whole-genome sequencing, exome sequencing, or targeted resequencing of large gene panels. The main advantage of untargeted approaches is that they do not rely on recurrent genetic changes. Therefore, these methods are applicable to all patients including those who were diagnosed with synchronous metastases, where only limited tumor material is available. Furthermore, these methods can identify novel changes that were not present in the primary tumor, which makes them useful for monitoring tumor evolution and the identification of resistance mechanisms and newly occurring therapy targets. Given that chromosomal copy number changes occur frequently in human cancer, we developed an approach allowing the mapping of tumor-specific copy number aberrations from plasma DNA employing next generation sequencing. Therefore, we use shallow sequencing depth with a benchtop high-throughput instrument (Illumina MiSeq; Illumina, Inc., San Diego, CA, USA) to examine the tumor genomes of patients with metastasized cancer at reasonable costs. This so-called plasma-Seq brings the power of whole-genome analysis to a more routine clinical benchtop setting [8, 11]. Using plasma-Seq we were able to monitor genetic evolution including the acquirement of novel copy number changes, such as focal amplifications and chromosomal polysomies in colorectal cancer patients as a response to anti-EGFR therapy [13]. Here we describe our methods for the noninvasive establishment of tumor-specific copy number changes beginning with the blood draw, plasma DNA extraction, library preparation, and sequencing to the bioinformatic analysis. The analysis workflow is displayed in Fig. 1.

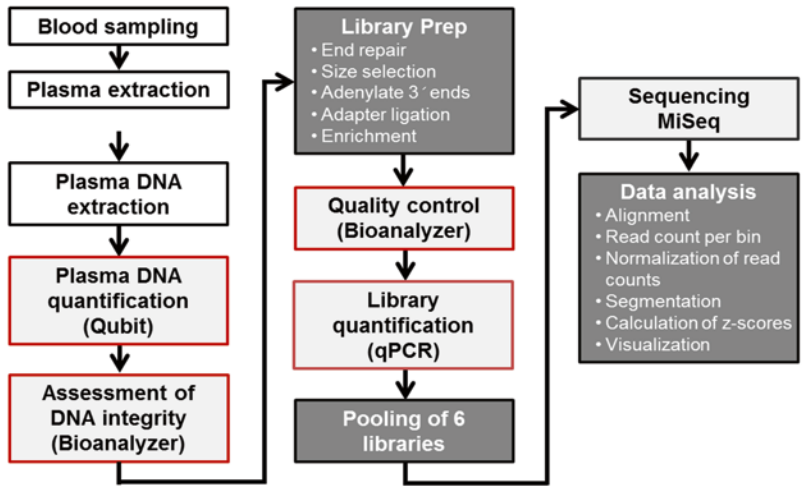

Fig. 1 Analysis workflow of plasma-Seq

2 Materials

2.1 Blood Sampling

1. 1 EDTA Vacutainer tube (9 ml) for plasma DNA isolation (BD Biosciences).
2. Syringe with 0.225 ml of 10 % neutral-buffered solution containing formaldehyde (NBF) (Sigma-Aldrich).

2.2 Extraction of Free Circulating DNA from Plasma

1. QIAamp DNA Mini Kit (Qiagen).
2. QIAGEN Proteinase K stock solution (store at room temperature, 15–25 °C).
3. Buffer AL (store at room temperature, 15–25 °C): Mix Buffer AL thoroughly by shaking before use. Buffer AL is stable for 1 year when stored at room temperature. If a precipitate has formed in Buffer AL, dissolve by incubating at 56 °C.
4. Buffer AW1* (store at room temperature, 15–25 °C): Buffer AW1 is supplied as a concentrate. Before using for the first time, add the appropriate amount of ethanol (96–100 %) to Buffer AW2 concentrate as indicated on the bottle. Buffer AW1 is stable for 1 year when stored closed at room temperature.
5. Buffer AW2* (store at room temperature, 15–25 °C): Buffer AW2 is supplied as a concentrate. Before using for the first time, add the appropriate amount of ethanol (96–100 %) to Buffer AW2 concentrate as indicated on the bottle. Buffer AW2 is stable for 1 year when stored closed at room temperature.
6. Nuclease-free water.
7. Water bath or heating block at 56 °C.
8. Speed Vac centrifuge (Eppendorf).
9. 2100 Bioanalyzer (Agilent).
10. Agilent DNA High Sensitivity Kit.

2.3 Quantification of Free Circulating DNA from Plasma with Qubit

1. Qubit® 3.0 Fluorometer (Life Technologies).
2. Qubit® dsDNA HS Assay Kit (Life Technologies).
3. Thin-wall, clear 0.5 ml PCR tubes.

2.4 Library Preparation

TruSeq® Nano DNA Sample Preparation kit (Illumina).

2.4.1 End Repair

End Repair Mix 2 (ERP2).

Resuspension buffer (RSB).

Sample Purification Beads (AMPure XP beads) (SPB).

1.5 ml microcentrifuge tubes.
0.2 ml PCR tubes.
Freshly prepared 80 % ethanol (EtOH).

2.4.2 A-Tailing

A-Tailing Mix.
Resuspension buffer (RSB).
RNase/DNase-free strip tubes.

2.4.3 Adapter Ligation

DNA Adapter Indices A or B.
Ligation mix 2 (LIG2).
Resuspension buffer (RSB) 1.
Sample Purification Beads (AMPure XP beads) (SPB).
Stop ligation buffer.
0.2 ml PCR tubes or stripes.
Freshly prepared 80 % ethanol (EtOH), 800 μl per sample.

2.4.4 Enrichment

Enhanced PCR mix (EPM).
PCR primer cocktail (PPC).
Sample Purification Beads (AMPure XP beads) (SPB).
RSB.
PCR tubes.

2.4.5 Validation

Bioanalyzer Agilent.
Agilent DNA 7500 Kit.

2.4.6 Quantification

Fast SYBR® Green Master Mix (Life Technology).
LibQuant_F: 5′ AATGATACGGCGACCACCGAGAT 3′.
LibQuant_R: 5′ CAAGCAGAAGACGGCATACGA 3′.
Real-time PCR instrument.

2.4.7 Pooling of Libraries and Sequencing

MiSeq (Illumina).
MiSeq Reagent Kit v3 (150 cycles).
HT1 (hybridization buffer), thawed and pre-chilled.
1.0 N NaOH, molecular biology grade.
Tris-Cl 10 mM, pH 8.5 with 0.1 % Tween 20 (General lab supplier).

2.4.8 Bioinformatics

Basic Linux system.
Python scripts from Baslan et al. [15].

bwa (http://bio-bwa.sourceforge.net/) [16].

samtools (http://samtools.sourceforge.net/) [17].

R (http://www.r-project.org/) [18].

R-package CGHweb (http://compbio.med.harvard.edu/CGHweb/Rpackage.html) [19] including the R-packages needed by CGHweb: waveslim, quantreg, snapCGH, cghFLasso, FASeg, GLAD, GDD, gplots.

3 Methods

3.1 Blood Sampling

1. After blood sampling 0.225 ml NBF should be immediately added to the blood in the EDTA tube to stabilize cell membranes and to impede additional cell lysis that might further dilute free circulating DNA with "normal DNA" from these cells (*see* **Notes 1** and **2**).
2. Samples should be gently inverted, stored at RT, and further processed within 2 h. As soon as the samples arrive at the laboratory, plasma isolation should be started immediately.

3.2 Plasma Extraction from Whole Blood

1. Fill the whole blood into a 15 ml tube.
2. Centrifuge tubes at 200 × *g* for 10 min.
3. Perform a subsequent centrifugation step at 1600 × *g* for 10 min (*see* **Note 4**).
4. Collect the supernatant (plasma without any cells) and transfer it to a new 15 ml tube and spin at 1600 × *g* for 10 min (*see* **Note 4**).
5. Carefully transfer plasma to a new sterile 1.5 ml Eppendorf by aliquoting to 1 ml and store at –80 °C for future use (*see* **Note 3**).

3.3 Extraction of Free Circulating DNA from Plasma

Plasma DNA extraction is performed using QIAamp DNA Mini Kit, Qiagen. The protocol is slightly modified from "QIAamp® DNA Mini Kit and QIAamp DNA Blood Mini Kit Handbook."

1. Isolate plasma DNA either from 1 ml freshly prepared plasma or from 1 ml of stored plasma. In the latter case thaw plasma on room temperature and proceed immediately after thawing.
2. For the extraction of 1 ml plasma pipet 50 µl QIAGEN Proteinase K into the bottom of two 2 ml microcentrifuge tubes (*see* **Note 5**).
3. Add 500 µl plasma to each of the microcentrifuge tubes.
4. Add 500 µl Buffer AL to the samples. Mix by pulse-vortexing for 15 s.
5. Incubate at 56 °C for 10 min. (DNA yield reaches a maximum after lysis for 10 min at 56 °C. Longer incubation times have no effect on yield or quality of the purified DNA.)

6. Briefly centrifuge the microcentrifuge tube to remove drops from the inside of the lid.
7. Add 500 µl ethanol (96–100 %) to the samples, and mix again by pulse-vortexing for 15 s. After mixing, briefly centrifuge the tube to remove drops from the inside of the lid.
8. Carefully apply 700 µl of the mixture from **step 6** to the QIAamp Mini spin column (in a 2 ml collection tube) without wetting the rim. Close the cap, and centrifuge at 6000 × *g* (8000 rpm) for 1 min. Remove flow-through, apply the remaining volume of the mixture to the column, and repeat centrifugation.
9. Repeat **step 7** until the mixture from both tubes from **step 6** has been transferred to the spin column.
10. Place the QIAamp Mini spin column in a clean 2 ml collection tube, and discard the tube containing the filtrate (*see* **Note 6**).
11. Carefully open the QIAamp Mini spin column and add 500 µl Buffer AW1 without wetting the rim. Close the cap and centrifuge at 6000 × *g* (8000 rpm) for 1 min. Place the QIAamp Mini spin column in a clean 2 ml collection tube, and discard the collection tube containing the filtrate.
12. Open the QIAamp Mini spin column and add 500 µl Buffer AW2 without wetting the rim. Close the cap and centrifuge at full speed (20,000 × *g*; 14,000 rpm) for 3 min (*see* **Note 7**).
13. Place the QIAamp Spin Column in a new 2 ml collection tube (not provided) and discard the collection tube with the filtrate. Centrifuge at full speed for 1 min.
14. Place the QIAamp Mini spin column in a clean 1.5 ml microcentrifuge tube and discard the collection tube containing the filtrate. Carefully open the QIAamp Mini spin column and add 60–90 µl of nuclease-free water. Incubate at room temperature (15–25 °C) for 5 min and then centrifuge at 6000 × *g* (8000 rpm) for 1 min.
15. Proceed with quantification or store samples at –20 °C.

3.4 Quantification of Plasma DNA Using Qubit dsDNA HS Assay Kit

1. Set up the number of 0.5 ml tubes you will need for two standards and the number of samples that are measured, and label the tubes.
2. Prepare the Qubit™ working solution by diluting the Qubit™ dsDNA HS reagent 1:200 in Qubit™ dsDNA HS buffer. Use a clean plastic tube (and no glass container) each time you make the working solution (*see* **Note 8**).
3. *Note*: The final volume for measuring is 200 µl. Each of the two standard tubes will require 190 µl of working solution, and each sample tube will require 195 µl. Prepare sufficient working solution to accommodate all standards and samples.

4. Preparing of the standards: Pipet 190 µl of working solution into each of the tubes used for standards and add 10 µl of each Qubit™ standard to the appropriate tube and mix by vortexing 2–3 s, being careful not to create bubbles.
5. Preparing the samples: Load 5 µl of your samples and add 195 ml of working solution to the tube. Mix by vortexing for 2–3 s (*see* **Note 9**).
6. Incubate tubes at room temperature for 2 min.
7. On the Home Screen of the Qubit® 2.0 Fluorometer, press DNA, and then select dsDNA High Sensitivity as the assay type.
8. Press "Read new standard" to run a new calibration and follow the instructions on the screen. Insert the tube containing Standard #1, close the lid, and press "Read." Then remove Standard #1 and insert the tube containing Standard #2, close the lid, and press "Read." Remove Standard #2.
9. Insert a sample tube into the Qubit 2.0 Fluorometer, close the lid, and press "Read."
10. Upon completion of the sample measurement, press "Calculate Stock Conc." The Dilution Calculator Screen containing the volume roller wheel is displayed. Select the volume of your original sample (5 µl) that you have added to the assay tube. When you stop scrolling, the Qubit® 2.0 Fluorometer calculates the original sample concentration based on the measured assay concentration.
11. Select the unit for your original sample concentration by touching the desired unit in the unit selection pop-up window. To close the unit selection pop-up window, touch anywhere on the screen outside.
12. Insert the next sample, and "Read Next Sample."
13. Repeat sample readings until all samples have been read.

3.5 Assessment of DNA Integrity on an Agilent Bioanalyzer

For comparable results the amount of cfDNA should be normalized before loading the Bioanalyzer chip. 800 pg seems to be the optimal amount for analyzing the DNA integrity of cfDNA since healthy controls show only one peak at 160 bp with this amount whereas tumor patients often show an additional peak at 320 bp. However, for samples with very low concentration the Bioanalyzer may be omitted. Examples for Bioanalyzer profiles of a monophasic and biphasic size distribution are shown in Fig. 2.

1. Calculate the volume of your sample that contains 1600 pg.
2. Concentrate the volume to 2 µl in a SpeedVac Eppendorf centrifuge (Program V-AQ, room temperature) and load 1 µl corresponding to a High Sensitivity Bioanalyzer chip.
3. Analyze the chip on a 2100 Agilent Bioanalyzer.

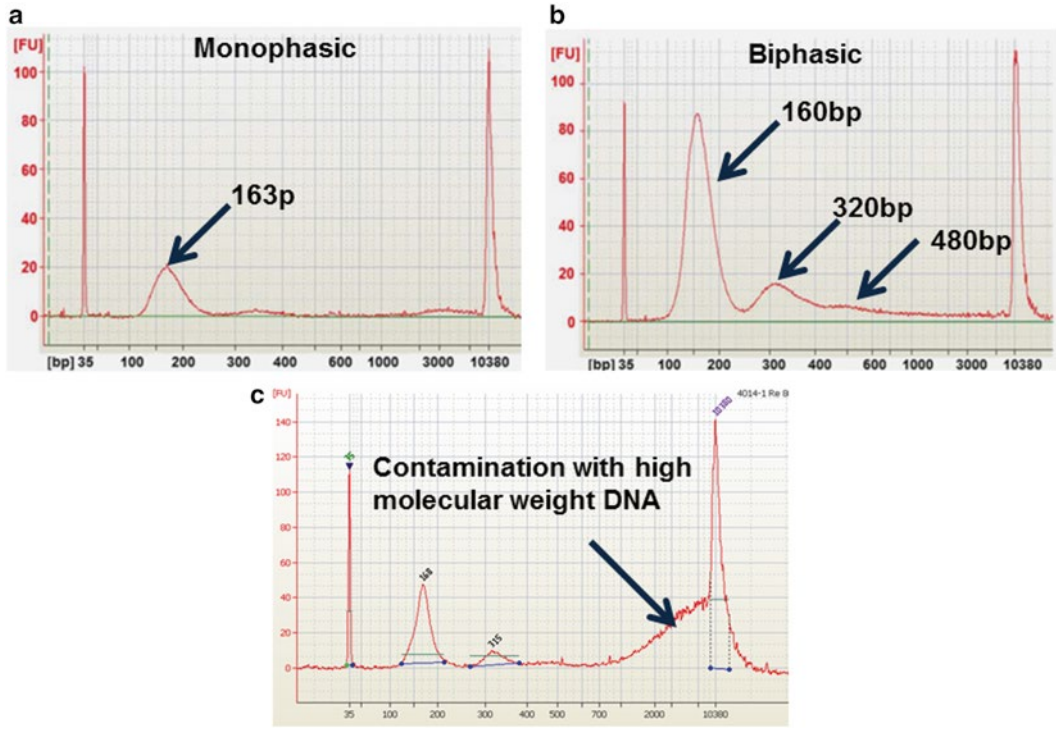

Fig. 2 Examples of size distribution of plasma DNA. (**a**) An enrichment of fragments in the range of 160 bp can be observed representing a monophasic size distribution. (**b**) Biphasic size distribution with an additional peak in the range of 320 bp. (**c**) Fragments larger than 100 bp indicate contamination with normal DNA from blood cells

4. You should observe at least one peak with a maximum of approximately 160 bp (monophasic size distribution). In some samples further peaks corresponding to multiples of 160 bp might be observed (biphasic size distribution) (*see* Fig. 1 and **Note 10**).

3.6 Library Preparation

Library preparation is performed using the TruSeq Nano DNA Sample Preparation kit. However, our protocol includes several changes (*see* **Note 11**).

3.6.1 End Repair

1. Use 5–10 ng of DNA as input amount; adjust the volume to 60 µl with RSB in a 200 µl PCR-tube.
2. Centrifuge the thawed end repair mix 2 tube to 600 × *g* for 5 s.
3. Add 40 µl of end repair mix 2 to the tube containing the fragmented DNA and mix by gently pipetting the entire volume up and down ten times.
4. Incubate the tube at 30 °C for 30 min in a thermal cycler. Choose with preheat lid option and set to 100 °C. Hold at 4 °C.
5. Remove the tube at 4 °C.

6. Dilute AMPure Beads (Sample Purification Beads) (*see* **Note 12**). Determine the amount of Sample Purification Beads and PCR-grade water needed to combine to prepare a diluted bead mixture: Sample Purification Beads: # of samples × 160 µl × 0.85 = µl Sample Purification Beads. PCR-grade water: # of samples × 160 µl × 0.15 = µl PCR-grade water.
7. Add 160 µl of the diluted bead mixture to a 1.5 ml Eppendorf tube and add 100 µl of End Repair Mix. Gently pipette the entire volume up and down ten times to mix thoroughly.
8. Incubate at room temperature for 10 min.
9. Place the tube on a magnetic stand at room temperature until the liquid appears clear (approximately 5–10 min).
10. Remove and discard the supernatant.
11. Leave the tube on the magnetic stand and add 200 µl of freshly prepared 80 % EtOH to each tube without disturbing the beads.
12. Incubate at room temperature for 30 s, then remove, and discard all of the supernatant from each tube. Take care not to disturb the beads.
13. Repeat **steps 8** and **9** once for a total of two 80 % EtOH washes.
14. Leave the tube on the magnetic stand and dry it at room temperature for 15 min to dry.
15. Remove the tube from the magnetic stand and resuspend the dried pellet with 17.5 µl RSB.
16. Incubate tube at room temperature for 2 min.
17. Place the tube back on the magnetic stand at room temperature for 5 min or until the liquid appears clear.
18. Transfer 15 µl of the clear supernatant from each tube to a new 0.2 ml PCR tube.

3.6.2 Adenylate 3′ Ends

1. Thaw the A-Tailing Mix and centrifuge the tube to 600 × *g* for 5 s.
2. Add 12.5 µl of thawed A-Tailing Mix to each tube containing the samples from the end repair and mix gently by pipetting the entire volume up and down ten times.
3. Place the tube on a pre-programmed thermal cycler and run the program as follows: Choose the preheat lid option and set to 100 °C, 37 °C for 30 min, 70 °C for 5 min, 4 °C for 5 min, and hold at 4 °C.
4. When the thermal cycler temperature has been at 4 °C for 5 min, remove the tube from the thermal cycler and briefly spin down the liquid. Proceed immediately to adapter ligation.

3.6.3 Adapter Ligation

1. Thaw the adapter tubes and centrifuge the thawed tubes to 600 × *g* for 5 s.
2. Centrifuge the stop ligation buffer tube to 600 × *g* for 5 s.
3. Add 2.5 μl of RSB to tube with the adenlyated samples.
4. Add 2.5 μl of ligation mix 2 to each tube.
5. Add 2.5 μl of the appropriate thawed DNA Adapter Index to tube and mix by gently pipetting the entire volume up and down ten times.
6. Briefly spin down the tube on a pre-programmed thermal cycler and run the program as follows: Choose the thermal cycler pre-heat lid option and set to 100 °C, 30 °C for 10 min, Hold at 4 °C.
7. Remove the tube from the thermal cycler and add 5 μl of stop ligation buffer. Mix gently pipetting the entire volume up and down ten times.
8. Vortex the Sample Purification Beads for at least 1 min or until they are well dispersed, then add 42.5 μl of the Sample Purification Beads to tube mix by gently pipetting the entire volume up and down ten times.
9. Incubate at room temperature for 5 min.
10. Place the tube on the magnetic stand at room temperature for 5 min or until the liquid appears clear.
11. Remove and discard 80 μl of the supernatant from tube and take care not to disturb the pellet.
12. With the tube remaining on the magnetic stand, add 200 μl of freshly prepared 80 % EtOH to each well without disturbing the beads.
13. Incubate at room temperature for 30 s, then remove, and discard all of the supernatant. Take care not to disturb the beads.
14. Repeat **steps 12** and **13** once for a total of two 80 % EtOH washes.
15. With the tube remaining on the magnetic stand, let the samples air dry at room temperature for 5 min. Remove and discard any remaining EtOH with a 10 μl pipette.
16. Add 52.5 μl of RSB to the tube and remove tube from the magnetic stand.
17. Resuspend the beads by repeatedly dispensing the RSB over the bead pellet until it is immersed in the solution, and then gently pipette the entire volume up and down ten times to mix thoroughly.
18. Incubate at room temperature for 2 min.
19. Place the tube back on the magnetic stand at room temperature for 5 min or until the liquid appears clear.

20. Transfer 50 μl of the clear supernatant from each tube to a new 1.5 ml Eppendorf tube. Take care not to disturb the beads.
21. Vortex the Sample Purification Beads until they are well dispersed.
22. Add 50 μl of mixed Sample Purification Beads to each tube for a second clean up, mix and incubate at room temperature for 5 min.
23. Place the tube on the magnetic stand at room temperature for 5 min or until the liquid appears clear.
24. Remove and discard 95 μl of the supernatant. Take care not to disturb the beads.
25. Add 200 μl of freshly prepared 80 % EtOH to each well and incubate at room temperature for 30 s. Take care not to disturb the beads.
26. Remove and discard all of the supernatant.
27. Repeat **steps 24** and **25** once for a total of two 80 % EtOH washes.
28. With the tube remaining on the magnetic stand, let the samples air-dry at room temperature for 5 min.
29. Remove and discard any remaining EtOH with a 10 μl pipette.
30. Add 27.5 μl of RSB to each tube and then remove tubes from the magnetic stand.
31. Resuspend the beads by repeatedly dispensing the RSB over the bead pellet until it is immersed in the solution, and then gently pipette the entire volume up and down ten times to mix thoroughly.
32. Incubate at room temperature for 2 min.
33. Place the tube on the magnetic stand at room temperature for 5 min or until the liquid appears clear.
34. Transfer 25 μl of the clear supernatant to a new 0.2 ml PCR tube.

3.6.4 Enrich DNA Fragments

1. Add 5 μl thawed PCR primer cocktail to each tube from the adapter ligation.
2. Add 20 μl thawed enhanced PCR Mix to each well of the PCR plate and mix gently by pipetting the entire volume up and down ten times to mix.
3. Close the tubes and place them into a pre-programmed thermal cycler.
4. Run the following program:
   (a) Choose the preheat lid option and set to 100 °C.
   (b) 95 °C for 3 min.

(c) 25 cycles of:

- 98 °C for 20 s.
- 60 °C for 15 s.
- 72 °C for 30 s.

(d) 72 °C for 5 min.

(e) Hold at 4 °C.

5. Remove tubes from thermal cycler and spin down the liquid and transfer to a 1.5 ml tube.
6. Vortex the Sample Purification Beads until they are well dispersed.
7. Add 50 μl mixed Sample Purification Beads to each tube 5 containing 50 μl of the PCR amplified library and mix well mix gently by pipetting the entire volume up and down ten times to mix.
8. Incubate the PCR plate at room temperature for 5 min.
9. Place the tubes on the magnetic stand at room temperature for 5 min or until the liquid is clear.
10. Remove and discard 95 μl of the supernatant from each tube.
11. With the PCR plate on the magnetic stand, add 200 μl freshly prepared 80 % EtOH to each tube without disturbing the beads.
12. Incubate at room temperature for 30 s, and then remove and discard all of the supernatant.
13. Repeat **steps 8** and **9** one time for a total of two 80 % EtOH washes.
14. With the tube on the magnetic stand, let the samples air-dry at room temperature for 5 min. Remove and discard any remaining EtOH from each tube with a 10 μl pipette.
15. With the tube on the magnetic stand, add 32.5 μl RSB to each well of the PCR plate.
16. Remove tubes from the magnetic stand.
17. Resuspend the beads by repeatedly dispensing the RSB over the bead pellet until it is immersed in the solution. Mix gently by pipetting the entire volume up and down ten times to mix.
18. Incubate at room temperature for 2 min.
19. Place the tube on the magnetic stand at room temperature for 5 min or until the liquid is clear.
20. Transfer 30 μl of the clear supernatant from to a new tube.
21. Proceed to library validation or store the library at –15 to –25 °C.

3.6.5 Validate Library

1. Run 1 µl of the library on a Bioanalyzer for qualitative purposes only. Proceed to library validation or store the library at −15 to −25 °C. Examples for successful library preparations are shown in Fig. 3.

3.6.6 Quantification of Libraries

To achieve the highest data quality on the Illumina MiSeq accurate quantification is of utmost interest. Although you can use fluorometric quantification methods that use dsDNA binding, qPCR is the most accurate methods in order to achieve optimized cluster densities across every lane of a flow cell. As a standard we use a library that achieved optimal cluster density in a MiSeq run. Alternatively you can use the PhiX control library or commercially available kits.

1. Prepare a 2× serial dilution of your standard (PhiX or exciting library from a previous run) starting from 50 to 1.56 pM.
2. Based on the Bioanalyzer result, prepare a 10 nM working dilution of your library.
3. For qPCR quantification dilute the library 1:500, 1:1000, and 1:2000.
4. Prepare a 96-well reaction plate and configure the plate for three replicates of each of the standard and library dilutions and calculate the number of reaction needed for the qPCR. A possible plate configuration for quantification 6 libraries is displayed in Fig. 4.
5. Prepare a master mix according to the number of samples of 10 µl of Fast SYBR® Green Master Mix (2×) and 0.5 µl of the 10 µM primers LibQuant_F and LibQuant_R and 7 µl PCR-grade water.
6. Transfer 18 µl of the master mix to each well of the 96-well plate.
7. Add 2 µl of your samples to the wells.
8. In your real-time software program choose “Absolute Quantification.”
9. Define the number and ratios of you standard dilutions and assign them to the wells containing the standard samples. Then define the targets (libraries to be quantified) and assign them to the wells in the reaction plate.
10. Run the reaction plate on a qPCR instrument using the following program:
    (a) 95 °C for 20 s.
    (b) 40 cycles of:
        - Denature 95 °C for 3 s.
        - Anneal/extend 60 °C for 30 s.

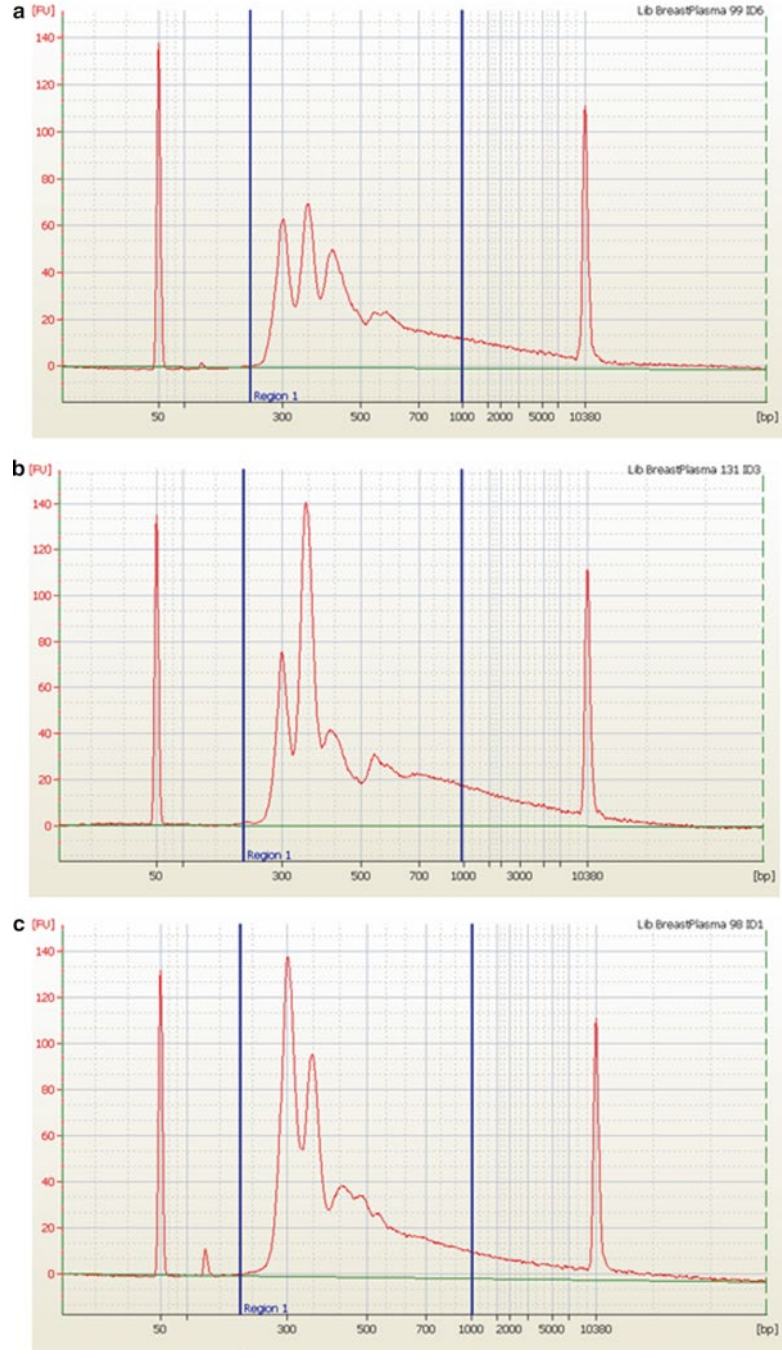

Fig. 3 Examples of library preparations form plasma DNA. Due to its fragmentation plasma DNA libraries do not show a normal size distribution of DNA fragments as it would be expected for shotgun libraries from high-molecular-weight DNA after fragmentation

	1	2	3	4	5	6	7	8	9	10	11	12
A	S Control 50 pM	S contol 25 pM	S contol 12.5 pM	S contol 6.25 pM	S contol 3.13 pM	S contol 1.6 pM	U Lib1 1:500	U Lib1 1:1000	U Lib1 1:2000	U Lib2 1:500	U Lib2 1:1000	U Lib2 1:2000
B	S Control 50 pM	S contol 25 pM	S contol 12.5 pM	S contol 6.25 pM	S contol 3.13 pM	S contol 1.6 pM	U Lib1 1:500	U Lib1 1:1000	U Lib1 1:2000	U Lib2 1:500	U Lib2 1:1000	U Lib2 1:2000
C	S Control 50 pM	S contol 25 pM	S contol 12.5 pM	S contol 6.25 pM	S contol 3.13 pM	S contol 1.6 pM	U Lib1 1:500	U Lib1 1:1000	U Lib1 1:2000	U Lib2 1:500	U Lib2 1:1000	U Lib2 1:2000
D	U Lib3 1:500	U Lib3 1:1000	U Lib3 1:2000	U Lib4 1:500	U Lib4 1:1000	U Lib4 1:2000	U Lib5 1:500	U Lib5 1:1000	U Lib5 1:2000	U Lib6 1:500	U Lib6 1:1000	U Lib6 1:2000
E	U Lib3 1:500	U Lib3 1:1000	U Lib3 1:2000	U Lib4 1:500	U Lib4 1:1000	U Lib4 1:2000	U Lib5 1:500	U Lib5 1:1000	U Lib5 1:2000	U Lib6 1:500	U Lib6 1:1000	U Lib6 1:2000
F	U Lib3 1:500	U Lib3 1:1000	U Lib3 1:2000	U Lib4 1:500	U Lib4 1:1000	U Lib4 1:2000	U Lib5 1:500	U Lib5 1:1000	U Lib5 1:2000	U Lib6 1:500	U Lib6 1:1000	U Lib6 1:2000
G	NTC	NTC	NTC									
H	NTC	NTC	NTC									

Fig. 4 Example of a plate configuration for quantification of plasma DNA libraries using qPCR. A total of six libraries can be concomitantly analyzed in one plate. *S* standard, *U* unknown samples

11. When the run is complete, check the NTC wells for any amplification. There should be no amplification.
12. Check for any outliers in you replicates are >0.5 Ct and omit these from you analysis.
13. Check whether all library dilutions are within the range of the standard curve. In case a dilution is out of range omit these samples from the analysis.
14. Check the threshold and adjust it in case it is not set appropriately.
15. Export the analysis results and calculate a mean concentration of your samples by taking the original dilution into account (1:500, 1:1000, 1.2000).

3.7 Pooling and Preparing Libraries for the Sequencing

1. Dilute the libraries according to the concentrations from the qPCR 4 nM.
2. Pool a total of six libraries by transferring 5 µl of each library into a 1.5 ml tube (*see* **Note 13**).
3. Prepare 1 ml of 0.2 N NaOH (800 µl laboratory-grade water + 200 µl 1.0 N NaOH) (*see* **Note 14**).
4. For denaturation transfer 5 µl of your library pool to a fresh 1.5 ml tube and add 5 µl freshly diluted 0.2 N NaOH.
5. Vortex briefly to mix spin down the sample solution.
6. Incubate for 5 min at room temperature.

7. Add 990 µl of the pre-chilled HT1 buffer to the tube. Your library is now concentrated to 20 pM in 1 mM NaOH.
8. Place the denatured library pool on ice until you are ready to proceed to final dilution.
9. The final dilution should be adjusted to our sequencing instrument. Based on our experience a final dilution of 8–12 pM results in optimal cluster density for a MiSeq Reagent Kit v3 (150 cycle V3) run (*see* **Note 15**).

3.8 Bioinformatics

For the analysis of Plasma-Seq, a depth-of-coverage algorithm is most appropriate. That is, we count the amount of reads in previously specified genomic regions (often called bins, or windows). These raw read counts must be normalized since several factors (such as GC-count) may introduce a bias in the results. Our analysis algorithm is based on the procedure described by Baslan et al. [15], who used this approach to detect copy-numbers from single-nucleus sequencing experiments [20].

Firstly, the pseudo-autosomal region of the chromosome Y is masked, since it is impossible to differentiate between the copy on the chromosome Y and the corresponding part on chromosome X [15]. We divide the genome into 50,000 regions of an average length of about 56 kbp, with each region containing the same amount of mappable positions. This was done by generating synthetic 150 bp reads from the hg19 genome for each position and mapping them back to check whether a perfect match coming from that position would yield an alignment [15]. Hence, some genomic windows (e.g., regions containing repeats, segmental duplications) are larger than average.

We then map the resulting reads to the hg19 genome and count reads within each of the 50,000 genomic regions. Since the amount of reads within each genomic region depends not only on the copy number but on the GC content of that region, we correct for GC content of each genomic region using LOWESS-smoothing. Moreover, GC-corrected read counts are corrected using the mean read counts of non-tumor controls (raw sequencing data of a set of 20 controls without any sign of malignant disease are available at EBI-EGA https://www.ebi.ac.uk/ega/home under the accession number EGAS00001000451 [11]).

In a further step, regions having similar read counts are grouped using existing segmentation algorithms and means of each copy number segments are calculated. To reliably identify segments with aberrant copy numbers and to increase sensitivity we calculate z-scores for each segment by subtracting the mean read counts of healthy controls and dividing by the standard-deviation (SD). We define a significant change in the regional representation of plasma DNA as > 3 SDs from the mean representation of the healthy controls for the bins in the corresponding segment.

3.8.1 Setup

You can skip the preparation step if you already have files containing the bin boundaries and the corresponding GC contents. Bin boundaries for synthetic 150 bp reads using BWA for alignment are available on request from the authors.

1. Download the hg19 reference genome (e.g.:http://hgdownload.cse.ucsc.edu/goldenPath/hg19/bigZips/chromFa.tar.gz).
2. Mask the pseudo-autosomal region of the chromosome Y using the script provided in [15]: (hg19.chrY.psr.py).
3. Combine the FASTA files to a single multi-entry FASTA files. Make sure to use the PAR-masked chromosome Y file.

```
cat chr1.fa chr2.fa chr3.fa chr4.fa chr5.fa chr6.fa
   chr7.fa chr8.fa chr9.fa chr10.fa chr11.fa chr12.
   fa chr13.fa chr14.fa chr15.fa chr16.fa chr17.fa
   chr18.fa  chr19.fa  chr20.fa  chr21.fa  chr22.fa
   chrX.fa chrY.fa > hg19.fa
```

4. Create an index for bwa using the PAR masked multi-entry FASTA file.

```
bwa index -p hg19_par_masked hg19.fa
```

5. Generate synthetic 150 bp reads for each position on the hg19 genome using the script provided in [15]: (hg19.generate.reads.k50.py; modify to output 150 bp reads). This script generates FASTQ files, each containing 150 million reads.
6. Align the synthetic 150 bp reads back to the PAR-masked hg19 genome.

```
bwa aln -f <SAI File> hg19_par_masked <FASTQ File>

bwa samse -f <SAM File> hg19_par_masked <SAI File>
   <FASTQ File>
```

7. Create a list of chromosome sizes using the script provided in [15] (hg19.chrom.sizes.py).
8. Create the "goodzones" file: i.e., create a list of contiguous blocks, of which every position can be aligned back to the original position with bwa (hg19.bowtie.goodzones.k50.py).
9. Count the number of mappable positions on each chromosome using the script provided in [15]*hg19.chrom.mappable.bowtie.k50.py*.
10. Compute the bin boundaries for 50,000 genomic bins (hg19.bin.boundaries.50k.py).
11. Sort the bin boundaries and compute GC-content for each bin (hg19.varbin.gc.content.50k.bowtie.k50.py).

3.8.2 Analysis

1. Align FASTQ files to PAR-masked hg19 genome using bwa. Replace the text within the parentheses with the appropriate file names.

```
bwa aln -f <SAI File> hg19_par_masked <FASTQ File>
```

```
bwa samse -f <SAM File> hg19_par_masked <SAI File>
   <FASTQ File>
```

2. Convert Text-based SAM file to BAM file.

```
samtools view -S -b -o <BAM File> <SAM File>
```

3. Remove PCR duplicates using samtools rmdup and convert back to SAM.

```
samtools rmdup -s <BAM File> <RMDUP BAM File>

samtools sort <RMDUP BAM File> <Sorted RMDUP BAM
   File>

samtools view <Sorted RMDUP BAM File> > <Sorted RMDUP
   SAM File>
```

4. Count reads in bins (varbin.50k.sam.py from [15]). The output of this script is a text-based file containing bin positions, raw read counts per bin and read counts normalized by the median read count (to account for varying sequencing yields per sample).

```
varbin.50k.sam.py <Sorted RMDUP SAM File> <Bincounts
   File> <Statistics File>
```

5. Postprocessing and normalization in R (modified from SRR054616.cbs.r script from Baslan [15]), Load R

```
R
```

6. Load library CGH Web.
   library("CGHweb")
7. Define lowess function to correct for GC-content.

```
lowess.gc <- function(jtkx, jtky) {

     jtklow <- lowess(jtkx, log(jtky), f=0.05)

     jtkz <- approx(jtklow$x, jtklow$y, jtkx)

     return(exp(log(jtky) - jtkz$y))

}
```

8. Define postprocess function.

```
postprocess <- function(indir, outdir, bad.bins,
   varbin.gc, varbin.data, sample.name, alt.sample.
   name, alpha, nperm, undo.SD, min.width) {

gc <- read.table(varbin.gc, header=T)

bad <- read.table(bad.bins, header=F)

chrom.numeric <- substring(gc$bin.chrom, 4)

chrom.numeric[which(gc$bin.chrom == "chrX")] <- "23"

chrom.numeric[which(gc$bin.chrom == "chrY")] <- "24"

chrom.numeric <- as.numeric(chrom.numeric)

thisRatio <- read.table(paste(indir, varbin.data,
   sep="/"), header=F)
```

```
names(thisRatio) <- c("chrom", "chrompos", "abspos",
   "bincount", "ratio")

thisRatio$chrom <- chrom.numeric

a <- thisRatio$bincount + 1

thisRatio$ratio <- a / mean(a)

thisRatio$gc.content <- gc$gc.content

thisRatio$lowratio <- lowess.gc(thisRatio$gc.con-
   tent, thisRatio$ratio)

a <- quantile(gc$bin.length, 0.985)

thisRatioNobad <- thisRatio[which(bad[, 1] == 0),]

write.table(thisRatio,file=paste(sample.name, ".cor-
   rected.bincounts", sep=""), sep="\t", row.
   names=FALSE)

# replace <Mean control read counts> with actual
   filepath

controlsRatio <-read.table(<Mean control read
   counts>, header=F)

controlsRatio$ratio<-controlsRatio$V5

controlsRatio$ratio[which(controlsRatio$ratio ==
   0)] <- 0.001

controlsRatio$lowratio<- lowess.gc(thisRatio$gc.
   content, controlsRatio$ratio)

thisRatio$normlowratio <- thisRatio$lowratio /
   controlsRatio$lowratio

printDataframe <- data.frame(chrom=thisRatio$chrom,
   pos=thisRatio$chrompos,gc=thisRatio$gc.content,
   ratio = thisRatio$ratio, lowratio=thisRatio
   $lowratio, controlRatio = controlsRatio$lowratio,
   normratio = thisRatio$normlowratio)

 #cghweb analysis

CGHweb_ratios<-data.frame(ProbeID=(1:length(thisRat
   io$chrom)),Chromosome=thisRatio$chrom,LogRatio=
   log(thisRatio$normlowratio, 2),Position=thisRati
   o$chrompos)

runCGHAnalysis(CGHweb_ratios, BioHMM = FALSE,
   UseCloneDists = FALSE, Lowess = FALSE, Lwidth =
   15, Wavelet = FALSE, Wlevels = 3, Runavg =
   FALSE,Rwidth = 5, CBS = TRUE, alpha = 0.05, Picard
   = FALSE, Km = 20,S = -0.5, FusedLasso = FALSE,
   fluv = FALSE, FDR = 0.5,rsm = FALSE, GLAD = TRUE,
   qlambda = 0.999,FASeg = FALSE, sig = 0.025, delta
   = 0.1, srange = 50, fineTune = FALSE, Quantreg =
   FALSE, lambda = 1,minLR = -2, maxLR = 2, Threshold
   = 0.2,genomeType = "HG19", tempDir = getwd(),
   resultDir = "CGHResults")

}
```

9. Call postprocess function (replace brackets (<>) with actual filepaths). CGHWeb creates a directory (CGHResults) containing plots and a text file (Table_of_aCGH_smoothed_profiles.txt) containing the segmented bin counts.

```
postprocess(indir=".", outdir=".", bad.bins=<BAD BINS>, varbin.gc=<GC Content File>, varbin.data=<Bincounts File>, sample.name=<Sample name>, alt.sample.name="", alpha=0.05, nperm=1000, undo.SD=1.0, min.width=5)
```

10. Extract copy number segment boundaries and mean log2-ratios from Table_of_aCGH_smoothed_profiles.txt using Perl. The first command-line argument is the Table_of_aCGH_smoothed_profiles.txt and the s argument is the output (text) file containing Segment boundaries and mean log2-ratios. The script is available on request from the authors.

11. For each segment z-scores are calculated by summing up GC-corrected bincounts of bins within that segment for the sample and each of the controls. The mean of the sums of the controls are subtracted from the sample bincount sum and divided by the standard deviation of sums of the controls. The script and corrected bincounts of controls are available on request from the authors.

12. Results can be plotted using R. Specify the output file in <Output File>.(*see* **Note 16**)

```
ratio<-read.table("Table_of_aCGH_smoothed_profiles.txt", header=TRUE);
png(filename = <Output File>, width = 2280, height = 218,
    units = "px", pointsize = 20, bg = "white", res = NA)
par(mar=c(4,0,0,0))
count<-1
widths<-vector(length=24)
for (i in c(1:24)) {
   ch <- which(ratio$Chromosome==i)
   widths[count]<-max(ratio$Position[ch])
   count<-count+1
}
nf <- layout(matrix(c(1,2,3,4,5,6,7,8,9,10,11,12,13,14,15,16,17,18,19,20,21,22,23,24), 1, 24, byrow=TRUE), widths=widths)
for (i in c(1:24)) {
    chrom <- which(ratio$Chromosome==i)
    if (length(chrom)>0) {
```

```
    plot(ratio$Position[chrom],ratio$LogRatio[chro
  m],ylim  =  c(-2,2),yaxt="n",xlab  =  paste
  ("chr",i),ylab = "log2-ratios",pch = ".",col =
  colors()[201])
       points(ratio$Position[chrom],ratio$Summary
  [chrom], pch = ".", col = colors()[88],cex=3)
  chrom <- which(ratio$Chromosome==i& ratio$Summary
  > 0.2)
     points(ratio$Position[chrom],ratio$Summary[ch
  rom], pch = ".", col = colors()[136],cex=3)
  chrom <- which(ratio$Chromosome==i& ratio$Summary
  < -0.2)
     points(ratio$Position[chrom],ratio$Summary[ch
  rom], pch = ".", col = colors()[461],cex=3)
       abline(h=0)
}
}
dev.off()
```

4 Notes

1. Blood tubes should be inverted the tube several times in order to prevent coagulation and to preserve blood cells from bursting that might dilute the fraction of circulating tumor DNA.
2. High-molecular-weight DNA on a Bioanalyzer profile indicates contamination with DNA from blood cells (*see* Fig. 2c).
3. Hemolysis and released haem may interfere with subsequent amplification methods. Therefore, presence of hemolysis should be documented for troubleshooting.
4. All centrifugation steps for plasma extraction should be done with the brake and acceleration powers set to zero.
5. QIAamp Mini kit: do not add QIAGEN Protease or proteinase K directly to Buffer AL.
6. QIAamp Mini kit: Close each spin column in order to avoid aerosol formation during centrifugation. Centrifugation at full speed will not affect the yield or purity of the DNA. If the lysate has not completely passed through the column after centrifugation, centrifuge again at higher speed until the QIAamp Mini spin column is empty.
7. QIAamp Mini kit: Residual Buffer AW2 in the eluate may cause problems in downstream applications. Therefore, an additional centrifugation step may be performed to eliminate buffer residuals.
8. Qubit: Use only thin-wall, clear 0.5 ml PCR tubes.

9. If plasma DNA concentration is below the detection limit of Qubit, either use larger volumes of plasma DNA or concentrate the sample in a speed Vac. The sample can be anywhere in the range of 1 and 20 µl. Add working solution so that the final volume in each tube after adding sample is 200 µl.
10. Based on our experience the likelihood of identifying copy number aberrations is higher in samples with a biphasic size distribution on a Bioanalyzer.
11. During library preparation there several save stopping points. Samples can be stored at −15 to −25 °C for up to 7 days after end repair, adapter ligation, PCR amplification, and validation.
12. In the Protocol AMPure Beads are referred to as "Sample Purification Beads." Before use remove SPB from 2 to 8 °C storage and let stand for at least 30 min to bring them to room temperature.
13. When pooling six libraries in one run be aware that only libraries with different indices can be pooled in one run.
14. Always prepare freshly diluted NaOH for library denaturation.
15. When using a MiSeq Reagent 150 cycle kit you should obtain a cluster density of 1200–1400 kg/mm^2. Based on our experience approximately 85–95 % of clusters should pass the filters and more than 90 % of reads should be above Q30 (Fig. 5a, b). Pooling should result in the same amount of reads for all samples (Fig. 5c, d).
16. Exemplary copy number profiles are displayed in Fig. 6.

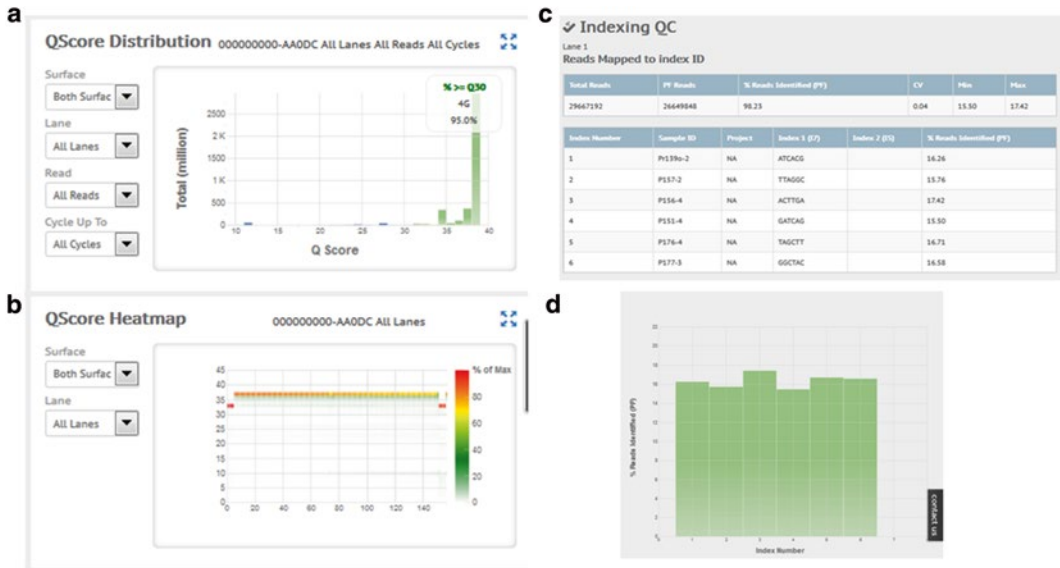

Fig. 5 Quality parameters of pooling and sequencing on an Illumina MiSeq. (**a**) Distribution of quality scores of all reads. (**b**) Heat map of quality scores. (**c**,**d**) Distribution of reads across all samples

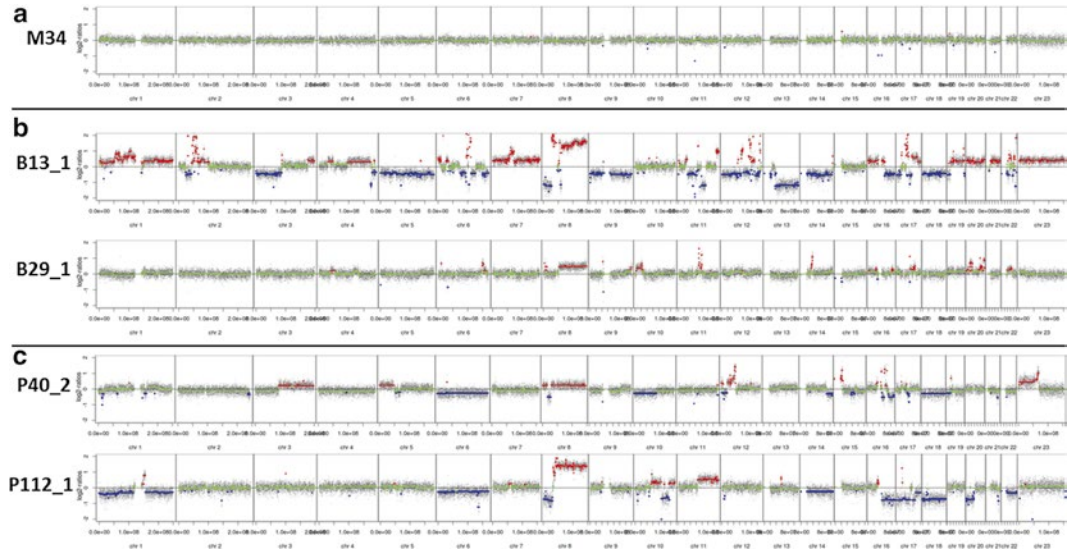

Fig. 6 Example of copy number profiles established with the plasma-Seq approach. (**a**) Copy number profile of a male control shows no copy number changes across the genome. (**b**) Copy number profiles of two plasma DNA samples from breast cancer patients. A variety of copy number changes including focal amplifications that are frequently detected in breast cancer can be observed. Even in samples with lower amount of tumor DNA (lower panel) copy number changes can be observed. (**c**) Copy number profiles of two plasma DNA samples from prostate cancer patients

References

1. Jung M, Klotzek S, Lewandowski M et al (2003) Changes in concentration of DNA in serum and plasma during storage of blood samples. Clin Chem 49:1028–1029
2. Lui YY, Chik KW, Chiu RW et al (2002) Predominant hematopoietic origin of cell-free DNA in plasma and serum after sex-mismatched bone marrow transplantation. Clin Chem 48:421–427
3. Bettegowda C, Sausen M, Leary RJ et al (2014) Detection of circulating tumor DNA in early- and late-stage human malignancies. Sci Transl Med 6:22ra424
4. Chan KC, Jiang P, Chan CW et al (2013) Noninvasive detection of cancer-associated genome-wide hypomethylation and copy number aberrations by plasma DNA bisulfite sequencing. Proc Natl Acad Sci U S A 110:18761–18768
5. Chan KC, Jiang P, Zheng YW et al (2013) Cancer genome scanning in plasma: detection of tumor-associated copy number aberrations, single-nucleotide variants, and tumoral heterogeneity by massively parallel sequencing. Clin Chem 59:211–224
6. Diehl F, Schmidt K, Choti MA et al (2008) Circulating mutant DNA to assess tumor dynamics. Nat Med 14:985–990
7. Forshew T (2012) Noninvasive identification and monitoring of cancer mutations by targeted deep sequencing of plasma DNA. Sci Transl Med 4:136ra68
8. Heidary M, Auer M, Ulz P et al (2014) The dynamic range of circulating tumor DNA in metastatic breast cancer. Breast Cancer Res 16:421
9. Heitzer E, Auer M, Hoffmann EM et al (2013) Establishment of tumor-specific copy number alterations from plasma DNA of patients with cancer. Int J Cancer 133:346–356
10. Heitzer E, Auer M, Ulz P et al (2013) Circulating tumor cells and DNA as liquid biopsies. Genome Med 5:73
11. Heitzer E, Ulz P, Belic J et al (2013) Tumor-associated copy number changes in the circulation of patients with prostate cancer identified

through whole-genome sequencing. Genome Med 5:30

12. Heitzer E, Ulz P, Geigl JB (2014) Circulating tumor DNA as a liquid biopsy for cancer. Clin Chem 61:112
13. Mohan S, Heitzer E, Ulz P et al (2014) Changes in colorectal carcinoma genomes under anti-egfr therapy identified by whole-genome plasma DNA sequencing. PLoS Genet 10:e1004271
14. Murtaza M (2013) Non-invasive analysis of acquired resistance to cancer therapy by sequencing of plasma DNA. Nature 497:108–112
15. Baslan T, Kendall J, Rodgers L et al (2012) Genome-wide copy number analysis of single cells. Nat Protoc 7:1024–1041
16. Li H, Durbin R (2009) Fast and accurate short read alignment with burrows-wheeler transform. Bioinformatics 25:1754–1760
17. Li H, Handsaker B, Wysoker A et al (2009) The sequence alignment/map format and samtools. Bioinformatics 25:2078–2079
18. R:. R: A language and environment for statistical computing. http://www.R-project.org
19. Lai W, Choudhary V, Park PJ (2008) Cghweb: a tool for comparing DNA copy number segmentations from multiple algorithms. Bioinformatics 24:1014–1015
20. Navin N, Kendall J, Troge J et al (2011) Tumour evolution inferred by single-cell sequencing. Nature 472:90–94

Chapter 6

The Methylated DNA Immunoprecipitation [MeDIP] to Investigate the Epigenetic Remodeling in Cell Fate Determination and Cancer Development

Silvia Masciarelli, Teresa Bellissimo, Ilaria Iosue, and Francesco Fazi

Abstract

Epigenetic mechanisms such as DNA methylation, posttranslational modifications of histone proteins, remodeling of nucleosomes, and the expression of noncoding RNAs contribute to the regulation of gene expression for the cell fate determination and tissue development. The disruption of these epigenetic mechanisms, in conjunction with genetic alterations, is a decisive element for cancer development and progression. The cancer phenotype is characterized by global DNA hypomethylation and gene-specific hypermethylation. The methylated DNA immunoprecipitation [MeDIP] is a useful approach currently used to clarify the functional consequences of DNA methylation on cell fate determination and cancer development.

Key words Epigenetic remodeling, DNA methylation, MeDIP, 5-Methyl-cytosine, CpG island, Chromatin immunoprecipitation, Cancer chemoprevention

1 Introduction

Epigenetics is defined as a series of heritable changes in the regulation of gene expression, resulting from chromatin structure modifications at specific loci without changes in the DNA sequence [1]. The methylation of DNA and the posttranslational modifications of histone proteins represent the main epigenetic mechanisms that profoundly impact the chromatin structure [2, 3]. The DNA methylation is a process normally used by mammalian cells for the maintenance of proper regulation of gene expression [4]. The DNA methylation consists in the conjugation of a methyl group to the cytosine residues at cytosine-phosphate-guanine (CpG) dinucleotides [2]. The enzymes responsible for the methylation of DNA are known as DNA methyltransferases (DNMTs) [5]. In human genome CpG dinucleotides are slightly uncommon and

Sabrina Strano (ed.), *Cancer Chemoprevention: Methods and Protocols*, Methods in Molecular Biology, vol. 1379,
DOI 10.1007/978-1-4939-3191-0_6,

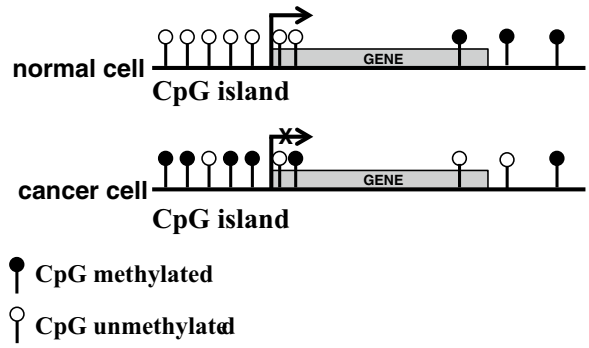

Fig. 1 DNA methylation of tumor-suppressor gene in normal and cancer cell

asymmetrically distributed within CpG-rich regions (also known as CpG islands) or within low-density CpG regions. In human cells, while the majority of the CpG dinucleotides are methylated, especially those located in areas of repetitive sequences, thought to preserve chromatin stability, the CpG islands usually remain unmethylated, except for specific regions such as the inactive X-chromosome and the imprinted genes [2, 6]. Interestingly, about 60 % of human gene promoters contain CpG islands and the methylation of these promoter regions generally correlates with the transcriptional gene silencing. Indeed, the methylation of DNA could prevent the binding of specific transcription factors or promote the recruitment of methylated DNA-binding proteins, such as MeCP2, which, by attracting co-repressor complexes at the surrounding regions, contribute to gene silencing [2].

The disruption of epigenetic mechanisms, in conjunction with genetic alterations, is a decisive element for cancer onset and progression [7, 8]. Cancer phenotype is characterized by a gene-specific hypermethylation resulting in the transcriptional silencing of tumor-suppressor genes and by a global DNA hypomethylation contributing to chromosomal instability and activation of key genes involved in tumorigenesis (Fig. 1) [9, 10].

In neoplastic cells, the evaluation of the methylation degree of DNA in relation to gene expression changes may be relevant not only for the identification of the epigenetic basis of tumor development but also to assess the cancer risk or to supply new insight into therapeutic response and cancer prevention [11–15]. Of note, emerging evidences in the last decade are pointing out that different synthetic or natural chemopreventive agents known to reduce or delay the occurrence of malignant phenotype, like the retinoic acid (RA), strongly impact the epigenetic regulation of gene expression [16]. Different methodologies are now available to clarify the relevance of these chromatin remodeling events on cancer chemoprevention.

Much of the information about the distribution of DNA methylation throughout the human genome has been obtained using

different methods such as the enzyme digestion, the sodium bisulphite treatment, and the methylated DNA immunoprecipitation (MeDIP) [17]. Enzyme digestion uses endonucleases sensitive or insensitive to the methylation of DNA. A problem with this type of analysis is that it is limited to those cytosine residues located within methylation-sensitive restriction endonuclease sites. Sodium bisulphite treatment is a powerful tool to uncover the methylation profile of each CpG within a region of interest [18]. Under the appropriate condition sodium bisulphite induces the deamination of unmethylated cytosines but not 5-methylcytosine (5-mC) residues [18]. Various analyses can be performed with this modified DNA: bisulfite sequencing, methylation-specific PCR, high-resolution melting curve analysis and next-generation sequencing [19, 20]. The MeDIP method is based on the affinity purification of methylated DNA using an antibody directed against the 5-mC residues [21]. The affinity-enriched DNA after purification can be used in sequence specific analyses when combined with PCR techniques or for genome-wide analysis. This chapter describes step by step the MeDIP methodology (Fig. 2).

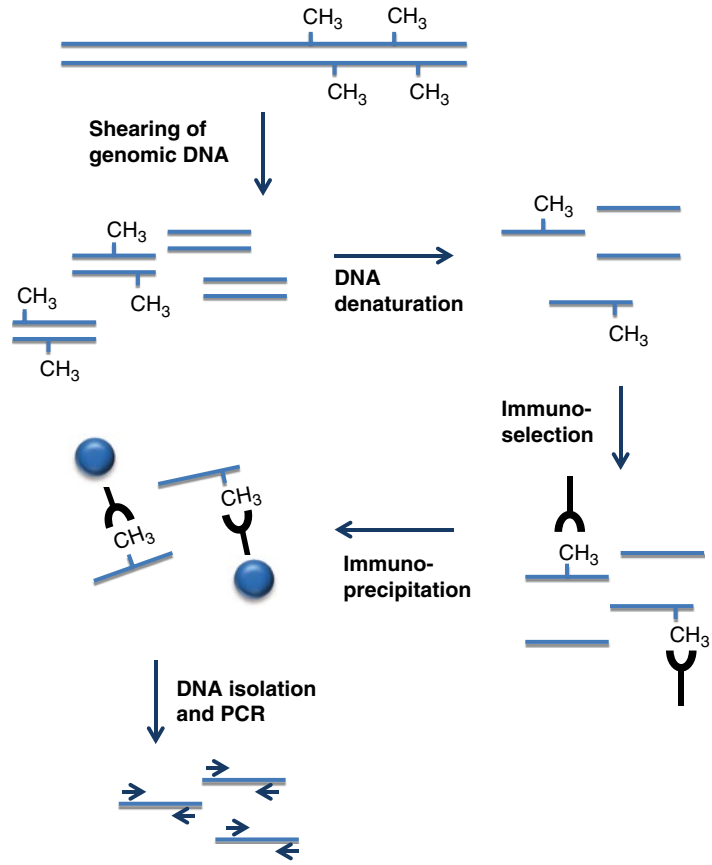

Fig. 2 MeDIP methodology

2 Materials

All solutions are prepared by using ultrapure water and analytical grade reagents.

2.1 Buffers

1. *Salting-out DNA extraction buffer*: 10 mM Tris–HCl pH 8.1, 150 mM NaCl, 2 mM EDTA pH 8.0. Store at 4 °C.
2. *Immunoprecipitation buffer*: 0.01 % SDS, 1.1 % Triton X-100, 1.2 mM EDTA pH 8.0, 16.7 mM Tris–HCl pH 8.1, 167 M NaCl and protease inhibitors.
3. *Low-salt wash buffer*: 0.1 % SDS, 1 % Triton X-100, 2 mM EDTA pH 8.0, 20 mM Tris–HCl pH 8.1, 150 mM NaCl.
4. *High-salt wash buffer*: 0.1 % SDS, 1 % Triton X-100, 2 mM EDTA pH 8.0, 20 mM Tris–HCl pH 8.1, 500 mM NaCl.
5. *LiCl wash buffer*: 0.25 M LiCl, 1 % NP40, 1 % sodium deoxycholate, 1 m MEDTA pH 8.0, 10 mM Tris–HCl pH 8.1.
6. *Elution buffer*: 1 % SDS, 0.1 M $NaHCO_3$.
7. *Tris-EDTA* [*TE*] *buffer*: 10 mM Tris–HCl pH 8.1, 1 mM EDTA pH 8.0.
8. *Ice-cold PBS buffer 1*×: 137 mM NaCl, 2.7 mM KCl, 10 mM Na_2HPO_4, 1.8 mM KH_2PO_4, 1 m $MCaCl_2 \cdot 2H_2O$, 0.5 mM $MgCl_2 \cdot 6H_2O$. Store at 4 °C.

3 Methods

3.1 Cell Collection and Lysis

1. Pellet suspension culture or trypsinize adherent cells and collect cells. Centrifuge at 300 × *g* for 5 min at 4 °C.
2. Discard the supernatant. Suspend cells in 10 ml ice-cold PBS. Centrifuge at 300 × *g* for 5 min at 4 °C. Discard the supernatant. Repeat this step.
3. Suspend 25–50 × 10^6 cells in 3 ml Salting-out DNA extraction buffer on ice (15 ml tubes); add 75 μl SDS 20 % and 30 μl 20 mg/ml Proteinase K (*see* **Note 1**).
4. Incubate the samples with shaking at 37 °C for 12–18 h in tightly capped tubes.

3.2 Extraction and Purification of DNA

1. Add 1.6 ml saturated 6 M NaCl and shake vigorously for 15 s.
2. Spin at 1400 × *g* for 15 min at RT.
3. Save supernatant and pour it in a 50 ml tube; add 2 volumes of 100 % ethanol and mix gently; DNA immediately precipitates.

4. Recover DNA by centrifugation at 1400 × *g* for 5 min.
5. Wash precipitated DNA extensively in 70 % ethanol (recommended: five washes 1 h each in 20–30 ml of 70 % ethanol).
6. Decant ethanol and air-dry the pellet.
7. Resuspend the pellet of DNA at 1 mg/ml in TE until dissolved. Shake gently at room temperature or at 65 °C for several hours to facilitate solubilization.
8. Store at 4 °C.

3.3 DNA Shearing

1. In a 1.5 ml tube, dissolve the DNA in TE to reach 0.1 μg/μl.
2. Use a final volume of 300 μl of DNA in 1.5 ml tubes.
3. Shear the DNA by sonication (5 cycles of 10 s ON/30 s OFF) to reduce DNA length to 200–500 bp. Cool samples on ice between pulses.
4. Check the sheared DNA on agarose gel (*see* **Note 2**).

3.4 Methylated DNA Immunoprecipitation and Washes

1. Dilute 1 μg (10 μl) of sonicated DNA in 50 μl TE.
2. Denature for 10 min in boiling water and immediately cool on ice for 10 min.
3. Quickly perform a short spin at 4 °C.
4. Dilute DNA sample 20-fold in immunoprecipitation buffer. Keep a portion of this dilution (1 %) to check the amount of input DNA present in different samples before immunoprecipitation.
5. To reduce nonspecific background, pre-clear diluted sample with 80 μl of Protein A Agarose/Salmon Sperm DNA—50 % Slurry (or previously saturated with 1 μg/μl sonicated salmon sperm in 1 ml immunoprecipitation buffer for 2 h at 4 °C) for 30 min at 4 °C with agitation.
6. Pellet beads by brief centrifugation (1000 RPM at 4 °C in a microfuge, ~1 min) and collect the supernatant fraction (*see* **Note 3**).
7. Add 5 μl of 5mC antibody to the supernatant fraction and incubate overnight at 4 °C with rotation (*see* **Note 4**). For a negative control, perform an immunoprecipitation in the absence of antibody (No Ab sample).
8. Add 60 μl of Protein A Agarose/Salmon Sperm DNA—50 % Slurry (or previously saturated with 1 μg/μl sonicated salmon sperm in 1 ml immunoprecipitation buffer for 2 h at 4 °C) for 1 h at 4 °C with rotation to collect the antibody/5mC complex.

9. Pellet beads by gentle centrifugation (1000 RPM at 4°C in a microfuge, ~1 min) (*see* **Note 3**). Carefully remove the supernatant that contains unbound, nonspecific DNA. Wash the beads for 3–5 min on a rotating platform with 1 ml of each of the buffers listed in the order as given below:

   (a) Low-salt wash buffer (one wash); (b) high-salt wash buffer (one wash); (c) LiCl wash buffer (one wash); (d) TE buffer (two washes).

10. After the last wash, discard the last traces of TE buffer. The immunoprecipitated methylated DNA is bound to the beads.

3.5 DNA Elution and Purification

1. Elute immune complex from the antibody by adding 250 μl of freshly prepared elution buffer to the pelleted beads. Vortex briefly to mix and incubate at room temperature for 15 min with rotation. Spin down beads, and carefully transfer the supernatant fraction (eluate) to another tube and repeat elution. Combine eluates (total volume =~500 μl).
2. Add 490 μl of freshly prepared complete elution buffer to the input samples (10 μl).
3. Add 1 volume of phenol/chloroform/isoamyl alcohol (25:24:1).
4. Centrifuge for 10 min at 13,000 RPM at RT in a microfuge. Transfer the top aqueous phase into a new 1.5 ml tube.
5. Add 1 volume of chloroform/isoamyl alcohol (24:1).
6. Centrifuge for 10 min at 13,000 RPM at RT in a microfuge. Transfer the top aqueous phase into a new 1.5 ml-tube.
7. Add 2 volumes of ice-cold 100 % ethanol and 20 μg of glycogen as a carrier. Mix well. Leave at –80 °C for 30 min.
8. Centrifuge for 25 min at 13,000 RPM at 4°C in a microfuge. Carefully remove the supernatant and add 500 μl of ice-cold 70 % ethanol to the pellet.
9. Centrifuge for 10 min at 13,000 RPM at 4°C in a microfuge. Carefully remove the supernatant. Air-dry samples for 30 min at room temperature to evaporate the remaining ethanol.
10. Suspend the DNA by adding 50 μl TE to the immunoprecipitated and input samples (*see* **Note 5**).

3.6 PCR Analysis of Immunoprecipitated DNA

Detect specific sequences from immunoprecipitated and input DNA samples by PCR or real-time PCR, using 20 ng of total input DNA and 2 μl of MeDIP DNA. The efficiency of Methyl DNA immunoprecipitation of particular genomic loci can be calculated from qPCR data and reported as a percentage of starting material: % (MeDNA-IP/total input).

4 Notes

1. If the cells are not completely disrupted during the cell lysis step keep attention do not use too many cells for the indicated amount of buffer.
2. To check the quality of DNA after the sonication do not load too much sample on 1 % agarose gel and run slowly.
3. Do not spin beads at high speed.
4. To ensure efficient immunoprecipitation it is important to test increasing amounts of antibody during the setting of the protocol.
5. Samples can be frozen at different steps of the protocol: genomic DNA, sheared DNA and immunoprecipitated DNA.

Acknowledgement

The work was supported by AIRC Start-up grant 4841.

References

1. Chen T, Dent SY (2014)- Chromatin modifiers and remodellers: regulators of cellular differentiation. Nat Rev Genet 15:93–106
2. Jones PA (2012) Functions of DNA methylation: islands, start sites, gene bodies and beyond. Nat Rev Genet 13:484–492
3. Portela A, Liz J, Nogales V et al (2013) DNA methylation determines nucleosome occupancy in the 5′-CpG islands of tumor suppressor genes. Oncogene 32:5421–5428
4. De Carvalho DD, You JS, Jones PA (2010) DNA methylation and cellular reprogramming. Trends Cell Bio 20:609–617
5. Brenner C, Fuks F (2006) DNA methyltransferases: facts, clues, mysteries. Curr Top Microbiol Immunol 301:45–66
6. Chaligne R, Heard E (2014) X-chromosome inactivation in development and cancer. FEBS Lett 588:2514–2522
7. Jones PA, Baylin SB (2007) The epigenomics of cancer. Cell 128:683–692
8. Easwaran H, Tsai HC, Baylin SB (2014) Cancer epigenetics: tumor heterogeneity, plasticity of stem-like states, and drug resistance. Mol Cell 54:716–727
9. Taberlay PC, Jones PA (2011) DNA methylation and cancer. Prog Drug Res 67:1–23
10. Estecio MR, Issa JP (2011) Dissecting DNA hypermethylation in cancer. FEBS Lett 585:2078–2086
11. Baylin SB, Jones PA (2011) A decade of exploring the cancer epigenome - biological and translational implications. Nat Rev Cancer 11: 726–734
12. Figueroa ME, Lugthart S, Li Y et al (2010) DNA methylation signatures identify biologically distinct subtypes in acute myeloid leukemia. Cancer Cell 17:13–27
13. Fazi F, Racanicchi S, Zardo G et al (2007) Epigenetic silencing of the myelopoiesis regulator microRNA-223 by the AML1/ETO oncoprotein. Cancer Cell 12:457–466

14. Fazi F, Zardo G, Gelmetti V et al (2007) Heterochromatic gene repression of the retinoic acid pathway in acute myeloid leukemia. Blood 109:4432–4440
15. Schoofs T, Muller-Tidow C (2011) DNA methylation as a pathogenic event and as a therapeutic target in AML. Cancer Treat Rev 37(Suppl 1):S13–S18
16. Gerhauser C (2013) Cancer chemoprevention and nutriepigenetics: state of the art and future challenges. Top Curr Chem 329:73–132
17. Laird PW (2010) Principles and challenges of genomewide DNA methylation analysis. Nat Rev Genet 11:191–203
18. Reinders J, Paszkowski J (2010) Bisulfite methylation profiling of large genomes. Epigenomics 2:209–220
19. Kristensen LS, Hansen LL (2009) PCR-based methods for detecting single-locus DNA methylation biomarkers in cancer diagnostics, prognostics, and response to treatment. Clin Chem 55:1471–1483
20. Li LC (2007) Designing PCR primer for DNA methylation mapping. Methods Mol Biol 402:371–384
21. Sorensen AL, Collas P (2009) Immunoprecipitation of methylated DNA. Methods Mol Biol 567:249–262

Chapter 7

LC-MS-Based Metabolomic Investigation of Chemopreventive Phytochemical-Elicited Metabolic Events

Lei Wang, Dan Yao, and Chi Chen

Abstract

Phytochemicals are under intensive investigation for their potential use as chemopreventive agents in blocking or suppressing carcinogenesis. Metabolic interactions between phytochemical and biological system play an important role in determining the efficacy and toxicity of chemopreventive phytochemicals. However, complexities of phytochemical biotransformation and intermediary metabolism pose challenges for studying phytochemical-elicited metabolic events. Metabolomics has become a highly effective technical platform to detect subtle changes in a complex metabolic system. Here, using green tea polyphenols as an example, we describe a workflow of LC-MS-based metabolomics study, covering the procedures and techniques in sample collection, preparation, LC-MS analysis, data analysis, and interpretation.

Key words Chemoprevention, Phytochemical, Metabolism, Metabolomics, LC-MS

1 Introduction

Cancer is a leading cause of disease-related mortalities over the world. In the United States, nearly one fourth of deaths are due to cancer [1]. Compared to invasive and costly surgical procedures, chemotherapy, and radiotherapy, chemoprevention is a promising approach to block and suppress carcinogenesis, especially for the people in high risk of cancer due to genetic background or environmental factors. Phytochemicals in plants (herbs and vegetables) are considered as a reliable and accessible source of chemopreventive agents since the efficacy of plant extracts against carcinogenesis has been largely attributed to specific phytochemicals, such as indole-3-carbinol in cruciferous vegetables and polyphenols in green tea [2–4]. Therefore, identifying potent chemopreventive phytochemicals and characterizing the mechanisms of their anticarcinogenic activities are the main goals of ongoing chemoprevention research.

Sabrina Strano (ed.), *Cancer Chemoprevention: Methods and Protocols*, Methods in Molecular Biology, vol. 1379,
DOI 10.1007/978-1-4939-3191-0_7,

Metabolism plays an essential role in the bioactivities of phytochemicals against carcinogenesis. On one hand, how a phytochemical is disposed in a biological system through absorption, distribution, metabolism, and excretion (ADME) determines the concentration and duration of phytochemical presence in target sites as well as whether bioactivation or detoxification biotransformation occurs to the phytochemical. On the other hand, since cancer is a metabolic disease, how a phytochemical affects the metabolism of a biological system could have major impacts on its chemopreventive activity. Studies in recent years have shown that uncontrolled proliferation of tumor cells is driven by dysregulated nutrient and energy metabolism. For example, aerobic glycolysis in cancer cells channels glucose metabolism toward lactate production in the presence of adequate oxygen [5], producing the intermediates that can be utilized for anabolic activities in growing cells, such as biosynthesis of fatty acids, nonessential amino acids, nucleic acids, and intracellular antioxidants [6, 7]. It has been shown that chemopreventive phytochemicals could affect diverse metabolic pathways, resulting in suppressing effects on tumor cells [8, 9]. Therefore, examining the metabolic interactions between phytochemicals and biological systems is essential for understanding and predicting the chemopreventive effects of phytochemicals.

Systems biology tools, such as genomics, transcriptomics, and proteomics, have been adopted to characterize the cancer prevention activities of phytochemicals due to their capacity for discovering molecular mechanisms in transcriptional and translational levels [10]. However, these platforms have clear disadvantages in elucidating the metabolic interactions between phytochemicals and biological systems since the central players of these metabolic interactions, which are phytochemical metabolites and endogenous metabolites, are not directly examined by these tools. In this regard, metabolomics, as a platform that is capable of detecting subtle metabolic changes in a complex biological system, has become a very effective tool for investigating chemical and metabolic events in chemoprevention. Untargeted metabolomics has been used to identify novel anticancer phytochemicals and examine biotransformation of phytochemicals [11, 12]. Furthermore, the values of metabolomics in characterizing chemopreventive phytochemical-induced metabolic events has also been discussed [13].

In this chapter, we describe a protocol for liquid chromatography-mass spectrometry (LC-MS)-based metabolomic investigation of chemopreventive phytochemical-induced metabolic events. Using green tea polyphenols (GTP) as an example, the procedures, techniques, and considerations in sample collection, preparation, LC-MS analysis, data analysis, and interpretation are described and discussed.

2 Materials

Following the general procedure of animal-based investigation of phytochemical-elicited metabolic events, the materials in metabolomics studies are categorized as the items for sample collection, sample preparation, LC-MS analysis, and data analysis, respectively (*see* **Note 1**). All solutions are prepared with LC-MS grade water, organic solvents, and analytical grade reagents. Unless indicated otherwise, all solutions are stored at room temperature.

2.1 Sample Collection in Animal Experiment

1. Animal: 8-week-old male C57/BL6 mice are used in this case study.
2. Chemopreventive phytochemical: The GTP extract used in this case study contains more than 50 % epigallocatechin gallate (EGCG).
3. Experimental diet: AIN93G-purified diet is used in this case study.
4. Metabolic cages (Tecniplast).
5. Lancet for submandibular bleeding.
6. Surgical apparatus for tissue collections.
7. 1.5 mL Eppendorf tubes for urine, serum, and fecal samples.
8. Cryogenic tubes for tissue collection.
9. Serum separator tubes (BD Microtainer™).
10. Liquid nitrogen.

2.2 Sample Preparation

1. Methanol for sample fractionation.
2. Chloroform for sample fractionation.
3. *n*-Butanol for dissolving lipid fraction.
4. 2 mL flat-bottom centrifuge tubes.
5. Tissue homogenizer.
6. Centrifuge.
7. Internal standards (*see* **Note 2**).
8. Reagents for derivatizing amino-containing metabolites: freshly prepared 3 mg/mL dansyl chloride (DC) in acetone, 10 mM sodium carbonate in water.
9. Reagents for derivatizing carboxylic acids, aldehydes, and ketones: freshly prepared reaction mixture containing 1 mM 2-hydrazinoquinoline (HQ), 1 mM 2,2′-dipyridyl disulfide (DPDS), and 1 mM triphenylphosphine (TPP) in acetonitrile (ACN).

2.3 LC-MS Analysis (See Note 3)

1. LC system: ACQUITY™ ultra-performance liquid chromatography (UPLC) system (Waters).
2. High-resolution MS system: SYNAPT quadrupole time-of-flight (QTOF) MS system (Waters).
3. ACQUITY UPLC BEH C18 column, 1.7 μm, 2.1 mm × 50 mm (Waters).
4. ACQUITY UPLC BEH C8 column, 1.7 μm, 2.1 mm × 50 mm (Waters).
5. ACQUITY UPLC BEH Amide column, 1.7 μm, 2.1 mm × 100 mm (Waters).
6. Mobile-phase A1 for analyzing general metabolites: H_2O containing 0.1 % formic acid (v/v).
7. Mobile-phase B1 for analyzing general metabolites: ACN containing 0.1 % formic acid (v/v).
8. Mobile-phase A2 for analyzing triglycerides and nonpolar lipids: H_2O:ACN (6:4, v:v) containing 10 mM ammonium formate and 0.1 % formic acid.
9. Mobile-phase B2 for analyzing triglycerides and nonpolar lipids: Isopropyl alcohol (IPA):ACN (9:1, v:v) containing 10 mM ammonium formate and 0.1 % formic acid.
10. Mobile-phase A3 for analyzing HQ-derivatized metabolites: H_2O containing 0.05 % acetic acid (v/v) and 2 mM ammonium acetate.
11. Mobile-phase B3 for analyzing HQ-derivatized metabolites: H_2O:ACN (5:95, v:v) containing 0.05 % acetic acid (v/v) and 2 mM ammonium acetate.
12. Lock mass: 500 pg/μL leucine encephalin in 50 % ACN (v/v) with 0.1 % formic acid (v/v).
13. LC sample vials.
14. Nitrogen gas for desolvation and ionization in MS system.
15. Argon gas for MSMS fragmentation analysis.
16. Software for operating the LC-MS system and acquiring LC-MS data: MassLynx™ software (Waters).

2.4 Data Analysis (See Note 4)

1. Software for processing LC-MS data:MassLynx™ (Waters).
2. Software for deconvoluting LC-MS data: Markerlynx™ (Waters).
3. Software for multivariate data analysis (MDA): SIMCA-P+™ (Umetrics).
4. Chemical standards for confirming the structures of interested metabolites.

3 Methods

The methods described here aim to detect the metabolic differences between control and phytochemical-treated animals. Following the general procedure of animal-based investigation of phytochemical-elicited metabolic events, the methods in metabolomics studies are categorized as the methods in animal treatment and sample collection, sample preparation, LC-MS analysis, and data analysis, respectively.

3.1 Animal Treatment and Sample Collection (See Notes 5 and 6)

In this case study, mice are housed under controlled temperature and lighting conditions (20-22°C and a 14-h/10-h light/dark cycle). Two groups of mice are acclimated for 3 days on control diet (AIN93G diet) before the treatment. Then one group of mice is switched to GTP diet (AIN93G + 0.12 % GTP) for 2 weeks.

1. Urine and fecal samples: Urine and fecal samples are collected by housing the mice in metabolic cages for 24 h, and then transferred to 1.5 mL Eppendorf tubes. All urine and fecal samples are stored at -80°C.
2. Serum samples: Blood is collected in serum separator tubes by submandibular bleeding. After clotting at room temperature, blood samples are centrifuged at 3000 × *g* to separate serum and blood cells. All serum samples are stored at -80°C.
3. Tissue collection: After the mice are euthanized by carbon dioxide, the liver and other tissue samples are harvested into cryogenic tubes and then snap-frozen in liquid nitrogen. All tissue samples are stored at -80°C.

3.2 Sample Preparation (See Note 7)

In this case study, the metabolism of GTP is determined by metabolomic analysis of urine and fecal samples while the influences of GTP on endogenous metabolism are examined by metabolomic analysis of serum and tissue samples.

1. Precipitation: To remove proteins and particles in biofluid samples through solvent denaturation and centrifugation.
   (a) Urine: Mix 40 μL of urine sample with 160 μL of 50 % aqueous ACN (v/v) in a 1.5 mL Eppendorf tube, and then centrifuge at 18,000 × *g* for 10 min. Transfer supernatant to a LC vial for LC-MS analysis.
   (b) Serum: Mix 5 μL of serum sample with 195 μL of 66 % aqueous ACN (v/v) in a 1.5 mL Eppendorf tube, and then centrifuge at 18,000 × *g* for 10 min. Transfer supernatant to a LC vial for LC-MS analysis.
2. Fractionation: To prepare aqueous and lipid fractions of serum and tissue samples (*see* **Note 8**).

(a) Tissue: Homogenize 100 mg of tissue sample with 0.5 mL of methanol in a 2 mL flat-bottom centrifuge tube using a mechanical homogenizer. The homogenate is then mixed with 0.5 mL of chloroform and 0.4 mL of water. After vortex and 10-min centrifugation at 18,000 × *g*, aqueous and lipid phases are separated by tissue debris. The upper aqueous phase is ready for direct LC-MS analysis or further chemical derivatization. The lower lipid phase is dried under nitrogen and then reconstituted in 0.5 mL of *n*-butanol for LC-MS analysis.

(b) Serum: Mix 20 μL of serum sample with 100 μL of methanol in a 1.5 mL Eppendorf tube, and then add 100 μL of chloroform and 80 μL of water. After vortex and 10-min centrifugation at 18,000 × *g*, aqueous and lipid phases are separated. The upper aqueous phase is ready for direct LC-MS analysis or further chemical derivatization. The lower lipid phase is dried under nitrogen and then reconstituted in 100 μL of *n*-butanol for LC-MS analysis.

3. Derivatization: To facilitate the detection of metabolites that have poor retention in LC system or poor ionization in MS system under general analytical conditions, samples are derivatized prior to LC-MS analysis.

(a) DC derivatization for analyzing the metabolites with amino group. Mix 5 μL of sample (serum, urine, or tissue extract) with 5 μL of 100 μM *p*-chlorol-L-phenylalanine (internal standard), 50 μL of 10 mM sodium carbonate, and 100 μL of DC acetone solution (3 mg/mL) in sequence. After 10-min incubation at 60°C, the reaction mixture is centrifuged at 18,000 × *g* for 10 min, and the supernatant is transferred to an LC vial.

(b) HQ derivatization for analyzing carboxylic acids, aldehydes, and ketones. Mix 5 μL of test sample with 100 μL of freshly prepared reaction mixture containing 1 mM DPDS, 1 mM TPP, and 1 mM HQ in ACN. Incubate at 60°C for 30 min, quickly chill on ice and then mix with 100 μL of H_2O. After centrifugation at 18,000 × *g* for 10 min, transfer the supernatant into an LC vial for LC-MS analysis.

3.3 LC-MS Analysis (See Note 9)

In this case study, LC-MS analysis of control and GTP treatment samples is conducted using a UPLC-QTOFMS system (*see* **Note 10**).

1. LC system: In general, 5 μL of processed sample is injected into a UPLC system and separated by a gradient of mobile phase over a 10-min run at flow rate 0.5 mL/min (*see* **Note 11**).

(a) Using mobile-phase A1 and B1 at 40°C, nonpolar metabolites in urine, fecal extract, and DC-derivatized samples

could be separated in C18 column while polar metabolites could be retained in amide column (*see* **Note 12**).

(b) Using mobile-phase A2 and B2 at 60°C, lipids, including phospholipids and triglycerides, in serum and tissue extracts, could be separated in C18 or C8 columns.

(c) Using mobile-phase A3 and B3 at 40°C, HQ-derivatized samples could be separated in C18 column.

2. MS system:

(a) General parameters of MS analysis: Capillary voltage and cone voltage for electrospray ionization (ESI) are maintained at 3 kV and 30 V for positive-mode detection, and at -3 kV and -35 V for negative-mode detection, respectively. Source temperature and desolvation temperature are set at 120°C and 350°C, respectively. Nitrogen is used as both cone gas (50 L/h) and desolvation gas (600 L/h) and argon as collision gas. Tandem MS (MS/MS) fragmentation is performed with collision energy ranging from 15 to 40 eV.

(b) Calibration for accurate mass measurement: The QTOF mass spectrometer is calibrated with sodium formate solution (range m/z 50–1000) and monitored by the intermittent injection of the lock mass leucine enkephalin ($[M+H]^+ = 556.2771$ m/z and $[M-H]^- = 554.2615$ m/z) in real time.

3.4 Data Analysis (See Note 13)

In this case study, untargeted metabolomics approach is adopted to identify GTP metabolites in urine.

1. Data deconvolution: Chromatographic and spectral data of LC-MS analysis are deconvoluted by MarkerLynx™ software (*see* **Note 14**) to construct a data matrix that comprises samples, metabolites (represented by retention time and m/z ratio), and signal intensity.
2. MDA: The data matrix is further exported into SIMCA-P+™ software, and transformed by mean-centering and *Pareto* scaling. Based on the complexity and quality of the data, either unsupervised such as principal components analysis (PCA), or supervised MDA, such as partial least squares-discriminant analysis (PLS-DA) and orthogonal partial least squares (OPLS), are adopted to analyze the data matrix. Major latent variables in the data matrix are defined in a scores scatter plot of defined multivariate model.
3. Marker identification and structural analysis: Potential biomarkers are identified by analyzing ions contributing to the principal components in the loadings plot. The chemical identities of biomarkers are determined by accurate mass measurement, elemental composition analysis, MS/MS fragmentation, database search (*see* **Note 15**), and comparisons with authentic standards.

Using the materials and methods described in this protocol, urine samples from control and GTP-treated mice are harvested, prepared, and analyzed by a UPLC-QTOFMS system in negative mode. The LC-MS data are deconvoluted to a data matrix (Fig. 1a), which contains the information on samples, metabolites, and signals. The data matrix is further processed by MDA to generate a PLS-DA model, in which the urine samples from control and GTP-treated mice are clearly separated (Fig. 1b). The urinary metabolites affected by GTP treatment are identified in a loadings S-plot, which reveals the metabolites contributing to the separation of two sample groups in a multivariate model (Fig. 1c). Two urinary metabolites increased by GTP treatment are further characterized as 3-hydroxyphenylvaleric acid sulfate (I), a general bacterial metabolite of catechins, and epicatechin sulfate (II), a metabolite of EGCG and other polyphenols in GTP (Fig. 1d, e).

4 Notes

1. Enlisted are the items used in the GTP case study. The selection of animal, phytochemical, reagent, instrument, and software should be based on the experiment design of each metabolomics study.
2. Spiking internal standards to the samples could facilitate the efforts to monitor the efficacy of sample preparation and the performance of LC-MS system. The choices of internal standards includes table isotope-labeled metabolites, halogenated metabolites, or other unnatural analogs of phytochemicals or endogenous metabolites.
3. A UPLC-QTOF system is used in this case study, which could be changed to other types of high-resolution LC-MS systems. Column and mobile phases could also be changed according to the experiment design and instrument availability.
4. Other commercial software and free public platforms are also available for processing LC-MS data [14, 15].
5. Considerations on animal experiment: (a). Avoid or minimize the influences of confounding factors, such as gender, age, strain, and environment, when selecting animals for control and phytochemical treatment. (b). Basal components of animal diets used in control and phytochemical treatments should be the same.
6. Considerations on sample collection: (a). Different types of samples contain different types of metabolites, and can reflect different aspects of phytochemical-elicited changes in the metabolome. In general, urine and fecal samples could be used for identifying or profiling the metabolites of chemopreventive

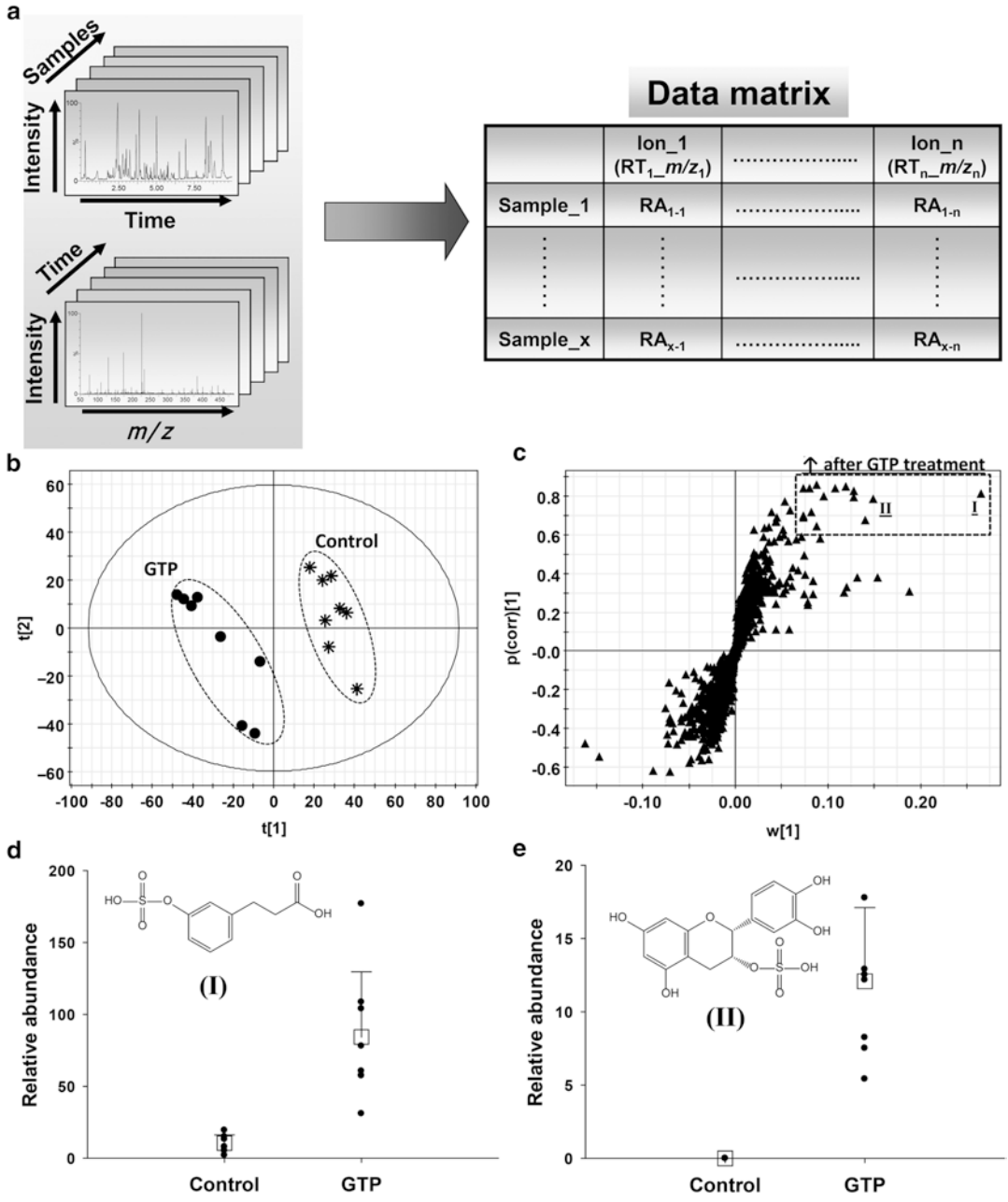

Fig. 1 LC-MS-based metabolomic investigation of GTP-induced changes in urine metabolome. (**a**) Deconvolution of LC-MS data to a multivariate data matrix. RA stands for the relative abundance of single ion count in total ion count of a chromatogram; RT stands for the retention time in LC column. (**b**) Scores plot of a PLS-DA model on the urine samples from control and GTP-treated mice ($n = 8$). The t[1] and t[2] values represent the respective scores of each sample in the principal component 1 and 2 of the model. (**c**) S loadings plot for identifying the metabolites contributing to the separation of control and GTP samples in the model. Two metabolites increased by GTP treatment are labeled (I: 245.106 *m*/*z* and II: 369.0279 *m*/*z*). (**d**, **e**) Structures of metabolites I and II and their relative abundances (individual values and mean ± S.D.) in control and GTP samples

phytochemicals, while blood and tissue samples could reveal the phytochemical-induced changes in endogenous metabolism. (b). The procedures in sample collection should maintain the chemical integrity of biological samples and avoid significant degradation or changes.

7. Considerations on sample preparation: (a). For untargeted metabolomics, the procedures of sample preparation should aim to maintain the integrity of metabolome in acquired samples through avoiding or minimizing the formation of new chemical species or the degradation of existing metabolites [16]. (b). For targeted metabolomics, appropriate procedures, such as solid-phase extraction, could be adopted to enrich the interested metabolites.
8. A modified Folch method is used to separate aqueous and lipid fractions [17].
9. Considerations on LC-MS analysis: (a). For untargeted metabolomics, a MS system with high-resolution capacity to determine accurate mass and broad dynamic range to measure signal intensity is preferred for structural elucidation of interested metabolites and multivariate data analysis. (b). Selections of LC column, mobile phase, column temperature, and ionization condition are based on the chemical properties of samples and metabolites, such as polarity, reactivity, and ionization efficiency.
10. Enlisted conditions and parameters are specifically for the UPLC-QTOF system used in this case study. Different conditions and parameters are expected for other LC-MS systems.
11. The gradient usually starts with low percent of organic phase (mobile phase B), and then gradually increases to high percent of B. At the end of 10-min run, the gradient returns to the starting gradient for the next sample. For example, A1-B1 mobile phase is used to separate urine samples in the GTP case study. The gradient profile starts at 0.5 % B1 with a flow rate of 0.5 mL/min for 0.5 min and then rises to 20 % B1 at 4 min and 95 % B1 at 8 min. At 8.1 min, the gradient is increased to 100 % B1. At 9.1 min, the gradient returns to 0.5 % B1.
12. Different to C8 and C18 column, Amide column uses hydrophilic interaction chromatography (HILIC) to retain metabolites that are too polar to be retained by reversed-phase chromatography.
13. Considerations on data analysis: (a). General procedure of data analysis in untargeted metabolomics include data deconvolution, multivariate data analysis, marker identification, bioinformatics, structural confirmation, and potential mechanistic investigation. (b). Targeted metabolomics focuses on identification and quantification of targeted metabolites.

14. The multivariate data matrix is generated through centroiding, deisotoping, filtering, peak recognition and integration. The signal intensity of each ion is calculated by normalizing the single ion counts (SIC) versus the total ion counts (TIC) in the whole chromatogram.
15. Databases for metabolite identification and structural analysis: Human Metabolome Database (http://www.hmdb.ca/), Kyoto Encyclopedia of Genes and Genomes (KEGG, http://www.genome.jp/kegg/), METLIN database (http://metlin.scripps.edu/), Lipid Maps (http://www.lipidmaps.org/), BioCyc (http://biocyc.org/), Spectral Database for organic compounds (http://sdbs.riodb.aist.go.jp).

Acknowledgements

Research projects in Dr. Chi Chen's lab are supported in part by an Agricultural Experiment Station project MIN-18-082 from the United States Department of Agriculture (USDA). We thank all the members in Dr. Chi Chen's lab for their help in preparing this protocol.

References

1. Jemal A, Siegel R, Xu J et al (2010) Cancer statistics, 2010. CA Cancer J Clin 60(5):277–300
2. Chen C, Kong ANT (2005) Dietary cancer-chemopreventive compounds: from signaling and gene expression to pharmacological effects. Trends Pharmacol Sci 26(6):318–326
3. Yang CS, Wang X, Lu G et al (2009) Cancer prevention by tea: animal studies, molecular mechanisms and human relevance. Nat Rev Cancer 9(6):429–439
4. Ahmad A, Sakr WA, Rahman KM (2010) Anticancer properties of indole compounds: mechanism of apoptosis induction and role in chemotherapy. Curr Drug Targets 11(6):652–666
5. Vander Heiden MG, Cantley LC, Thompson CB (2009) Understanding the Warburg effect: the metabolic requirements of cell proliferation. Science 324(5930):1029–1033
6. Gatenby RA, Gillies RJ (2004) Why do cancers have high aerobic glycolysis? Nat Rev Cancer 4(11):891–899
7. Lunt SY, Vander Heiden MG (2011) Aerobic glycolysis: meeting the metabolic requirements of cell proliferation. Annu Rev Cell Dev Biol 27:441–464
8. Tan AC, Konczak I, Sze DM et al (2011) Molecular pathways for cancer chemoprevention by dietary phytochemicals. Nutr Cancer 63(4):495–505
9. Lee KW, Bode AM, Dong Z (2011) Molecular targets of phytochemicals for cancer prevention. Nat Rev Cancer 11(3):211–218
10. Urich-Merzenich G, Zeitler H, Jobst D et al (2007) Application of the "-omic-" technologies in phytomedicine. Phytomedicine 14(1):70–82
11. Kersten RD, Dorrestein PC (2009) Secondary metabolomics: natural products mass spectrometry goes global. ACS Chem Biol 4(8):599–601
12. Chen V, Staub RE, Baggett S et al (2012) Identification and analysis of the active phytochemicals from the anti-cancer botanical extract Bezielle. PLoS One 7(1):e30107
13. Wang L, Chen C (2013) Emerging applications of metabolomics in studying chemopreventive phytochemicals. AAPS J 15(4):941–950

14. Sugimoto M, Kawakami M, Robert M et al (2012) Bioinformatics tools for mass spectroscopy-based metabolomic data processing and analysis. Curr Bioinform 7(1):96–108
15. Blekherman G, Laubenbacher R, Cortes DF et al (2011) Bioinformatics tools for cancer metabolomics. Metabolomics 7(3):329–343
16. Villas-Boas SG, Mas S, Akesson M et al (2005) Mass spectrometry in metabolome analysis. Mass Spectrom Rev 24(5):613–646
17. Folch J, Lees M, Sloane Stanley GH (1957) A simple method for the isolation and purification of total lipides from animal tissues. J Biol Chem 226(1):497–509

Chapter 8

^{1}H NMR Metabolomic Footprinting Analysis for the In Vitro Screening of Potential Chemopreventive Agents

Luca Casadei and Mariacristina Valerio

Abstract

Metabolomics is the quantification and analysis of the concentration profiles of low-molecular-weight compounds present in biological samples. In particular metabolic footprinting analysis, based on the monitoring of metabolites consumed from and secreted into the growth medium, is a valuable tool for the study of pharmacological and toxicological effects of drugs. Mass spectrometry and nuclear magnetic resonance (NMR) are the two main complementary techniques used in this field. Although less sensitive, NMR gives a direct fingerprint of the system, and the spectra obtained contain metabolic information that can be distilled by chemometric techniques.

In this chapter, we present how metabolomic footprinting can be used to assess in vitro a potential chemopreventive molecule as metformin.

Key words Chemoprevention, Metabolomics, Footprinting analysis, NMR spectroscopy, Principal component analysis, Euclidean distance

1 Introduction

One of the most promising preventive approach to the increased incidence of cancer [1, 2] is chemoprevention, which is defined as the use of natural, synthetic, or biological agents to reverse, suppress, or prevent either the first stages of carcinogenesis or the premalignant progression [3].

The first step to identify a chemopreventive agent is the use of epidemiological or preclinical activity or structure-activity relationship data. Then all the potential chemopreventive agents must pass through preclinical and clinical trials. The use of metabolomic analysis can be effective in many preclinical and clinical stages.

In this chapter, we show the use of ^{1}H-NMR metabolomic-based analysis for the first stage of preclinical study: the in vitro screening of a potential chemopreventive agent in relevant cell models.

Sabrina Strano (ed.), *Cancer Chemoprevention: Methods and Protocols*, Methods in Molecular Biology, vol. 1379,
DOI 10.1007/978-1-4939-3191-0_8,

For a comprehensive description of the biochemical responses of an organism to a drug intervention, the use of a non-target approach such as metabolomics can be indispensable in capturing global changes in biochemical networks and pathways within cells. Therefore, a metabolomic approach may allow us to disentangle the mysteries of a comprehensive description of the biochemical responses of an organism to a drug intervention: instead of assuming an *a priori* mechanistic hypothesis, a metabolomic approach offers the chance to capture global changes in biochemical networks and pathways in a "target-independent" way. The application of metabolomic techniques to characterize tumor-specific metabolic shifts in drug response is well established [4–6].

The metabolism of living cells produces in the culture medium a very unique metabolic footprint [7]. All the variations in the physiological state of cells due to environmental conditions or drug administration can be distinguished by differences in the profile of extracellular metabolites [8].

The analysis of extracellular metabolites, also known as metabolic footprinting, shows some advantages over the analysis of intracellular compounds, often referred as metabolic fingerprinting [9]. For instance, the intracellular metabolism is more dynamic and therefore, the turnover of most metabolites is extremely fast requiring an efficient quenching of cell metabolism, followed by an effective separation of intra- and extracellular metabolites and subsequent extraction of intracellular compounds [9]. Furthermore, the concentration of intracellular metabolites in cell extracts are lower compared with concentrations in extracellular samples. For these reasons, measurements of intracellular metabolites are time-consuming, economically demanding and subject to technical difficulties, which very often result in relatively poor reproducibility. In addition, there are several biochemical processes that are specifically related to the extracellular media, such as the degradation of complex substrates, and these can only be assessed by measuring the degradation products in the extracellular medium [10].

In this chapter, we show as case study the analysis of diverse molecular subtypes of human breast cancer cell lines, namely BT-474, MCF-7 and SUM-159-PT, in the presence or absence of metformin.

2 Materials

2.1 Medium Sample Collection

1. Collect at least 1.5 ml for sample in 2 ml Eppendorf tube.
2. Lyophilize each sample or dry to solid using a vacuum concentrator (*see* **Note 1**).

2.2 Reagents for Sample Preparation

1. Na_2HPO_4, 99 %, anhydrous.
2. NaH_2PO_4, 99 %, anhydrous.

3. Sodium salt of 3-(trimethylsilyl) propionic-2,2,3,3-d_4 acid, 98 atom % D (TSP).
4. Sodium azide (NaN_3).
5. D_2O, 99.9 atom % D.

2.3 Equipment

1. 500 MHz spectrometer (Bruker BioSpin Corp., Billerica, MA, USA, or Agilent Technologies, Santa Clara, CA, USA, or Jeol Ltd., Akishima, Tokyo, Japan). However, 400 or 600 MHz NMR instruments are commonly used in metabolomic studies.
2. Lyophilizator or vacuum concentrator.
3. Analytical balance.
4. 1.5 ml Eppendorf tubes.
5. Micropipettes and pipette tips.

2.4 Software for Data Analysis

Several commercial and free licensed software packages are available for NMR data processing, post-processing, and statistical analysis. Only the most widely used software are reported.

1. Software for processing NMR data: TopSpin (Bruker BioSpin Corp., Billerica, MA, USA), VNMRJ (Agilent Technologies, Santa Clara, CA, USA), MetaboLab [11] in the MATLAB programming environment (MathWorks, Inc., Natick, MA).
2. Software for post-processing NMR data: ACD/NMR processor (Advanced Chemistry Development Inc. (ACD/Labs), Toronto, ON, Canada), MetaboLab [11] in the MATLAB programming environment (MathWorks, Inc., Natick, MA).
3. Software for multivariate data analysis: SIMCA-P+ (Umetrics, Umeå, Sweden), PLS-Toolbox (Eigenvector Research, Manson, WA) in MATLAB.

3 Methods

3.1 Phosphate Buffer for NMR Sample Preparation

1. Prepare the 0.1 M D_2O (99.9 atom % D) phosphate buffer solution at pH 7.4 by mixing Na_2HPO_4 0.08 M (1.14 % w/v), NaH_2PO_4 0.02 M (0.24 % w/v), TSP 1 mM (0.017 % w/v) and NaN_3 10 mM (0.065 % w/v).

3.2 Sample Preparation for NMR Spectroscopy

1. Dissolve each sample in 700 µl of 0.1 M D_2O phosphate buffer solution at pH = 7.4.
2. Homogenize samples by using a vortex mixer for 1 min.
3. Centrifuge samples at 10,000 RCF for 10 min at room temperature to remove protein pellets. After centrifugation, transfer 600 µl of each resulting supernatant into a 5 mm NMR tube.

3.3 Acquisition, Processing, and Post-processing of NMR Data

3.3.1 NMR Setup

1. Set temperature to 298 K.
2. Properly position a representative sample inside the probe and leave for 5 min to equilibrate the sample temperature.
3. For obtaining a good signal-to-noise ratio: adjust the probe-head tuning and matching; lock and shim the sample on D_2O; calibrate the 90° pulse length; determine the power, length, and frequency offset for HDO signal suppression by using the presaturation pulse.
4. Once an optimal signal is obtained, transfer the setting parameters to the other samples (*see* **Notes 2–4**).

3.3.2 Two-Dimensional 2D ^{1}H J-Resolved

For the analysis of culture media, J-resolved pulse sequence is used to observe resonances better, as they are partially or completely buried in a typical 1D medium spectrum. This sequence improves the quality of the metabolic information extracted.

1. Acquire 2D ^{1}H J-resolved (JRES) NMR spectra using a double-spin echo sequence [12], suppressing the residual water signal with the presaturation technique.
2. Use the following parameters to acquire the JRES spectra: transients per increment, 4; total increments, 32; dummy scans, 16; data points, 16k; spectral width for direct (F2 or chemical shift) dimension, 6 kHz; spectral width for indirect (F1 or J-coupling) dimension, 40 Hz; relaxation delay, 2 s (approximately 11 min of acquisition for sample).
3. Process the NMR data carrying out the following operations: zero-fill the F1 data to 256 data points; multiply each free induction decay (FID) with a combined sine-bell/exponential function in the F2 dimension and a sine-bell function in the F1 dimension; apply Fourier transform to each dimension; tilt the spectra by 45°; symmetrize the spectra about F1 dimension; calibrate chemical shifts to the TSP methyl protons at 0.00 ppm; apply a zero-order baseline correction of spectrum.
4. Export the proton-decoupled skyline projections (p-JRES) in a suitable format (arrange the exported 1D-skyline projections into a matrix of N samples (rows) by M variables (columns)) for subsequent post-processing treatment.

3.3.3 NMR Data Post-processing

NMR data post-processing is a necessary step of metabolomics pipeline to extract useful information related to the state of cell. This step helps to avoid sources of variation in the data, such as dilution effect, subtle changes in chemical shifts, line-widths and baseline across series of spectra, which can interfere with the outcome of the statistical analysis, leading to false deductions.

NMR data post-processing usually includes exclusion of non-informative regions, binning, normalization, scaling, and data export for subsequent multivariate statistical analysis.

1. Remove the regions in the spectra that contain only noise and/or exogenous peaks. Therefore, exclude the spectral regions outside the window 0.5 (including TSP signal) and 9.0 ppm and those containing the residual water (δ 4.7–5.0 ppm) and drug peaks.
2. Reduce the dimensionality of data splitting the p-JRES spectra into small segments (bins or buckets) with variable widths ranging from 0.01 to 0.04 ppm to ensure that each bin contains the same signals throughout all the spectra. If local peak shifts across series of spectra are still observed, compress groups of bins into single bins or alignment the spectra. Then, integrate the signal within each bin (*see* **Note 5**).
3. Normalize the binned spectra by applying the Probabilistic Quotient Normalization (PQN) [13, 14] method to make spectra comparable:
   (a) Set the total spectral area of every spectrum to 100.
   (b) Calculate as reference spectrum the median spectrum (median of each variable/bin area) of control samples.
   (c) Calculate the quotient between the area of each spectral bin of the considered spectrum and that of the corresponding bin in the reference spectrum.
   (d) Calculate the median of all quotients.
   (e) Divide all variables of the considered spectrum by the median quotient.
   (f) Repeat the **steps c–e** for all spectra.
4. Scaling the data by applying the generalized log (g-log) transformation [15, 16] to make the variables within spectra comparable:
   (a) Estimate the g-log transformation parameter (λ) by maximum likelihood method using a set of five replicate measurements.
   (b) Obtain these five replicates from a single homogeneous pool of media from control and drug-treated cells. Process the replicate spectra as described above (i.e., selection of exclusion regions, binning and normalization).
5. Mean centred the data: subtract the mean value of each variable from the original data of that bin.

3.4 Statistical Analysis of NMR Data

1. Reduce the data by using principal component analysis (PCA). This process assigns to each sample score relative to each extracted component (principal component, PC). The extracted components are each other independent by construction, thus they are non-overlapping features of the studied system. Use the component scores to plot PC maps of the samples which best provide an indication of the differences between the classes in terms of metabolic similarity.

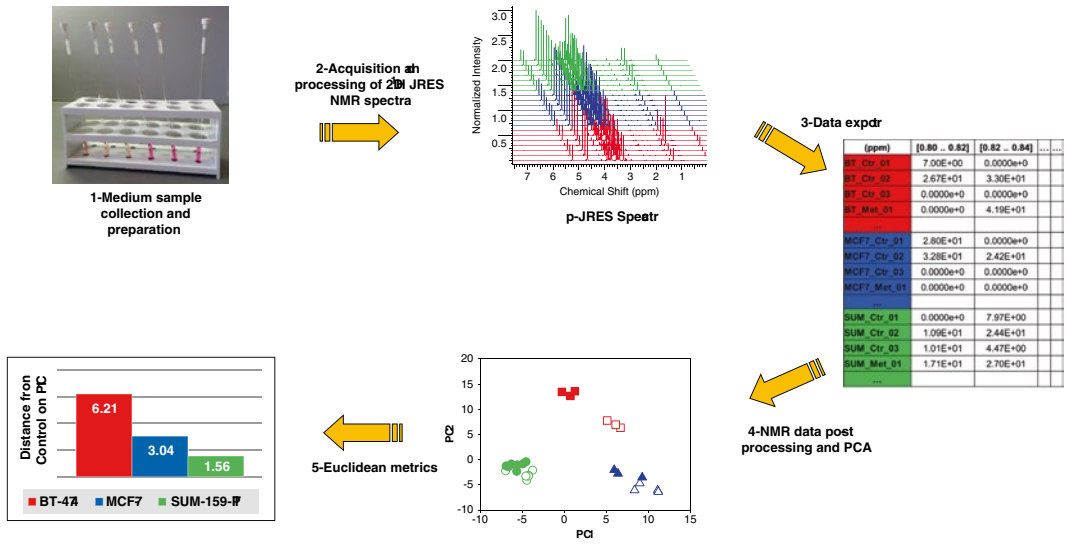

Fig. 1 Flowchart of ^{1}H NMR metabolomics footprinting analysis for the *in vitro* screening of potential chemopreventive agents

2. Carry out separate inferential statistics (*t*-test) on the different component scores, so to check for the statistical significance of the between groups differences.
3. Calculate the Euclidean distances between the centroids of each sample group (i.e., the barycenters of each sample group). This allows for a direct and easy estimation of the treatment effect on the metabolic components by examining the average difference in each PC score between control and treated groups. The fact components are each other independent by construction guarantees for the relevance of Euclidean metrics [17, 18].

We used the footprinting analysis protocol described above (Fig. 1) to investigate the metabolic responses of mammospheres from different molecular subtypes of human breast cancer, namely BT-474, MCF-7 and SUM-159-PT, to low dose of metformin. After NMR data post-processing, we applied PCA to a dataset of treated and untreated medium samples of the three cell lines. This produced a solution with five significant components, which together explain about 60 % of the total variability of the system. The PCA are depicted in Fig. 2, which shows score plot for the first two model components. A *t*-test was applied to these component scores in order to compare all the specific pairs of treated and untreated groups. The results highlight significant differences between the two groups on PC1 for BT-474 culture cells and on PC2 for BT-474, MCF-7, and SUM-159-PT (*see* Table 1).

Given that component scores are standardized to zero mean and unit standard deviation over the whole data set, we can measure the treatment effect on the metabolic components by

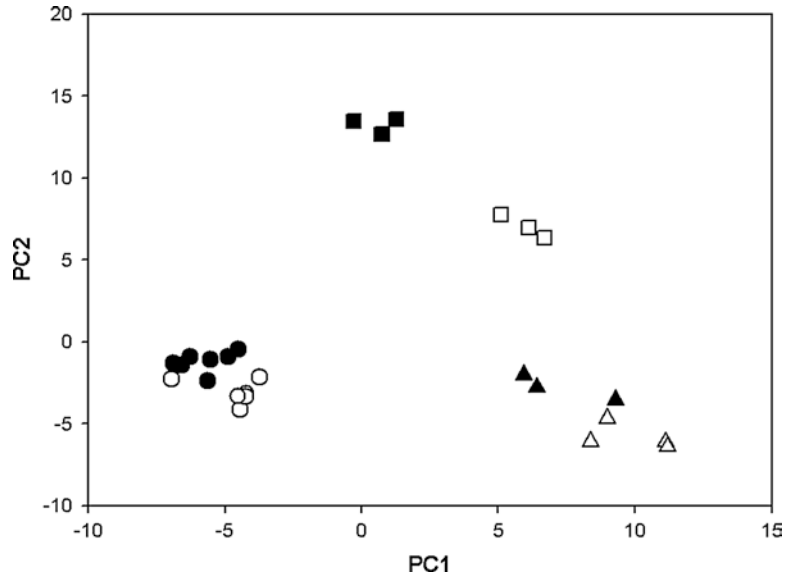

Fig. 2 Overview of the PCA model built on the pJRES NMR dataset of media samples of control and metformin-treated cultures per each cell lines. The score plot of the first two components (PC1 versus PC2) shows the differentiation between untreated and metformin-treated samples. Medium samples collected from BT-474, MCF-7, and SUM-159-PT untreated cell cultures are represented as *open squares*, *triangles*, and *circles*, respectively, those of treated cell cultures as *filled squares*, *triangles*, and *circles*, respectively

Table 1

Average differences in PC1 and PC2 scores between untreated and treated groups

	Cell line		
PCs	**BT-474**	**MCF-7**	**SUM-159-PT**
PC1	5.40**	–	–
PC2	6.21***	3.04**	1.56**

Statistics: $p<0.05$; **, $p<0.01$; ***, $p<0.001$

examining the average difference in each PC score between control and treated groups. The distance between centroids of control and treated groups is 5.40 for BT-474 on PC1 and 6.21 for BT-474, 3.04 for MCF-7, and 1.56 for SUM-159-PT on PC2 (*see* Table 1). Thus, the results indicate that the treatment has a marked line specific effect. The maximum difference between untreated and treated groups (and, therefore, the maximum drug effects) is observed for BT-474 on PC1. No metabolic differences between control and treated groups are observed for MCF-7 and SUM-159-PT cells on PC1. Still metformin alters the metabolic

pathways described by PC2 in all cell lines with a major effect of the drug on BT-474 cells and a minor effect on SUM-159-PT.

In summary, ^{1}H-NMR metabolomic profiles of BT-474, MCF-7 and SUM-159-PT cell culture media display significant differences between metformin-treated and untreated cells in all breast cell lines, even with some differences between the cell lines.

4 Notes

1. If you cannot lyophilize the medium samples immediately after collection, store them at −80 °C.
2. For each experiment, the magnetic field homogeneity must be optimized through an accurate shimming. To check if a sample is properly shimmed, you can observe the full-width at half-maximum of lactate peak that should be less than 1.7 Hz, (before applying apodization) and symmetric shape. TSP peak is not a reliable signal to check the quality of shimming due to the huge amount of proteins present in the sample, which influence its line-width because TSP binds to proteins.
3. Samples must be acquired in randomized order.
4. It is useful to run standard solution to identify potential impurities arising from reagents and preparation procedures.
5. The most common method of spectral binning is the so-called equidistant binning, i.e. each spectrum is divided into bins with fixed width, typically 0.04 ppm. The weakness of this method is that, under certain experimental conditions, single peaks can be divided into two neighboring bins, generating artifacts. To avoid this problem, several mathematical algorithms [19–22] have been developed to vary the individual size bin. For example, ACD intelligent bucketing method (ACD/NMR processor, Advanced Chemistry Development Inc. (ACD/Labs), Toronto, ON, Canada), a combination of equidistant binning and non-equidistant binning, sets the bucket divisions at local minima (within the spectra) to ensure that each resonance is in the same bin throughout all spectra.

Acknowledgements

We thank Prof. Cesare Manetti, supervisor of NMR Laboratory of Chemistry Dpt., “Sapienza” University of Rome. We thank all the members of Dr. Giovanni Blandino’s and Dr. Sabrina Strano’s laboratories, Italian National Cancer Institute “Regina Elena,” Rome, Italy, for many years of collaboration in the metformin project. We are grateful to Dr. Alessandro Giuliani, Dpt. of Environment and Primary Prevention, Istituto Superiore di Sanità, Rome, Italy, for his useful comments and suggestions on the data analysis.

References

1. Parkin DM, Bray F, Ferlay J et al (2005) Global cancer statistics, 2002. CA Cancer J Clin 55:74–108
2. Jemal A, Siegel R, Ward E et al (2008) Cancer statistics, 2008. CA Cancer J Clin 58:71–96
3. Sporn MB (1976) Approaches to prevention of epithelial cancer during the preneoplastic period. Cancer Res 36:2699–2702
4. Griffin JL, Shockcor JP (2004) Metabolic profiles of cancer cells. Nat Rev Cancer 4:551–561
5. Spratlin L, Serkova NJ, Eckhardt SG (2009) Clinical applications of metabolomics in oncology: a review. Clin Cancer Res 15:431–440
6. Tiziani S, Kang Y, Choi JS et al (2011) Metabolomic high-content nuclear magnetic resonance-based drug screening of a kinase inhibitor library. Nat Commun 2:545–555
7. Kell DB, Brown M, Davey HM et al (2005) Metabolic footprinting and systems biology: the medium is the message. Nat Rev Microbiol 3:557–565
8. Allen J, Davey HM, Broadhurst D et al (2003) High-throughput classification of yeast mutants for functional genomics using metabolic footprinting. Nat Biotechnol 21:692–696
9. Villas-Bôas SG, Højer-Pedersen J, Akesson M et al (2005) Global metabolite analysis of yeast: evaluation of sample preparation methods. Yeast 22:1155–1169
10. Villas-Bôas SG, Noel S, Lane GA et al (2006) Extracellular metabolomics: a metabolic footprinting approach to assess fiber degradation in complex media. Anal Biochem 349:297–305
11. Ludwig C, Günther UL (2011) MetaboLab - advanced NMR data processing and analysis for metabolomics. BMC Bioinform 12:366
12. Thrippleton MJ, Edden RA, Keeler J (2005) Suppression of strong coupling artefacts in J-spectra. J Magn Reson 174:97–109
13. Dieterle F, Ross A, Schlotterbeck G et al (2006) Probabilistic quotient normalization as robust method to account for dilution of complex biological mixtures. Application in H-1 NMR metabolomics. Anal Chem 78:4281–4290
14. Dieterle F, Riefke B, Schlotterbeck G et al (2011) NMR and MS methods for metabolomics. Methods Mol Biol 691:385–415
15. Purohit PV, Rocke DM, Viant MR et al (2004) Discrimination models using variance-stabilizing transformation of metabolomic NMR data. OMICS 8:118–130
16. Parsons HM, Ludwig C, Gunther UL et al (2007) Improved classification accuracy in 1-and 2-dimensional NMR metabolomics data using the variance stabilising generalised logarithm transformation. BMC Bioinform 8:234–250
17. Blandino G, Valerio M, Cioce M et al (2012) Metformin elicits anticancer effects through the sequential modulation of DICER and c-MYC. Nat Commun 3:865–876
18. Cioce M, Valerio M, Casadei L et al (2014) Metformin-induced metabolic reprogramming of chemoresistant ALDH^{bright} breast cancer cells. Oncotarget 5:4129–4143
19. Dieterle F, Ross A, Schlotterbeck G et al (2006) Metabolite projection analysis for fast identification of metabolites in metabonomics. Application in an amiodarone study. Anal Chem 78:3551–3561
20. Davis RA, Charlton AJ, Godward J et al (2007) Adaptive binning: an improved binning method for metabolomics data using the undecimated wavelet transform. Chemometr Intell Lab 85:144–154
21. De Meyer T, Sinnaeve D, Van Gasse B et al (2008) NMR-based characterization of metabolic alterations in hypertension using an adaptive, intelligent binning algorithm. Anal Chem 80:3783–3790
22. Anderson PE, Mahle DA, Doom TE et al (2011) Dynamic adaptive binning: an improved quantification technique for NMR spectroscopic data. Metabolomics 7:179–190

Chapter 9

Comet Assay in Cancer Chemoprevention

Raffaela Santoro, Maria Ferraiuolo, Gian Paolo Morgano, Paola Muti, and Sabrina Strano

Abstract

The comet assay can be useful in monitoring DNA damage in single cells caused by exposure to genotoxic agents, such as those causing air, water, and soil pollution (e.g., pesticides, dioxins, electromagnetic fields) and chemo- and radiotherapy in cancer patients, or in the assessment of genoprotective effects of chemopreventive molecules. Therefore, it has particular importance in the fields of pharmacology and toxicology, and in both environmental and human biomonitoring. It allows the detection of single strand breaks as well as double-strand breaks and can be used in both normal and cancer cells. Here we describe the alkali method for comet assay, which allows to detect both single- and double-strand DNA breaks.

Key words Comet assay, DNA damage, DNA repair, Single-cell gel electrophoresis (SCGE), Genotoxic stress, Double-strand breaks (DSB), Single-strand breaks (SSB)

1 Introduction

The first method for comet assay was described in 1990 [1], when migration of the DNA from a single cell was observed as a comet, having high-molecular-weight DNA in the head and migrating fragments (i.e., damaged DNA) in the tail. The concept of tail moment was introduced as the product between the amount of DNA in the tail and the tail length, and a software which could measure it was developed. Comet assay can be used to assess the heterogeneity of DNA damage in a cell population: it has been first used in cells treated with bleomycin [2] and then to monitor the chemoresistance of human cancers and 3D cultures [3–5]. It is now well established as a method to detect DNA damage caused by chemo- and radiotherapeutic treatments on tumours [6–8], as well as to measure the extent of DNA repair in cancer cells [9–12]. Comet assay founds its application in (1) biomonitoring of DNA damaging exposure (DNA damage due to air, soil and water pollution, and to radiation exposure, such as after the Chernobyl accident) [13–18], (2) biomonitoring of phytochemical effects (such

Sabrina Strano (ed.), *Cancer Chemoprevention: Methods and Protocols*, Methods in Molecular Biology, vol. 1379,
DOI 10.1007/978-1-4939-3191-0_9,

as green tea, cranberry juice, carotenoids) [19–21], and (3) in cancer, although some studies in lung and prostate cancer have shown no differences in the levels of DNA damage in tumours as compared to control cells [22–30].

It is important to notice that there are some limitations to the comet assay. The samples should be viable as the presence of specific lesions cannot be detected in apoptotic or necrotic cells. Tissue disaggregation should be fast but gentle in order to minimize DNA damage due to sample handling. The number of cells that can be analysed is limited, as individual scoring of the comets does not allow to analyze more than 40–50 slides per day.

Two variations of the comet assay exist: one (neutral method) can detect only double-strand breaks (DSB), while the other (alkali method, which we describe here) can detect both single- and double-strand breaks.

2 Materials

Prepare all solutions using ultrapure water (deionized water purified to attain 18 MΩ cm at 25 °C) and analytical grade reagents. Always place 70 % volume of ultrapure water in the cylinder before adding solid reagents. When they are completely dissolved, adjust the volume. Use special care when weighing and dissolving solid NaOH. Store all reagents at room temperature, unless indicated otherwise.

1. Agarose-coated microscopy slides.
   (a) One-end-frosted microscopy slides. Store them at –20 °C in their own package.
   (b) Normal melting agarose (NMA) solution: 1 % NMA in ultrapure water. Dissolve 300 mg NMA in 30 ml ultrapure water in a glass bottle and heat in microwave at low power.
2. Low melting agarose (LMA solution): 1 % LMA in DPBS. Dissolve 100 mg LMA in 10 ml DPBS and heat in microwave at low power. Prepare 90 μl aliquots in microcentrifuge tubes (*see* **Note 1**).
3. Lysis solution: 2.5 M NaCl, 100 mM EDTA, 10 mM Tris base, 8 g/l NaOH, 1 % Triton X-100, 10 % DMSO. Dissolve 147.1 g NaCl anhydrous, 29.22 g EDTA, 1.21 g Tris base, 8 g NaOH in 1 l ultrapure water and store at room temperature. One hour before use, add 500 μl Triton X-100 and 5 ml DMSO to 50 ml lysis solution and store at +4 °C.
4. Electrophoresis running buffer: 300 mM NaOH, 1 mM EDTA, pH 13.0. Dissolve 12 g NaOH and 2.92 g EDTA in 1 l ultrapure water. pH will be 13.0. Store at room temperature.

5. Neutralization buffer: 0.4 M Tris-Cl, pH 8.0. Prepare 1 M Tris-Cl stock solution by dissolving 121 g Tris base in 1 l ultrapure water, adjust pH to 8.0 with HCl, and sterilize by autoclaving. Dilute 20 ml 1 M Tris-Cl, pH 8.0 to 50 ml with ultrapure water.
6. Propidium iodide staining solution: 20 μg/ml propidium iodide in DPBS. Dilute 1 mg/ml propidium iodide stock solution in DPBS. You will need 50 μl/slide.
7. Horizontal electrophoresis apparatus (tank and power supply).
8. Heat-block equipped with 1.5 ml tubes rack.
9. Fluorescence microscope equipped with an excitation filter of 515–560 nm, 100× magnification objective, and a CCD camera.
10. Computer and analysis software.

3 Methods

Carry out all the procedures at room temperature unless otherwise specified. The procedure cannot be paused until slides are dried (about 4–5 h from the beginning).

3.1 Treatment of Cells

Seed 5×10^4 cells in 35 mm diameter dishes on day 1. On day 2, pretreat the cells with melatonin (or another chemopreventive agent), then add the chemotherapeutic drugs of choice or irradiate with UV or γ-ray. On day 3 (24 h posttreatment), wash cells with DPBS, and then detach them with trypsin.

3.2 Preparing Agarose-Coated Slides

Remove microscopy slides from the –20 °C freezer. Cut the edge of a 1 ml pipette tip to enlarge its opening. Wipe each of the microscopy slides with a dry paper towel to remove condensation just prior to coat it with NMA (*see* **Note 2**). Hold the slide at a 45° angle onto the NMA containing glass bottle and pipette 500 μl NMA solution onto the slide, allowing excess solution to fall back into the bottle (Fig. 1). Lean it under the fume hood with the agarose-coated side facing upward. Allow the slides to dry for at least 30 min or until the agarose coating cannot be seen anymore. Mark the agarose-coated side of the slides (*see* **Note 3**).

3.3 Embedding Cells in LMA

Place a microcentrifuge tube containing LMA solution for each of your samples in a heat block previously set at 60 °C for 15 min to allow LMA to melt. Lower the temperature to 38 °C and use the aliquots only when they have reached this temperature (*see* **Note 4**). Place as many NMA-coated slides as your samples close to the heat block and mark them with samples names. In the meantime, collect cells, spin down briefly, and wash them with DPBS (200 μl for a 35 mm dish); spin down briefly and resuspend in 10 μl DPBS.

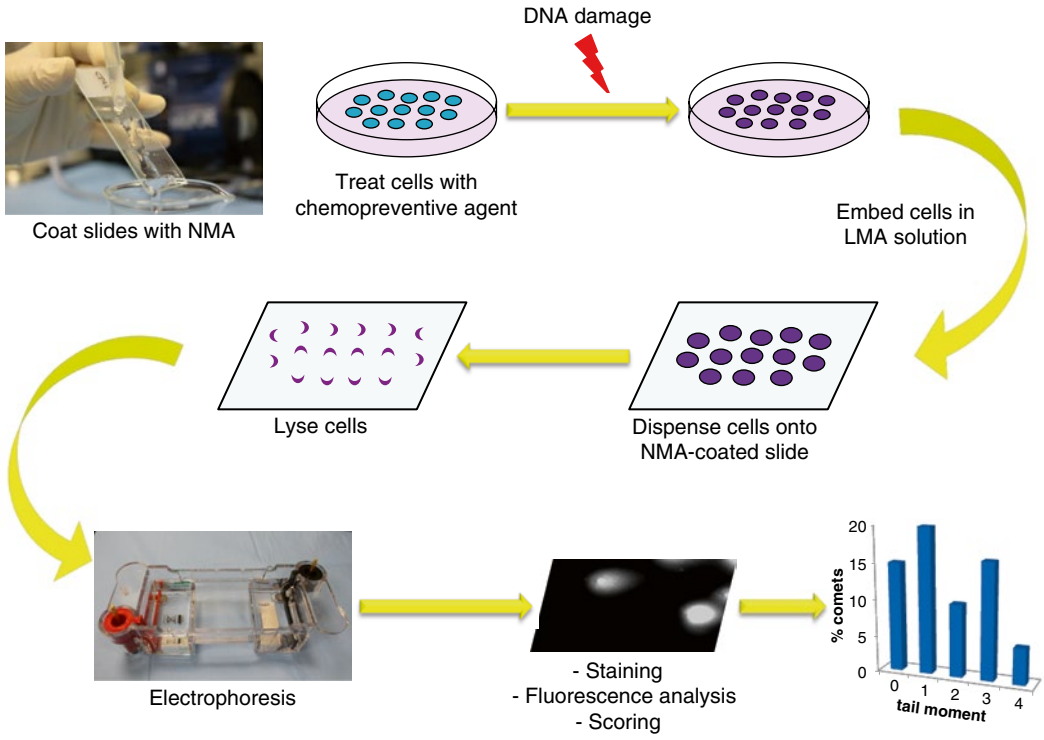

Fig. 1 Comet assay workflow. Comet assay procedure is indicated step by step

If LMA aliquots have not reached 38 °C, keep cells on ice to avoid DNA repair. Cut the edge of a 200 µl pipette tip and dispense sample into an aliquot of LMA solution. Mix and dispense immediately onto a NMA-coated slide (Fig. 1); cover with a cover slip and apply gentle pressure to spread cells. Avoid air bubbles. Repeat for all your samples. Let the cells-LMA solidify, and then remove cover slips.

3.4 Lysing Cells

Place the slides horizontally into a container and submerge them gently in cold lysis solution containing Triton X-100 and DMSO (Fig. 1). Incubate for 1 h at room temperature (*see* **Note 5**).

3.5 Equilibrating the Slides

Discard lysis solution and submerge the slides in running buffer for 20 min. Be gentle when pouring running buffer as agarose can come off the slides.

3.6 Running

Dispose the slides into a horizontal electrophoresis tank for nucleic acids and add as much running buffer as to cover the slides (Fig. 1). Run for 20 min at 300 mA and 0.6–1 V/cm length of the tank (*see* **Note 6**) to allow for proper run.

3.7 Neutralization of Samples

Gently remove the slides from the running tank and dispose them horizontally in a container. Gently wash with deionized water to remove running buffer. Submerge in neutralization buffer and incubate for 5 min. Repeat three times. Wash with deionized water.

3.8 Drying the Samples

Under a fume hood, hold the slides at a 45° angle and dispense 1 ml methanol onto the agarose with a pipet. Place horizontally and allow to completely dry (*see* **Note 7**).

3.9 Staining and Imaging

Slides can be stained by pipetting 50 μl propidium iodide solution (*see* **Note 8**) and covering with a cover slip. Samples can be visualized under a fluorescence microscope using an excitation filter of 515–560 nm. 100× magnification can be used to analyze comets (Fig. 1).

3.10 Scoring Comets

The extent of DNA damage will be estimated by both counting the comets and scoring the tail moment. Comets at the edge of the cover slips should not be taken into consideration as they usually do not run properly. In the case of melatonin, its presence strongly inhibits DNA damage hence comet tails disappear following melatonin pretreatment; thus either comets with tail or comets without tail will be observed. In the case of other pretreatments, the effect can be not so striking; thus assignment of a score to different kinds of comets is needed. There is a great number of softwares that analyze the percentage of DNA in the head or in the tail and the tail moment (i.e., the product between the amount of DNA in the tail and the tail length). Otherwise, visual scoring can be performed by measuring the tail length of each comet and assigning a score to each length, ranging from 0 for comets without tail to 4 for comets which almost lost their head and show almost all their DNA in the tail (Fig. 2).

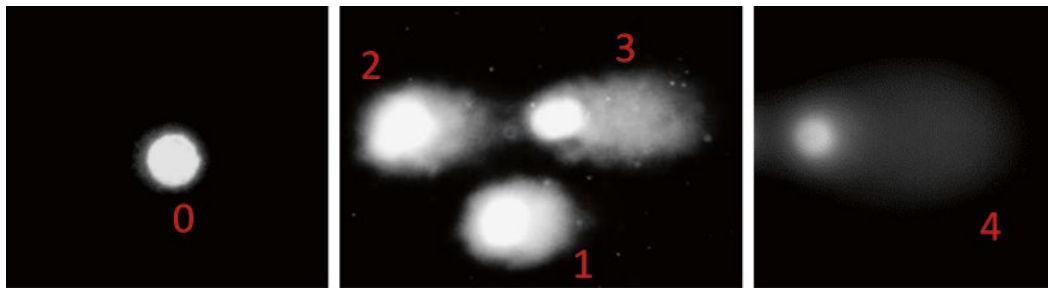

Fig. 2 Comets. Sample images are shown. Numbers in *red* indicate the score given to each comet according to the tail length

4 Notes

1. If sterile microcentrifuge tubes are used and LMA solution is dispensed when its temperature is still around 50–60 °C, aliquots can be stored for a few months. Prior to use be sure no contaminants have grown into LMA.
2. Removing condensation from microscopy slides is essential to avoid agarose comes off the slide while lysing cells or during the run.
3. Dry NMA-coated slides can be stored in a microscopy slides box at room temperature for a few months. Be sure to store them in a cool and dry place, possibly with desiccant.
4. If the cells are embedded into LMA at a temperature higher than 38 °C, DNA damage will occur.
5. Most cancer cells can be lysed by incubation in lysis solution for 1 h at room temperature. However, some cell types, such as Sk-Br-3, need a longer incubation. In these cases, incubate the slides over night at 4 °C. Such long incubation can cause NMA to come off the slides, therefore particular care should be used when handling them.
6. The length of the tank is measured from anode to cathode. In order to reach 300 mA and 0.6–1 V/cm, the volume of the running buffer should be adjusted.
7. Slides can be stored for up to 1 month before analysis. Store in a cool and dry place.
8. Slides stained with propidium iodide, as well as ethidium bromide, cannot be stored and therefore should be analyzed immediately.

References

1. Olive PL, Banath JP, Durand RE (1990) Heterogeneity in radiation-induced DNA damage and repair in tumor and normal cells measured using the "comet" assay. Radiat Res 122:86–94
2. Ostling O, Johanson KJ (1987) Bleomycin, in contrast to gamma irradiation, induces extreme variation of DNA strand breakage from cell to cell. Int J Radiat Biol Relat Stud Phys Chem Med 52:683–691
3. Olive PL, Banath JP (1993) Detection of DNA double-strand breaks through the cell cycle after exposure to X-rays, bleomycin, etoposide and 125IdUrd. Int J Radiat Biol 64:349–358
4. Olive PL, Banath JP (1997) Multicell spheroid response to drugs predicted with the comet assay. Cancer Res 57:5528–5533
5. Olive PL, Johnston PJ, Banath JP et al (1998) The comet assay: a new method to examine heterogeneity associated with solid tumors. Nat Med 4:103–105
6. Almeida GM, Duarte TL, Steward WP et al (2006) Detection of oxaliplatin-induced DNA crosslinks in vitro and in cancer patients using the alkaline comet assay. DNA Repair (Amst) 5:219–225
7. Dorie MJ, Kovacs MS, Gabalski EC et al (1999) DNA damage measured by the comet assay in head and neck cancer patients treated with tirapazamine. Neoplasia 1:461–467
8. Olive PL, Durand RE, Jackson SM et al (1999) The comet assay in clinical practice. Acta Oncol 38:839–844
9. Ostling O, Johanson KJ (1984) Microelectrophoretic study of radiation-

induced DNA damages in individual mammalian cells. Biochem Biophys Res Commun 123:291–298

10. Santoro R, Marani M, Blandino G et al (2012) Melatonin triggers p53Ser phosphorylation and prevents DNA damage accumulation. Oncogene 31:2931–2942
11. Santoro R, Mori F, Marani M et al (2013) Blockage of melatonin receptors impairs p53-mediated prevention of DNA damage accumulation. Carcinogenesis 34:1051–1061
12. Singh NP, Mccoy MT, Tice RR et al (1988) A simple technique for quantitation of low levels of DNA damage in individual cells. Exp Cell Res 175:184–191
13. Coronas MV, Pereira TS, Rocha JA et al (2009) Genetic biomonitoring of an urban population exposed to mutagenic airborne pollutants. Environ Int 35:1023–1029
14. Moller P, Loft S (2010) Oxidative damage to DNA and lipids as biomarkers of exposure to air pollution. Environ Health Perspect 118:1126–1136
15. Mondal NK, Mukherjee B, Das D et al (2010) Micronucleus formation, DNA damage and repair in premenopausal women chronically exposed to high level of indoor air pollution from biomass fuel use in rural India. Mutat Res 697:47–54
16. Pandey AK, Bajpayee M, Parmar D et al (2005) DNA damage in lymphocytes of rural Indian women exposed to biomass fuel smoke as assessed by the Comet assay. Environ Mol Mutagen 45:435–441
17. Piperakis SM, Petrakou E, Tsilimigaki S (2000) Effects of air pollution and smoking on DNA damage of human lymphocytes. Environ Mol Mutagen 36:243–249
18. Valverde M, Rojas E (2009) Environmental and occupational biomonitoring using the Comet assay. Mutat Res 681:93–109
19. Collins AR, Olmedilla B, Southon S et al (1998) Serum carotenoids and oxidative DNA damage in human lymphocytes. Carcinogenesis 19:2159–2162
20. Duthie SJ, Jenkinson AM, Crozier A et al (2006) The effects of cranberry juice consumption on antioxidant status and biomarkers relating to heart disease and cancer in healthy human volunteers. Eur J Nutr 45:113–122
21. Glei M, Habermann N, Osswald K et al (2005) Assessment of DNA damage and its modulation by dietary and genetic factors in smokers using the Comet assay: a biomarker model. Biomarkers 10:203–217
22. Gabelova A, Farkasova T, Gurska S et al (2008) Radiosensitivity of peripheral blood lymphocytes from healthy donors and cervical cancer patients; the correspondence of in vitro data with the clinical outcome. Neoplasma 55:182–191
23. Kosti O, Goldman L, Saha DT et al (2011) DNA damage phenotype and prostate cancer risk. Mutat Res 719:41–46
24. Lorenzo Y, Provencio M, Lombardia L et al (2009) Differential genetic and functional markers of second neoplasias in Hodgkin's disease patients. Clin Cancer Res 15:4823–4828
25. Mckenna DJ, Mckeown SR, Mckelvey-Martin VJ (2008) Potential use of the comet assay in the clinical management of cancer. Mutagenesis 23:183–190
26. Pavlov VV, Aleshchenko AV, Antoshchina MM et al (2010) Molecular-cellular characteristic of blood lymphocytes in Hodgkin lymphoma. Radiats Biol Radioecol 50:508–513
27. Santos RA, Teixeira AC, Mayorano MB et al (2010) Basal levels of DNA damage detected by micronuclei and comet assays in untreated breast cancer patients and healthy women. Clin Exp Med 10:87–92
28. Sigurdson AJ, Jones IM, Wei Q et al (2011) Prospective analysis of DNA damage and repair markers of lung cancer risk from the Prostate, Lung, Colorectal and Ovarian (PLCO) Cancer Screening Trial. Carcinogenesis 32:69–73
29. Synowiec E, Stefanska J, Morawiec Z et al (2008) Association between DNA damage, DNA repair genes variability and clinical characteristics in breast cancer patients. Mutat Res 648:65–72
30. Vasavi M, Vedicherala B, Vattam KK et al (2010) Assessment of genetic damage in inflammatory, precancerous, and cancerous pathologies of the esophagus using the comet assay. Genet Test Mol Biomarkers 14:477–482

Chapter 10

Angiogenesis Assays

Dhanya K. Nambiar, Praveen K. Kujur, and Rana P. Singh

Abstract

Neoangiogenesis constitutes one of the first steps of tumor progression beyond a critical size of tumor growth, which supplies a dormant mass of cancerous cells with the required nutrient supply and gaseous exchange through blood vessels essentially needed for their sustained and aggressive growth. In order to understand any biological process, it becomes imperative that we use models, which could mimic the actual biological system as closely as possible. Hence, finding the most appropriate model is always a vital part of any experimental design. Angiogenesis research has also been much affected due to lack of simple, reliable, and relevant models which could be easily quantitated. The angiogenesis models have been used extensively for studying the action of various molecules for agonist or antagonistic behaviour and associated mechanisms. Here, we have described two protocols or models which have been popularly utilized for studying angiogenic parameters. Rat aortic ring assay tends to bridge the gap between in vitro and in vivo models. The chorioallantoic membrane (CAM) assay is one of the most utilized in vivo model system for angiogenesis-related studies. The CAM is highly vascularized tissue of the avian embryo and serves as a good model to study the effects of various test compounds on neoangiogenesis.

Key words Neoangiogenesis, Rat aortic ring, Matrigel, Angiogenesis, Chorioallantoic membrane, Egg, Blood vessel

1 Introduction

Angiogenesis is an important step in the growth and progression of solid tumors and it starts with the need for the cancer/tumor to obtain sustained blood supply. Hence angiogenesis or the formation of new blood vessels from pre-existing vessels is one of the most important steps in tumor growth and progression. The switch from dormant tumor mass less than 2 mm^3 in size to an actively growing tumor, initiates a step forward in tumor progression [1]. The supply of blood vessels also facilitates the movement of these cancer cells from the primary site of the tumor to distant parts, leading to metastases. Since Judah Folkman in his landmark paper highlighted the importance of angiogenesis [2], many tools and techniques have been developed to understand the basic biology behind the process of angiogenesis and the factors which could

Sabrina Strano (ed.), *Cancer Chemoprevention: Methods and Protocols*, Methods in Molecular Biology, vol. 1379,
DOI 10.1007/978-1-4939-3191-0_10,

work either as pro-angiogenic or anti-angiogenic [3]. This has also led to the development of many agents and pharmaceutical interventions, which target the process of tumor angiogenesis, thereby limiting the growth of tumor. However, in some pathological situations such as wound closure or diabetic retinopathy, there may be a need to induce angiogenesis [4].

Angiogenesis is a complex process, which involves multiple steps including endothelial cell proliferation, migration, tube formation, microvasculature development and branching, pericyte recruitment, and tissue remodeling [5]. All these processes are intricately governed by various growth factors, matrix remodeling enzymes, and other proteins. Hence, in order to understand and develop targets for inhibiting angiogenesis, many in vitro, ex vivo, and in vivo models have been used successfully. Each of these models has its own advantages and disadvantages. Currently, the most commonly used models for angiogenesis include Matrigel tube formation assay, invasion/migration using Boyden chamber, rabbit ear chamber, the rat dorsal skin, corneal angiogenesis in rodents, chick chorioallantoic membrane (CAM) assay, Matrigel plug assay, and most recently zebrafish (*Danio rerio*) embryos have also been utilized to study the mechanisms of angiogenesis. Here we describe two of these models, which have been used successfully to study or mimic the process of angiogenesis.

1.1 3D-Ex Vivo Aortic Ring Angiogenesis Assay

This was first developed by Nicosia and Offinette as an ex vivo model [6]. Though many in vitro assays have been developed for the study of angiogenesis, most of which utilize the endothelial cell function as a parameter of measurement. However, these assays do not show involvement or the role of adjacent blood vessels and other surrounding cells. The endothelial tube formation assay which is used in majority of the studies is an example of this aspect. In addition, tube formation cannot be equated to actual blood vessel formation. Hence, the aortic ring assay, which basically studies the role of both endothelial cells and pericytes is a good way to recapitulate in vivo angiogenesis [7]. Also, this assay mimics the time period taken for the vessel formation under in vivo condition.

1.2 Chick Chorioallantoic Membrane Assay

The chick development process from fertilization to hatching takes around 21 days. The chick has four extraembryonic membranes including the yolk sac, amnion, chorion and the allantois. After the fertilization occurs, the allantois grows rapidly between the 4th and the 11th day of the development. During the process, the mesodermal layer of the allantois joins with the mesoderm of the chorion to form a fused double mesodermal layer known as the chorionic allantoic membrane [8]. Till day 8 of the development, the primitive blood vessels continue to grow and form a network of capillaries. The growth of CAM vasculature happens rapidly

from 4th to the 11th day, after which the endothelial cell mitotic index reduces dramatically and eventually completes by 18th day of development. The rapid development of blood vessel in this model and its ease of manipulation makes it one of the most economical and widely used in vivo models for screening the agonist and antagonist behavior of various agents against angiogenesis [7, 8, 9, 10]. The agent to be tested is applied focally onto the developed CAM. The test agent is usually introduced in the form of small filter disks or polymerized materials such as methylcellulose, gelatin or any other biologically inert synthetic polymer. It is quick and semi-quantifiable, economical, and good for the screening of many novel pro- or antiangiogenic agents. The measurement parameters which can be obtained from this assay include blood vessel number, density, branch point number, diameter, and blood flow. Test of an anti-angiogenic agent is based on the development of an avascular zone or a zone of inhibition at the site of application. The avascular zone diameter is an indicative of anti-angiogenic ability of the compound.

2 Materials

2.1 3D- Ex Vivo Aortic Ring Angiogenesis Assay

1. Animal: Rat or mice (adult C57BL/6 mice of 7–12 weeks of age).
2. Penicillin-streptomycin (10,000 U/ml penicillin and 10 mg/ml streptomycin). Use 1 % pen-strep antibiotic.
3. Sterile cold PBS containing 1 % pen-strep solution.
4. Matrigel (basement membrane matrix).
5. Endothelial cell growth media (with Bullet Kit).
6. 48-Well cell culture plate.
7. Syringe (1 ml).
8. Needles (27-G).
9. Dissection kit: Sterile—scalpel, forceps, blunt and fine scissors.
10. 70 % Ethanol.

2.2 Chick Chorioallantoic Membrane Assay

1. Fertilized chicken eggs.
2. 2 ml syringes with 21-G needle.
3. 5 ml syringes with 27-G needle.
4. Curved pointed forceps and small dissecting scissors.
5. Filter-paper disk (Whatman, catalog number: 1441150).
6. 1 % aqueous methyl cellulose.
7. 70 % ethanol.
8. Scotch tape.
9. Humidified incubator (37–38 °C).

10. Complete endothelial cell culture medium with supplements.
11. Phase-contrast microscope fitted with a camera.
12. 25- or 26-G hypodermic needles and 1 ml syringes.

3 Methods

3.1 3D-Ex Vivo Aortic Ring Angiogenesis Assay

3.1.1 Mice/Rat Dissection

1. For the experiment mice/rat (8–12 weeks) could be used. The animal is sacrificed by CO_2 asphyxiation and/or cervical dislocation.
2. The animal is wiped thoroughly with 70 % ethanol and transferred to the laminar flow by mounting on a surgical wax tray such that the ventral side is facing upwards and the limbs are extended out and fixed on the board.
3. Using a scissor an incision is made and the skin over the ventral side is opened up.
4. A cut is now made around the rib cage and the chest cavity is opened up through the sternum. Holding the heart using a forceps, lungs and the heart are lifted up for the best view of the thoracic aorta. Next, these organs are removed/cut out, so that the spine is visible. The thoracic aorta could be seen as a white line running along the length of the spine covered with a fat layer.
5. Grasping the anterior end of the aorta with a forceps, the aortic connections to the spine is detached by finely running the scissor below it. Now the aorta is cut at the posterior end and holding it by the forceps, a cut is made now at the anterior end. This would give us a good length of the thoracic aorta, which is transferred to a petri dish containing chilled PBS with 1 % antibiotic.

3.1.2 Sectioning into Aortic Rings

1. Keeping the aortic tissue in PBS, with the help of the forceps and scalpel, the attached fat layer or adventia is slowly removed without damaging the aorta. Using the 27-G needle fixed to 1 ml syringe flush out any remnant blood from the vessels. (*Note*: Be gentle but firm while cleaning the aorta walls making sure not to damage the aortic wall, as the sprouting density is affected by mechanical damage to vessel endothelium.)
2. Using a sharp blade, clean and uniform horizontal sections (rings) of 0.5–1 mm thickness are made. (*Note*: Keep the ring thickness as uniform as possible, since it affects the overall rate of sprouting.) The rings are rinsed well with PBS and transferred to a fresh petri dish containing sterile PBS for further cleaning. (*Note*: At this stage, the aortic rings can be stored at 4 °C for 3–4 h in PBS.)

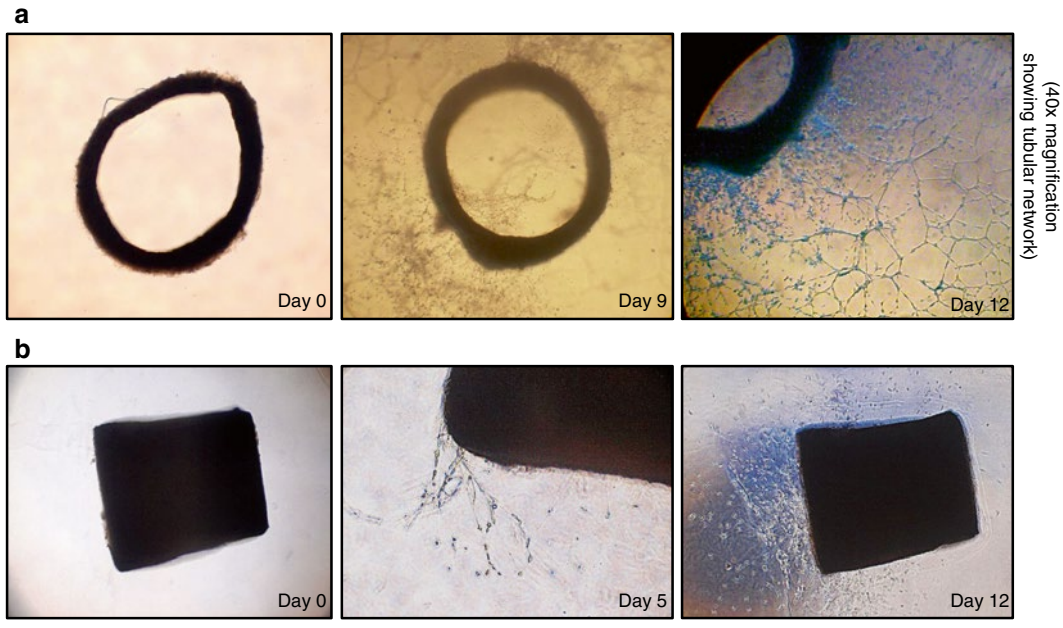

Fig. 1 Development of capillary outgrowth from aortic ring assay. Representative images showing the rat aortic ring kept on Matrigel (**a**) with the luminal axis parallel to the well. The *upper left panel* shows the ring immediately after being embedded (day 0), the *middle panel* shows capillary outgrowths on day 9 of the assay, and the *right panel* shows the 40× magnification of tubular network at day 12; (**b**) with the luminal axis perpendicular to the well. The *lower left panel* shows the ring immediately after being embedded (day 0). The *middle panel* represents the early stages of microvessel sprouting at day 5, and the right panel shows capillary outgrowth at the end of day 12

3.1.3 Matrigel Coating and Embedding of Rings

1. The Matrigel, which is thawed overnight and maintained at 4 °C, is now taken out and transferred to the hood for coating the wells of the 48-well plates.
2. Using pre-chilled pipette tips, pipette out 150 μl of Matrigel into each well of the 48-well plate. Make sure not to leave any bubble and keep the surface even.
3. Now take the aortic ring one by one and place one ring in each of the wells with either the luminal surface parallel (Fig. 1a) or perpendicular (Fig. 1b) to the well. Transfer the plate to 37 °C incubator and allow it to solidify for 30 min. (*Note*: Make sure that the Matrigel is added to each well singly, in order to prevent early solidification and improver embedding. Do not place multiple rings in a single well, as the sprouts from the individual rings will interfere with the growth and hamper capillary formation.)

4. Now, 100 μl of Matrigel was added on top of the ring for proper embedding of the ring. The Matrigel was now allowed to solidify at 37 °C for 30 min.
5. Once the ring is fixed/embedded, 500 μl endothelial cell growth media containing 5 % FBS and 1 % antibiotic was added to the well slowly from the sides without disturbing the embedded ring.

3.1.4 Culture Conditions and Drug Treatment

1. The plates are re-fed with fresh media every 3–4 days, by gently pipetting out the spent media and replacing it with fresh endothelial cell growth medium.
2. For testing any agent, the agent is pre-mixed with the media to achieve the required concentration and added to the wells.
3. Transfer the plate into the 37 °C incubator for 12–14 days to see tube formation and sprouting from the aortic vessel into the Matrigel (Fig. 1).
4. The plate should be observed periodically for any contamination and photographs of the rings are taken at regular intervals. (*Note*: The microscopic pictures should be taken at different focuses as the microvessel grows into the 3-D matrix making it difficult to visualize all the vessels under a single focus.)
5. The microvessel growth obtained doing the experiment could be quantified by live phase-contrast microscopy. The number of sprouts starting from a specific point on the ring, count each microvessel emerging from the main ring. The data could be quantified in terms of sprouting density, microvessel per ring etc. In order to do statistical calculations for the result, a minimum of 5–8 rings per sample or treatment should be sufficient. (*Note*: A total of 20–25 rings can be obtained, on average, from an adult thoracic aorta.)

3.2 Chick Chorioallantoic Membrane Assay

3.2.1 Preparation of the Egg for CAM Assay

1. Fertilized eggs are obtained from a certified poultry farm and stored at 4 °C. (*Note*: At 4 °C, the eggs are viable for more than 2 weeks.) To begin the experiment, the eggs are sterilized by wiping with 70 % ethanol and transferred to the incubator at 37–38 °C (~37.5 °C) with a humidity level of 60–70 %. The temperature in the incubator was monitored and the eggs are turned back and forth regularly. The first incubation day is called the zero day (Fig. 2a).
2. After 3 days post-incubation, make a small hole at the pointed side of the egg using the 21-G needle and 2 ml syringe. Now gently pull out 1.5–2 ml of albumin from the egg. Return the eggs to the incubator placing them horizontally. (*Note*: This process allows to make space for experimental manipulation, keeping the CAM intact, without injury.)
3. On day 4 of incubation, using a 21-G needle make a small hole on the blunt end of the egg and puncture the natural air sac on

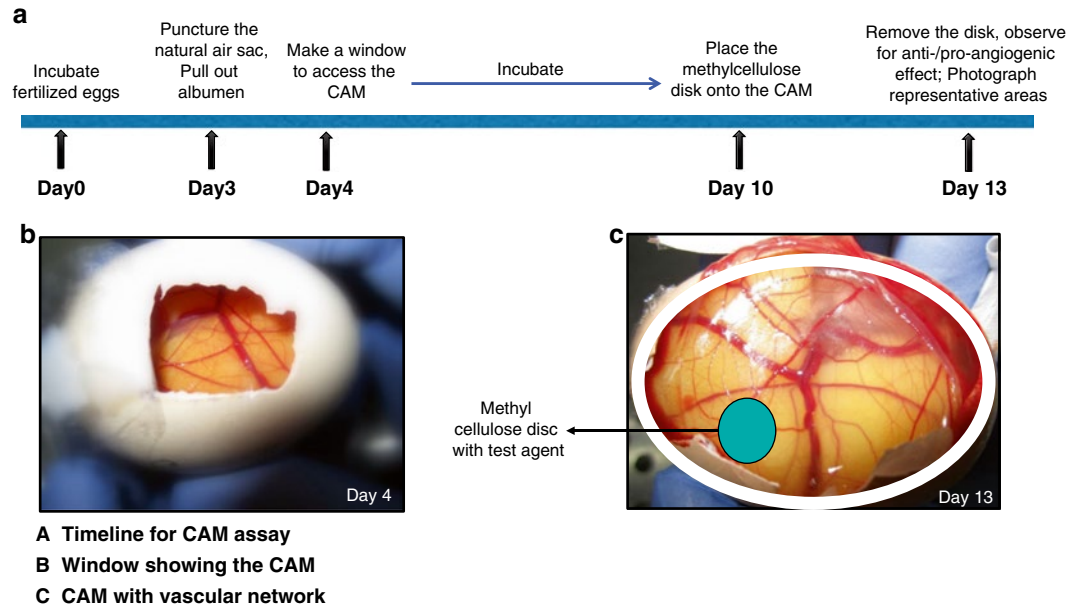

Fig. 2 CAM in vivo angiogenesis model. (**a**) The panel depicts the timeline of the major steps involved in in vivo CAM assay. (**b**) The panel shows the window cut out of the fertilized egg to provide access to the CAM, at day 4 of incubation. (**c**) The panel shows representative image of a CAM at day 13, showing placement of a methyl cellulose disk for evaluation of pro-/anti-angiogenic molecules

the larger side right behind the shell. (The 3rd–4th day after incubation is the best time to make a hole, as the embryo has already formed, the chorioallantoic membrane begins to form.)

4. Now in between the two holes made, using sharp forceps slowly cut out a small window (1 cm square) into the egg shell. (*Note*: Make sure that the egg shell covering does not fall inside onto the CAM, as it will stimulate inflammatory response.) (Fig. 2b).
5. At this stage, any nonviable egg can be identified and disposed off. The window is now covered using a scotch tape in order to maintain humidity and for proper development and the vitality of the embryo.
6. Return the viable eggs back to the incubator in a horizontal orientation such that the window is on the top and accessible for sample application. Continue the incubation undisturbed, until the sample application day (10th day of incubation).

3.2.2 Application of the Sample/Modulator

1. Prepare a 1 % w/v aqueous solution of methylcellulose, autoclave to sterilize, cool and store at 4 °C till use.
2. On the day of application, mix equal volumes of 1 % methylcellulose and sample/drug in the desired concentration in 10 µl volume for each egg. Mix thoroughly. Control methylcellulose disks are made with the vehicle used to dissolve the sample/agent/drug.

3. Pipette 10 μl of the mixture on the circular disks cut out from the Whatman paper using hole punch. The filter disk are now air-dried under the laminar flow.
4. The eggs are now examined for viability and then grouped randomly such that there are at least 5 eggs per sample or treatment. (*Note*: Experimental setup should begin with at least 10 eggs per group, as 10–20 % eggs are sometimes unviable.)
5. Now remove the scotch tape covering the window. Using a sterile forceps slowly place the filter disk onto the CAM. (*Note*: Make sure that the egg is not tilted or moved too much as it will lead to displacement of the filter disk on the CAM thereby diluting the effect.) (Fig. 2c).
6. Reseal the egg window with the tape and place the eggs back in the incubator for another 3 days.
7. On 13th day, examine the CAM area for angiogenesis especially at the site of disc application.
8. The CAM is now photographed to record the effect on microvessel formation and capillary networking.

3.3 3D-Ex Vivo *Aortic Ring Angiogenesis Assay - Advantages*

1. Mimics most steps of the angiogenic process.
2. Easier to perform and handle.
3. Comparatively less expensive.
4. Excludes the role of inflammatory cells which are generally known to show an involvement in other in vivo models.
5. The vessels have lumen.
6. Many samples can be analyzed with a single mouse or rat.

3.4 *Chick Chorioallantoic Membrane Assay - Advantages*

1. CAM assay is highly advantageous in terms of its ease of manipulation and economical nature.
2. Large number of samples/agents can be screened at once.
3. Compared to other in vivo assays, to perform CAM assay, we do not need animal ethics protocol approval and other stringent measures to be followed as long as the experiment is terminated by 18th day of development.

3.5 *Chick Chorioallantoic Membrane Assay - Limitations*

1. The main limitation of CAM assays is the nonspecific inflammatory reactions that may develop as a result of the grafted material.
2. Another drawback is that, when test material is placed on preexisting vessels, the neovascularization and the re-arrangement of vessels cannot be distinguished clearly from each other.
3. Another problem is that often the polymers do not adhere to the CAM surface and are prone to movement over CAM surface, which might dilute the effect of the drug/agent.

References

1. Bhat TA, Singh RP (2008) Tumor angiogenesis – a potential target in cancer chemoprevention. Food Chem Toxicol 46:1334–1345
2. Folkman J (1971) Tumor angiogenesis: therapeutic implications. N Engl J Med 285:1182–1186
3. Norrby K (2006) In vivo models of angiogenesis. J Cell Mol Med 10:588–612
4. Chung AS, Ferrara N (2011) Developmental and pathological angiogenesis. Annu Rev Cell Dev Biol 27:563–584
5. Potente M, Gerhardt H, Carmeliet P (2011) Basic and therapeutic aspects of angiogenesis. Cell 146:873–887
6. Nicosia RF, Ottinetti A (1990) Growth of microvessels in serum-free matrix culture of rat aorta. A quantitative assay of angiogenesis in vitro. Lab Invest 63:115–122
7. Baker M, Robinson SD, Lechertier T et al (2012) Use of the mouse aortic ring assay to study angiogenesis. Nat Protoc 7:89–104
8. Mareel M, Bocxlaer SV (1994) Chorion allantois membrane (CAM) assay. http://users.telenet.be/jojoba/doc/experiments/1.pdf.pp1-8
9. Ribatti D, Nico B, Vacca A et al (2001) Chorioallantoic membrane capillary bed: a useful target for studying angiogenesis and anti-angiogenesis. In Vivo 324:317–324
10. Bhat TA, Nambiar D, Pal A et al (2012) Fisetin inhibits various attributes of angiogenesis *in vitro* and *in vivo*-implications for angioprevention. Carcinogenesis 33:385–393

Chapter 11

AlgiMatrix™-Based 3D Cell Culture System as an In Vitro Tumor Model: An Important Tool in Cancer Research

Chandraiah Godugu and Mandip Singh

Abstract

Routinely used two-dimensional cell culture-based models often fail while translating the observations into in vivo models. This setback is more common in cancer research, due to several reasons. The extracellular matrix and cell-to-cell interactions are not present in two-dimensional (2D) cell culture models. Diffusion of drug molecules into cancer cells is hindered by barriers of extracellular components in in vivo conditions, these barriers are absent in 2D cell culture models. To better mimic or simulate the in vivo conditions present in tumors, the current study used the alginate based three-dimensional cell culture (AlgiMatrix™) model, which resembles close to the in vivo tumor models. The current study explains the detailed protocols involved in AlgiMatrix™ based in vitro non-small-cell lung cancer (NSCLC) models.

The suitability of this model was studied by evaluating, cytotoxicity, apoptosis, and penetration of nanoparticles into the in vitro tumor spheroids. This study also demonstrated the effect of EphA2 receptor targeted docetaxel-loaded nanoparticles on MDA-MB-468 TNBC cell lines. The methods section is subdivided into three subsections such as (1) preparation of AlgiMatrix™-based 3D in vitro tumor models and cytotoxicity assays, (2) free drug and nanoparticle uptake into spheroid studies, and (3) western blot, IHC, and RT-PCR studies.

Key words 3D culture models, AlgiMatrix™, Alginate, Extracellular matrix, Cytotoxicity, 2D cell cultures, Cell-to-cell interaction, In vivo environment, Nanoparticles, Nanostructured lipid carries, AlamarBlue, Spheroids

Abbreviations

CSCs	Cancer stem cells
DIO-NLC	DIO dye-loaded NLC
EGF	Epidermal growth factor
ECM	Extracellular matrix
FGF	Fibroblast growth factor
FBS	Fetal bovine serum
IHC	Immunohistochemistry
NSCLC	Non-small-cell lung cancer
NLC	Nanostructured lipid carriers
OCT	Optimal cutting temperature

Sabrina Strano (ed.), *Cancer Chemoprevention: Methods and Protocols*, Methods in Molecular Biology, vol. 1379,
DOI 10.1007/978-1-4939-3191-0_11,

RT-PCR	Reverse transcription-polymerase chain reaction
SEM	Scanning electron microscopic
TNBC	Triple-negative breast cancer
2D	Two dimensional
3D	Two dimensional

1 Introduction

Most of the cancer researchers usually depend on two-dimensional (2D) in vitro models and on experimental animal models to understand the complex pathophysiology of tumors such as angioneogenesis, tumor cell invasion, and metastatic mechanisms. Tumor cells in in vivo conditions are well organized to maintain cell-cell and cell-extracellular matrix (ECM) interactions and paracrine signaling events. These interactions are crucial for tumor cells to proliferate, survive and invade, further, may also decide the chemotherapeutic performance of drugs. However, in conventional 2D-based in vitro tumor models, most of these in vivo conditions and ECM effects are not possible to create. Therefore, the anticancer results obtained in monolayer 2D models may not translate the same pattern of results in actual in vivo tumor models. Due to this difference, the promising anticancer effects observed with several agents often resulted in no activity when studied in in vivo models. These discrepancies suggested the need of developing high-throughput in vitro tumor models, which mimic the in vivo conditions perfectly. Recently several studies indicated the promising potential of 3D models in simulating the in vivo conditions. ECM-mediated signals can be restored using 3D cultures. Functional in vitro tumor models that are representative of in vivo tumor progression have been rapidly evolving. Several 3D-based tumor spheroid models demonstrated the remarkable resistance to anticancer drugs by limiting the penetration into the tumor spheroid cells. The role of cell-cell and cell-ECM interactions required for tumor progression cannot be studied in 2D monolayer cell culture models, whereas in 3D models these types of interactions can be mimicked [1]. Therefore, 3D culture-based tumor models may have beneficial role in cancer research. The widespread application of 3D model systems is stuck by the unavailability of appropriate biocompatible materials that present ease of use, experimental flexibility, and ability to translate from in vitro to in vivo applications [2]. Among the different 3D models available, alginate scaffold-based (AlgiMatrix™) models possess the advantage of being an animal-free product and stability at room temperature (2). Due to highly porous (pore size 50–150 μm) nature of the alginate matrix, cells grow as multicellular spheroids. The translucent nature of the 3D jelly scaffolds makes these spheroids easily visualized under the microscope and sizes can be measured in the intact matrix. It is our

hypothesis that the use of 3D alginate scaffold lung tumor model will simulate in vivo conditions to screen the efficacy of drug candidates and will be more effective than the use of traditional monolayer 2D cultures.

In the current study, we have developed the in vitro tumor models based on AlgiMatrix™-based 3D cultures using non-small-cell lung cancer cells (NSCLCs). This study explains the detailed procedure involved in the development of tumor spheroids and demonstrates the anticancer effects of chemotherapeutic agents. This study also demonstrates the cancer stem cell-based spheroid growth characteristics using H1650 NSCLC stem cells. Further, we also studied the uptake of nanoparticles into spheroids. The details of AlgiMatrix™-based in vitro tumor model optimization and anticancer evaluation was reported in our previous reports [3].

2 Materials

1. Alginate-based 3D culture scaffolds (AlgiMatrix™) in 96- and 6-well plate formats (*see* **Notes 1** and **2**), relevant supplies such as firming buffer, matrix dissolving buffer (Composition), and AlamarBlue (Composition) were supplied by Life Technologies Corporation. Cleaved caspase-3 kit was purchased from Cell Signaling Technology. All the cell culture plasticware supplies were purchased from Corning, Inc. Epidermal growth factor (EGF) and fibroblast growth factor (FGF) were purchased from Sigma Aldrich.
2. AlamarBlue dye was used to quantify the live cells present in the 3D matrix (*see* **Note 3**), which produces fluorescence after internalization into viable cells. The fluorescent intensity indicates the number of viable cells.
3. The human Non Small Cell Lung Cancer (NSCLC) cell lines A549, H460, H1650 cell lines and MDA-MB-468 triple negative breast cancer (TNBC) cell lines were procured from ATCC.
4. The cell culture media suitable for each cell line was procured from Invitrogen Technologies. All the cell culture supplies such as trypsin and antibiotic mix were purchased from Invitrogen Technologies.
5. DMEM/F12K (50:50) media was used for 549 cells and RPMI media was used for H460 and H1650 cells. MDA-MB-468 cells were grown in DMEM media. 10 % fetal bovine serum (FBS) was used to grow the spheroids in 3D matrices and while performing the anticancer/cytotoxicity studies 5 % FBS was maintained.
6. H1650 cancer stem cells (CSCs) were grown in DMEM media, this media was supplemented with important growth factors

like EGF and FGF. The stemness of these cells was conformed from the SOX-2 expression by western blotting.

7. All the cancer cell lines were grown in conventional monolayer cultures in 250 cm^2 cell culture flasks according to the standard cell culture procedures before incorporating into 3D AlgiMatrix™ scaffolds (*see* **Note 4**).
8. Fluorescent dye DIO was purchased from Molecular Probes, and dye-loaded nanoparticles (nanostructured lipid carriers, NLC) were prepared as per the reported methods [4].
9. Different anticancer drugs such as doxorubicin, docetaxel, gemcitabine, cisplatin, 5-fluorouracil, and camptothecin were purchased from Sigma Aldrich, St. Louis, MO.
10. Rest of the materials used in this protocol can be procured from any molecular biology consumables suppliers.

3 Methods

3.1 Preparation of AlgiMatrix™-Based 3D In Vitro Tumor Models and Cytotoxicity Assays

1. Different NSCLC cell lines were harvested according to the standard procedures and suspended in suitable medium and incorporated into the 3D culture wells.
2. Both 96- and 6-well plates were used to develop the in vitro tumor models. In 96-well plates, different cell densities (*see* **Note 5**) were suspended in 100 μL of suitable media. In the case of 6-well plates, the cell density of 250000 cells/well were suspended in 2000 μL of media (*see* **Note 6**).
3. The cell suspension was distributed uniformly throughout the each 3D AlgiMatrix™ scaffold and incubated for 20–30 min. This incubation results in formation of jellylike scaffolds, in which cells are suspended.
4. The deposited cells will migrate into the large pores present (pore sizes of 50–150 μm) in the 3D matrix and grow as compact spheroids. After 20–30 min, to ensure the complete immersion of 3D scaffolds in the media, additional amount of media was added to each well.
5. To each 96-well plate wells another 200 μL of media and to each 6-well plate wells 3 ml of media were added and plates were kept in incubator at 37 °C with 5 % CO_2. Cell culture media was changed every alternative day.
6. Our preliminary studies suggested that for 96-well plates 10,000–20,000 cells/well and for 6-well plates 0.25 million cells/well are optical cell densities. Therefore, throughout this protocol indicated cell densities were used. The cell densities may vary depending upon the growth rate of the cells lines.

7. The effect of culture duration time on spheroid size and number was optimized. Based on our previous findings, the duration of the culture was optimized as 14 days.
8. Cell culture media was changed every alternative day, cells were allowed to grow in the 3D scaffolds for 2 weeks. During this period, spheroid number and sizes were measured.
9. The spheroid number and size was observed by inverted microscope. During the microscopic examination excess amount of media was removed from the wells, all visible spheroids and their sizes were measured every third day. Once measurements of all the spheroids are over, if needed scaffolds were inverted and observed under microscope.
10. It is possible to observe the spheroids growing in the 3D alginate scaffold without dissolving the matrix or removing media. During 14 days of spheroid growth, the size of spheroid and number of spheroids in each well were measured/counted on an inverted microscope. From each well an average of 8–10 fields were used for these measurements. The effect of anticancer drugs on spheroids number and size distribution was studied during the anticancer evaluations.
11. The anticancer effects of drugs on 3D culture models: Our preliminary studies suggested that after 7 days of 3D culture of cancer cells, the spheroids attained >100 μm in size, which suggest the suitability of 3D models for drug treatments.
12. Drug treatment was given at 7, 9, and 11 days post cell seeding. At each treatment time point, drug was exposed for 24 h, followed by a 24 h wash period. Cisplatin, gemcitabine, 5-fluorouracil, and camptothecin at concentration ranges of 1–400 μM were used. After the last dose (13th day), the effect of these anticancer drugs on spheroid number and size distribution was studied. Finally, cell viability was estimated by AlamarBlue assay in the intact matrix.
13. Cell viability study by using AlamarBlue dye: 14 days after the culture/drug treatment of cells in 3D scaffolds, the cell viability was estimated by AlamarBlue assay. This assay detects the viable cells based on their metabolic activity, which is based on the conversion of a non-fluorescent dye to the red fluorescent dye resorufin in response to chemical reduction of growth medium resulting from cell growth. 10 % of AlamarBlue was added to each well and incubated at normal cell culture conditions. After 1 h, plates were read for fluorescence intensity at 530 and 590 nm wavelength for excitation and emission, respectively.
14. The standard curve (cell number vs. fluorescence intensity) was plotted to quantify the number of cells present in 3D scaffolds.

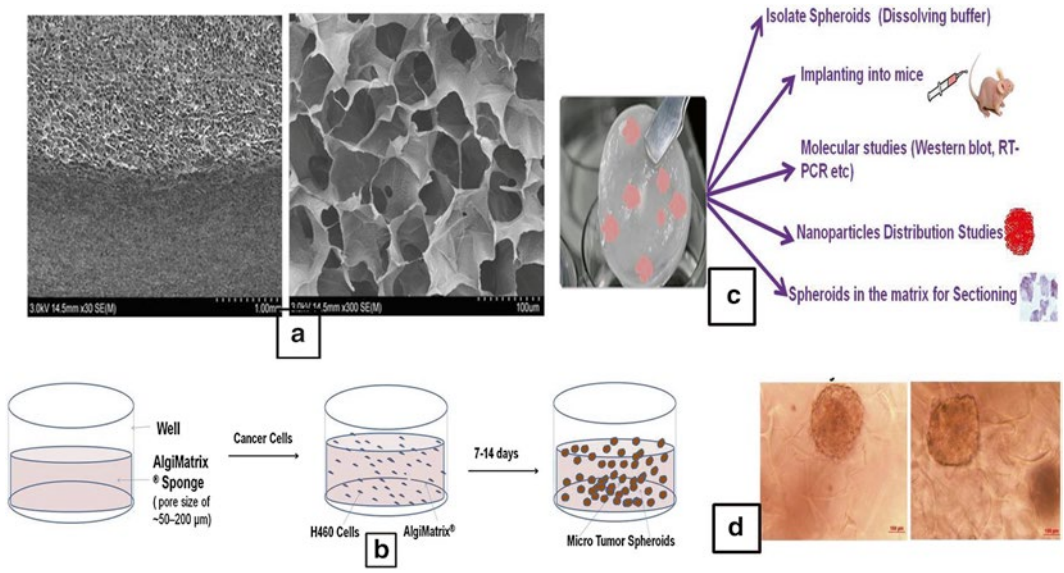

Fig. 1 AlgiMatrix™ 3D culture system. Scanning electron microscopic (SEM) images of 3D alginate scaffolds at lower resolution (*left panel*, 30 K) and higher resolution (*right panel*, 300 K), figure shows pore sizes in the matrix to accumulate the cells and grow them as spheroids (**a**). (**b**) The schematic representation of 3D alginate scaffold wells and how spheroids are formed and grown in the 3D alginate scaffold cell culture system upon seeding the cells into the porous alginate media. (**c**) The schematic representation of possible applications of AlgiMatrix™ scaffold culture models and (**d**) representative photomicrographs of in vitro tumor spheroids captured from intact 3D scaffolds (this figure is reproduced and modified from Ref. 3)

15. While studying the cytotoxicity of anticancer drugs, based on intensity of fluorescence, the percentage of cell viability was measured against different concentrations of anticancer drugs and IC_{50} values were calculated.
16. Results (IC_{50} values) were compared with 2D culture systems (Fig. 1 and Table 1).

3.2 Free Drug and Nanoparticle Uptake into Spheroids

In recent times nanotechnology demonstrated to play important role in cancer drug delivery. There are already few nanotechnology-based drug formulations clinically used in cancer therapy and further lot of research is going on to improve cancer diagnosis, chemoprevention, and therapy [5]. These 3D models can be used for the evaluation of nanoparticle formulation. For nanoformulations to produce the desired effects, they need to penetrate several barriers before reaching the tumor cells. In our 3D models also we demonstrated in vitro tumor distribution and cancer cell uptake of nanoparticles was studied. The detailed procedure for nanoparticle study is explained in following steps.

1. Free drug and nanoparticles uptake into spheroids: A549, H460, or MDA-MB-468 cells were grown in AlgiMatrix™ 6-well plates for 1–2 weeks in suitable medium as per our

Table 1
Comparative analysis of IC_{50} values of various anticancer drugs in 2D and 3D systems. Each data point is represented as mean ± sem (n=5-6). @P<0.001 Vs respective 2D groups (Data was reproduced from [3])

	IC50Value(μM)							
	H460 Cells		A549 Cells		H1650 Parental Cells		H1650 Stem Cells	
Drugs	2D	3D	2D	3D	2D	3D	2D	3D
Cisplatin	3.47 ± 0.45	84.26 ± 5.63@	4.2 ± 0.2	75.79 ± 4.52@	2.09 ± 0.98	66.13 ± 7.36@	4.84 ± 0.62	126.14 ± 12.42@
Gemcitabine	2.33 ± 0.16	91.07 ± 7.01@	2.56 ± 0.45	87.31 ± 9.64@	2.68 ± 0.58	103.72 ± 9.68@	6.03 ± 0.84	177.79 ± 14.03@
5-Fluorouracil	3.62 ± 0.52	120.94 ± 12.65@	3.21 ± 1.58	99.17 ± 6.24@	2.63 ± 0.37	100.44 ± 8.92@	6.87 ± 0.46	148.31 ± 6.56@
Camptothecin	2.59 ± 0.74	69.72 ± 7.82@	1.36 ± 0.17	89.74 ± 7.45@	4.48 ± 0.81	51.84 ± 4.81@	7.49 ± 1.05	95.46 ± 10.68@

standardized protocols. Once the spheroids attained suitable sizes (in 14 days spheroids attain approximately 200–250 μ in size).

2. Nanoparticle uptake studies were performed either on intact AlgiMatrix™ scaffolds or on isolated spheroids from 3D matrix.
3. In 3D matrix intact spheroids, DIO dye-loaded NLCs were added to the AlgiMatrix™ wells. Plates were kept for shaking (100 rpm) and incubated in CO_2 incubator. After 2–4 h cell culture medium containing excess of NLCs was removed and spheroids were either isolated from 3D scaffolds after dissolving the matrix by using dissolving buffer or intact spheroids in 3D scaffolds were fixed in suitable fixative medium (*see* **Note 7**).
4. In the isolated spheroid studies, 3D matrix scaffold was dissolved in dissolving buffer (*see* **Note 8**) the resultant spheroid suspensions were isolated by centrifugation.
5. Isolated spheroids were resuspended in PBS (pH 7.4) and incubated with either free doxorubicin or DIO oil-loaded nanostructured lipid carrier (NLC) nanoparticles. DIO dye-loaded NLC were prepared according to our previous method [4]. Two hours after the incubation, spheroids were washed with PBS twice to remove the unbound free doxorubicin and NLCs.
6. The spheroids were spread on microscopic slides using cytospin and observed under fluorescent microscope. Fluorescent images were captured and intensity was calculated.

7. For doxorubicin and for DIO-NLC 470 and 585 nm and 484 and 501 nm were used as excitation and emission wavelengths.
8. In another set of experiments the relative uptake of free drug and NLC in 2D and 3D models were performed and fluorescent intensities were measured by adjusting the total cell number.
9. The uptake was expressed in terms of relative fluorescence and results were compared between free doxorubicin and nanoparticle groups.
10. In another set of experiments, we have evaluated the role of targeted nanoparticles on in vitro intratumoral penetration in 3D scaffolds. We have chosen EphA2 receptor-targeted nanoparticles, because these receptors are over-expressed in many solid tumors, including triple-negative breast cancer [6]. The YSA peptide selectively binds to EphA2 receptors. Therefore, we have prepared YSA peptide-coated nanoparticles and used for tumor uptake studies (*see* **Note 9**). Rest of the procedure for nanoparticle uptake into spheroids was kept similar (Fig. 2).

3.3 Western Blot, IHC, and RT-PCR Studies

The response of cancer cells towards anticancer drugs may vary when studied in 2D monolayer systems or 3D spheroid based in vitro tumor model systems. In addition to the several intracellular pathways, several extracellular and cell-cell signaling events may play role in tumor development, metastasis, and anticancer drug responses. Therefore, mechanistic studies may provide the valuable information of how cancer cells are behaving differently when grown in 2D and 3D systems and how drugs produce cytotoxicity differently when grown in 3D systems compared to monolayer cultures. We also performed the western blot, IHC, and RT-PCR analysis to understand different mechanisms. The details of these steps were as follows.

1. Sample preparation for western blot analysis: After treatment with respective drugs in both culture systems, spheroids were isolated from AlgiMatrix™ scaffold and spheroids were mixed with RIPA lysis buffer and homogenized to disrupt the spheroids. In the case of 2D culture systems also similar extraction procedures were followed. The rest of the procedure was as per the standard protocols to prepare the protein samples for western blot analysis [7].
2. Immunohistochemical (IHC) analysis of spheroids: After isolating the spheroids from 3D matrices, they were spread on the microscopic slide by cytospin. On these spheroids IHC can be performed to study the expression of different markers (*see* **Note 10**).

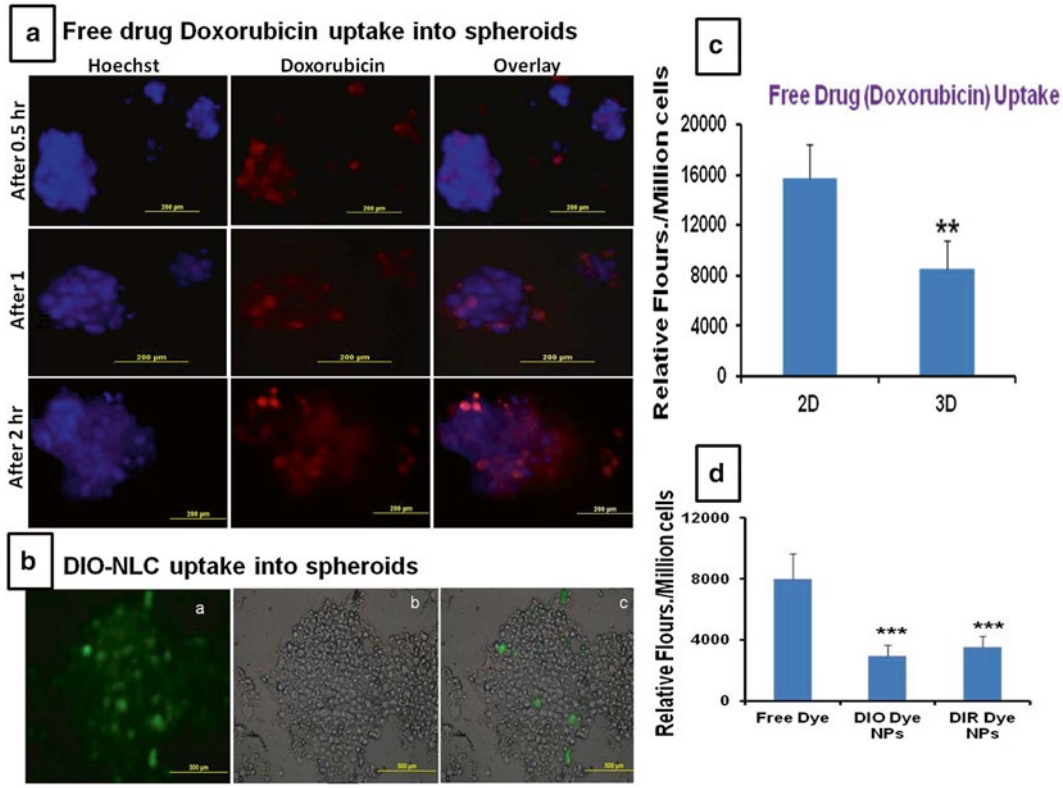

Fig. 2 Drug and nanoparticles uptake by spheroids. (**a**) Representative images of free drug doxorubicin uptake into H1650 parental cell spheroids at different incubation time points. (**b**) Representative Images of the DIO-NLC nanoparticle uptake into H1650 parental cell spheroids (*a*) fluorescent, (*b*) bright-field, and (*c*) merged image. The fluorescent images clearly indicates the nanoparticles uptake into spheroids, (**c**) Relative fluorescence intensities of free doxorubicin uptake and dye loaded NLC NPs into 3D spheroids and comparison with 2D uptake intensities and (**d**) Comparative uptake (relative fluorescent intensities) of free drug and nanoparticles (DIO and DIR loaded NPs) into spheroids (this figure is reproduced and modified from Ref. 3)

3. As a standard marker, we have studied expression profile of cleaved caspase 3 in response to anticancer treatment and expression pattern was compared between 2D and 3D systems.
4. Chemotherapeutic drug induced apoptotic cell death was evaluated by studying the expression of cleaved caspase 3. IHC was performed according to the recommended IHC kit protocol [3].
5. For RT-PCR analysis, either fresh isolated spheroids or spheroids stored in RNAlater were used for RNA extraction. The RNA extraction procedure we had followed was according to our previous methods [8]. The expression of antiapoptotic Bcl-2 mRNA was performed according to standard protocols and results were compared between 2D and 3D systems (Figs. 3 and 4).

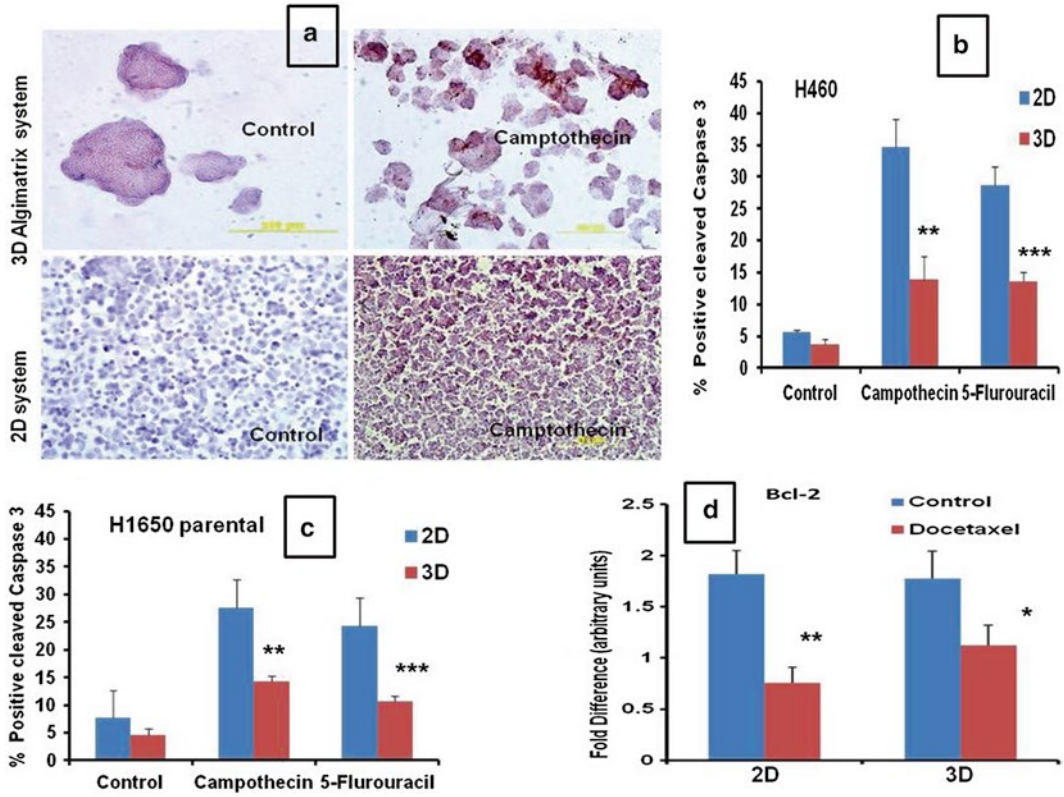

Fig. 3 Immunohistochemistry and RT-PCR analysis. (**a**) Representative images of Immunohistochemistry of H1650 parental cells or spheroids grown in 2D and 3D culture systems for cleaved caspase-positive cells and effect of camptothecin and 5-fluorouracil on cleaved caspase expression. Comparative immunohistochemistry of (**b**) H460 and (**c**) H1650 parental cells or spheroids grown in 2D and 3D culture systems for cleaved caspase 3-positive cells. (**d**) RT-PCR analysis of RNA isolated from 2D and 3D culture systems and effect of docetaxel on Bcl-2 expression in H460 cells (this figure is reproduced from Ref. 3)

6. Data analysis and statistics: Data was represented as mean ± SEM. One-way ANOVA followed by Tukey's test was used to compare the statistical difference among the groups. *P* value <0.05 was considered as statistically significant.

4 Notes

1. 3D alginate scaffold is a nontoxic and biodegradable ready-to-use sponge made from lyophilized alginate gel, which supports a cell culture model resembling normal cell characteristics and morphology. AlgiMatrix™ is a chemically defined, highly porous (>90 %) 3D scaffold and cell recovery from 3D alginate scaffold is achieved with the use of dissolving buffer, a nonenzymatic solution which dissolves the scaffold within a few minutes but leaves the cellular aggregates intact for further processing and/or analysis.

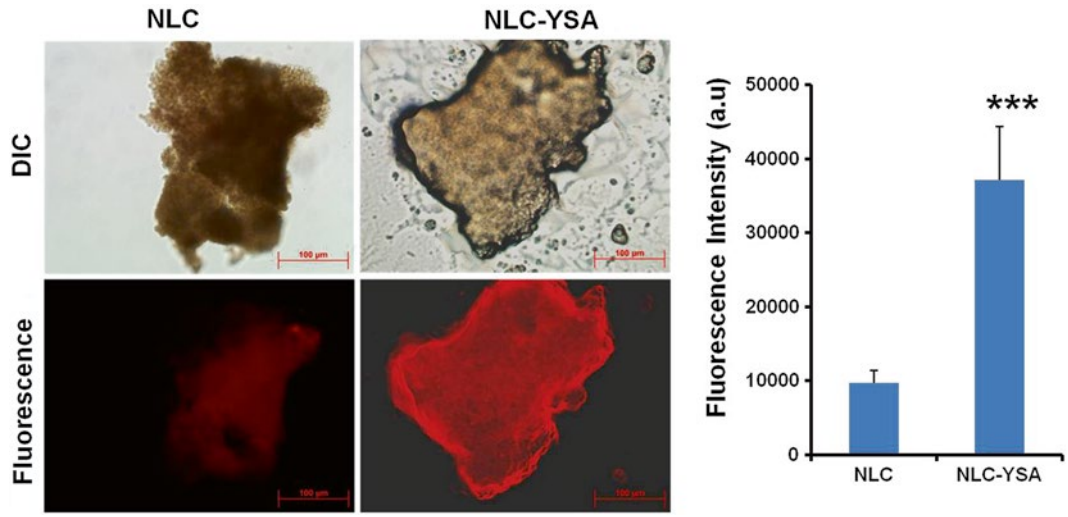

Fig. 4 EphA2 receptor targeted nanoparticles uptake into spheroids: Figure shows the representative photomicrographs of DIR dye-loaded NLC non-targeted and YSA peptide-coated EphA2 receptor targeted nanoparticles uptake images in MDA-MB-468 spheroids. *Right panel* shows the quantification of NLC-YSA uptake into spheroids. This clearly demonstrates the increased uptake of nanoparticles when targeted with over-expressed EphA2-specific peptides

2. Sterile packed 3D AlgiMatrix™ plates (96- and 6-well plates, each well of the plate supplied with packed alginate matrix suitable for cell growth) were used to grow the cells.
3. Alginate-based 3D culture scaffolds (AlgiMatrix™) are interchangeably used with 3D matrix
4. To grow H1650 stem cells in 2D culture-based monolayer culture, the culture plates need to be coated with laminin prior to use.
5. In each well of 96-well plates, preliminary studies were performed to optimize the suitable cell number required for each well by using cell numbers from 1000 to 35000 cells/well.
6. In the 6-well plates, firming buffer was added to cell suspension to increase the firmness of the 3D matrix gels, so that scaffolds would become more flexible to handle during the culture.
7. Though this procedure explained the drug and nanoparticle uptake into isolated spheroids, these studies can also be performed on intact 3D AlgiMatrix™ matrices in which spheroids are growing.
8. The dissolving buffer of 2 ml was added to each well and incubated for 10 min at 37 °C, which results in the complete loss of alginate matrix.
9. EphA2 receptors are over expressed on various types of tumors and YSA peptide found to have selective binding to these

receptors; therefore, coating/conjugating the YSA peptide on to nanoparticles may increase the tumor cell uptake.

10. Cryosectioned in vitro tumor spheroids can also be used for the IHC analysis. The intact AlgiMatrix™ along with spheroids can be embedded in OCT medium and cryosectioned; these sections can also be used for drug uptake and IHC studies.

References

1. Kim JB (2005) Three-dimensional tissue culture models in cancer biology. Semin Cancer Biol 15:365–377
2. Prestwich GD (2007) Simplifying the extracellular matrix for 3-D cell culture and tissue engineering: a pragmatic approach. J Cell Biochem 101:1370–1383
3. Godugu C, Patel AR, Desai U et al (2013) AlgiMatrix™ based 3D cell culture system as an in-vitro tumor model for anticancer studies. PLoS One 8:e53708
4. Patlolla RR, Chougule M, Patel AR et al (2010) Formulation, characterization and pulmonary deposition of nebulized celecoxib encapsulated nanostructured lipid carriers. J Control Release 144:233–241
5. Wicki A, Witzigmann D, Balasubramanian V et al (2015) Nanomedicine in cancer therapy: challenges, opportunities, and clinical applications. J Control Release 200:138–157
6. Patel AR, Chougule M, Singh M (2014) EphA2 targeting pegylated nanocarrier drug delivery system for treatment of lung cancer. Pharm Res 31:2796–2809
7. Godugu C, Patel AR, Doddapaneni R et al (2013) Inhalation delivery of Telmisartan enhances intratumoral distribution of nanoparticles in lung cancer models. J Control Release 172:86–95
8. Godugu C, Patel AR, Doddapaneni R et al (2014) Approaches to improve the oral bioavailability and effects of novel anticancer drugs berberine and betulinic acid. PLoS One 9, e89919

Chapter 12

Cancer Gastric Chemoprevention: Isolation of Gastric Tumor-Initiating Cells

Federica Mori, Valeria Canu, Laura Lorenzon, Alfredo Garofalo, Giovanni Blandino, and Sabrina Strano

Abstract

Gastric cancer is an important healthcare problem and represents the second leading cause of death for malignant disease worldwide. In the Western world, the diagnosis is done at late stage when treatments can be only palliative. Searches for new therapeutic regimens as well as for new biomarkers are in progress.

To reduce cancer mortality is crucial the prevention of the lesion at earlier stages. Therefore, new bullets to prevention are needed.

Nowadays, studies relating to different kinds of tumor are unanimous in considering cancer stem cells (CSCs) as "the core" of the tumor and the responsible of tumor chemoresistance and relapse.

This chapter aims to provide the instructions to (1) isolate, (2) grow, and (3) validate, both in vivo and in vitro, the gastric CSC subpopulation.

Key words Gastric cancer, Chemoprevention, Cancer stem cells, Patient-derived xenograft, Chemoresistance

1 Introduction

Gastric cancer (GC) is the fourth most common cancer worldwide, with higher incidence in Asian countries [1]. Even though many breakthroughs have been done in the diagnosis as well as in the therapy strategies, it remains the second leading cause of cancer-related death [2]. Surgery is the main treatment option, with chemotherapy as adjuvant therapy, but the 5-year survival rate is still poor (<20 %) [3]. In the last decades, aim of GC prophylaxis is to include primary and secondary prevention strategies. Chemoprevention is by definition, the use of any chemicals (vitamins, pharmaceuticals, minerals) at any stages of carcinogenesis to reduce tumor incidence [2]. Regarding GC, among the most pursued strategies applied in chemoprevention are the *Helicobacter pylori* eradication; diet; nonsteroidal anti-inflammatory drugs; and COX-2 inhibitor supplementation [2]. All these approaches have

Sabrina Strano (ed.), *Cancer Chemoprevention: Methods and Protocols*, Methods in Molecular Biology, vol. 1379,
DOI 10.1007/978-1-4939-3191-0_12,

been demonstrated to be promising either in in vitro or in in vivo studies [2, 4]. At this point an important consideration about the canonical in vitro and in vivo models must be done. It is frustrating but it is a matter of fact that several powerful new therapeutic approaches fail when they reach the Phase III clinical trials [5]. This unfortunately happens because (1) in vitro-cultured cell lines diverge from the tumor they have been originated from, with irreversible alterations in the gene expression pattern and (2) in vivo mouse xenografts derived from human cell lines, although useful in predicting targeted agents responsiveness, failed in the translation of the oncological therapeutics into the clinical settings, due to the failure in the reproduction of the tumor microenvironment and its interaction with the immune system [5]. To better overcome these limitations, it is essential to focus on models that possess invaluable clinical predictive power. Studies conducted in the last years indicate that in order to test the efficacy of a chemotherapeutic as well as of a chemopreventive protocol, there are two main predictive strategies:

- Tumor graft models (also known as: patient-derived xenograft or PDXs).
- Cancer stem cell (CSC) cultures.

Both strategies imply the manipulation of NOD-SCID mice, a mouse strain that lacks natural killer cells and is more immunodeficient than the nude one. PDX approach consists in the transplantation of a sample derived directly from the patient tumor and collected fresh from the surgery. The sample, after a brief digestion, that could be either mechanic or chemical or both, is transplanted heterotopically or ortotopically in the host. Considering that a single animal recipient could not catch the inherent variability of each cancer, more than one engraftment is performed from a single tumor to preserve tumor heterogeneity. Once engrafted, the PDX is allowed to grow till an ethically sustainable burden and then it is excised, processed and transplanted into another mouse. Because of their origin, PDXs permit to manage with xenografts that maintain most of the molecular characteristics of the parental tumors [5].

Similar to the PDXs' innovative contribution to the in vivo approach is the enrollment of CSCs in the in vitro studies. In 2006, during an American Association of Cancer Research workshop, CSCs have been defined as: "cells within the tumor that possess the capacity for self-renewal and that can cause the heterogeneous lineages of cancer cells that constitute the tumor" [6]. Moreover, CSCs are almost univocally considered the cells inside the tumor that are responsible for the chemo- and radioresistance as well as for the relapse and, not least, a connection between CSCs and metastasis has also been hypothesized [7]. Due to these characteristics and abilities, CSCs can be considered "the core" of the tumor,

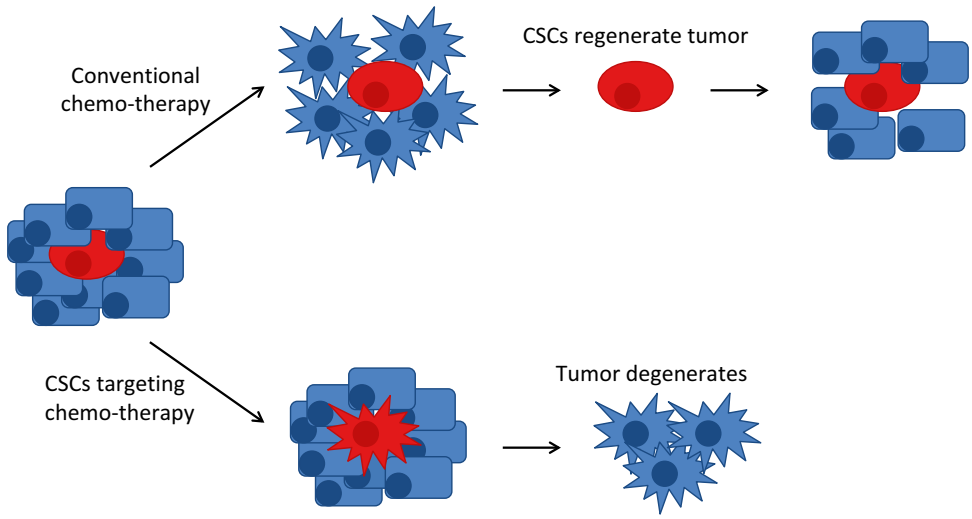

Fig. 1 CSCs within the bulk of the tumor are less sensitive to the conventional therapies. While the tumor cells are killed, CSCs survive and lead to the tumor recurrence. On the contrary, a CSCs targeting therapy is more effective in killing CSCs and this lead to the tumor degeneration and the patient is recovered

the cells that need to be hit by the targeted therapy in order to cure and eradicate the tumor (Fig. 1). As in part described in the CSCs definition, the characteristics that need to be satisfied to define a subpopulation of cells isolated from a human tumor specimen as a CSC culture are:

- Stability and ability to grow in non-adherent culture conditions.
- Capacity to reconstitute the cellular heterogeneity in vitro and to originate and recapitulate in vivo the tumor of origin.
- Chemoresistance.

Obtaining a gastric cancer stem cell (GCSC) culture is an important primary step in the development of new gastric cancer therapies. GCSCs were identified for the first time in 2009 by Takaishi et al. [8], who were also able to isolate them by using the CD44 surface marker. From that time on the isolation and characterization protocols have been improved, new surface (EpCAM; CD133, Musashi-1) [9, 10]. Andenzymatic (ALDH) [9] markers have been identified and novel tumorigenicity experiments have been settled up [9, 11, 12].

The aim of this chapter is to provide guidelines that could be useful for the isolation and propagation of GCSCs from human primary gastric cancer sample [11].

2 Materials

2.1 Equipment

1. Cell culture unit.
2. Sterile scalpels, scissors and forceps.
3. 2, 5, 10 ml Pasteur pipettes.
4. 15, 50 ml centrifuge tubes.
5. Centrifuge.
6. 70, 35 μm nylon meshes.
7. Ultralow adhesion dishes and 6 wells plates.
8. 1 ml Syringe.
9. FACS-based sorter.

2.2 Materials and Reagents

1. Phosphate-buffered saline (PBS).
2. RPMI 1640 medium.
3. Neurobasal-A medium.
4. Ciprofloxacin.
5. Streptomycin.
6. Penicillin.
7. Ceftazidime.
8. Amphotericin-B.
9. HEPES.
10. Collagenase type-III.
11. DTT.
12. 0.8 % Ammonium chloride potassium phosphate solution.
13. Trypan Blue Cell Staining Reagent.
14. Accutase.
15. Matrigel.
16. 5-Fluorouracil.
17. Doxorubicin.
18. Vinblastine.
19. Paclitaxel.

3 Methods

3.1 Isolation of GCSCs from Human Gastric Cancer Sample

The informed consent of the patient is mandatory before collecting any samples.

Sterile conditions must be carried out for all the steps, which should be carried out under a cells fume hood.

1. Collect the tumor specimen of about 1 cm^3 of volume (*see* **Note 1**).
2. Transfer the samples from the surgery room to the lab in a 50 ml Falcon, containing 25 ml PBS supplemented with antibiotics (4 mg/ml ciprofloxacin, 120 μg/ml penicillin, 100 μg/ml streptomycin) (*see* **Notes 2** and **3**).
3. Wash the samples three times with the PBS antibiotics solution (*see* **Note 3**).
4. Transfer the tumor sample into a 60 mm plate with 1 ml PBS antibiotics and by the aim of scissors or scalpels, mechanically disaggregate the tissue into small pieces (1–2 mm^3).
5. Collect the minced sample and incubate in PBS 6.5 mM DTT solution at room temperature for 15 min (in order to remove mucus contamination).
6. After centrifugation gently wash the fragments with the PBS antibiotics solution.
7. Resuspend the sample in 5 ml digestion medium (serum-free RPMI 1640 supplemented with 2 mmol/l L-glutamine, 120 μg/ml penicillin, 100 μg/ml streptomycin, 50 μg/ml ceftazidime, 0.25 μg/ml amphotericin-B, 20 mmol/l HEPES) and after resuspension add Collagenase typeIII (200 U/ml) and hyaluronidase (20 U/ml). Incubate for 1 h at 37 °C to allow the enzymatic disaggregation.
8. Serially filter the digested sample through 70 and 35 μm nylon meshes.
9. Resuspend the sample in 0.8 % ammonium chloride lysis buffer for 5 min on ice, to remove red blood cells.
10. Gently centrifuge the sample (10 min 300×*g*) at room temperature.
11. Resuspend the cells in sphere medium (Neurobasal-A medium supplemented with 2 mM L-glutamine, 120 μg/ml penicillin, 100 μg/ml streptomycin, B27, 50 ng/ml EGF, 50 ng/ml FGF-2).
12. Seed the cells in 100 mm ultralow adhesion cell culture plates at the density of 10^5 cells/ml.
13. Grow cells for 7–10 days in order to allow their recovery and propagation. Add fresh medium and growth factors every 3 days (*see* **Note 4**).

3.2 GCSC Sorting

1. Collect the culture of the gastric cells obtained from the tumor sample disaggregation (Subheading 3.1) and wash with PBS.
2. Incubate the cells with 2 ml Accutase for 5 min at 37 °C 5 % CO_2.
3. Centrifuge the cells suspension at 800×*g* for 5 min and wash with PBS 1×.

4. Resuspend the cells at a concentration of 5×10^5/100 μl in 0.6 % human immunoglobulins for 10 min on ice, in order to reduce antibodies nonspecific binding (*see* **Note 5**).
5. Wash the cells in PBS1×.
6. Resuspend the antibodies in PBS 1 % bovine serum albumin.
7. Stain the cells with the anti-human ESA-APC (clone EBA-1; Becton-Dickinson, San Jose, CA) and anti-human CD44-FITC antiboby (clone G44-26; BD Biosciences, San Diego, CA), following the manufacturer's instruction (*see* **Note 6**).
8. To exclude stromal cells, simultaneously stain the isolated gastric cells with anti-human CD3-PE.Cy5 (clone UCHT1: BD Biosciences), CD10-PE.Cy5 (clone HI10a:BD Biosciences), and CD45-PE.Cy5 (clone HI30BD: Biosciences).
9. Perform the FACS sorting following the manufacturer's instruction.
10. Resuspend the cells in sphere medium (Neurobasal-A medium supplemented with 2 mM L-glutamine, 120 μg/ml penicillin, 100 μg/ml streptomycin, B27, 50 ng/ml EGF, 50 ng/ml FGF-2) for cell culture propagation.

    OR

11. Resuspend the cells in RPMI 1640 supplemented with 10 % FBS, 20 mM HEPES and 2 mM L-glutamine for subsequent in vivo injection.

3.3 Propagation of GCSC Culture

1. After about 10 days from seeding, the first spheres of GCSCs from **step 10** of Subheading 3.2 can be observed in suspension. Collect the culture medium and the floating cells in a 15 ml Falcon tube.
2. Centrifuge the cell suspension at 800 × *g* for 5 min. Keep the supernatant for **step 6**.
3. Wash the cells with PBS 1×.
4. Incubate the cells with 2 ml Accutase for up to 10 min at 37 °C 5 % CO_2 (*see* **Note 7**).
5. Centrifuge the cell suspension at 800 × *g* for 5 min.
6. Resuspend the cells pellet in fresh sphere medium (Neurobasal-A medium supplemented with 2 mM L-glutamine, 120 μg/ml penicillin, 100 μg/ml streptomycin, B27, 50 ng/ml EGF, 50 ng/ml FGF-2). Add the conditioned medium previously collected at the final dilution of 30 % on the total medium (*see* **Note 8**).

3.4 GCSCs In Vivo Tumorigenic Assay

1. Every step in the manipulation of the mice must be conducted following the Guidelines for Ethical Treatment of Animals. Due to the chemoresistance that CSCs convey to the tumor

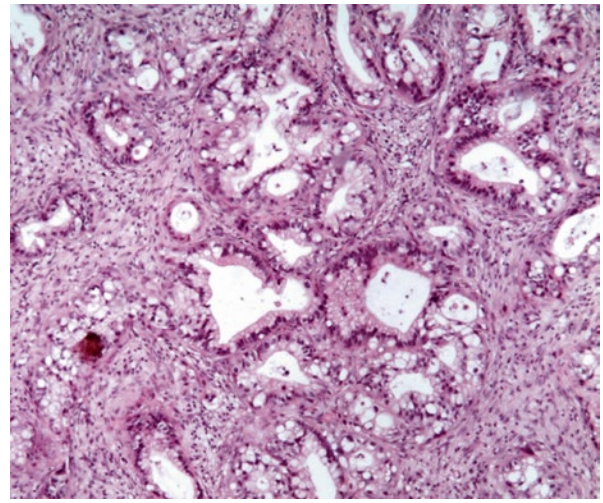

Fig. 2 GCSCs isolated in our laboratory (data not published) from a primary human gastric adenocarcinoma (ADK) were injected in a NOD-SCID female mouse. GCSCs grown subcutaneously as a xenograft that was excised after 3 weeks and H/E stained for the histological analysis. As shown in the reported figure, GCSCs gave rise to a tumor that recapitulates the gastric ADK of origin

they belong to, engrafted xenograft derived from GCSCs can be considered a useful model to test the efficacy of novel or already existing anticancer drugs (Fig. 2).

(a) Evaluate GCSC (from **step 11** of Subheading 3.2) viability by Trypan blue staining.

(b) Resuspend GCSCs in PBS 1× at the final concentration of 10^6 cells/100 μl.

(c) Prepare a 1:1 GCSCs: Matrigel (BD Biosciences) dilution.

(d) Inject 200 μl of GCSCs/Matrigel suspension subcutaneously into the dorsal side of the right flank of NOD-SCID mice (*see* **Note 9**).

(e) Check the mice clinical parameters twice a week.

(f) Sacrifice the animals after 5 months, or when a tumor volume of 500 mm^3 is measured.

(g) Fix the collected tumor in 4 % buffered formalin, cut 4 μm sections and perform the Haematoxylin/Eosin staining.

3.5 GCSC Cell Chemoresistance Assay

1. Evaluate GCSC (from Subheading 3.3) viability by Trypan blue staining.
2. Seed the GCSCs at a density of 1.5×10^4 cells/well in a 96-well plate.

3. The day after, treat the cells with four incremental doses of different anticancer drugs:
   (a) 5-Fluorouracil (10 nM to 1 mM).
   (b) Doxorubicin (10 nM to 10 μM).
   (c) Vinblastine (10 nM to 10 μM).
   (d) Paclitaxel (10 nM to 10 μM).
4. Measure cell viability after 48 h by the aim of the ATPlite 1step Luminescence Assay System, following the Perkin Elmer instructions and reading the plate by a luminometer (*see* **Note 10**).

4 Notes

1. If the operator is not used to deal with primary cancers gross anatomy, the sample should be collected with the help of an expert pathologist, in order to avoid necrotic areas.
2. A critic step of this protocol is the time between the sample collection from the patient and the starting of its processing. To avoid tissue deterioration, it is recommended to reduce this interval to no more than 2 h, and to keep the samples in PBS antibiotics at 4 °C.
3. Stomach is one of the human body organs that are directly connected with the outside, so it is naturally contaminated. In order to remove the native contamination and the one that can derive from the manipulation during the sample collection, it is essential to perform all the first passages using washing solutions and digestion medium supplemented with antibiotics. In case of considerable contamination antibiotics can be added to the culture medium and maintained during the first growth passages.
4. Due to previously cited limitations and to the inner variability of the quality of the samples, the success in isolating and growing primary cancer stem cells culture may vary. Usually a 60–70 % of viable culture is obtained.
5. GCSCs growing in spheres structures need to be digested with Accutase (**step 2** of Subheading 3.2) to be isolated and sorted. However, sometimes the Accutase digestion cannot be effective enough, in this case it would be useful to add EDTA (2 μM) to the cell suspension before sorting the labeled cells.
6. Epithelial specific antigen (ESA) is a synonym for EpCAM. However—as reported in the literature—this acronym should no longer be used (On the abundance of EpCAM on cancer stem cells [13].
7. During the 10-min incubation with Accutase (**step 4** of Subheading 3.3) pass the cell suspension once or twice into a 5 ml Pasteur pipette, to facilitate spheres disaggregation.

8. Maintaining a 30 % of the conditioned medium in the total sphere medium after the spheres disaggregation and seeding helps the survival and propagation of the GCSCs, due to the growth factors and cytokines that it contains.
9. In order to avoid Matrigel solidification (that would irreversibly damage the cell suspension), keep the 1 ml syringe and the GCSCs/Matrigel suspension refrigerated till the moment of the injection.
10. Due to the difficulty in having precise replicates of the GCSCs seeding, even though the spheres are disaggregated, it is recommended to perform the ATPlite 1step Luminescence Assay at least in quintuplicate, to reduce standard deviation as much as possible.

References

1. Fock KM, Katelaris P, Sugano K et al (2009) Second Asia-Pacific consensus guidelines for helicobacter pylori infection. J Gastroenterol Hepatol 24(10):1587–1600
2. Leung WK, Sung JJ (2006) Chemoprevention of gastric cancer. Eur J Gastroenterol Hepatol 18(8):867–871
3. Anderson WF, Camargo MC, Fraumeni JF et al (2010) Age-specific trends in incidence of noncardia gastric cancer in US adults. JAMA 303(17):1723–1728
4. Ford AC (2011) Chemoprevention for gastric cancer. Best Pract Res Clin Gastroenterol 25(4–5):581–592
5. Siolas D, Hannon GJ (2013) Patient-derived tumor xenografts: transforming clinical samples into mouse models. Cancer Res 73(17): 5315–5319
6. Clarke MF, Dick JE, Dirks PB et al (2006) Cancer stem cells--perspectives on current status and future directions: AACR workshop on cancer stem cells. Cancer Res 66(19): 9339–9344
7. Mani SA, Guo W, Liao MJ et al (2008) The epithelial-mesenchymal transition generates cells with properties of stem cells. Cell 133(4):704–715
8. Takaishi S, Okumura T, Tu S et al (2009) Identification of gastric cancer stem cells using the cell surface marker CD44. Stem Cells 27(5):1006–1020
9. Li K, Dan Z, Nie YQ (2014) Gastric cancer stem cells in gastric carcinogenesis, progression, prevention and treatment. World J Gastroenterol 20(18):5420–5426
10. Jiang J, Zhang Y, Chuai S et al (2012) Trastuzumab (herceptin) targets gastric cancer stem cells characterized by CD90 phenotype. Oncogene 31(6):671–682
11. Han ME, Jeon TY, Hwang SH et al (2011) Cancer spheres from gastric cancer patients provide an ideal model system for cancer stem cell research. Cell Mol Life Sci 68(21): 3589–3605
12. Xu G, Shen J, Ou Yang X et al (2013) Cancer stem cells: the 'heartbeat' of gastric cancer. J Gastroenterol 48(7):781–797
13. Gires O, Klein CA, Baeuerle PA (2009) On the abundance of EpCAM on cancer stem cells. Nat Rev Cancer 9(2):143

Chapter 13

Isolation of Chemoresistant Cell Subpopulations

Claudia Canino and Mario Cioce

Abstract

Chemoresistance is a major challenge for cancer therapy and drives tumor relapse. The emergence, within the treated tumor mass, of specific cancer cell subpopulations endowed with high tolerance to the microenvironment stress induced by therapy is being growingly recognized as a mechanism of tumor progression. To obtain detailed information with regard to the pathways underlying survival, expansion, and microenvironmental cross talk of such chemoresistant cell subpopulations may be instrumental for cancer chemoprevention. Additionally, the obtained cell subpopulations may be used for direct screening of cancer chemopreventive compounds, in appropriate experimental settings. Here we report detailed experimental procedures that we and others have setup in order to obtain cell cultures enriched for chemoresistant cells from both malignant pleural mesothelioma specimens and primary cell cultures. We provide indications for the purification and characterization of those chemoresistant cell populations and to generally validate the obtained enriched cell populations for their chemoresistance.

Key words Mesothelioma, Chemoresistance, Pemetrexed, Cisplatin, FACS, ALDH, Primary culture

1 Introduction

Chemotherapy treatment represents a very important aspect of cancer management. However, it appears more and more evident that development of resistance to therapy greatly influences tumor relapse and negatively shapes patient prognosis. One mechanism of tumor resistance which is gaining growing attention is the emergence of specific chemoresistant cell subpopulations within the tumor mass [1]. This is of translational relevance, since combined therapies including stemlike cell-targeting agents exhibit improved efficacy [2, 3]. A hierarchical organization and micro environmental control may underlie the function of such cell subpopulations. We have shown that pemetrexed and cisplatin treatment of malignant pleural mesothelioma (MPM) cell lines and primary cultures trigger the emergence of cell subpopulations endowed with chemoresistance properties (MPM-CICs-chemotherapy-induced cells). The latter represent a small fraction of unsorted, untreated MPM cell populations and their number is

Sabrina Strano (ed.), *Cancer Chemoprevention: Methods and Protocols*, Methods in Molecular Biology, vol. 1379,
DOI 10.1007/978-1-4939-3191-0_13,

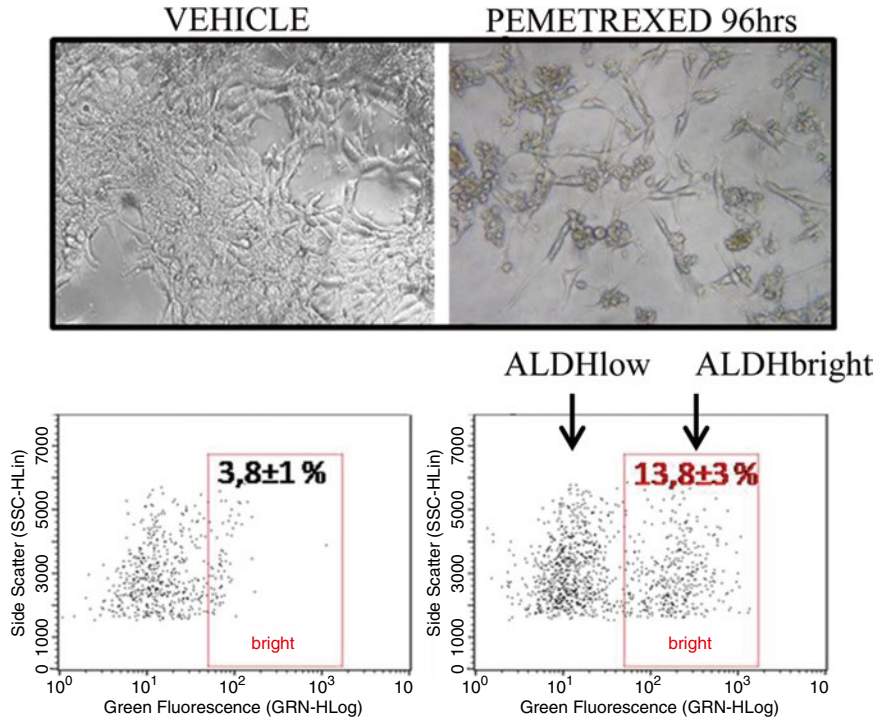

Fig. 1 Pemetrexed treatment induces chemoresistant mesothelioma cell subpopulations. *Upper*. Representative micrographs of vehicle- or pemetrexed-treated mesothelioma cells. *Lower*. Quantitation of ALDH^{bright} cells by FACS from the same cells as in *upper panel*

increased by pemetrexed (and cisplatin) treatment [4] (Fig. 1). MPM-CICs exhibit high levels of aldehyde dehydrogenase (ALDH) activity and can be tracked in unfractionated tumor cell populations by means of this (Fig. 1). Purified ALDH^{bright} MPM cells are chemoresistant as compared to ALDH^{low} cells (Fig. 2): additionally, their number inversely correlates with survival of xenografted host mice [4]. The present chapter aims at describing the protocols we and others have recently setup to identify, enrich and characterize chemoresistant cell subpopulations (ALDH^{bright} cells) from both cell lines and primary cultures. We (and others) have found that the criteria listed below identify cell subpopulations with chemoresistance properties in vitro and in vivo, enrichment for early-differentiation stemlike markers, and ability to reconstitute tumor heterogeneity in vitro and in vivo. The protocols reported here have been applied to successfully isolating mesothelioma [4, 5] and lung cancer (unpublished) cell subpopulations from both cell lines and primary samples. Additionally, we report procedures for the stable selection and enrichment for chemoresistant cell subpopulations.

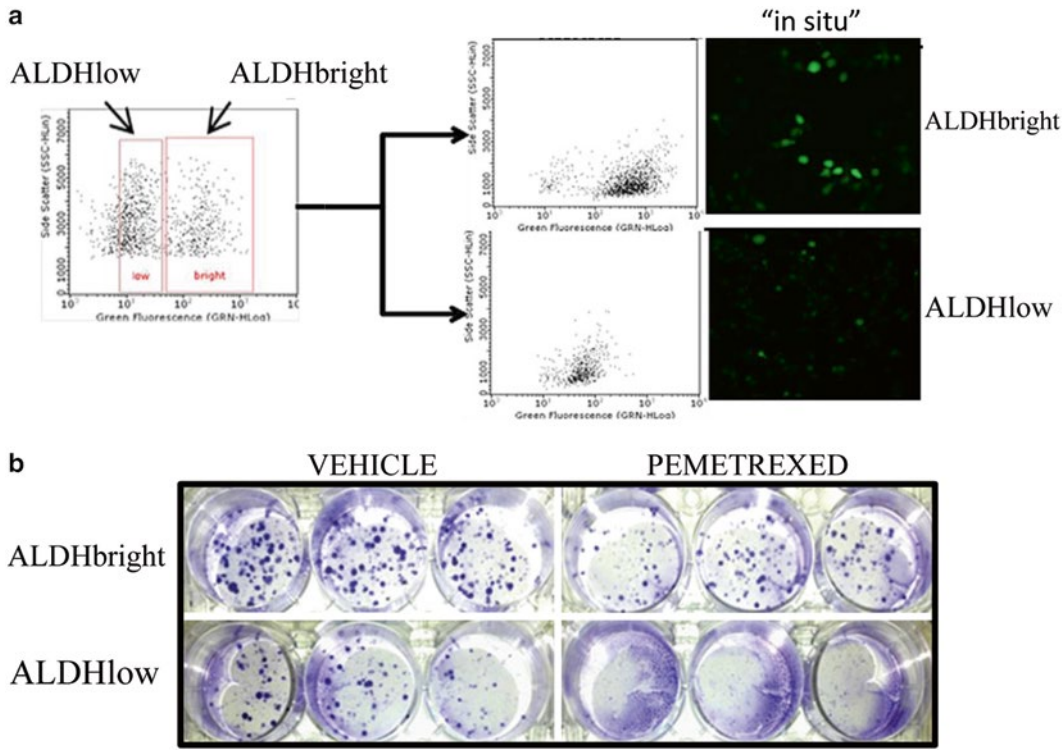

Fig. 2 Features of purified ALDH^{bright}mesothelioma cells. (**a**) Scheme used for FACS-based sorting of ALDH^{bright} and ALDH^{low} cells. (**b**) The ALDH^{bright} cells are chemoresistant. Clonogenic assay. Representative micrographs of CFA assays. Adapted with permission from Oncogene. 2012;31(26):3148–3163

2 Materials

This is a general protocol for the isolation, selection, and maintenance of primary MPM and lung cultures of chemoresistant cells. The resulting cell subpopulations can be used as a tool for the identification of tumor-initiating cells and early progenitor-targeting drugs [6]. The protocol is suitable for both solid specimens and pleural effusion which will be discusses in separate sections below.

2.1 Disaggregation and Cell Culture Reagents

1. PBS: Phosphate-buffered saline. Dissolve the following in 800 ml distilled H_2O: 8 g of NaCl, 0.2 g of KCl 1.44 g of Na_2HPO_4, 0.24 g of KH_2PO_4. Adjust pH to 7.4 with HCl. Adjust volume to 1000 ml with additional distilled H_2O. Sterilize by autoclaving.
2. Collagenase type IV (300 U/ml). Weigh 100 mg of Collagenase Type IV powder and transfer to 150 ml DMEM-F12 medium. When the collagenase is completely dissolved filter-sterilize the solution (0.22 μm) and tighten the cap (the solution is stable

for 14 days after preparation at 4 °C). Prepare the working dilution in DMEM-F12 + 50 mM HEPES cell culture medium according to the specific activity indicated from the manufacturer.

3. Hyaluronidase (100 U/ml). Use Type IV-S from bovine testes (cell culture or embryo-tested). Prepare a stock solution at 10 mg/ml in DMEM-F12 + 50 mM HEPES cell culture medium. Filter-sterilize (0.22 μm), aliquot, and store at –20 °C. The stock solution is stable for 3 months. Prepare the working dilution in DMEM-F12 + 50 mM HEPES cell culture medium according to the specific activity indicated from the manufacturer.
4. Red blood lysis buffer. Dissolve the following in 100 ml distilled H_2O:NH4Cl 8.02 g; NaHCO3 (sodium bicarbonate) 0.84 g; EDTA (disodium) 0.37 g. Store at 4 °C for 6 months. Prepare the working solution by diluting $10n$ times the stock solution in distilled water. Keep cold until use.
5. FBS: Non-heat-inactivated fetal bovine serum.
6. Digestion medium: DMEM-F12 (1:1) + GLUTAMAX supplemented with 1 % BSA-FAF and 5 μg/ml human insulin.
7. Growth medium: DMEM F12 (1:1) + GLUTAMAX supplemented with 5 % non-heat-inactivated FBS, insulin (5 μg/ml).
8. Selection medium: DMEM F12 (1:1) + GLUTAMAX supplemented with 5 % non-heat-inactivated FBS.
9. Freezing medium: 90 % non-heat-inactivated FBS-10 % DMSO.
10. Human recombinant insulin. Dissolve insulin in cell culture grade water at 1–10 mg/ml. Adjust the pH to 2.0–3.0 with diluted HCl. Filter using a low protein-binding filter with a pore size of 0.2 μm. Store at –20 °C for 2 months.
11. BSA-FAF: Bovine serum albumin-fatty acid free.
12. Ciprofloxacin.
13. ACCUTASE Cell detachment solution.
14. Trypan Blue Cell Staining Reagent. Weight 0.2 g Trypan Blue in 99.8 ml distilled water. Filter at 0.22 μm. Dilute the stock solution five times in PBS1× before cell staining.
15. ALDEFLUOR kit (Stem Cell Technologies).
16. SYTOX Dead cell staining reagent.
17. Pemetrexed. Dissolve pemetrexed disodium initially in DMSO at a concentration of 4 mg/ml and further dilute with cell culture medium to the desired concentration.
18. Cisplatin. Dissolve in DMSO at 50 mg/ml and further dilute with cell culture medium to the desired concentration.

2.2 Equipment

1. Scalpels and microdissecting forceps.
2. 5 ml Pasteur pipette.
3. 15 ml centrifuge tubes.
4. 50 ml centrifuge tubes.
5. Centrifuge capable of running at $\geq 300 \times g$.
6. Nylon mesh (70 μm).
7. Cell culture setup.
8. CORNING #3261 for 100 mm Ultralow attachment dishes or alternatively, sterile Petri dishes not treated for cell culture.
9. Polycarbonate FACS tubes.
10. A suitable cytofluorimeter for FACS analysis.
11. A suitable FACS-based sorter.

3 Methods

3.1 Isolating MPM Cells from Clinical Specimens

3.1.1 Procedure for Isolating MPM Cells from Surgical Specimens (See **Notes 1** and **2**)

1. Wash the tumor specimen three times with PBS1× supplemented with ciprofloxacin 4 mg/ml. Submerge three times for 5 min the sample in three different 50 ml tubes filled with 25 ml of antibiotic solution. To disaggregate the solid tumor follow three sequential steps (in a tissue-culture sterile hood) (*see* **Note 3**).
2. Manually cut the solid tumor into ≤1.5 mm pieces with scalpels in a sterile 60 mm Petri dish with 1 ml PBS1×.
3. Enzymatic disaggregation: Resuspend tumor pieces in a T-25 cell culture flask with 5 ml of digestion medium. After resuspension, add collagenase (final concentration 50 U/ml) and hyaluronidase (final concentration 20 U/ml) to the tumor suspension and leave cells in the incubator for 2 h at 37 °C, 5 % CO_2. Every 15 min resuspend the semi-digested tumor with a 5 ml sterile Pasteur pipette by gently pipetting up and down to disperse tumor pieces.
4. Filter the digested material through a sterile nylon mesh (70 μm) in a 50 ml tube. Wash the filter with PBS1× and collect the flow-through.
5. Transfer the filtered material to a 15 ml centrifuge tube.
6. Spin at $300 \times g$ for 10 min at room temperature (RT).
7. Resuspend the pellet in growth medium supplemented with ciprofloxacin (4 μg/ml) (*see* **Note 4**). Assess the number of live cell with Trypan Blue exclusion method.
8. Seed cells in low-adhesion cell culture dishes at a cell density $\geq 1–1.5 \times 10^6$ cells/ml (*see* **Note 5**). Grow cells for 10 days by adding 25 % fresh medium every 3 days. After 10 days, a relatively homogeneous population of mesothelioma cells (virtually devoid of adhering macrophages, lymphocytes, fibroblasts) [5] can be observed in culture (*see* **Note 6**).

3.1.2 Procedure for Isolating MPM Cells from Pleural Effusions

1. Collect the pleural effusion in 15 ml FALCON tubes diluted 1:1 with PBS1× supplemented with ciprofloxacin 4 μg/ml.
2. Harvest cells by centrifugation at 300×*g* for 10 min at room temperature (RT). Keep the cell-free medium (supernatant–pleural effusion) (*see* **Note** 7). Filter (0.22 μM) the supernatant-pleural effusion for subsequent use.
3. Resuspend cells in red blood lysis buffer (10 bed pellet volumes). Incubate for 5 min at room temperature (RT).
4. Centrifuge (300×*g* for 10 min) and discard supernatant.
5. Resuspend the pellet in growth medium supplemented with ciprofloxacin (4 μg/ml) and add 30 % (vol/vol) of the previously collected cell-free conditioned medium (from **step 2**). Count total live cell number with Trypan Blue.
6. Seed cells in low-adhesion cell culture dishes at a cell density ≥1–1.5×10^6 live cells/ml. Size of the dish must be chosen according to the available number of cells in order to achieve the desired concentration. Grow cells for 10 days by adding 25 % fresh medium every 3 days. After 10 days, a relatively homogeneous population of mesothelioma cells (virtually devoid of adhering macrophages, lymphocytes, fibroblasts but still comprising both adherent and floating elements) can be observed in culture (Fig. 3).
7. The MPM primary cultures can be propagated for a limited length of time (8–12 weeks) as follows.

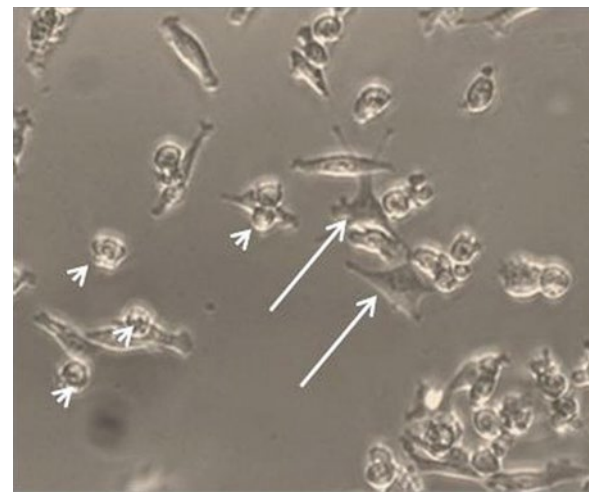

Fig. 3 Representative micrograph of a MPM cell culture (from a malignant pleural effusion) at 2 weeks after seeding. *Arrows*: adherent, fibroblast-like cells. *Arrowheads*: loosely adherent, rounded cells. Reproduced with permission from http://www.bio-protocol.org/e285

3.2 Propagation of MPM Cultures

1. Collect cell culture medium in a centrifuge tube (*see* **Note 8**). Wash the adherent cells with 3–5 ml of PBS1× and add it to the collected cell culture medium. This contains loosely adherent or floating cells. PBS1× should be ≤30 % final volume in the collection tube.
2. Wash cells again with PBS1×, discard PBS1× and add Accutase (1.5 ml/dish).
3. Incubate cells in the incubator for 5 min at 37 °C, 5 % CO_2. Harvest the detached cells with the collected cell culture medium/PBS1× washing from **step 1**. Collect cells by centrifugation at 300 × *g* for 10 min at room temperature (RT). Do not discard the supernatant.
4. Resuspend the pellet in growth medium. Count total live cell number with Trypan Blue exclusion method.
5. Seed cells in low-adhesion cell culture dishes at a density ≤0.5×10^6 live cells/ml. To achieve the required cell concentrations dilute the harvested cells with the previously collected supernatant. The dilution medium must represent ≥of the 30 % of the final cell culture volume in the dish.

3.3 Selection of Chemoresistant Cell Subpopulations

3.3.1 Determining the CC_{50} (See **Note 9**)

1. Seed a small aliquot of the obtained cell populations (pooled: adherent and floating cells—"probe cells") in 96 wells at 1500-cell well in selection medium. Treat the cells 24 h later with at least 9–12 points of doses (we usually test cisplatin + pemetrexed, a current line of treatment for MPM) in duplicate wells (*see* **Note 10**).
2. At 24, 48, and 72 h from the treatment evaluate viability by either Trypan Blue counting of detached cells or by SYTOX staining of the detached cells by FACS (*see* **Notes 11** and **12**).
3. Calculate CC_{50} (*see* **Note 13**).

3.3.2 Start Selection for Chemoresistant Cell Subpopulation

1. After having empirically determined the CC_{50}, add the appropriate volume of selecting agents (for MPM: cisplatin + pemetrexed) to the larger cell culture without further addition of fresh cell culture medium. Incubate for 7 dd without renewing the culture medium.
2. After 7 dd, a sharp increase of chemoresistant cell subpopulations is expected [4]. Such cell subpopulations may be analyzed by FACS and enriched by FACS sorting for their aldehyde dehydrogenase (ALDH) activity components as follows.

3.4 FACS-Based Identification of $ALDH^{bright}$ Cells

1. Collect whole-cell populations (adherent + loosely attached cells) by centrifugation. Detach the adherent fraction by Accutase treatment as previously described.
2. Centrifuge the cell suspension at 300 × *g* for 10 min to pellet the cells.

3. Discard the supernatant.
4. Resuspend the cell pellet with 10 ml of PBS1× to remove residual Accutase.
5. Centrifuge the cell suspension as before. Aspirate and discard the rinse solution.
6. Resuspend the cells at 1×10^6 cells/ml (range $0.5–1 \times 10^6$ cells/ml) at room temperature (15–25 °C) with ice cold ALDEFLUOR® assay buffer.
7. For each sample, have ready a test (ALDH substrate, BAA: BODIPY®-aminoacetate, 1:200) and a "control" (15 UM) ALDH inhibitor:DEAB, diethylaminobenzaldehye + BAA).
8. Incubate the "test" and "control" samples between for 45 min (range 30–60 min) in a 37 °C 5% CO^2 incubator, light protected. Allow free diffusion of the oxygen/CO_2 (keep the tubes uncapped!).
9. Following incubation, centrifuge the "test" and "control" tubes at 4 °C for 5 min at 300 × *g*. Carefully aspirate the supernatant without disturbing the cell pellet. Resuspend the cell pellet in 0.5 ml of ice cold ALDEFLUOR® assay buffer and place samples immediately on ice. To exclude dead cells from data acquisition, add SYTOX® Red Dead Cell Stain (Life Technologies) which allows nonproblematic detection of both $ALDH^{bright}$ and dead/dying cells with compromised cell membrane permeability.
10. For details on flow cytometer setup and data acquisition, refer to the product information sheet provided with the ALDEFLUOR® Assay Kit or go to: http://www.stemcell.com/technical/01700-PIS.pdf. (*see* **Note 14**). Briefly, the cells endowed with high ALDH activity will be gated as the brightest cells on the FITC axis (test tube) whose fluorescence disappears after inhibition of the ALDH enzyme with DEAB ("control" tube). Cells acquiring fluorescence independently of DEAB treatment do not possess ALDH activity but rather fluoresce because of passive diffusion of the ALDH substrate (BAA). FACS-based purification of $ALDH^{bright}$ cells. Perform FACS-sorting according to the manufacturer's instructions of your FACS sorting instrument.

3.5 Freezing or Propagation of Purified ALDHbright Cells

The obtained cells can be used immediately after sorting for gene expression/microRNA profiling, frozen or seeded for propagation and further selection.

1. Freezing of FACS-sorted cells.

   Freshly sorted cells can be collected by centrifugation and directly resuspended in freezing medium (*see* **Note 15**).

2. Propagation of the FACS-sorted ALDH^{bright} cells (*see* **Notes 16–20**).

   For the propagation of the sorted cells, please refer to point Subheading 3.2.

4 Notes

1. Please *note* that all the procedures described below involving the use of patient samples must be pre-approved by the Ethical Committee.
2. Critical step: The time interval from tumor resection and processing must be kept to a minimum, ideally ≤2 h.
3. Critical step: To prevent undesired contamination, work under sterile condition at all steps and whenever possible. Do not allow alcohol, staining reagents or disinfectants to come in contact with the specimen.
4. Ciprofloxacin prevents contamination of the material from non-sterile handling of the tumor specimens during the harvesting of the sample.
5. The obtained tumor digests consist initially of a heterogeneous population, comprising but not limited to mesothelioma cells, macrophages, immune infiltrate, stromal cells, adipocytes, and remnant red blood cells. However, within 72–96 h from seeding most of the cells in culture consist of mesothelioma cells, since the mentioned accompanying cell subpopulations will not propagate in the experimental conditions used here, as revealed by morphological observations and clonogenic assays (55) (and unpublished observations). The obtained populations have been shown to originate MPM-like tumors when injected into NOD/SCID mice with very high resemblance to the originating tumor [4].
6. A typical yield of 1×10^6 cells can be obtained from a 100 mg solid specimen. A typical yield of 10×10^6 cells can be obtained from 30 to 50 ml freshly collected pleural effusion (after removal of red blood cells, RBC).
7. The reason to keep the conditioned medium during propagation of the MPM cultures is its enrichment for growth factors and cytokines produced by the MPM cells which favors survival and propagation of the cells especially at early steps of establishing the culture [7].
8. For the propagation of the primary cell cultures, always collect both floating (or loosely adherent) and adherent cell subpopulations. It is very important to keep conditioned medium during harvesting of the cells and to add it back to cell culture during the establishment of primary cultures. All the volumes

listed below refer to 100 mm dishes. Please vary volumes of solutions according the size of the cell culture dishes used.

9. This protocol requires, first, to determine the sensitivity (CC_{50}) of the isolated cell cultures (a probe aliquot of the obtained culture) to the chemotherapy agents. The CC_{50} is defined as the concentration of drug (alone or in combination) capable of eliciting a 50 % reduction in the number of viable cells. After that, a larger fraction of the culture will be selected, at the identified CC_{50} dosages, for 7 dd to elicit the emergence of chemoresistant cell subpopulations
10. Please include appropriate vehicles and do not exceed 0.5 % final concentration if DMSO or other organic solvents are used as a vehicle.
11. Please *note* that this assay will not distinguish, at this stage, between cytostatic or cytotoxic effects of the treatments.
12. Other viability assays can be used to evaluate the effect of the treatments. However, we have empirically found the mentioned to be of broader utility as being not influenced by metabolic status of the cells or changes in plasma membrane composition induced by some chemotherapy agents.
13. CC_{50} can be calculated manually or by using commercially available software, such as KALEIDAGRAPH, SIGMAPLOT, or GRAPHPAD. In case of combined treatment, the drug interactions must be taken in consideration to unravel "additive" or synergistic interaction between the treatments.
14. The aldehyde dehydrogenases (ALDH) are enzymes ubiquitously expressed in developing tissues and adult liver where they act as either as a detoxifying enzymes and as a metabolic modulators. Cancer cells endowed with high ALDH activity (generally named $ALDH^{bright}$ because of the intracellular accumulation of a fluorescent ALDH substrate, as opposed to $ALDH^{low}$, which do not exhibit substrate accumulation) have been isolated from a variety of solid tumors, including breast, lung, ovary, prostate, osteosarcoma, and glioblastoma and shown to contribute protumorigenic features [7–9].
15. Alternatively, a serum-free, methylcellulose containing-freezing medium can be used. No differences in the biological features of the sorted cells (clonogenicity and chemoresistance) were observed when comparing the two methods. However, the lack of DMSO in the freezing medium significantly affects the viability of the frozen cells (from four representative MPM primary cultures).
16. This protocol may be generally applicable to other solid tumors (breast, prostate, glioblastoma) proven that important differences residing in the different biological context of the tissues examined will be taken into consideration (i.e., hormone

sensitivity). In order to fulfill the definition of "chemoresistant," the isolated cell subpopulations must exhibit resistance (time dependent and over a broad range of concentrations) to the currently used chemotherapeutics, specific for the tumor/tissue studied. Resistance to therapeutics should be defined as relative to untransformed nonimmortalized (if available) cell cultures derived from apparently unaffected tissue or at least from immortalized, untransformed cell cultures.

17. The isolated cell subpopulations should be at least partially propagable under the selective conditions mentioned. The selected cell subpopulations should exhibit ability to reconstitute the cell culture heterogeneity in vitro or the tissue heterogeneity in vivo. This indicates potential for tumor relapse.
18. Inter-patient variability. Please keep in mind that working with patient samples is intrinsically complex. First, the rate of successful isolation and propagation can vary (we obtain 70 % of successful isolation/maintenance of primary cultures). Second. A significant inter-patient variability (due to different underlying health status, to different stages of the disease, to the presence of potentially undiagnosed lesions impinging on altered tumor microenvironment) is normally observed when patient-derived primary cell cultures for a specific biological function. The latter problem can be overcome by using larger number of specimens in order to obtain statistical support to the observed phenomena.
19. The FACS-based selection for high aldehyde dehydrogenase-expressing cells ($ALDH^{bright}$) identifies a heterogeneous population of chemoresistant cells. The $ALDH^{bright}$ cell population is intrinsically heterogeneous, in terms of cell cycle status, expression of membrane markers and, possibly, pathway activation. However, the described procedure undoubtedly enriches for chemoresistant cell subpopulations, as described by us and others in MPM, lung, breast, GBM, and prostate.
20. Be aware that, as shown by us and others [4, 8, 9], the isolated $ALDH^{bright}$ cells do spontaneously generate $ALDH^{low}$ cells in culture in a unidirectional way. This is partially independent of the drug selection process. For MPM, $ALDH^{bright}$ cell number drops significantly within the first 2 weeks of culture, after FACS sorting.

Acknowledgement

M.C. was supported by the NYU Cancer Institute Cancer Center Support Grant's Developmental Project Program (P30CA016087).

References

1. Abdullah LN, Chow EK (2013) Mechanisms of chemoresistance in cancer stem cells. Clin Transl Med 2(1):3
2. Cojoc M, Mabert K, Muders MH et al (2015) A role for cancer stem cells in therapy resistance: Cellular and molecular mechanisms. Semin Cancer Biol 31:16–27
3. Vidal SJ, Rodriguez-Bravo V, Galsky M et al (2014) Targeting cancer stem cells to suppress acquired chemotherapy resistance. Oncogene 33(36):4451–4463
4. Canino C, Mori F, Cambria A et al (2012) SASP mediates chemoresistance and tumor-initiating-activity of mesothelioma cells. Oncogene 31(26): 3148–3163
5. Cioce M, Canino C, Goparaju C et al (2014) Autocrine CSF-1R signaling drives mesothelioma chemoresistance via AKT activation. Cell Death Dis 5:e1167
6. Cioce M, Gherardi S, Viglietto G et al (2010) Mammosphere-forming cells from breast cancer cell lines as a tool for the identification of CSC-like- and early progenitor-targeting drugs. Cell Cycle 9(14):2878–2887
7. Lanfrancone L et al (1992) Human peritoneal mesothelial cells produce many cytokines (granulocyte colony-stimulating factor [CSF], granulocyte-monocyte-CSF, macrophage-CSF, interleukin-1 [IL-1], and IL-6) and are activated and stimulated to grow by IL-1. Blood 80(11):2835–2842
8. Cortes-Dericks L, Froment L, Boesch R et al (2014) Cisplatin-resistant cells in malignant pleural mesothelioma cell lines show ALDH(high) CD44(+) phenotype and sphere-forming capacity. BMC Cancer 14:304
9. Luo Y, Dallaglio K, Chen Y et al (2012) ALDH1A isozymes are markers of human melanoma stem cells and potential therapeutic targets. Stem Cells 30(10):2100–2113

Chapter 14

Autophagy in Cancer Chemoprevention: Identification of Novel Autophagy Modulators with Anticancer Potential

Yuanzhi Lao and Naihan Xu

Abstract

Cancer cells have the ability to tolerate extreme conditions, autophagy-related stress tolerance enables cancer cells to survive by maintaining energy production that leads to cell growth and therapeutic resistance. Insufficient activation of autophagy in nutrient-deprived cancer cells may sensitize cancer cells to a broad array of chemotherapeutic agents and ionizing radiation. Therefore, identification of novel autophagy modulators with lower toxicity and better therapeutic index would be beneficial for cancer therapy. Here, we describe several currently used biochemical methods to assess autophagic activity and lysosomal function in cultured cancer cells. We also discuss both in vitro and in vivo assays to clarify the anticancer potential of novel autophagy modulators.

Key words Autophagy, Lysosome, Autophagosome, Immunofluorescence, Flow cytometry, GFP-LC3, Cathepsin, DQ-BSA, Cell death, Cancer, Caloric restriction

1 Introduction

Autophagy is an evolutionarily conserved membrane process that results in the transporting of cellular contents to lysosomes for degradation [1–4]. The execution of autophagy involves a group of evolutionarily conserved autophagy-related (ATG) proteins [5, 6]. Microtubule-associated protein light chain 3 (LC3), a mammalian homolog of yeast Atg8, is known to exist on autophagosomes, and serves as a widely used marker for autophagosomes [7–9]. However, an accumulation of autophagosomes (can be measured by GFP-LC3 puncta or lipidated LC3-II on a western blot) is not always indicative of autophagy induction, it may reflect an inhibition of autophagy, which can occur by inhibiting autophagosome–lysosome fusion, or a lysosomal defect following inefficient degradation of autophagic substrates inside the lysosomes. To distinguish between bona fide induction of autophagy and impairment of autophagic degradation, it is necessary to monitor the dynamic process of cellular autophagic activity (autophagic

Sabrina Strano (ed.), *Cancer Chemoprevention: Methods and Protocols*, Methods in Molecular Biology, vol. 1379,
DOI 10.1007/978-1-4939-3191-0_14,

flux). Currently, several approaches have been developed to accurately assess autophagic activity in a giving biological setting, more specific agents will be identified to modulate autophagic activity and subsequently be used for anticancer treatment [7, 8].

The role of autophagy represents a "Janus face" within the context of cancer. Autophagy can function as a tumor suppression mechanism by removing damaged organelles and proteins and preventing genomic instability that drives tumorigenesis. However, autophagy has been shown to promote the survival of tumor cells from various forms of cellular stress within the tumor microenvironment [10–13]. To this end, modulating autophagy may be therapeutically useful and serve as a novel approach for enhancing the efficacy for existing cancer therapy. Compounds from natural herbs are important sources for drugs against a wide variety of diseases, including cancer. Several natural compounds have been identified to modulate autophagic activity and be used for anticancer treatment [14, 15]. Here, we discuss detail both in vitro and in vivo methods to unravel the complex mechanisms of novel autophagy modulators with anticancer potential.

2 Materials

2.1 Immunofluorescence Components

1. 1× PBS solution: Dissolve 8 g NaCl, 0.2 g KCl, 1.44 g Na_2HPO_4, 0.24 g KH_2PO_4 in 800 mL of deionized H_2O. Adjust the pH to 7.4 with 1 N HCl, and then add deionized H_2O to 1 L. Dispense the solution into aliquots and sterilize them by autoclaving before use. Store at room temperature.
2. Fixing solution: Add 4 g of paraformaldehyde powder to 80 mL of 1× PBS to a glass beaker in a ventilated hood. Heat to approximately 70 °C for 2 h until the powder is dissolved. Adjust the volume of the solution to 100 mL with 1× PBS. The solution can be aliquoted and frozen or stored at 4 °C for up to 1 month (*see* **Note 1**).
3. Permeabilizing solution: Add 250 μL of 100 % Triton X-100 to 100 mL of 1× PBS to yield 0.25 % Triton X-100. Store at room temperature (*see* **Note 2**).
4. Blocking buffer: Add 3 g of bovine serum albumin (BSA) powder to 80 mL of 1× PBS to a glass beaker. Place a sterile, magnetic stir bar in the beaker. Place the beaker on a stir plate, and turn on the stir plate to a low speed until the BSA powder is dissolved completely. Adjust the volume to 100 mL with 1× PBS. Store at 4 °C.
5. Antibodies: LAMP1 (D2D11) Rabbit mAb (Cell Signaling Technology, 9091) is diluted 100 times in blocking buffer. Alexa Flour 555 goat anti-rabbit IgG (H + L) (Life Technologies, A-21428) is diluted 250 times in blocking buffer.

6. Mounting medium: Vectashield mounting medium with 4′,6-diamidino-2-phenylindole (DAPI) (Vector Laboratories, H-1200) (*see* **Note 3**).

2.2 Fluorescent Probes

1. LysoTracker Red DND-99 (Molecular Probes, L-7528): Dilute the 1 mM stock solution to the final working concentration in the growth medium or 1× PBS. Store the stock solution at –20 °C and protect from light.
2. DQ™ Red BSA (Molecular Probes, D12051): Dissolve 1 mg of DQ™ Red BSA in 1 mL of 1× PBS to make a 1 mg/mL stock solution. The stock solution can be aliquoted and frozen or stored at 4 °C for several weeks. Add 2 mM sodium azide as a preservative. Protect from light.

2.3 Cathepsin Activity Assay Components

1. Cathepsin B activity assay kit (BioVision, 140-100). Store the kit at –20 °C.
2. Cathepsin D activity assay kit (BioVision, 143-100). Store the kit at –20 °C.
3. Corning 96-well plates, solid black polystyrene (Corning, 3650).

2.4 Agents for Flow Cytometry

1. Fixing solution: Add 70 mL of absolute ethanol to 30 mL of 1× PBS or distilled water. Keep the solution at 4 °C.
2. Propidium iodide (P4170, Sigma-Aldrich): Dissolve 10 mg powder in 1 mL of 1× PBS or deionized H_2O to yield 10 mg/mL stock solution. Store the stock solution at 4 °C. Protect from light.
3. RNase A (R6513, Sigma-Aldrich): Dissolve 10 mg powder in 1 mL of 1× PBS or deionized H_2O to yield 10 mg/mL stock solution. Store the stock solution at –20 °C.

3 Methods

3.1 Assessing Autophagosome–Lysosome Fusion

3.1.1 Live Cell Imaging of GFP-LC3 and LysoTracker Red

1. Plate HeLa cells stably overexpressing GFP-LC3 at a density of 2.0×10^5 cells per well in custom-made glass-bottomed 35-mm culture dishes, spread the cells evenly by gently rocking the dish back and forth.
2. Cells are cultured in complete tissue culture medium (DMEM + 10 % fetal bovine serum) and incubated at 37 °C in a humidified 5 % CO_2 incubator overnight.
3. Cells are treated with the test compound in complete tissue culture medium for a certain period of time at 37 °C. Set up control experiment at the same time. Cells are washed three times with prewarmed 1× PBS, then cultured in starvation medium (Earle's Balanced Salt Solution, Sigma) for 2–3 h to induce autophagy (*see* **Note 4**).

4. To stain lysosomes, cells are incubated with 50 nM LysoTracker Red DND-99 (Molecular Probes/Invitrogen) in 1 mL pre-warmed complete tissue culture medium for 30 min at 37 °C. Check the labeling of LysoTracker Red under the fluorescence microscope, and make sure that the dye is not overloaded.
5. Autophagosomes can be visualized by detecting GFP-LC3 puncta; lysosomes can be detected by LysoTracker Red DND-99 labeling. Live cell images of autophagosomes and lysosomes are captured by confocal microscope (*see* **Note 5**).

3.1.2 Immunofluorescent Staining of LAMP1

The retention of LysoTracker probes is likely to involve protonation at neutral pH. The intensity of LysoTracker dye can be changed by pH alteration. Therefore, we can use the antibody of LAMP1 (lysosomal-associated membrane protein 1), a marker protein for endosomal and lysosomal membranes, to confirm the observation from LysoTracker staining [16].

1. Prepare a 12-well tissue culture plate by adding sterilized 16 mm round glass cover slips in the well.
2. HeLa cells stably overexpressing GFP-LC3 are plated at a density of 2.0×10^5 cells/well. Cells are cultured at 37 °C in a humidified 5 % CO_2 incubator overnight.
3. Cells are treated the same as **step 3** in Subheading 3.1.1.
4. Cells are washed with 1× PBS to remove excess medium. Add 4 % paraformaldehyde solution to fix cells for 15 min at room temperature.
5. Cells are washed twice with 1× PBS and then incubated in 0.25 % Triton X-100/PBS solution to permeabilize the cell membrane to allow entry of the antibody. Permeabilize cells for 5 min at room temperature, followed by washing the cells three times with 1× PBS.
6. Cells are incubated with a blocking agent (3 % BSA in 1× PBS) to prevent nonspecific binding of the antibody. Block cells for 1 h at room temperature or overnight at 4 °C.
7. Dilute LAMP1 rabbit monoclonal antibody (Cell Signaling Technology, 9091) 100 times in blocking agent. Optimal antibody concentration should be determined by titration.
8. Place 20–25 μL diluted primary antibody on a 12-well plate covered with parafilm. Pick up the cover slip with tweezers carefully and lay it over the antibody solution to make sure the cells are in fully contact with the antibody. Cells are incubated with primary antibody for 1 h at room temperature or over night at 4 °C in a humid chamber (*see* **Note 6**).
9. Carefully pick up the cover slips and place them back to the 12-well plate. Wash cells three times with 1× PBS, 3 min each time.

10. Dilute Alexa Fluor 555 goat anti-rabbit (Invitrogen) 250 times in blocking agent. Cells are incubated with secondary antibody for 1 h at room temperature. The procedure is the same as primary antibody staining. Protect from light.
11. Carefully remove the cover slips as described for the primary antibody, wash cells three times with 1× PBS, 3 min each time.
12. To mount cover slips, we use Vectashield mounting medium with DAPI (Vectorlabs). Place an appropriate volume of Vectashield on a clean microscope slide. Carefully pickup the cover slip from the PBS solution, rinse with deionized water to get rid of excess salt. Dab off excess water with kimwipe by capillary action. Place the cover slip on the top of mounting medium and descend slowly to avoid air bubbles, suction off excess mounting medium, and seal with nail polish. Label the slides and keep them in microscope slide storage box. Store the slide box at 4 °C.
13. Images of GFP-LC3 and anti-LAMP1 are captured by confocal microscope.

3.1.3 Autophagosome–Lysosome Colocalization Analysis

The colocalization of autophagosomes and lysosomes can be analyzed by Pearson's correlation coefficient (PCC) calculation, which is one of the standard techniques applied in pattern recognition for matching one image to another in order to describe the degree of overlap between the two patterns [17]. The formula for PCC is given below for image consisting of red and green colors:

$$PCC = \frac{\sum_i (R_i - R_{\text{ave}}) \times (G_i - G_{\text{ave}})}{\sqrt{\sum_i (R_i - R_{\text{ave}})^2} \times \sqrt{\sum_i (G_i - G_{\text{ave}})^2}}$$

where Ri and Gi refer to the intensity values of pixel i from red and green images, respectively. R_{ave} and G_{ave} refer to the mean intensity of red and green images, respectively. PCC value ranges from −1 to 1, with a value of −1 representing a total lack of overlap between pixels from the images, and a value of 1 indicating perfect image registration. Quantification of PCC values may follow the steps below:

1. Most of the confocal microscope software provides analytical tool for PCC calculation. We use Olympus FluoView as an example in this protocol. The confocal images of GFP-LC3 and LysoTracker Red are acquired by 63× oil objective with Z stack less than 2 μm.
2. To calculate the PCC of interest cells, use any of the drawing/selection tools (i.e., polyline, *see* Fig. 1a), and then select "PCC measurement" from the Analyze menu; you will see a popup box with PCC values.

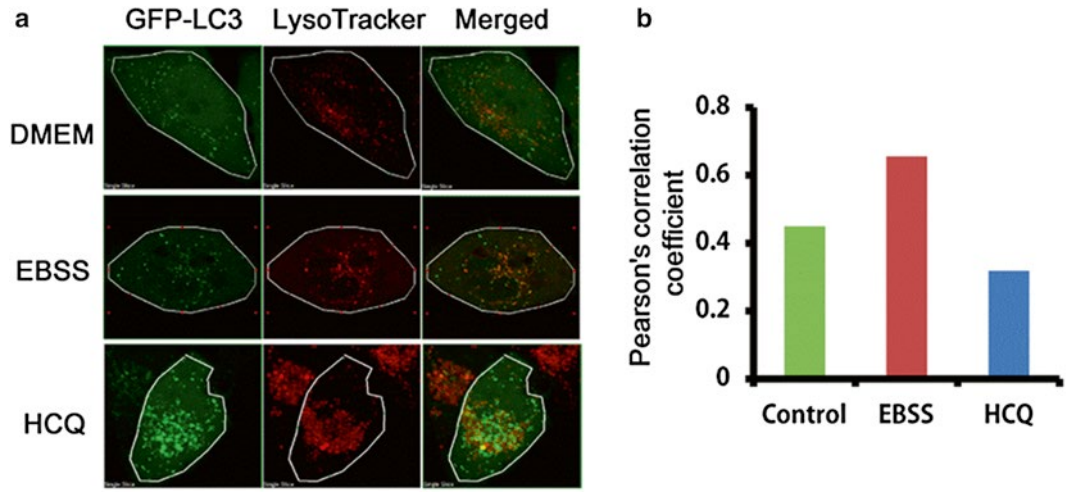

Fig. 1 Use PCC values to quantify the colocalization of autophagosomes and lysosomes. (*a*) HeLa cells overexpressing GFP-LC3 were treated with autophagy inhibitor HCQ for 4 h, or cultured in EBSS medium for 2 h to induce autophagy. Live cells images were captured by use of Olympus confocal microscope. (*b*) The colocalization of GFP-LC3 and LysoTracker Red was determined by quantifying the PCC values. More than 30 cells were counted in each condition and data (mean ± SD) are representative of two independent experiments

3. Repeat this step for the other cells you want to measure. Copy the data to Excel file and calculate the average value for each sample.
4. Use PCC values to quantify the colocalization of GFP-LC3 and LysoTracker (*see* Fig. 1). Accordingly, the colocalization of GFP-LC3 and LAMP1 can be determined the same way (*see* **Note 7**).

3.2 Monitoring Lysosomal Activity with DQ-BSA

To detect lysosomal activity, cells can be assayed for their activity to process DQ-BSA. These BSA derivatives are highly labeled with green or red BODIPY dyes that are strongly self-quenched. Proteolysis of the BSA conjugates result in dequenching and release of brightly fluorescent fragments. Thus, the use of DQ-BSA is useful for the visualization of intracellular proteolytic activity in a variety of applications [18]. To analyze lysosomal activity inside cells, the following procedures may be followed:

1. Prepare a 12-well tissue culture plate by adding sterilized 16 mm round glass cover slips in the well.
2. HeLa cells overexpressing GFP-LC3 are plated at a density of 2×10^5 cells/well on a 12-well tissue culture plate. Cells are cultured at 37 °C in a humidified 5 % CO_2 incubator.
3. When cells reach 50~70 % confluence, incubate cells with DQ™ Red BSA at a concentration of 10 μg/mL in complete tissue culture medium for 10~12 h at 37 °C in a humidified 5 % CO_2 incubator (*see* **Note 8**).

4. Cells are washed twice with prewarmed 1× PBS to remove excess probe in the medium.
5. Cells are incubated in Earle's Balanced Salt Solution for 2–3 h to induce autophagy. Nutrient starvation is usually used as positive control to allow for detection of DQ-BSA fluorescence.
6. Cells are treated with the test compound or bafilomycin A1 (5 nM) in either complete tissue culture medium or Earle's Balanced Salt Solution for a certain period of time at 37 °C. Bafilomycin A1 is a V-ATPase inhibitor which inhibits autolysosome maturation and lysosomal degradation, it can be used as a negative control.
7. Aspirate medium from cells and fix them in 4 % paraformaldehyde solution for 15 min at room temperature.
8. Wash cells twice with 1× PBS, mount the cover slips onto glass slides using Vectashield or other mounting media. Aspirate excess mounting media from the slide and seal cover slips in place with nail polish. Store the slides at 4 °C and protect from light.
9. Images of GFP-LC3 and DQ™ Red BSA are captured by confocal microscope. The fluorescence intensities of DQ™ Red BSA are analyzed by Image J software (*see* **Note 9**).
10. Select the cell of interest using any of the drawing/selection tools (i.e., circle, *see* Fig. 2a), and then select "Measure" from the Analyze menu; you will see a popup box with a stack of values. Repeat this step for the other cells you want to measure. Select a region without fluorescence as background.
11. Select all the data in the Results window, copy and paste into an Excel worksheet, calculate the integrated fluorescence intensity of DQ™ Red BSA by subtracting the background readings (*see* Fig. 2b).

3.3 Assessing Lysosomal Cathepsin Activity

Autophagy involves the proteolytic degradation of cellular components in lysosomes, which requires the activity of proteases. Lysosomal cathepsins help to maintain cellular homeostasis by participating in the degradation of heterophagic and autophagic materials [19]. Tumor invasion and metastasis are associated with altered lysosomal trafficking and increased expression of cathepsins, especially the cysteine cathepsins—cathepsin Band the aspirate cathepsins—cathepsin D [20]. Therefore, inhibiting cathepsin activity could a useful therapeutic strategy for cancer therapy.

To assess cathepsin B and cathepsin D activities in different experimental conditions, the following protocol may be followed:

1. HeLa cells are plated at $4\sim5\times10^5$ cells per well and cultured in complete tissue culture medium (DMEM + 10 % fetal bovine serum) in a 6-well tissue culture plate at 37 °C in a humidified 5 % CO_2 incubator overnight.

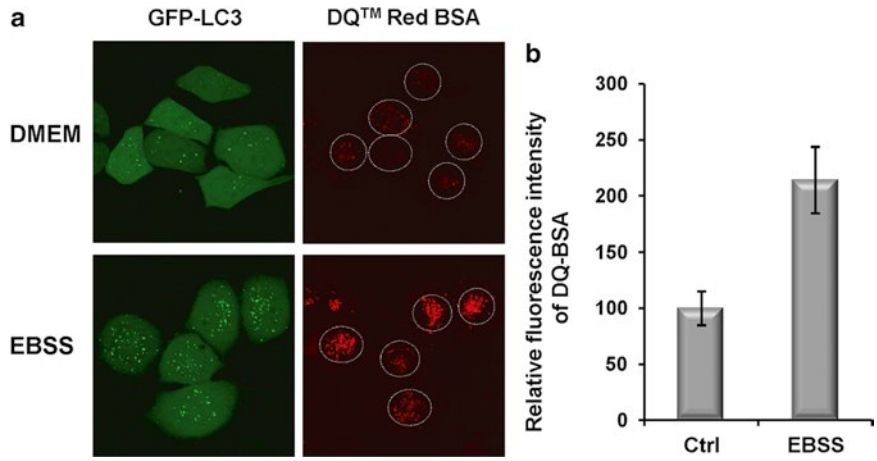

Fig. 2 Using DQ-BSA to monitor lysosomal activity. (*a*) HeLa cells overexpressing GFP-LC3 were incubated with DQ™ Red BSA (10 μg/mL) for 10 h. Cells were washed three times with prewarmed PBS and cultured in complete DMEM medium or EBSS medium for 2 h. Cells were fixed with 4 % paraformaldehyde and then mounted on coverslips. Images of GFP-LC3 and DQ™ Red BSA were captured by confocal microscope. (*b*) Quantification of DQ™ Red BSA fluorescence intensity by use of Image J software. More than 100 cells were counted in each sample group. Data represented as means ±SD from three independent experiments

2. When cells reach 70~80 % confluence, treat cells with DMSO or the test compound at a certain period of time points.
3. Cells are harvested with Trypsin-EDTA, count the cell number to make sure the total amount of cells is at least 1×10^6 cells/sample. Resuspend cells in 1 mL of 1× PBS. Transfer cell suspension to Eppendorf tubes and centrifuge at 200 × *g* for 5 min in a microcentrifuge and discard supernatant.
4. For cathepsin B activity assay: add 50 μL chilled CB lysis buffer to each Eppendorf tube; For cathepsin D activity assay, lyse cells in 100 μL chilled CD lysis buffer in each Eppendorf tube. Resuspend the pellet by pipetting up and down a few times. Incubate cells on ice for 10 min (*see* **Note 10**).
5. Centrifuge at top speed (13,000 × *g*) in a microcentrifuge for 5 min. Transfer the supernatant to a new Eppendorf tube.
6. Use Bradford protein assay kit to calculate the protein concentration of the samples (*see* **Note 11**).
7. For cathepsin B activity assay: Add 100 μg of the cell lysate into each well in a black 96-well plate. Bring the total volume to 50 μL with CB lysis buffer. For cathepsin D activity assay: add 5–10 μg of the cell lysate into each well in a black 96-well plate. Bring the total volume to 50 μL with CD lysis buffer.

For blank, add 50 μL CB or CD lysis buffer without cell lysate. We usually do triplicates for all samples we have (*see* **Note 12**).

8. Prepare a master assay mix, for each assay:

   Cathepsin B assay mix:

   50 μL of CB reaction buffer

   2 μL of substrate (10 mM Ac-RR-AFC)

   Cathepsin D assay mix:

   50 μL of CD reaction buffer.

   2 μL of substrate (1 mM GKPILFFRLK(Dnp)-D-R-NH2)-MCA).

   Mix the master assay mix, and add 52 μL of the assay mix into each assay wells; thus the total volume in each assay well is 102 μL.

9. Warp the 96-well plate with aluminum foil paper to protect from light. Incubate the plate at 37 °C incubator for 1–2 h.
10. The fluorescence can be measured in a fluorometer. For cathepsin B activity assay, read fluorescence at Ex/Em = 400/505 nm; for cathepsin D activity assay, read fluorescence at Ex/Em = 328/460 nm.
11. The cathepsin activity can be determined by the following (*see* **Note 13**):

    Cathepsin B/D activity = $(RFU_{sample} - RFU_{blank})/\mu g$ protein

3.4 Accessing the Anticancer Activity in Vitro

Insufficient autophagy in nutrient-deprived cancer cells would be beneficial for cancer therapy. If the compound you tested is a potent autophagic inhibitor, then it is interesting to examine whether the compound increases the sensitivity of cancer cells to metabolic stress. Flow cytometry analysis is a powerful method to access the effect on cell cycle and cell death. To analyze the number of dead cells, the following protocol may be followed:

1. Plate HeLa cells at a density of 2×10^5 cells per well in a 12-well plate, spread the cells evenly by gently rocking the dish back and forth. Cells are cultured at 37 °C in a humidified 5 % CO_2 incubator overnight.
2. Cells are treated with compound or DMSO in complete tissue culture medium or starvation medium (Earle's Balanced Salt Solution) at 37 °C for a certain period of time points.
3. Cells are harvested with trypsin-EDTA. Transfer cell suspension to Eppendorf tubes and centrifuge at 200 × *g* for 5 min in a microcentrifuge and discard supernatant. Cells are washed with 1× PBS twice at 200 × *g* in a tabletop centrifuge for 5 min; aspirate the supernatant (*see* **Note 14**).

4. To fix cells, add 1 mL of cold 70 % ethanol (in PBS or deionized water) drop by drop into the cell pellet while vortexing. Then incubate cells on ice for 1 h or overnight at 4 °C (*see* **Note 15**).
5. Centrifuge at 200 × *g* in a microcentrifuge for 5 min to spin down the cells, and then wash cells with 1× PBS to remove the excess ethanol.
6. Prepare stain solution, and add 5 μL of PI solution (10 mg/mL) and 1 μL of RNase A solution (10 mg/mL) to 500 μL PBS. Apply stain solution to the Eppendorf tubes, and cells are vortexed gently and incubated for 30 min at room temperature. Protect from light.
7. The sub-G_1 cells can be detected by Flow Cytometry analysis. First, measure the forward scatter (FSC) and side scatter (SSC) to identify single cells. DNA content is acquired at PI channel with cell counts as *Y*-axis and PI intensity as *X*-axis. The sub-G1 fraction is considered as dead cells (*see* **Note 16**).

3.5 Accessing the Anticancer Activity in Vivo

Xenograft tumor animal model is a convenient and ideal approach to evaluate the anticancer activity in vivo. Caloric restriction is the most physiological inducer of autophagy [21, 22]. To test the anticancer effect of the compound under metabolic stress in vivo, caloric restriction diet can be applied.

1. Preparation of HeLa cells: HeLa cells grow in complete tissue culture medium.
   4 h before harvesting, replace medium with fresh medium to remove dead and detached cells. HeLa cells are harvested by trypsin–EDTA and washed with 1× PBS twice. Centrifuge at 200 × *g* for 5 min, and aspirate the supernatant. After cell counting, cells are suspended in 300 μL 1× PBS containing required number of cells per injection. Normally, 1.0×10^6 to 3.0×10^6 cells are needed per injection.
2. Preparation of nude mice: 4~6-week-old BALB/c nude mice are suitable for xenograft model for HeLa cells. To estimate the food intake, the mice weight and the amount of food intake are monitored every day. Caloric restriction (fed with 70 % of food intake) can be applied by monitoring the food intake based on the animal body weight.
3. Tumor injection: Clean and sterilize the inoculation area of the mice with 70 % ethanol. Mix cells and draw the cells into a syringe without a needle. Inject cells subcutaneously into the lower flank of the mice with 27 G needle.
4. Drug treatment: After tumor injection, the mice are randomly divided to individual group and the drug can be administrated right after injection or few weeks after tumor injection. The

tested compound can be administrated by several methods, including oral administration, intravenous injection, intraperitoneal injection, hypodermic injection, and intratumoral injection. The solvent is used as a negative control (*see* **Note 17**).

5. Antitumor effect evaluation: During tumor development, the tumor diameters are measured by caliper. The tumor volume in mm^3 is calculated by the formula: volume = $(\text{width})^2 \times (\text{length})/2$. After the tumor volume is larger than 1000 mm^3, the animals are sacrificed by euthanasia and the tumor is resected immediately. The tumor weight of each animal can be analyzed as the indicator for antitumor effect of tested compounds.

4 Notes

1. Paraformaldehyde is toxic, make sure you take the necessary safety precautions to prevent contact with the powder. Paraformaldehyde is difficult to dissolve into solution. Slowly raise the pH by adding a couple of drops of 1 N NaOH to the solution will be helpful. Once paraformaldehyde is in solution, allow it to cool to room temperature.
2. Undiluted Triton X-100 is a viscous fluid. We usually prepare a 10 % Triton X-100 stock on hand. Add 10 mL of 100 % Triton X-100 to 100 mL of 1× PBS to yield 10 % Triton X-100. Store the stock solution at room temperature. If fix cells using organic solvents such as methanol or acetone, no permeabilization step needed following fixation.
3. There are numerous commercial and homemade mounting medium are available for making permanent slides. The choice of the right mounting medium depends on several factors, such as compatibility with specimen, refractive index, shrinkage, durability, cost, and ease of use.
4. A negative control experiment can be set up at the same time. Some widely used autophagy inhibitors, such as bafilomycin A_1 (a specific inhibitor of vacuolar-type H^+-ATPase) and chloroquine/hydrochloroquine (CQ/HCQ) (lysosomotropic agent) have been reported to impair fusion between autophagosomes and lysosomes (*see* Ref. 8).
5. Cells can be fixed after LysoTracker staining. Cells are fixed in 4 % paraformaldehyde solution for 15 min at room temperature. After two times wash with 1× PBS, samples can be stored at 4 °C for a couple of days. Protect from light.
6. We find that primary antibody incubation at 37 °C for 40–60 min gives better signal. Raising the incubation temperature can increase stringency and reduce nonspecific background.

7. The different expression level of GFP-LC3 may cause large variation of the PCC calculation. We suggest using GFP-LC3 stable expressed cells and choosing those cells with similar expression level when acquiring images.
8. Some people suggest that the incubation time for DQ-BSA staining is 1 h at 37 °C. However, we find that the signal is very weak if the incubation time is too short. It is better to stain the cells for longer time.
9. When acquiring images, make sure the detection parameters of the confocal microscope (e.g., gain and offset values) remain the same for all the samples. Therefore, we can compare the fluorescence intensity between different samples.
10. There are several commercial cathepsin activity assay kits available. The components and the procedure are very similar between different assay kits. You can choose any one of the assay kit for your study.
11. This step can be done at later time after finishing the activity assay. You can add the same volume of cell lysate to 96-well plate for the assay.
12. Cathespin B activity assay need much more lysate (100 μg/well) than cathespin D activity assay (5–10 μg/well). Our suggestion is to set up more culture plates for cathespin B activity assay.
13. The cathepsin activity can also be expressed as RFU/million cells. If desired, the relative cathepsin activity can be normalized and represented as fold increase by comparing with untreated control sample.
14. We find that cells under EBSS nutrient starvation sometimes are very sticky and difficult to be harvested by trypsinization. To isolate the single cell for flow cytometry detection, researchers can extend the period of trypsin treatment, pipette cells gentle after centrifuge, and pipette cells after fixation.
15. The fixed solution can be stored at –20 °C for a couple of days.
16. We find that sometimes the sub-G_1 population detected by flow cytometry is far less than the number of dead cells we observe under the microscope, which might be due to the loss of dead cells when fixing and washing samples. In this case, we can measure the uptake of propidium iodide in live cells. Propidium iodide is excluded by viable cells but can penetrate cell membrane of dying or dead cells.
17. To assess the anticancer activity in vivo, some widely used anticancer drugs (e.g., etoposide, 5-FU, paclitaxel, docetaxel) should be applied as positive control.

Acknowledgement

This work was supported by National Natural Science Foundation of China (NSFC) (21272135 and 81173485) and Overseas High-caliber Personnel Foundation of Shenzhen (KQC201109050084A).

References

1. Xie Z, Klionsky DJ (2007) Autophagosome formation: core machinery and adaptations. Nat Cell Biol 9:1102–1109
2. Rubinsztein DC, Marino G, Kroemer G (2011) Autophagy and aging. Cell 146:682–695
3. Rosenfeldt MT, Ryan KM (2009) The role of autophagy in tumour development and cancer therapy. Expert Rev Mol Med 11:e36
4. Mathew R, Karantza-Wadsworth V et al (2007) Role of autophagy in cancer. Nat Rev Cancer 7:961–967
5. Mizushima N, Klionsky DJ (2007) Protein turnover via autophagy: implications for metabolism. Annu Rev Nutr 27:19–40
6. Levine B, Deretic V (2007) Unveiling the roles of autophagy in innate and adaptive immunity. Nat Rev Immunol 7:767–777
7. Klionsky DJ, Abeliovich H, Agostinis P et al (2008) Guidelines for the use and interpretation of assays for monitoring autophagy in higher eukaryotes. Autophagy 4:151–175
8. Mizushima N, Yoshimori T, Levine B (2010) Methods in mammalian autophagy research. Cell 140:313–326
9. Kabeya Y, Mizushima N, Ueno T et al (2000) LC3, a mammalian homologue of yeast Apg8p, is localized in autophagosome membranes after processing. EMBO J 19:5720–5728
10. White E (2007) Role of the metabolic stress responses of apoptosis and autophagy in tumor suppression. Ernst Schering Foundation symposium proceedings. p 23–34
11. Jin S, White E (2007) Role of autophagy in cancer: management of metabolic stress. Autophagy 3:28–31
12. Karantza-Wadsworth V, Patel S, Kravchuk O et al (2007) Autophagy mitigates metabolic stress and genome damage in mammary tumorigenesis. Genes Dev 21:1621–1635
13. Wu WK, Coffelt SB, Cho CH et al (2012) The autophagic paradox in cancer therapy. Oncogene 31:939–953
14. Zhou J, Hu SE, Tan SH et al (2012) Andrographolide sensitizes cisplatin-induced apoptosis via suppression of autophagosome-lysosome fusion in human cancer cells. Autophagy 8:338–349
15. Lao Y, Wan G, Liu Z et al (2014) The natural compound oblongifolin C inhibits autophagic flux and enhances antitumor efficacy of nutrient deprivation. Autophagy 10:736–749
16. Saftig P, Klumperman J (2009) Lysosome biogenesis and lysosomal membrane proteins: trafficking meets function. Nat Rev Mol Cell Biol 10:623–635
17. Dunn KW, Kamocka MM, McDonald JH (2011) A practical guide to evaluating colocalization in biological microscopy. Am J Physiol Cell Physiol 300:C723–C742
18. Vazquez CL, Colombo MI (2009) Assays to assess autophagy induction and fusion of autophagic vacuoles with a degradative compartment, using monodansylcadaverine (MDC) and DQ-BSA. Methods Enzymol 452:85–95
19. Repnik U, Stoka V, Turk V et al (2012) Lysosomes and lysosomal cathepsins in cell death. Biochim Biophys Acta 1824:22–33
20. Kroemer G, Jaattela M (2005) Lysosomes and autophagy in cell death control. Nat Rev Cancer 5:886–897
21. Levine B, Klionsky DJ (2004) Development by self-digestion: molecular mechanisms and biological functions of autophagy. Dev Cell 6:463–477
22. Bergamini E, Cavallini G, Donati A et al (2003) The anti-ageing effects of caloric restriction may involve stimulation of macroautophagy and lysosomal degradation, and can be intensified pharmacologically. Biomed Pharmacother 57:203–208

Chapter 15

Protocol for a Steady-State FRET Assay in Cancer Chemoprevention

Marjolein C.A. Schaap, Andreia M.R. Guimarães, Andrew F. Wilderspin, and Geoffrey Wells

Abstract

Cancer chemoprevention is an important strategy to prevent, reverse, or suppress the development of cancer. One of the target pathways that has emerged in recent years is the Keap1-Nrf2-ARE system that regulates the protection of cells against various carcinogens and their metabolites. Increased concentrations of the redox transcription factor nuclear factor erythroid 2-related factor 2 (Nrf2) induces the activation of antioxidant and phase 2 detoxifying genes. Nrf2 is regulated by substrate adaptor protein Kelch-like ECH-associated protein 1 (Keap1) that can target Nrf2 for ubiquitination and degradation by the proteasome. The interaction between Nrf2 and Keap1 can be disrupted at the protein–protein interface in order to increase Nrf2 activity for potential therapeutic purposes. This chapter describes a protocol for a steady-state fluorescence or Förster resonance energy transfer (FRET) assay to examine the Keap1–Nrf2 protein–protein interaction (PPI), to investigate the effects of Nrf2 mutations on Keap1 binding and finally to identify potential inhibitors of this PPI. In the assay system Keap1 is conjugated to an YFP protein at the *N*-terminus whereas an Nrf2-derived 16-mer peptide containing a high-affinity "ETGE" motif is conjugated to a CFP protein at the *N*-terminus.

Key words FRET, Keap1, Nrf2, Protein–protein interactions, Peptide inhibitors, Small-molecule inhibitors

1 Introduction

The substrate adaptor protein Kelch-like ECH-associated protein 1 (Keap1) and the transcription factor nuclear factor erythroid 2-related factor 2 (Nrf2) are important components in the regulation of cellular cytoprotective responses upon exposure to redox stress and reactive xenobiotics [1]. Nrf2 regulates the expression of antioxidant response element (ARE) driven gene products, whereas Keap1 controls free Nrf2 concentrations by binding to the transcription factor and targeting it for ubiquitination and degradation by the proteasome. Several electrophilic natural products (e.g., sulforaphane, curcumin) are able to activate Nrf2 by modifying

Sabrina Strano (ed.), *Cancer Chemoprevention: Methods and Protocols*, Methods in Molecular Biology, vol. 1379,
DOI 10.1007/978-1-4939-3191-0_15,

reactive cysteine residues within Keap1 resulting in conformational changes that inhibit Nrf2 ubiquitination [2–4].

The protein–protein interaction (PPI) site consists of two sequences in the Nrf2 Neh2 domain (a low affinity "DLG" motif, residues 24–31, and a high affinity "ETGE" motif, residues 78–82) that form β-hairpin structures that each occupies a binding pocket in one of the two β-propeller Kelch domains present in a Keap1 dimer [5–8]. Disrupting this PPI interface by direct competition forms a potential alternative strategy to induce Nrf2 activity with compounds that lack electrophilic properties. We and others have demonstrated that peptides with sequences based on the high affinity ETGE motif from Nrf2 and small molecules are capable of inhibiting the Keap-Nrf2 PPI by occupying the Kelch domain-binding pocket [9, 10].

Fluorescence or Förster resonance energy transfer (FRET) is a technique that is applied widely to understanding and quantifying biomolecular interactions. Usually this involves labelling proteins or nucleic acids and their binding partners with fluorescent donor and acceptor species; the presence, absence or change in intensity of a FRET signal can be used to indicate the degree of interaction between the two species. The FRET principle is based on the overlap of the donor fluorescence emission spectrum of one fluorophore with the acceptor excitation spectrum of an adjacent fluorophore. When the fluorescent species are brought into close proximity (<10 nm), a proportion of the energy used to excite the donor fluorophore is directly transferred to the acceptor fluorophore. As a result, the fluorescence emission of the donor is decreased and the emission of the acceptor is increased [11].

An advantage of using green fluorescent protein (GFP) and its derivatives as fluorophores is that in some cases the stability of the interacting proteins can be improved significantly by conjugation. Cyan fluorescent protein (CFP) and yellow fluorescent protein (YFP) possess a suitable spectral overlap to form a good FRET pair, and when coupled to the partners of two interacting proteins are ideally suited to report on their proximity. We proposed that the approach would be suitable to monitor a variety of PPIs found in cancer pathways and as a homogenous (single step) assay would be more able to rapidly screen large compound libraries than heterogenous assays such as ELISA. Thus we initially developed such a protein–protein interaction assay for the HIF1α/p300 interaction using these GFP conjugates and screened a small panel of inhibitors [12]. We were particularly interested in detailing how this approach could be further applied to identify potential inhibitors of the Keap1-Nrf2 PPI. In this chapter we describe a step-by-step protocol for a steady-state FRET assay to study the PPI between the Keap1 Kelch domain and a 16-mer Nrf2-derived peptide containing a high-affinity ETGE motif, which we developed and applied in our previous work [13]. In this assay, the donor fluorophore, CFP,

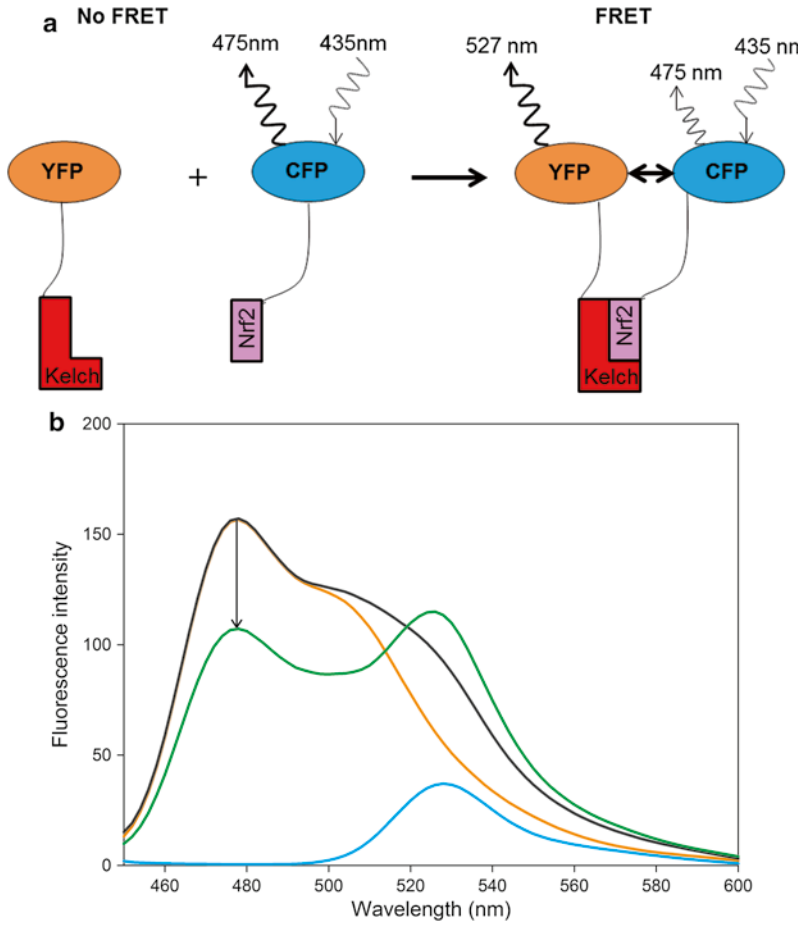

Fig. 1 (**a**) FRET diagrams of the YFP-Kelch and CFP-Nrf2 protein constructs. The *double-headed arrow* indicates FRET between the two fusion proteins. (**b**) An example of the fluorescence emission spectra of the FRET pair (*green*), YFP-Kelch alone (*orange*), CFP-Nrf2 (*blue*), and the sum of YFP-Kelch and CFP-Nrf2 (*black*). The *arrow* indicates the typical decrease in CFP emission when FRET occurs between the two fusion proteins

is fused to the ETGE motif-containing 16-mer Nrf2 derived peptide (CFP-Nrf2) and the acceptor fluorophore, YFP, is fused to the human Keap1 Kelch domain (YFP-Kelch) (Fig. 1).

We describe details for the protein expression and purification of CFP-Nrf2-wild-type (WT), CFP-Nrf2-E79Q, YFP-Kelch, and YFP proteins, together with step-by-step experimental conditions for a titration experiment in which fluorescence emission spectra are recorded after the addition of YFP-Kelch or unconjugated YFP (accounts for nonspecific interactions) to a fixed concentration of CFP-Nrf2 or CFP-Nrf2-E79Q (Fig. 2). The CFP-Nrf2-E79Q protein construct contains a point mutation in the Nrf2 ETGE consensus-binding motif (residues 78–82) that exhibits low binding affinity for the Keap1 Kelch domain [14]. This CFP conjugated Nrf2 mutant protein is used as an example to demonstrate

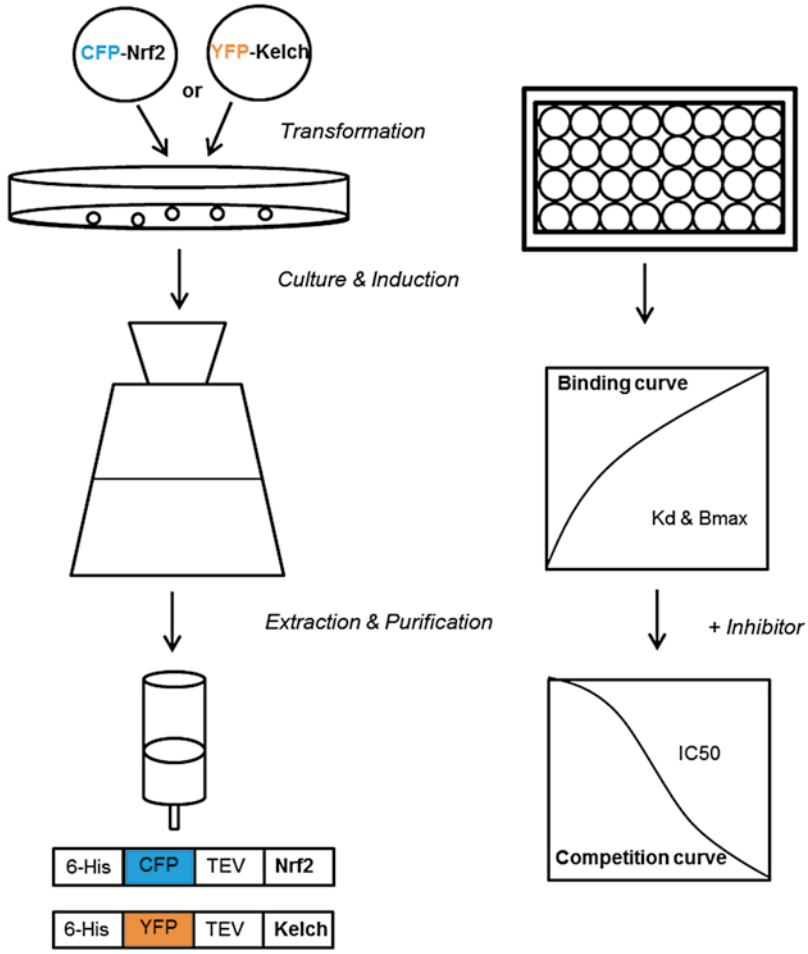

Fig. 2 A schematic overview of our step-by-step protocol for a steady-state FRET assay. The figure shows the transformation of the CFP-Nrf2 and YFP-Kelch plasmid constructs in Rosetta 2 (DE3) cells followed by their protein expression, extraction, and purification. Finally, the fusion proteins are used in a titration (binding) assay and the potency of inhibitors of the PPI is evaluated in a competition assay

specificity of the Keap1–Nrf2 PPI. The efficiency of FRET (FE) is determined by measuring the decrease in donor fluorescence emission at 480 nm. The change in FE with concentration of the interacting proteins can be used to determine the protein–protein binding affinity. We describe a protocol for a competition assay format to evaluate compounds that competitively inhibit the Keap1–Nrf2 PPI. The reduction in FE can be observed upon addition of increasing concentrations of an inhibitor to the CFP-Nrf2 and YFP-Kelch protein mixture and can be used to determine IC_{50} values. We have shown that the FRET assay can be applied to quantify protein–protein binding and to screen Nrf2 derived peptides for the inhibition of the Keap1-Nrf2 PPI. Recent work in our

lab has revealed that the inhibition potential of representative small molecule inhibitors can also be studied with our assay.

The protocol that we describe has the potential to be modified for use in time-resolved (TR) FRET assays by switching to a lanthanide chelate donor and matched acceptor fluorophores. TR-FRET is a modified FRET method that exploits the long emission half-life of lanthanide fluorophores to reduce the impact of background fluorescence interference on measurements [15].

2 Materials

Prepare all (buffer) solutions fresh each day using ultrapure water (prepared by purified deionized water).

2.1 Protein Expression and Purification Reagents

1. Plasmid constructs pET28c-eCFP-TEV-Nrf2-WT, pET28c-eCFP-TEV-Nrf2-E79Q, pET28c-eYFP-TEV-Kelch, and pET28c-eYFP (Fig. 3) [13, 16] (*see* **Notes 1** and **2**).
2. Competent Rosetta 2 (DE3) cells (Novagen). Store at −80 °C.
3. Luria-Bertani (LB) Broth (in 1 L): 10 g NaCl, 10 g tryptone and 5 g yeast extract. The solution is autoclaved, then cooled to a "hand-warm" temperature and kanamycin solution (30 μg/mL) is added.
4. LB-kanamycin (LB-kan) agar plates (in 1 L): 10 g NaCl, 10 g tryptone and 5 g yeast extract, 1.5 g agar. The solution is autoclaved, cooled to a "hand-warm" temperature and kanamycin solution (30 μg/mL) is added. The solution is dispensed into plates and stored at 4 °C.
5. Isopropyl β-d-1-thiogalactopyranoside (IPTG, Sigma-Aldrich) solution: A 1 M stock solution in water, filter sterilized. Stored at −20 °C.
6. Sonicator (Soniprep 150).

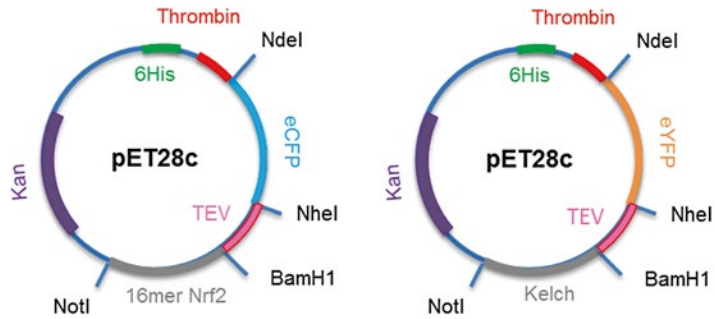

Fig. 3 The pET28c plasmid constructs containing a kanamycin (Kan) resistance gene, a 6-histidine tag (6His), a thrombin, a tobacco etch virus (TEV) recognition site, and eCFP or eYFP and a 16-mer Nrf2 or a Keap1 Kelch domain, respectively [13, 16]

7. Imidazole (Sigma-Aldrich).
8. Extraction buffer: 20 mM Tris–HCl pH 7.4, 150 mM NaCl, 30 mM imidazole, 0.5 mM DTT, 0.5 mM EDTA, 5 % glycerol and 50 μL/g of bacterial pellet protease inhibitor cocktail: AEBSF, bestatin, E-64, pepstatin A, and phosphoramidon (Sigma-Aldrich). Store at 4 °C.

   Purification buffer: 20 mM Tris–HCl pH 7.4, 0.5 M NaCl, and 0.5 mM DTT. Store at 4 °C.
9. 5 mL His-Trap FF columns (GE Healthcare).
10. Amicon Ultra-15 centrifugal filter units 10 and 30 K (Millipore).
11. Dialysis buffer: 20 mM Tris–HCl pH 7.4, 150 mM NaCl, 0.5 mM DTT, and 1 mM EDTA. Store at 4 °C.
12. Dialysis membrane: Tubing Spectra/Por 1 dialysis membrane 3.3 mL/cm, MWCO 6000–8000 (Spectrum labs).
13. Syringe filters 0.22 μm (Millipore) and 10–25 mL syringes.
14. SDS-PAGE gel components and Coomassie blue staining.

2.2 Protein Quantification by Intrinsic GFP Absorbance

1. FRET buffer: 20 mM Tris–HCl pH 7.4 buffer containing, 0.5 mM DTT, 0.1 mM EDTA, and 5 % v/v glycerol (*see* **Note 3**).
2. Quartz cuvette, 10 mm square cuvette (1 mL) (Helma).
3. UV spectrophotometer (Perkin Elmer).

2.3 Titration (Binding) and Competition Assays

1. Flat bottom black 96-well plates (Corning).
2. Inhibitors (peptides or small molecules).
3. Multichannel pipettes.
4. Multi-well fluorescence plate reader (Pherastar, BMG Labtech).

3 Methods

Keep proteins on ice between protein purification steps.

3.1 Protein Expression and Purification

3.1.1 Bacterial Transformation

1. Place sterile 0.5 mL microcentrifuge tubes on ice. Add 50 μL of thawed competent Rosetta 2 (DE3) cells and 1 μL of plasmid constructs (pET28c-eCFP-TEV-Nrf2-WT, pET28c-eCFP-TEV-Nrf2-E79Q, pET28c-eYFP-TEV-Kelch, and pET28c-eYFP) to the pre-cooled microcentrifuge tubes. Incubate the mixture on ice for 45 min. Heat-shock the cells at 42 °C for 90 s and then place the tubes with cells on ice for 2 min. Add 400 μL of LB-broth to cells and incubate at 37 °C whilst shaking at 220 rpm for 45 min. Disperse the cell mixture on LB-kan agar plates and incubate at 37 °C for 12–16 h (*see* **Note 4**).

2. On the following day, pick one single colony from the LB-kan agar plate and add to 5 mL of LB-kan medium. Incubate the cell mixture at 37 °C whilst shaking at 220 rpm for 12–16 h.

3.1.2 Protein Expression

1. On the next day, add 1 mL of the overnight grown culture to 1 L of LB-kan medium. Incubate the 1 L bacterial culture at 37 °C until the cells reach the exponential growth phase (OD_{600nm} = 0.4–0.6). Induce protein expression by adding IPTG (1 mM final concentration) and incubate at 21 °C for 16 h.
2. On the following day, pellet the cells at 6,000 × *g* at 4 °C for 30 min. Keep the pellet on ice for further purification steps or store at −80 °C.

3.1.3 Protein Extraction and Purification

1. Resuspend the bacterial pellets in extraction buffer and sonicate the suspension on ice for 5 min with 15 s of rest between each 15 s cycle of sonication (*see* **Note 5**). Pellet the cells by centrifugation (27,000 × *g*, 4 °C) for 40 min and filter the supernatant through a 0.22 μM filter. Wash a 5 mL His-Trap FF column with 30 mL of dH_2O and equilibrate with a solution of imidazole (30 mM in purification buffer). Add the filtered supernatant to the 5 mL His-Trap FF column and pass through the column at an approximate flow rate of 0.5 mL/min (drop-wise). Collect the eluent and store on ice; this fraction can be used to determine the amount of unbound (contaminant) protein. Wash the column with 50 mL of imidazole solution (30 mM in purification buffer) and 10 mL of a more concentrated imidazole solution (50 mM in purification buffer). Collect the eluent fractions and store on ice. Elute the protein from the column using 10 mL volumes of a gradient solvent system (100–300 mM imidazole in purification buffer). Collect the fractions and store on ice. To monitor purification, samples should be removed from each fraction and subjected to SDS-PAGE followed by Coomassie Brilliant Blue staining (Fig. 4). Transfer the selected eluted protein fractions to a dialysis membrane and separate each protein fraction with dialysis clips (*see* **Note 6**). Dialyze the protein fractions in 2 L dialysis buffer at 4 °C in the dark whilst stirring for 16–24 h.
2. The next day, collect the dialyzed protein fractions in 15 mL tubes and place them on ice. Concentrate the protein fractions to 1 mL volume using Amicon Ultra-15 centrifugal filter units MWCO 10 K for the CFP-Nrf2 (WT or E79Q) proteins and 30 K MWCO for the YFP-Kelch proteins (*see* **Notes 7** and **8**).

   Add 10 % glycerol to the concentrated protein fractions to prevent ice-crystals from forming upon freezing. Aliquot the proteins into 250 μL samples then flash-freeze in liquid nitrogen and store at −80 °C (*see* **Note 9**).

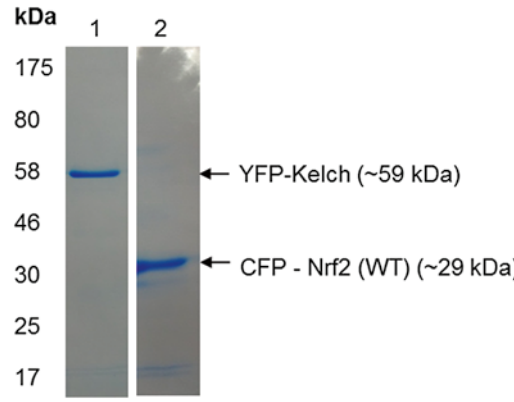

Fig. 4 A representative example of His-trap-purified CFP-Nrf2 and YFP-Kelch proteins analyzed on a 10 % SDS-PAGE gel

3.2 Protein Quantification by Intrinsic GFP Absorbance (See Note 10)

1. Clean a quartz cuvette with 70 % ethanol then dH_2O.
2. Set the spectrophotometer to zero with the cuvette containing 1 mL of FRET buffer using a wavelength of $\lambda = 435$ nm for the CFP tagged proteins and $\lambda = 514$ nm for the YFP-tagged protein, respectively (*see* **Note 11**).
3. Thaw the concentrated proteins ((CFP-Nrf2 (WT or E79Q) and YFP-Kelch)) on ice.
4. Add 20 μL of concentrated protein to 980 μL of FRET buffer in the cuvette (50× diluted).
5. Cover the cuvette with parafilm and mix by inversion. Measure the absorbance of the diluted protein at the appropriate wavelength.
6. Calculate the CFP-Nrf2 (WT or E79Q) or YFP-Kelch protein concentrations using the Beer-Lambert law: $A = \varepsilon lc$ ((A = absorbance, ε = molar extinction coefficient ($M-1\ cm-1$), l = path length of the cuvette (cm) and c = concentration (M)). Extinction coefficients of $83400\ M^{-1}\,cm^{-1}$ and $28750\ M^{-1}\,cm^{-1}$ should be used for YFP and CFP respectively. Calculate the stored protein concentrations by adjusting for the dilution factor of the measured solutions.

3.3 Titration (Binding) Assay (See Notes 12 and 13)

Perform the assays at room temperature (RT). Table 1 may be used as a sample template for the plate layout for the titration assays. Three replicates are recommended.

1. Rinse black 96-well plates 3× with dH_2O and leave to dry.
2. Calculate volume FRET buffer needed in μL for each well in one plate (Fig. 5) (*see* **Note 14**).
3. Add FRET buffer alone to the designated blank wells (Table 1).

Table 1
An example template of a plate layout for titration assays

	1	2	3	4	5	6	7	8	9	10	11	12
A	**0.01 μM YFP-(Kelch)**			**0.40 μM YFP-(Kelch)**			0.11 μM CFP-Nrf2 (WT or E79Q) + 0.11 μM YFP-(Kelch)					
B	**0.03 μM YFP-(Kelch)**			**0.50 μM YFP-(Kelch)**			0.11 μM CFP-Nrf2 (WT or E79Q) + 0.20 μM YFP-(Kelch)					
C	**0.05 μM YFP-(Kelch)**			*0.11 μM CFP-Nrf2 (WT or E79Q)*			0.11 μM CFP-Nrf2 (WT or E79Q) + 0.30 μM YFP-(Kelch)					
D	**0.07 μM YFP-(Kelch)**			0.11 μM CFP-Nrf2 (WT or E79Q) + 0.01 μM YFP-(Kelch)			0.11 μM CFP-Nrf2 (WT or E79Q) + 0.40 μM YFP-(Kelch)					
E	**0.09 μM YFP-(Kelch)**			0.11 μM CFP-Nrf2 (WT or E79Q) + 0.03 μM YFP-(Kelch)			0.11 μM CFP-Nrf2 (WT or E79Q) + 0.50 μM YFP-(Kelch)					
F	**0.11 μM YFP-(Kelch)**			0.11 μM CFP-Nrf2 (WT or E79Q) + 0.05 μM YFP-(Kelch)								
G	**0.20 μM YFP-(Kelch)**			0.11 μM CFP-Nrf2 (WT or E79Q) + 0.07 μM YFP-(Kelch)								
H	**0.30 μM YFP-(Kelch)**			0.11 μM CFP-Nrf2 (WT or E79Q) + 0.09 μM YFP-(Kelch)			Blank					

Assay wells containing YFP-Kelch protein alone are shown in *bold*, CFP-Nrf2 alone in *italic*, and a combination of the two proteins in *bold italic*. Blank assay wells are shown *underlined*

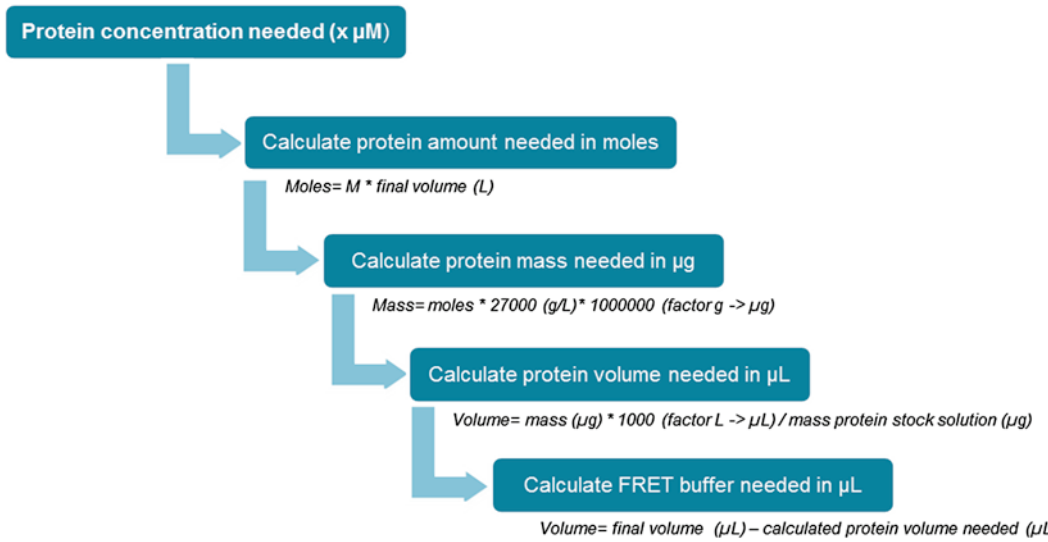

Fig. 5 Flowchart with formulas to calculate protein volume (μL) and FRET buffer volume (μL) given a certain protein concentration (μM). The CFP-Nrf2 and YFP-Kelch protein masses are calculated by using the extinction coefficients (83400 or 28750 M^{-1} cm^{-1}) and molecular weight (27,000 g/L) of CFP or YFP proteins, respectively

4. Calculate volume protein needed in μL for each well in one plate ((CFP-Nrf2 (WT or E79Q), YFP-Kelch, or unconjugated YFP)) in FRET buffer (Fig. 5) (*see* **Notes 15–17**).
5. Add 0.11 μM of CFP-Nrf2 (WT or E79Q) (final concentration) to the assay wells (Table 1) (*see* **Notes 18** and **19**).
6. Add 0.01–0.50 μM of YFP-Kelch or unconjugated YFP (final concentrations) to the assay wells (Table 1).
7. Cover the plate with aluminium foil and incubate on a plate shaker whilst shaking at 800 rpm at RT for 4 min.
8. Use a multi-well plate reader with an excitation filter of 430 nm and emission filters of 480 and 530 nm to measure the fluorescence emission intensity from the plate wells (*see* **Notes 20** and **21**).
9. Subtract the averaged blank values from each fluorescence value.
10. Calculate the FRET efficiencies of each protein combination using $\mathrm{FE} = 1 - \frac{F^{\mathrm{da}}}{F^{\mathrm{d}}}$

    where da = donor emission in the presence of the acceptor and d = donor emission in the absence of the acceptor.
11. Fit binding curves by nonlinear regression (linear binding, one site saturation) and determine K_d and B_{max} values using appropriate statistics software (e.g., Sigmaplot) (Fig. 6).

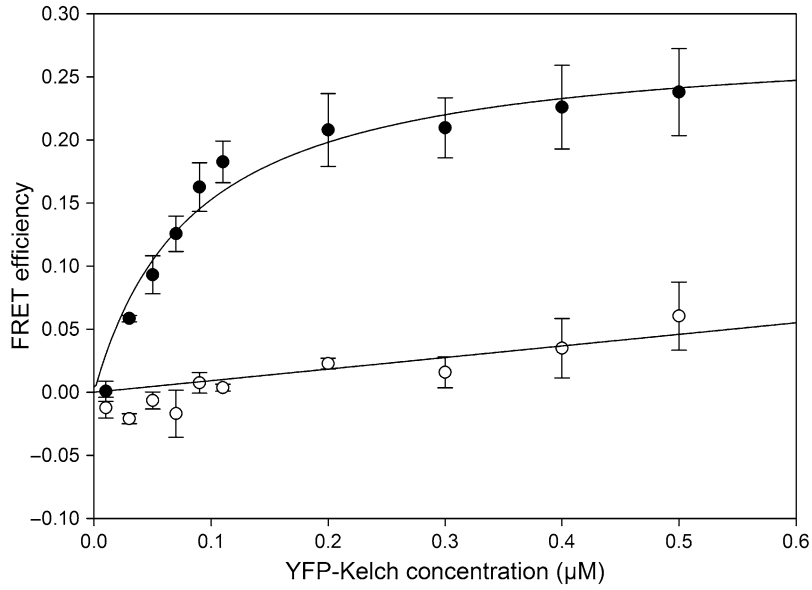

Fig. 6 An example of binding curves obtained with a fixed concentration of CFP-Nrf2-WT (*black rounds*) or CFP-Nrf2-E79Q (*white rounds*) titrated with variable concentrations of YFP-Kelch

Table 2
An example template of a plate layout for competition assays

	1	2	3	4	5	6	7	8	9	10	11	12
A	*0.11 μM CFP-Nrf2 (WT)*			+100 μM inhibitor			+0.01 μM inhibitor					
B	**0.20 μM YFP-Kelch**			+30 μM inhibitor			+0.003 μM inhibitor					
C	0.11 μM CFP-Nrf2 (WT) + 0.20 μM YFP-Kelch			+10 μM inhibitor			+0.001 μM inhibitor					
D	*0.11 μM CFP-Nrf2 (WT) + vehicle*			+3 μM inhibitor			+0.0003 μM inhibitor					
E	**0.20 μM YFP-Kelch + vehicle**			+1 μM inhibitor			+0.0001 μM inhibitor					
F	0.11 μM CFP-Nrf2 (WT) + 0.20 μM YFP-Kelch + vehicle			+0.3 μM inhibitor								
G				+0.1 μM inhibitor								
H				+0.03 μM inhibitor			Blank					

Assay wells containing YFP-Kelch protein alone are shown in *bold*, CFP-Nrf2 alone in *italic*, and a combination of the two proteins in *bold italic*. Inhibitor is added to a combination of the two proteins shown in *bold italic*. Blank assay wells are shown *underlined*

3.4 Competition Assay

Perform the assay at room temperature. Table 2 may be used as a template for competition assays. Three replicates are recommended.

1. Rinse black 96-well plates with dH_2O (×3) and leave to dry.
2. Calculate the volume of FRET buffer needed in μL for each well in one plate (Fig. 5) (*see* **Note 14**).
3. Add FRET buffer alone to the designated blank wells (Table 2).
4. Calculate volume protein need in μL for each well in one plate ((CFP-Nrf2 (WT) or YFP-Kelch)) in FRET buffer (Fig. 5) (*see* **Notes 15–17**).
5. Add 0.11 μM CFP-Nrf2 (WT) (final concentration) to the wells (Table 2) (*see* **Note 22**).
6. Add 0.20 μM YFP-Kelch (final concentration) to the wells (Table 2).
7. Prepare 1 % DMSO in FRET buffer solutions (vehicle control) and 100× diluted inhibitor in 1 % DMSO in FRET buffer solutions (*see* **Note 23**).
8. Add 10 μL of 100× diluted inhibitor in 1 % DMSO in FRET buffer solution (0.1 % DMSO final concentration) to the wells or 10 μL of 1 % DMSO in FRET buffer (vehicle control) (Table 2).
9. Cover the plate with aluminum foil and incubate the plate on a plate shaker at 800 rpm at RT for 4 min.

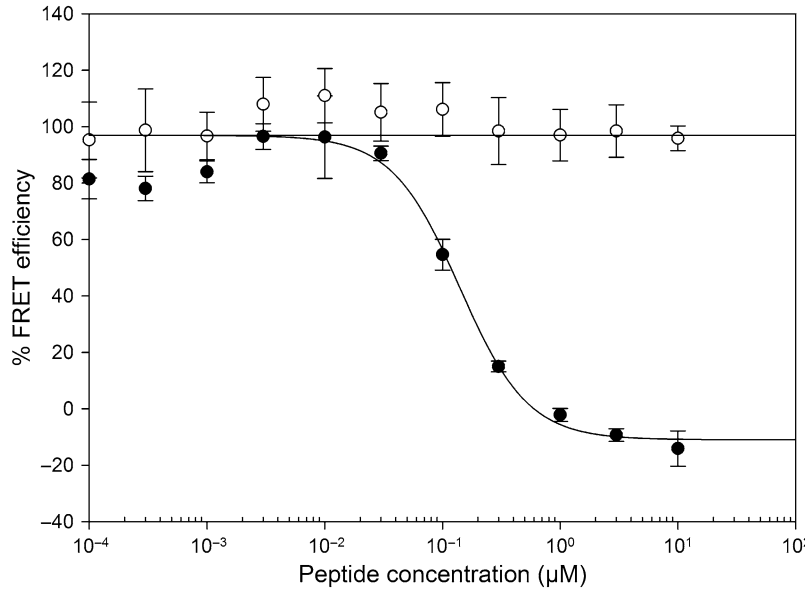

Fig. 7 An example of competition curves using fixed concentrations of CFP-Nrf2-WT and YFP-Kelch and variable concentrations of 16-mer peptide inhibitors Nrf2-WT (*black rounds*) and Nrf2-E79Q (*white rounds*)

10. Use a multi-well plate reader with an excitation filter of 430 nm and emission filters of 480 and 530 nm to measure the fluorescence emission intensity from each of the plate wells.
11. Subtract the averaged blank values from each fluorescence value.
12. Calculate FRET efficiencies of each protein combination using

$$\mathrm{FE} = 1 - \frac{F^{\mathrm{da+inhibitor}}}{F^{\mathrm{d+vehicle}}}$$

where da = donor emission in the presence of the acceptor and d = donor emission in the absence of the acceptor and vehicle is 0.1 % DMSO.

13. Calculate percentage FE using

$$\%\mathrm{FE} = 1 - \frac{FE^{\mathit{vehicle}} - FE^{\mathit{inhibitor}}}{FE^{\mathit{vehicle}}} * 100$$

14. Fit inhibition curves to a standard four-parameter logistic function and determine IC_{50} values using appropriate statistics software (e.g. SigmaPlot) (Fig. 7).

    For optional experiments *see* **Notes 24** and **25**.

4 Notes

1. Details on the design of the plasmid constructs (primer design and cDNA cloning) can be found in our publication [13].
2. Plasmid constructs: pET28c-eCFP-TEV-Nrf2-WT, pET28c-eCFP-TEV-Nrf2-E79Q, and pET28c-eYFP-TEV-Kelch were

used to express proteins: CFP-Nrf2-WT, CFP-Nrf2-E79Q, and YFP-Kelch, respectively. The terms eCFP and eYFP are used synonymously with CFP and YFP for simplicity.

3. A range of FRET buffer conditions were screened and optimized accordingly. Increasing the sodium chloride concentration was found to negatively impact the FE.
4. Use appropriate aseptic techniques for all bacterial work to maintain a sterile environment. Wear gloves and clean the work area with 70 % ethanol. Keep the competent bacterial cells on ice at all times and do not reuse an aliquot.
5. Wear protective ear defenders when sonicating. Make sure that neither bacterial (protein) suspension nor the sonicator becomes too warm.
6. The dialysis membrane has been chemically treated with sodium azide preservative agent, which needs to be removed by soaking the membrane in a large volume of dH_2O for 30 min. It is important to prevent drying out of the membrane.
7. Check for potential precipitation of the proteins to prevent assay inaccuracy.
8. Protect the fluorophore-fused proteins from light by covering tubes with aluminum foil.
9. Wear protective eye goggles and gloves when working with liquid nitrogen. Ensure a quick transfer to a −80 °C freezer after flash-freezing protein in liquid nitrogen.
10. Use were possible a fresh aliquot of protein and avoid repeated freeze-thawing. Determine protein concentrations before performing an assay. Protein concentrations can vary and may impact the reproducibility of the assay.
11. Prepare FRET buffer fresh every time when needed (DTT is unstable at room temperature).
12. Details on the optimization of the FRET assay can be found in our publication [13].
13. We recommend repeating the titration and competition assays at least three times to reduce experimental noise.
14. We optimized the final well volume to 100 μL.
15. We recommended preparing a spreadsheet template for protein concentration calculations.
16. Work relatively quick when adding the buffer, protein solutions (and inhibitors) to the assay wells since the protein degrades more quickly at room temperature and on exposure to light.
17. We found that using a multichannel pipette to add the buffer, protein solutions (and inhibitors) to the wells greatly enhanced the reproducibility of the assay.

18. Make sure to pipette the protein solution directly into the FRET buffer and avoid touching the walls of the assay wells.
19. Protein volumes used in the assay have been optimized to be at least 10 % of the total well volume. Protein volumes <10 μL were found to affect the assay accuracy and reproducibility. We found that a concentration of > 5 mg/mL of protein stock solution is essential to be able to dilute the protein in a high enough volume of FRET buffer and pipette protein volumes of > 10 μL/well.
20. Record the emission spectra of CFP-Nrf2 and YFP-Kelch separately to control for direct excitation of the fluorescent fusion proteins.
21. Select an assay well that will give the highest expected fluorescence signal to adjust the gain on the multi-well plate reader. Adjust the gain for each plate separately.
22. We found that a protein ratio of 0.11 μM CFP-Nrf2 (WT) and 0.20 μM YFP-Kelch to achieve 80 % of the maximal FE and was consequently used in our competition assays.
23. Inhibitors were dissolved in the vehicle DMSO. We found that a final DMSO concentration of >1 % v/v in the assay wells has a negative effect on the fluorescence emission spectra of the proteins. We recommend using a final concentration of 0.1% DMSO.
24. Optional: The Keap1–Nrf2 PPI is rapid and should be stable for up to 24 h. The PPI stability and the inhibition potency of peptides or small molecules can be tested by measuring the emission spectra of the proteins over a period of 24 h.
25. Optional: The Z' value, to assess the suitability of the assay for high throughput screening (HTS), can be determined using the experimental details described in the supplemental data section of our publication [13].
26. To verify fluorescence emission spectra from 400 to 600 nm, FRET can be recorded using a single sample unit. We have used a Perkin Elmer LS 55 luminescence spectrometer with 5 nm slit width, 1 nm interval and 1 s integration time.
27. All protein fusion constructs have a Tobacco Etch Virus (TEV) recognition site between the fluorophore and the protein. Therefore, the FRET signal between CFP-Nrf2 (WT) and YFP-Kelch proteins can be validated by addition of TEV protease to the protein mixture. The initial observed FRET signal in the protein mixture should decrease rapidly upon addition of the TEV protease.
28. Add inhibitor solution alone to the wells (no proteins) to determine whether compound fluorescence could interfere with the FRET signal.

29. Add inhibitor to CFP-Nrf2 (WT) or YFP-Kelch alone to identify possible effects (fluorescence interference) on emission spectra.

Acknowledgements

We thank Dr. Edwin Nkansah for kindly providing plasmids and Hei Leung for her contribution to the recombinant protein production. This work was supported by Cancer Research UK (C9344/A10268) and UCL School of Pharmacy.

References

1. Hayes JD, McMahon M, Chowdhry S et al (2010) Cancer chemoprevention mechanisms mediated through the Keap1-Nrf2 pathway. Antioxid Redox Signal 13(11):1713–1748
2. Zhang DD, Hannink M (2003) Distinct cysteine residues in Keap1 are required for Keap1-dependent ubiquitination of Nrf2 and for stabilization of Nrf2 by chemopreventive agents and oxidative stress. Mol Cell Biol 23(22):8137–8151
3. Dinkova-Kostova AT, Holtzclaw WD, Cole RN et al (2002) Direct evidence that sulfhydryl groups of Keap1 are the sensors regulating induction of phase 2 enzymes that protect against carcinogens and oxidants. Proc Natl Acad Sci U S A 99(18):11908–11913
4. Kobayashi M, Li L, Iwamoto N et al (2009) The antioxidant defense system Keap1-Nrf2 comprises a multiple sensing mechanism for responding to a wide range of chemical compounds. Mol Cell Biol 29(2):493–502
5. Tong KI, Katoh Y, Kusunoki H et al (2006) Keap1 recruits Neh2 through binding to ETGE and DLG motifs: characterization of the two-site molecular recognition model. Mol Cell Biol 26(8):2887–2900
6. Itoh K, Wakabayashi N, Katoh Y et al (1999) Keap1 represses nuclear activation of antioxidant responsive elements by Nrf2 through binding to the amino-terminal Neh2 domain. Genes Dev 13(1):76–86
7. Ahn, Y.H., Hwang Y, Liu H et al., Electrophilic tuning of the chemoprotective natural product sulforaphane. Proc Natl Acad Sci U S A. 107(21): p. 9590-5.
8. Lo SC, Li X, Henzl MT et al (2006) Structure of the Keap1:Nrf2 interface provides mechanistic insight into Nrf2 signaling. EMBO J 25(15):3605–3617
9. Hancock R, Bertrand HC, Tsujita T. et al. Peptide inhibitors of the Keap1-Nrf2 protein–protein interaction. Free Radic Biol Med. 52(2): 44-51.
10. Magesh S, Chen Y, Hu L (2012) Small molecule modulators of Keap1-Nrf2-ARE pathway as potential preventive and therapeutic agents. Med Res Rev 32(4):687–726
11. Clegg RM (2009) Förster resonance energy transfer—FRET what is it, why do it, and how it's done. In: Gadella TWJ (ed) Laboratory techniques in biochemistry and molecular biology. Elsevier BV, Urbana, p 38
12. Guimarães AMR. Screening molecular interactions for drug discovery, PhD thesis. 2013, UCL, School of Pharmacy: London.
13. Schaap M, Hancock R, Wilderspin A et al (2013) Development of a steady-state FRET-based assay to identify inhibitors of the Keap1-Nrf2 protein–protein interaction. Protein Sci 22(12):1812–1819
14. Shibata T, Ohta T, Tong KI et al (2008) Cancer related mutations in NRF2 impair its recognition by Keap1-Cul3 E3 ligase and promote malignancy. Proc Natl Acad Sci U S A 105(36):13568–13573
15. Qin QP, Peltola O, Pettersson K (2003) Time-resolved fluorescence resonance energy transfer assay for point-of-care testing of urinary albumin. Clin Chem 49(07):1105–1113
16. Nkansah E, Shah R, Collie GW et al (2013) Observation of unphosphorylated STAT3 core protein binding to target dsDNA by PEMSA and X-ray crystallography. FEBS Lett 587(7): 833–839

Chapter 16

3D Tumor Models and Time-Lapse Analysis by Multidimensional Microscopy

Dimitri Scholz and Nobue Itasaki

Abstract

The 3D culture is advantageous in reflecting the in vivo condition compared to the 2D culture; however, imaging 3D-cultured cells may be a challenge due to technical restrictions. Recent development of confocal spinning disc microscope system as well as sophisticated software has enabled us to monitor dynamism of cell movement in multiple dimensions. Here we describe the method for time-lapse imaging of 3D-cultured cancer cells co-cultured with non-cancerous cells and discuss current limitations and future perspectives.

Key words Three-dimensional culture, Time-lapse imaging, Multidimensional microscopy, Live cell imaging, Deconvolution

1 Introduction

The three-dimensional (3D) cell culture system is far more advantageous compare to the 2D culture in reflecting in vivo conditions in many aspects such as cell morphology, movement, cell–cell adhesion, cell polarity, and cancer cell malignancy [1]. The cytoarchitecture, which is critical for the function of epithelial cells as well as for the degree of malignancy of cancer cells, can be reestablished in the 3D culture with acquisition of apical-basal polarity and cell adhesion [2]. Cancer cells grown in 3D also show different metabolic pattern from those grown in 2D [3, 4]. Furthermore, cancer cells display different sensitivity and selectivity to anticancer drugs between 3D and 2D cultures [5–7]. These advantages postulate 3D culture not just a replacement of 2D culture but as a necessary system for in vitro cancer research. Despite the fact that such advantages had already been highlighted more than a decade ago [8], the method has not been accepted as widely as it deserves, partly due to unaccustomed technical requirements. Obtaining good quality of images of 3D materials under the microscope is a particular challenge, which may have hampered a wide usage of 3D culture.

Sabrina Strano (ed.), *Cancer Chemoprevention: Methods and Protocols*, Methods in Molecular Biology, vol. 1379,
DOI 10.1007/978-1-4939-3191-0_16,

In this chapter, we describe the method of 3D culture and following time-lapse filming that was employed in our recent studies [4], and concisely discuss other possible approaches. The method of analysing 3D-cultured cells by immunocytochemistry is also mentioned. Our studies are on dynamic interaction of cancer cells with non-cancerous epithelial cells using cell lines [4]. However, the method should be widely applicable to other types of studies such as the use of primary cells, drug test, and personalized medicine.

2 Materials

2.1 Cells

MDA-MB-231, breast cancer cell lines from American Type Culture Collection (ATCC), have been made to stably express green fluorescent protein (GFP). Likewise, Madin-Darby canine kidney (MDCK) cell line is mCherry labeled. While stable fluorescent labels are useful for time lapse imaging, they are not necessary for other purposes such as immunocytochemical or biochemical analyses. Primary cells can also be used. For non-fluorolabeled cells (e.g., primary cells) phase-contrast or differential interference contrast (DIC) allows live imaging. Combining fluorescent imaging with transmission light-based techniques are useful not only for detecting non-labeled cells but also for outlining fluorescent cells (*see* **Note 1**).

2.2 Reagents and Consumables

Before setting up 3D culture, cells can be maintained in 2D as usual. The reagents used for MDA-MB-231 and MDCK cells in this study were DMEM (sigma D5546), fetal calf serum (FCS) (Sigma F7524), Penicillin–streptomycin (Sigma P4333), Glutamax™ (Gibco 35050-038), and 0.25 % Trypsin–EDTA (Gibco 25200-056). For the 3D culture, Geltrex™ reduced growth factor basement membrane matrix (Gibco 12760-021) was used in this study. More widely used matrix, Matrigel [9], is anticipated to work in a similar way.

It is essential to use special imaging-grade dishes or slides with the cover slip-thin (150–190 μm) bottom. We got best results with products from ibidi (Germany), who provide a broad range of cell culture slides, dishes and gadgets (http://ibidi.com/home/). For our 3D time-lapse imaging, ibidi μ-dish (ibidi 81151) or μ-slide (ibidi 80426, 80421) were used. The plate does not need coating as the matrix is used for the 3D culture.

3 Methods

3.1 Cell Culture

The cell lines were cultured in DMEM containing 10 % FCS, 100 units/ml penicillin, 100 μg/ml streptomycin and 2 mM Glutamax™. All cells were incubated in a 37 °C humidified cham-

ber supplied with 5 % CO_2. The medium was replaced every 3 days and the cells were passaged once they were 80–90 % confluent using trypsin.

3.2 Three-Dimensional Co-cultures

The cells that have been cultured in 2D and reached near-confluent were trypsinized and suspended at 1×10^5 cells/ml in the culture medium. On the desired ibidi μ-dish, Geltrex™ was spread to form a thin layer on the surface and allowed to set in the incubator at 37 °C for 20 min (*see* **Note 2**). Cell dilutions were prepared containing MDA-MB-231 and MDCK cells at a desired ratio (1:1 in this study). The cell mix were then centrifuged at 1000 rpm ($188 \times g$) for 5 min at room temperature. The supernatant was aspirated off and the cells were resuspended in Geltrex™ in each tube. The amount of cells and gels should be optimized beforehand; it may depend on the speed of cell proliferation, length of incubation and purpose of the study. For time-lapse imaging of MDA-MB-231 and MDCK cells after 7–10 days of incubation, 1×10^5 of cells resuspending in 0.1 ml of Geltrex is optimal; however, this might be relatively sparse for other purposes.

The cells and the gel matrix were pipetted up and down to mix well. The mix was then pipetted on top of the already-set Geltrex™. The plate was incubated at 37 °C for 20 min to allow the matrix to set. The culture medium was then added slowly to cover the set-gel. The medium was replaced every 3 days and the cells were grown for 7–10 days. The cells may be grown for at least 14 days.

For immunocytochemical analyses, the above method were applied on the cover slips which had been put in culture wells. For example, 12 mm diameter round cover slips were put in 24-well-plate wells. After the culture, fixing, washing, and immunolabeling can be performed all in the well while keeping the cells in the matrix. Once secondary antibodies were washed off, the cover slip to which matrix containing the cells were attached was taken out of the well and mounted on a glass slide with mounting medium (e.g., Mowiol 4-88, Sigma 81381; Slowfade, Life Technologies S36938).

3.3 Multidimensional Live Cell Imaging

In this study, the Andor Revolution Laser Confocal spinning disc microscope system was used with the inverted Nikon Ti microscope, motorized XYZ Prior stage, and Andor iXon897 EM EMCCD camera operated by Andor IQ2.6 software. The microscope was equipped with a chamber keeping the cells at 37 °C with continuous supply of 5 % CO_2 and humid air. The experimental setup included sequential time-lapse acquisition (every 1–20 min) from 10 to 40 different XY fields, in two fluorescent channels, GFP and mCherry. For each time point and XY location, a *Z*-stack of 9–40 optical sections was acquired (*see* **Notes 3–5**).

If we consider the individual 3D with *Z*-stacks as 3D microscopy, then the time lapse of *Z*-stacks is 4D. When these

are performed at multiple positions of the field, it is 5D. With multiple-channel imaging, it is 6D. We hence use the term "multidimensional microscopy."

3.4 Data Analysis

Data sets resulting from multidimensional acquisition could be huge. *Z*-stacks of 30 layers at each XY position, in two colours at 120 time points (over 24 h) and 40 positions of XY fields, result in 288,000 individual frames. With an Andor EMCCD camera with 512×512 pixels and 14-bit digitalization, the resulted images were mounted in over 100 GB of raw data. It is therefore important to ensure a sufficient storage space available in the computer. During the acquisition, the data streamed directly to the hard drive, which prevented the complete loss of data even in case of power cut. The data were then sorted by the XY field of view and analyzed on a separate working station. We excluded those films where cells traveled outside of the field or went out of focus. Therefore, a multitude of fields are essential for the analysis and statistics. The usual workflow then included the 4D deconvolution (XYZT) for each remaining field of view using the Autoquant 3.0 software. Volume rendering, measurements and export in the form of single shots or movies were performed using Imaris 7.6 software.

It is very important to use a different computer for image analysis because of the following reasons: (a) The analysis may take hours during which the acquisition on the microscope would be prevented. (b) Different requirements have to be applied to those computers; while the "microscope" computer has to allow the fast data stream from the captured data and safe storage, the "off-line" working station has to possess a huge operative memory and a great graphic card.

3.5 The Current Setups, Limitations, and Future Perspectives

The live cell imaging is currently performed with an inverted microscope using transmission light, fluorescent light, or reflected light modes. To detect fluorescence-labeled proteins, detection of the fluorophore is the key part of imaging. Each of individual images is a two-dimensional projection. To acquire information of the third dimension, different approaches are currently used. The epi-fluorescent microscopy delivers blurry images because it captures the image of the whole thickness of the sample. It is therefore useful for acquiring images of thin monolayers of cells, especially under low magnifications. There is no advantage of using confocal microscope over epi-fluorescent one if you employ a 10×–40× lens for monolayer culture of HeLa cells or endothelial cells, for example. To get the volume information from epi-fluorescent image, a Z-stack of images followed by 3D deconvolution is required. In future, rotation of sample followed by tomography-like deconvolution is expected. Another advantageous usage of epi-fluorescent application is a quantitative measurement of

fluorescence such asCa^{++} imaging, because the whole *Z*-range of the object is illuminated and the whole fluorescence is collected by the detector.

In confocal microscopy (single pinhole or spinning disc), the out-of-focus light is blocked by the pinhole(s). The resulting image therefore represents an optical section. This makes confocal images unsuitable for fluorescence measurements. For volume reconstruction, multiple optical sections need to be captured and rendered *in silico*. Spinning disc confocal microscope is best for live imaging of relatively thin samples that do not exceed 30–50 μm in *Z*-dimension. Thicker samples such as 100 μm may be acceptable if they are well-labelled with a high signal-to-noise ratio. Otherwise, cross-talk of pinholes could deteriorate the result. For thicker samples, though, deconvolution is more effective.

If your sample is in the range of 50 μm–2 mm, the multiphoton microscope would be the choice, although microscope manufacturers claim to render up to 8 mm in thickness. If your sample is transparent eggs or embryos sized 100–1000 μm, the best microscopy of choice is Single Plane illumination microscopy (SPIM).

In all cases, the fluorescent microscopy may be combined with the transmission light microscopy (phase of differential interference contrast) to outline the live cells. For imaging metallic nanoparticles, we have developed and recommend to use the reflected mode that is fully compatible with the fluorescence [10].

4 Notes

1. Cell labeling
   To distinguish different cell types under the microscope, the use of cell lines stably expressing fluorescent proteins is the current method of choice. However, establishing coloured cell lines is time-consuming and sometimes not practical, especially for primary cells. To distinguish two cell populations, it is enough to label only one and then combine the fluorescent and transmission light microscopy. As such, distinguishing three different cell types requires two different labelings. We have not been confronted yet with a task to co-culture more than three different cell types. However, contemporary imaging technologies would allow differentiating three or more fluorescent proteins in the live mode.
2. 3D culture thickness
   It is best not to make a thick matrix for the optical reason. Nonetheless, the first bottom matrix layer is important for the 3D culture, because cells would stick to the bottom glass without it thus resulting in the 2D culture.

3. Parameter setting
   At the beginning and/or end of filming, snapshots may be taken with a larger number of *Z*-stack layers. If there are too many Z-stack layers during the film capture, it would take long time to scan all layers. The optimal *Z*-step should be 2–3 times smaller than the *Z*-resolution of the objective lens (Nyquist theorem). Further practical advice is available online: http://www.svi.nl/NyquistCalculator. Surely, a compromise between spatial and temporal resolution as well as sensitivity of the detector has to be found for each particular experiment. The same rule applies for XY-resolution, although we had less choice for it. For our biological system we used the 20×/NA0.70 PlanApo objective lens that covers a reasonably wide XY field while obtaining a good resolution.

   Different from a classical singe pinhole confocal microscope, the spinning disc pinholes are not flexible but are optimized for NA1.4 lenses. Nonetheless, we obtained decent confocal images with 20×/NA0.7 and even with 10×/NA0.45 lenses.

   For multipositional acquisition from a multi-well dish for many hours, only dry objective lens, not immersion oil lens, is possible to use, as immersion oil would be lost during the repetitive movement of the stage. A long-hour usage of oil objective lens may become possible if immersion oil is continuously supplied. Such a system with a nozzle for water immersion is already available for some Olympus microscopes, which opens a possibility in the development of similar nozzle systems on the oil or silicone objective lenses in the future (Figs. 1 and 2).

4. Acquisition protocol
   It appears to be better to scan all *Z*-stacks in one channel then scan again in another channel, rather than scanning all channels on one *Z* plane and moving to the next plane, because it takes shorter for the hardware to change the focal plane (less than 1 ms) than to change the channel (approximately 70 ms in our case).

5. Time-lapse interval setting
   Time lapse of every minute provides films of smooth movement of cells, however, other parameters such as the number of XY positions may need to be compromised. For example, in the condition of ten XY positions with 25 *Z*-stacks and two channels each, it takes 4 min 30 s for one round of scan in our setup; hence it was not possible to take time-lapse filming with an interval shorter than that. Time lapse of every 5 min is reasonably acceptable in detecting the cell movement. Different time-lapse intervals can be compared in our published literature [4].

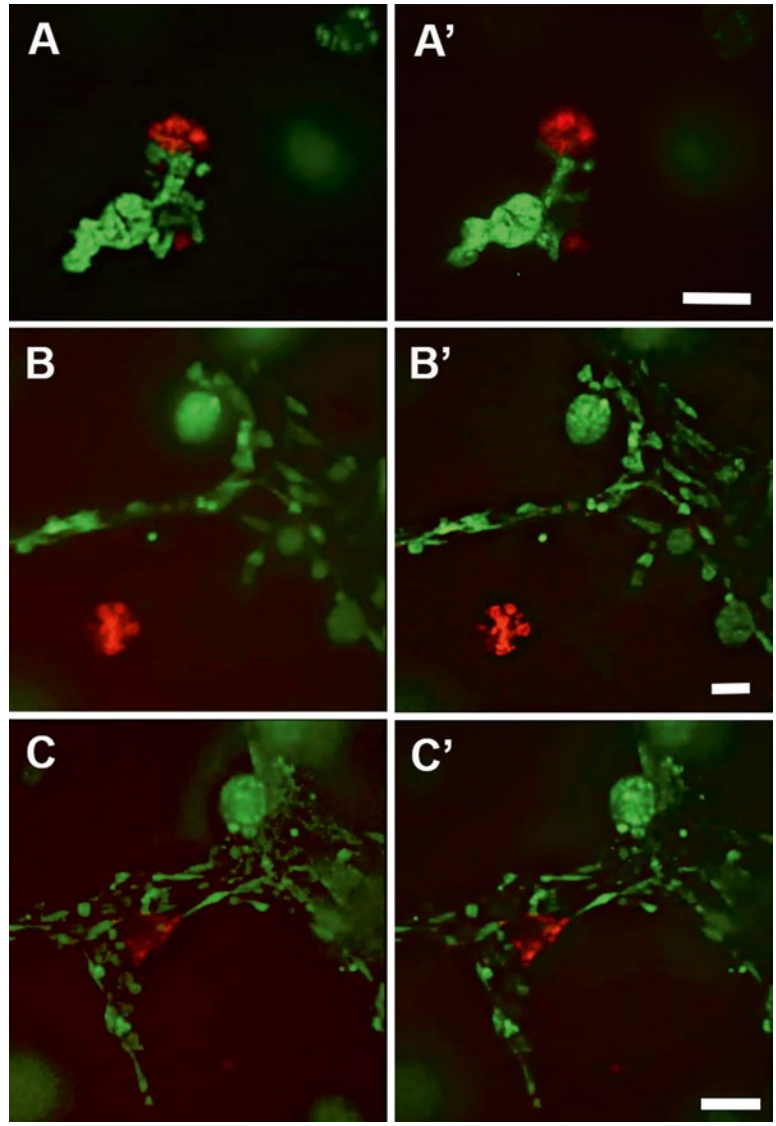

Fig. 1 The effect of deconvolution. Three examples of before and after deconvolution of snapshot images. A–C are snapshots of live images of 3D cultures whereas A′–C′ are deconvolved versions of A–C, respectively. Scale bars; A and C, 50 μm; B, 30 μm

Acknowledgements

We thank K. Welzel, L. Ivers, and F. Owolabi for their support and acquisition of images. This work was funded by University College Dublin Core Funding to NI.

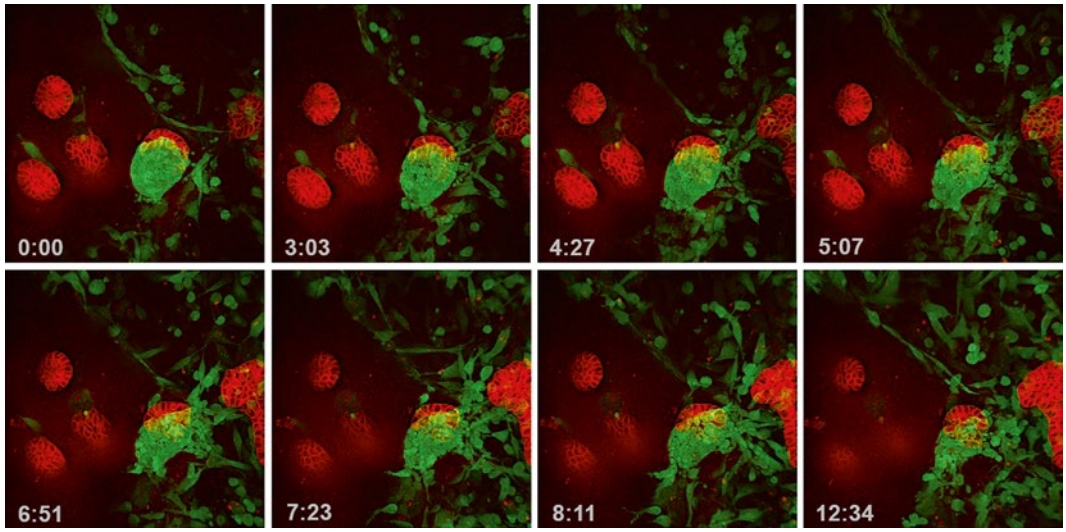

Fig. 2 Snapshots of a time lapse movie of 3D co-culture of MDA-MB-231 (*green*) and MDCK (*red*) cells, showing dynamism of MDA-MB-231 cells and rather static MDCK cells. The images were captured every 5 min at 25 *Z*-planes ($\Delta Z = 1.5$ μm; total *Z* range, 37.2 μm). Total duration of filming was 12 h 45 min. The image data were deconvolved

References

1. Kenny PA, Lee GY, Myers CA et al (2007) The morphologies of breast cancer cell lines in three-dimensional assays correlate with their profiles of gene expression. Mol Oncol 1(1):84–96
2. Weaver VM, Petersen OW, Wang F et al (1997) Reversion of the malignant phenotype of human breast cells in three-dimensional culture and in vivo by integrin blocking antibodies. J Cell Biol 137(1):231–245
3. Dhiman HK, Ray AR, Panda AK (2005) Three-dimensional chitosan scaffold-based MCF-7 cell culture for the determination of the cytotoxicity of tamoxifen. Biomaterials 26(9):979–986
4. Ivers LP, Cummings B, Owolabi F et al (2014) Dynamic and influential interaction of cancer cells with normal epithelial cells in 3D culture. Cancer Cell Int 14(1):108
5. Howes AL, Richardson RD, Finlay D et al (2014) 3-Dimensional culture systems for anti-cancer compound profiling and high-throughput screening reveal increases in EGFR inhibitor-mediated cytotoxicity compared to monolayer culture systems. PLoS One 9(9): e108283
6. Chambers KF, Mosaad EM, Russell PJ et al (2014) 3D cultures of prostate cancer cells cultured in a novel high-throughput culture platform are more resistant to chemotherapeutics compared to cells cultured in monolayer. PLoS One 9(11):e111029
7. Eichler M, Jahnke HG, Krinke D et al (2014) A novel 96-well multielectrode array based impedimetric monitoring platform for comparative drug efficacy analysis on 2D and 3D brain tumor cultures. Biosens Bioelectron. doi:10.1016/j.bios.2014.09.049
8. Abbott A (2003) Cell culture: biology's new dimension. Nature 424(6951):870–872
9. Kleinman HK, McGarvey ML, Hassell JR et al (1986) Basement membrane complexes with biological activity. Biochemistry 25(2): 312–318
10. Movia D, Gerard V, Maguire CM et al (2014) A safe-by-design approach to the development of gold nanoboxes as carriers for internalization into cancer cells. Biomaterials 35(9):2543–2557

Chapter 17

Antibody Array as a Tool for Screening of Natural Agents in Cancer Chemoprevention

Claudio Pulito, Andrea Sacconi, Etleva Korita, Anna Maidecchi, and Sabrina Strano

Abstract

The efficacy of a given drug resides mainly on its ability to specifically target disease mechanisms.

Natural products represent the leading source of bioactive molecules with a broad range of activities.

It is becoming increasingly clear that natural compounds exert their chemopreventive or antitumoral activities targeting simultaneously diverse cellular pathways. Here we describe the use of antibody array to assess the effects of natural compounds on the expression of multiple proteins and of their posttranslational modifications in cellular systems. This might turn to be a very flexible application for cancer chemoprevention studies.

Key words Antibody array, Natural agent, Cancer chemoprevention

1 Introduction

In the last decade, there was an increase in the investigations of several chemical or natural compounds according for their anticancer activities [1]. In particular, the natural compounds represent a challenge for scientists who often face the problem of finding out the molecular mechanisms through which they can exert their anticancer effects. This is because natural compounds are constituted by many heterogeneous molecules [2, 3]. Usually, a natural extract impacts on several pathways simultaneously and the final biological readout of treating people at high risk of cancer occurrence could be the reprogramming of different molecular perturbations. Recently, we showed that Cynara Scolymus leaf extracts impact on mesothelioma anticancer activities by impinging on different oncogenic signalling pathways [4]. This was evidenced using the Antibody array technology.

Based on these evidences, a high-throughput platform such as the Antibody Microarrays (AM) represents an efficient, accurate,

Sabrina Strano (ed.), *Cancer Chemoprevention: Methods and Protocols*, Methods in Molecular Biology, vol. 1379,
DOI 10.1007/978-1-4939-3191-0_17,

and sensitive technique for screening the protein expression profiles to investigate the molecular mechanisms of a natural extracts [5–10].

Different kinds of protein arrays are available. They differ on the number and the type of antibodies that are spotted on the surface of the slide. The advanced ones permit to analyze simultaneously more than one hundred protein and phospho-protein antibodies in order to discriminate which pathways are modulated by the chemoprevention agent tested. In addition, this kind of assays allows to save resources and to reduce the number of variables that can affect the experimental outcome.

AM are mainly based on the enzyme-linked immunosorbent assay (ELISA). The antibodies are directly immobilized on the AM slide surface in a specific order. Each antibody is often spotted in replicate and, positive and negative control are loaded on the AM slide in order to discriminate any technical problems such as background problems during data analysis. The detection is often based on an immunofluorescent reaction caused by the binding between the biotinylated protein and the dye-labeled streptavidin substrate. The sandwich assay involves the formation of a three-layered structure that consists in the immobilized antibody, the biotinylated protein and the dye-labeled streptavidin substrate [11].

In general, these assays can be used for analysis of protein extracts from cells, blood samples, and fresh, frozen, and/or FFPE tissues.

The protocol described below is a more detailed personal modification of the antibody array user's guide of Full Moon BioSystems, Inc. (754 N Pastoria Ave, Sunnyvale, CA 94085) (Fig. 1).

2 Materials

Before starting the experiment prepare all fresh solutions.

Each reagent needs a different temperature of warming before use (*see* Subheading 3).

The major part of the reagents is provided by the kit (Phospho Explorer Antibody Array, Cat. N. PEX100, Full Moon, BioSystems).

2.1 Protein Extraction

1. One to five million of cells.
2. 1× PBS (pH 7.4) (Gibco).
3. Thoma cell counting chamber.
4. Extraction buffer (Full Moon BioSystems).
5. Lysis beads (Full Moon BioSystems).
6. Vortexer.
7. Centrifuge.

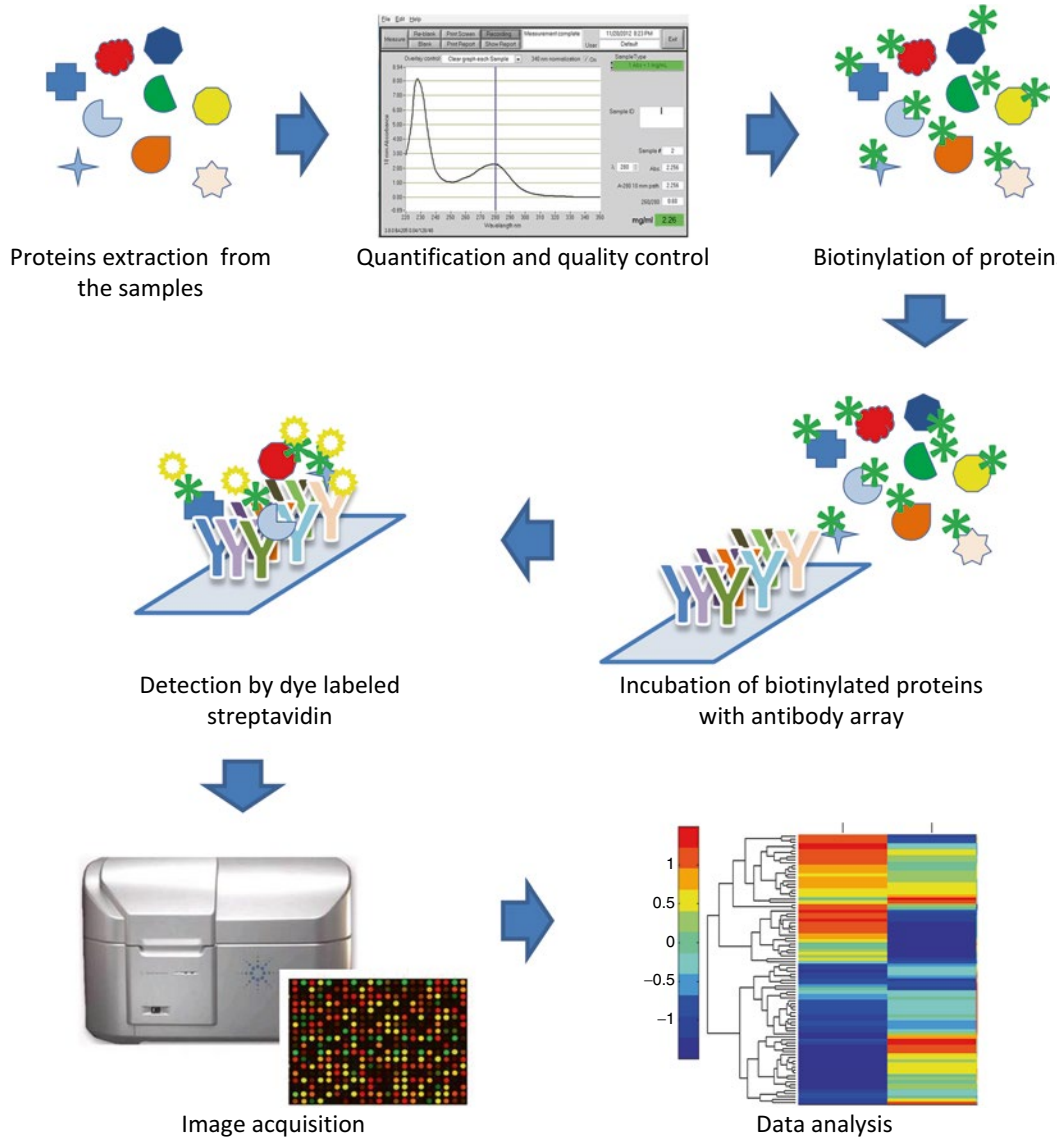

Fig. 1 Workflow

2.2 Lysate Purification and Quantification

1. Spin columns (Full Moon BioSystems).
2. Labeling buffer (Full Moon BioSystems).
3. Vortexer.
4. Centrifuge.
5. UV adsorption spectrophotometer (NanoDrop 1000 spectrophotometer, Thermo Scientific).

2.3 Protein Labeling

1. Biotin Reagent (Full Moon BioSystems).
2. *N*,*N*-Dimethylformamide (DMF) (Full Moon BioSystems).
3. Labeling buffer (Full Moon BioSystems).
4. Stop Reagent (Full Moon BioSystems).

2.4 Blocking and Coupling

1. Blocking reagent (Full Moon BioSystems).
2. Petri dish 100 × 15 mm.
3. Antibody microarray slides (Full Moon BioSystems).
4. Milli-Q grade water or dd H_2O.
5. Coupling reagent (Full Moon BioSystems).
6. Vortexer.
7. Coupling chambers (Full Moon BioSystems).
8. Labeled protein solution.
9. 10× Wash buffer (Full Moon BioSystems).
10. Orbital shaker [2].
11. 50 ml conical tube.

2.5 Detection

1. Cy3-Streptavidin (1 mg/ml) (#SA-5549, Vector).
2. Detection buffer (Full Moon BioSystems).
3. Petri dish 100 × 15 mm.
4. Milli-Q-grade water or dd H_2O.
5. 10× Wash buffer (Full Moon BioSystems).
6. Orbital shaker
7. 50 ml conical tube.
8. Centrifuge.

2.6 Scanning

1. Agilent Technologies G2505B Micro Array Scanner (Agilent Technologies).

2.7 Data Extraction

1. Gal file (Full Moon BioSystems).
2. Agilent feature extraction software (Agilent technologies).

2.8 Data Analysis

1. Antibody list (Full Moon BioSystems).
2. Array map (Full Moon BioSystems).
3. Matlab software (The MathWorks Inc.).

3 Methods

Please warm all the solution at the right temperature before use. The protocol allows to stop the procedure and stored the sample at −80 °C at the end of the lysate quantification and/or the protein labeling section.

3.1 Protein Extraction (See Note 1)

1. Wash twice the cell culture dishes with warm 1× PBS (37 °C).
2. Detach the cells by scraping (*see* **Note 2**) them from the dish in cold 1× PBS (4 °C).
3. Collect cells in a 15 ml conical tubes and centrifuge at 4 °C at 800 rpm for 5 min. Discard supernatant and suspend pellet with cold 1× PBS.
4. Calculate the amount of cells by using a Thoma counting cells chambers. Collect 1–2.5 million or 2.5–5 million of cells and centrifuge at 4 °C at 800 rpm for 5 min. Discard supernatant.
5. Resuspend the pellet in 100 μl (1–2.5 million) or 200 μl (2.5–5 million of cells) of extraction buffer.
6. Add a tube of lysis beads in each sample and mix by vortexing for 1 min.
7. Incubate the mixture on ice for 10 min.
8. Repeat vortexing every 10-min intervals for 60 min. Remember to place sample on ice between vortexing.
9. Centrifuge samples at 17500 × *g* for 20 min at 4 °C.
10. Transfer the supernatant (protein extract) to a clean tube (*see* **Note 3**).

3.2 Lysate Purification and Quantification

Warm to room temperature the following reagents before use: spin column and labeling buffer.

1. Remove the top column cap of the spin column and reconstitute the dry gel contained inside by adding 650 μl of labeling buffer.
2. Close the top column cap and vortex vigorously for 5 s (*see* **Note 4**).
3. Leave the hydrated column at room temperature for 30 min before use (*see* **Note 5**).
4. After hydration, remove excess fluid by spin the column in its wash tube at 800 × *g* for 2 min. Remove the top and the bottom tap before centrifuging.
5. Immediately transfer 100 μl of protein extract by dispensing the sample onto the center of the column without touch the gel surface.
6. Place the column in a new collection tube and spin them at 800 × *g* for 2 min.
7. Discard the spin column and collect the purified protein.
8. Measure the UV adsorption of the protein sample (*see* **Note 6**). Use labeling buffer as blank.
9. Store the sample at −80 °C or proceed to the next step.

3.3 Protein Labeling

Warm to room temperature the following reagents before use: DMF, biotin reagent, labelling buffer, stop reagent.

1. Prepare the DMF/biotin solution to final volume of 10 μg/μl by adding 100 μl of warm DMF to 1 mg of biotin.
2. Aliquot 100 μg of protein lysate in a new tube (collect 10–25 μl of lysate basing on the OD measured) (*see* **Note 7**).
3. Bring the protein lysate to 75 μl by adding labeling buffer.
4. Add 3 μl of DMF/biotin solution to the protein lysate and incubate it for 2 h at room temperature by mixing.
5. At the end of the 2 h stop the reaction by adding 35 μl of stop reagent. Incubate for 30 min at room temperature with mixing.
6. Store the sample at −80 °C or proceed to the next step.

3.4 Blocking and Coupling

Warm to 25–30 °C in a water bath the following reagents before use: blocking reagent, coupling reagent, and 10× wash buffer. Warm to room temperature the antibody microarray slides (*see* **Note 8**).

1. Prepare the blocking solution by adding 60 ml of warm blocking reagent to 1.8 g of dry milk.
2. Add 30 ml of blocking solution in a 100 × 15 mm Petri dish and submerge the slide in this solution. Submerge only one slide for Petri dish.
3. Incubate at room temperature for 45 min on an orbital shaker at 50 rpm.
4. After that, place the slide in a 50 ml conical tube.
5. Add 45 Milli-Q grade water or dd H_2O. Avoid to add water directly on the upper side of the slide. Shake gently for 10–20 s, discard the water and refill the tube with other 45 ml of water.
6. Repeat **step 5** ten times (*see* **Note 9**).
7. Place the slide in a free well of the coupling chamber. Before to place, shake off the excess of fluid from the slide.
8. During **step 6**, prepare the coupling solution by adding 12 ml of warm coupling reagent to 0,36 g of dry milk.
9. Add in a 15 ml conical tube, 6 ml of coupling solution and one tube of labeled samples previously stored at −80 °C (**step 6** of Subheading 3.3). Prepare a 15 ml of conical tube for each labeled sample.
10. Slowly pour the solution of point 8 into a free well. Submerge the slide of the coupling chamber containing the slide (*see* **Note 10**). Avoid to add the solution directly on the surface of the slide.

11. Incubate at room temperature for 2 h on an orbital shaker at 30 rpm.
12. During **step 10**, prepare the 1× wash solution by adding 100 m of warm 10× wash buffer to 900 ml of dd H_2O.
13. Transfer the slide in a new Petri dish previously filled with 30 ml of 1× wash solution.
14. Incubate at room temperature for 10 min on an orbital shaker at 60 rpm.
15. Discard 1× wash solution from the Petri dish and fill it with other 30 ml of 1× wash solution.
16. Repeat **steps 14** and **15** for other two times.
17. After that, place the slide in a 50 ml conical tube and add 45 Milli-Q-grade water or dd H_2O. Avoid to add water directly on the upper side of the slide. Shake gently for 10–20 s, discard the water, and refill the tube with other 45 ml of water.
18. Repeat **step 17** ten times (*see* **Note 9**).

3.5 Detection (see Note 11)

Warm to room temperature the following reagents before use: detection buffer, 1× wash solution.

1. Prepare Cy3-streptavidin solution by adding 30 μl of Cy3-streptavidin (1 mg/ml) to 60 ml of warm detection buffer.
2. Transfer the slide in a new Petri dish and slowly add 30 ml of Cy3-streptavidin solution.
3. Incubate at room temperature for 20 min on an orbital shaker at 50 rpm.
4. Transfer the slide in a new Petri dish previously filled with 30 ml of 1× wash solution.
5. Incubate at room temperature for 10 min on an orbital shaker at 60 rpm.
6. Discard 1× wash solution from the Petri dish and fill it with other 30 ml of 1× wash solution.
7. Repeat **steps 5** and **6** for other two times.
8. After that, place the slide in a 50 ml conical tube and add 45 Milli-Q-grade water or dd H_2O. Avoid to add water directly on the upper side of the slide. Shake gently for 10–20 s, discard the water, and refill the tube with other 45 ml of water.
9. Repeat **step 8** for ten times (*see* **Note 9**).
10. Shake off excess water from the slide and place the slide in a new 50 ml conical tube.
11. Dry the slide by centrifuging the 50 ml conical tube filled with the slide at 100 × *g* for 2 min at room temperature (*see* **Note 12**).

3.6 Scanning (see Note 13)

1. Put the slide in a slide holder for the Agilent microarray scanner with the barcode facing up in the slide holder.
2. Place assembled slide holder into an empty slot of the carousel.
3. Use an Agilent HD_GX_1 color protocol, with 5 μm scanning resolution, and green color channel, to scan the slide.

3.7 Data Extraction

1. Open the scanner slide image (.tiff) with the Agilent Feature Extraction software (*see* **Note 14**).
2. Flip the scanner slide image from left to lower right (landscape/portrait).
3. Convert the gal file (*see* **Note 15**) to a grid.csv file compatible with the Agilent software.
4. Open the grid (grid.csv) and adjust it on the scanner slide image thus to center each spot of the slide to each point of the grid.
5. Create a new project, change project properties, and run Feature Extraction for a non-Agilent image (*see* **Note 16**).
6. Proceed with data extraction.

3.8 Data Analysis

For data analysis and features selection we use Matlab software (The MathWorks Inc.).

1. A quality control of the signals is performed on negative and positive controls and checking intensity values of two different housekeeping protein such as GAPDH and ACTIN.
2. A quantile normalization between arrays and Z score transformation is performed to express the background corrected spot intensity values as unit of a standard deviation from the normalized mean of zero.
3. Features is selected basing on Z ratios calculated by taking the difference between the averages of the observed protein Z scores and dividing by the standard deviation of all the differences for that particular comparison [12]. A Z ratio higher than 1.5 is inferred as significant.
4. Unsupervised Hierarchical Clustering is used to investigate clusters of samples (Fig. 2).

4 Notes

1. Usually the kit provides only two antibody array assay slides; for this reason it is important to know if the treatment, that we want to test, has worked before performing the experiment. It is advisable to use an aliquot of the cells to test a positive read out.

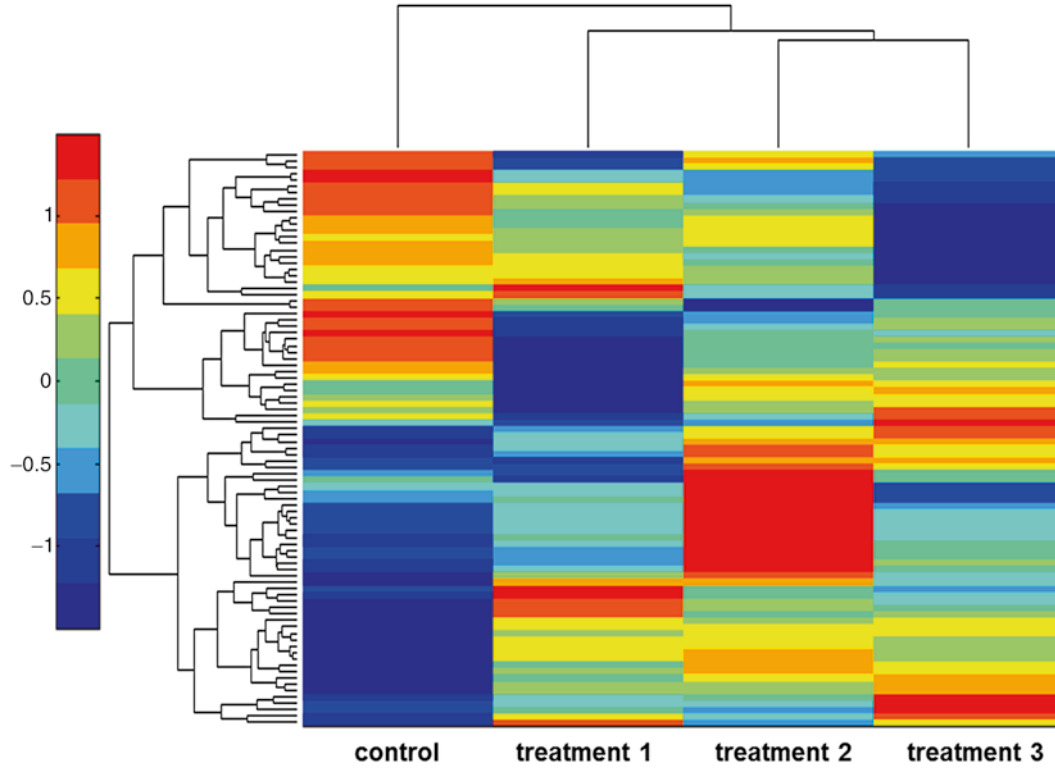

Fig. 2 Unsupervised hierarchical clustering example. Heat maps depicting phospho-protein levels of a control and three different treatments

2. Do not use trypsin to detach the cells: it could impair cell protein activity. Use only the lysis buffer provided by the kit to lysate the samples. Other buffers could impair the ELISA reaction.
3. The supernatant should appear clear. If it appears cloudy, centrifuge again at 17500 × *g* for 20 min at 4 °C. If it is still cloudy, store tubes at −70 °C for 15 min. Remove tubes from the freezer and immediately centrifuge at 14000 rpm for 20 min at 4 °C.
4. Spin column cap is provided of two caps one on top and one at bottom. After adding labelling buffer, remove air bubbles by sharply tapping the bottom of the column.
5. Reconstitute the spin column during the centrifuge of **step 9** of the protein extraction thus to allow an immediately purification of the protein samples.
6. Use proteins A280 program for the NanoDrop 1000 spectrophotometer (Thermo Scientific). The absorbance should be greater than four OD and the UV absorption spectrum should reveal two peaks one at 200–230 nm and one at 240–280 nm (Fig. 3). If the OD is lower than four, the protein must be

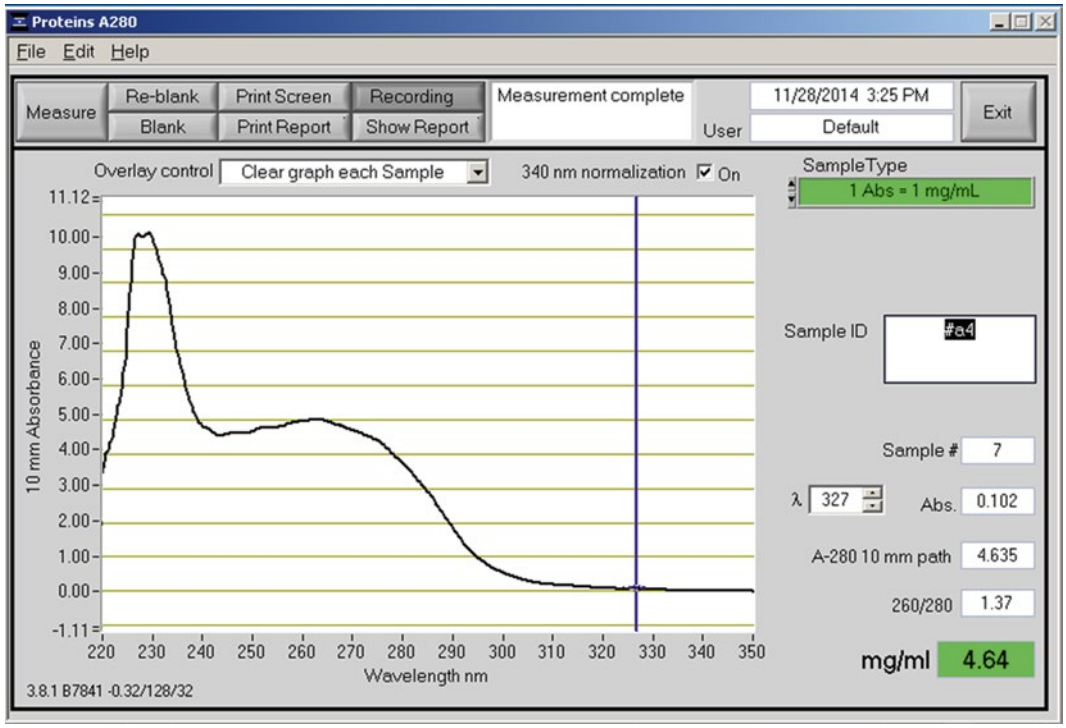

Fig. 3 UV absorption spectrum example of a clear cell lysate. The two peaks, 230 and 270 nm, are well separated

concentrated at 4 °C in a vacuum centrifuge. Moreover, if the protein lysate is not clear the peaks will not appear well separated. In this case it should necessary repeat procedure described in **Note 3**.

7. It is possible to use less than 100 μg of protein lysate, till to a minimum of 40 μg with a concentration of 2 μg/μl.
8. Warm the slides at room temperature for 30–45 min; after that, open the package and leave the slides for 10 min at room temperature in order to dry the surface of the slides. Please note that the side of the slide with the barcode labeled is the upper one and must face up.
9. After the last wash, the slide surface should appear uniformly smooth. If it does not happen repeat **step 5** of Subheading 3.4.
10. It is important to do **step 9** just after **step 6** of Subheading 3.4 in order to avoid the surface of the slide from becoming dry.
11. Perform these steps in the dark or cover with aluminum foil all the steps in which it used the Cy3-streptavidin solution.
12. It is very important to shake off the excess of fluid from the slide as quickly as possible in order to avoid spots formation

due to water evaporation, which could compromise the quality of scan image.

13. Here we described the procedure for scanning the slide with the Agilent Technologies G2505B Micro Array Scanner; however, it could be used other scanners which are compatible with 3 × 1 in. slides (76 × 25 mm).
14. Use Agilent Feature Extraction software or another one compatible with the scanner that is used.
15. The gal file is provided by the company that produced the microarray protein assay.
16. See the Agilent Feature Extraction software user's guide.

References

1. Steward WP, Brown K (2013) Cancer chemoprevention: a rapidly evolving field. Br J Cancer 109:1–7
2. Newman DJ, Cragg GM (2012) Natural products as sources of new drugs over the 30 years from 1981 to 2010. J Nat Prod 75(3):311–335
3. Danishefsky S (2010) On the potential of natural products in the discovery of pharma leads: a case for reassessment. Nat Prod Rep 27:1114–1116
4. Pulito C, Mori F, Sacconi A Cynara scolymus affects malignant pleural mesothelioma by promoting apoptosis and restraining invasion. Oncotarget 6(20):18134–50
5. Fan H, Yang L, Fu F et al (2012) Cardioprotective effects of salvianolic acid a on myocardial ischemia-reperfusion injury in vivo and in vitro. Evid Based Complement Alternat Med 2012:508938
6. Chung A, Chin YE (2009) Antibody array platform to monitor protein tyrosine phosphorylation in mammalian cells (Chapter 18). Methods Mol Biol 527:247–255
7. Sanchez-Carrayo M (2006) Antibody arrays: technical considerations and clinical applications in cancer. Clin Chem 52(9): 1651–1659
8. Pierobon M, Wulfkuhle J, Liotta L et al (2015) Phosphoproteomic analysis in oncological practice. Oncogene 34(7):805–814
9. Eke I, Schneider L, Forster C et al (2013) EGFR/JIP-4/JNK2 signaling attenuates cetuximab-mediated radiosensitization of squamous cell carcinoma cells. Cancer Res 73:297–306
10. Mitchell SJ, Martin-Montalvo A, Mercken EM et al (2014) The SIRT1 activator SRT1720 extends lifespan and improves health of mice fed a standard diet. Cell Rep 6:836–843
11. Lee JR, Magee DM, Gaster RS et al (2013) Emerging protein array technologies for proteomics. Expert Rev Proteomics 10:65–75
12. Cheadle C, Vawter MP, Freed WJ et al (2003) Analysis of microarray data using Z score transformation. J Mol Diagn 5:73–81

Chapter 18

South African Herbal Extracts as Potential Chemopreventive Agents: Screening for Anticancer Splicing Activity

Zodwa Dlamini, Zukile Mbita, and David Bates

Abstract

RT-PCR is an invaluable tool for the detection and characterization of mRNA. Cancer cell lines are treated with crude plant extracts and RNA is extracted and purified with DNase prior to RT-PCR. RT-PCR first-strand cDNA synthesis is done using random primers and can be refrigerated at 4 °C. PCR from the stored cDNA is performed using transcript-specific primers and electrophoresed on a molecular grade agarose gel to separate the splice variants.

Key words Anticancer splicing activity, Herbal plant extracts, RNA extraction, First-strand cDNA synthesis, DNase treatment, Agarose gel electrophoresis

1 Introduction

Traditional medicine use has a long history and is still the major source of medicine in developing countries. Approximately 70 % of the South African population consults traditional healers, perpetuating the need for scientific appraisal of traditional medicine as a means to establish its efficiency and safety [1]. Also, pharmacological and phytochemical insights into several plants have led to the discovery of novel chemicals and therefore novel drugs. The discovery of these drugs stresses the importance of using natural products and their derivatives to provide new target molecules for drug development.

Since the publication of the human genome, research has shown that the number of genes is considerably lower than that predicted from the known protein catalogue [2]. Posttranslational modification, such as splicing of immature messenger RNA (pre-mRNA), is fundamental for generating mature mRNAs ready to be translated into proteins. Additionally, through alternative splicing, a single gene is capable of generating multiple transcripts from a

Sabrina Strano (ed.), *Cancer Chemoprevention: Methods and Protocols*, Methods in Molecular Biology, vol. 1379,
DOI 10.1007/978-1-4939-3191-0_18,

common mRNA precursor and this mechanism allows for proteome complexity. This event leads to the production of distinct protein isoforms, which might have diverse and even antagonistic functions. Several genome-wide analyses indicate that more than 50 % of human genes present alternative spliced forms, suggesting that this mechanism has a major role in the generation of protein diversity [8]. Alternative splicing is important in normal development as a means of creating protein catalogue or diversity in complex organisms [9, 10]. Alteration of the normal process in cancer cells results in the production of previously nonexisting mRNAs or in the modification of tissue-specific ratios between normal mRNA isoforms [2]. Defects in mRNA splicing are crucial in the development of diseases [4–6]. The most common forms of splicing defects are genomic splice site mutations in more than 12 different types of cancers [7]. To be a cause of cancer an abnormal alternatively spliced product must presumably be expressed at a significant level compared with properly spliced product [3]. An individual splice form seen exclusively in cancer but not in healthy cells could be a candidate for a diagnostic, prognostic, or predictive biomarker. An association between differential expression of splicing isoforms and tumour progression has been shown for several proteins, such as MDM2 and survivin [2]. Currently, the analysis of cancer-specific alternative splicing is a promising step forward in basic and translational molecular biology [2].

Thus we have screened medicinal plants for anticancer splicing activity using semiquantitative RT-PCR in cancer cell lines.

2 Materials

Prepare all solutions with ultrapure water. Autoclave all solutions for tissue culture.

2.1 Culture Medium

Prepare culture medium for appropriate cell lines by adding the appropriate medium, serum, and supplemental reagents required for growth according to the cell line manufacturer.

2.2 Stock Solution for SRPIN 340

SRPIN 340 (28 mM in 100 % DMSO-Kept in a –20 °C freezer).

1. Make 400 µl 10 %/DMSO (28 mM SPRPIN 340).
2. Dilute to 10 % DMSO with tissue culture media before use. (40 µl 100 % DMSO/2,8 mM SRPIN 340 + 360 µl medium-400 µl 10 % DMSO/2800 µM SRPIN 340).

2.3 Plant Extract Preparation

1. Prepare a stock solution of 100 mg/ml in 10 ml tubes.
2. Filter-sterilize and keep in small aliquots (100 µl Eppendorfs) at –20 °C until use.

2.4 PCR Primers

1. Experimental primers.

   Forward primer: Transcript specific.

   Reverse primer: Transcript specific.

   Forward primer GC content ±50 %.

   Reverse primer GC content ±50 %.

2. VEGFxxx/VEGFxxxb PCR control.

   Forward Exon 7b:

   5′GGC AGC TTG AGT TAA ACG AAC G-3′

   Oligo %GC = 50 %.

   Oligo is 25 nt bases long.

   Reverse Exon 8b:

   3′UTR BamHI + GG (5′-G/GATCC-3′):

   5′-CCA GGA AAG ACT Gat aca gaa cga -3′

   Oligo % GC = 48 %.

   Oligo is 25 nt base long.

   130 bp VEGFxxxb, 64 bp VEGFxxx

3. HnRNPA2 primers.

   HnRNPA2 ex1-forward primer: 5′-GCG GCA GTA GCA GCA GCG CC-3′

   HnRNPA2 ex3-reverse primer: 5′-CTT ACG GAA CTG TTC CTT TTC TC-3′

4. MKNK2 PCR (EXON 13a and 13b) primers.

   MKNK2 ex11-forward primer: 5′-CCA AGT CCT GCA GCA CCC CTG G-3′

   MKNK2 ex13a-reverse primer: 5′-CAT GGG AGG GTC AGG CGT GGT C-3′

   MKNK2 ex13b-reverse primer: 5′-GAG GAG GAA GTG ACT GTC CCA C-3′

3 Methods

3.1 Tissue Culture

1. Grow cells in T75 flasks in an appropriate medium until confluent.
2. Trypsinize cells as follows: add 3 ml trypsin plus 3× (9 ml) culture medium with serum in a T75 flask.
3. Keep cells at the CO_2 incubator at 37 °C shortly until cells have detached from the flask.
4. Spin the cells down for 3 min at 3000 rpm (700 × *g*) in a microfuge at 4 °C (*see* **Note 1**).

5. Take out the media by suction using a pipette. Add 5 ml tissue culture medium and resuspend cells. Disperse or separate clumps of cells by using a syringe and a needle.
6. Take 10 µl cells in 90 µl medium/PBS/H2O (10× dilute).
7. Count on a hemocytometer. Seed approximately 40,000–80,000 cells per well (24-well plate).
8. Incubate cells at 37 °C in a CO_2 incubator until 50 % confluent and then treat the cells with your plant extracts/compounds for 24 h.

3.2 SRPIN 340 Control Experiments

Do the experiment in triplicates in a 24-well plate.

1. Seed cells until they are 50 % confluent before treatment.

   Dilution: Provide 6 × 5 ml tubes (Table 1).
2. Transfer 3000 µl media into each tube. From tubes 2–6 discard 1, 5, 10, 54, and 107 µl respectively and then replace with 1, 5, 10, 54, and 107 µl 2800 µM SRPIN 340, respectively, to attain concentrations from tubes 1–6 of 0, 1, 5, 10, 50, and 100 µM, respectively.
3. Do the treatment in triplicates for 24 h and stop the reaction by washing with 1× PBS three times before RNA extraction.

3.3 Plant Extract Treatments

1. Dilution: Provide 5 × 5 ml tubes (Table 2).
2. Transfer 500 ml media into each tube. From tubes 2–5 discard 50, 100, 150, and 250 µl, respectively, and then replace with

Table 1
SRPIN 340 dose–response control experiments

Tubes (5 ml)	1	2	3	4	5	6
Final concentration of SRPIN 340 in µM	0	1	5	10	50	100
Medium in µl	3000	2999	2995	2990	2946	2893
10 % SRPIN 340/2800uMDMSO in µl	0	1	5	10	54	107

Table 2
Herbal extract dose–response experiments (*see* Note 9)

Tubes (5 ml)	1	2	3	4	5
Final concentration of herbal extract in mg/ml	0	1	2	3	5
Medium in µl	5000	4950	4900	4850	4750
100 mg/ml herbal extract stock solution in µl	0	50	100	150	250

50, 100, 150, and 250 μl of the 100 mg/ml stock solution of plant extract, respectively, to attain concentrations from tubes 1–5 of 0, 1, 2, 3, and 5 mg/ml, respectively.

3. Treat cells on 24-well plates for 24 h.
4. Wash the cells three times with 1 ml 1× PBS to stop the reaction.

   Control: We always have an extra 5 ml tube of 10 μM SRPIN 340 (15 μl in 4.5 ml medium) for control treatment.

3.4 RNA Extraction with Tri Reagent

1. Move cells from the Class 11 tissue culture laboratory incubator to a fume hood.
2. Remove the medium and wash cells ×2 with 1 ml per each well of 1× PBS. Add 125 μl per each well of TRI Reagent (Sigma T9424)(*see* **Note 2**).
3. Lyse the cells by mixing the solution up and down several times with a pipette (mix the first well and then move the lysate to the replica well of the same clone).
4. Collect the homogenous lysate in a fresh 1.5 ml Eppendorf tube and leave the samples in incubation for 5 min at room temperature to ensure the complete dissociation of nucleoprotein complexes.
5. Add 100 μl of Chloroform (Sigma C2432) per 500 μl of TRI Reagent used and close tightly.
6. Shake vigorously by hand for 15 s and leave in incubation for 15 min at room temperature.
7. Centrifuge at 12,000 rpm (12,000 × *g*) for 15 min at 4 °C.
8. Transfer the upper aqueous phase to a fresh tube (three phases: a pink organic, lower phase (protein), a white/grey interphase (DNA), a colorless upper aqueous phase (RNA)).
9. Add 500 μl of cold isopropanol (Fluka 59304) per ml of TRI Reagent used, close tightly, shake vigorously for 15 s, and leave in incubation for 10 min at room temperature.
10. Pellet the RNA by centrifugation at 12,000 rpm (12,000 × *g*) for 10 min at 4 °C. Discard the supernatant and wash the gel-like pellet by adding 1 ml of cold 75 % ethanol per ml of TRI Reagent used.
11. Gently wash the samples and centrifuge at 10,000 rpm (7500 × *g*) for 5 min at 4 °C.
12. Discard the supernatant and briefly dry the pellet for 5–10 min at room temperature (do not overdry).
13. Dissolve the RNA by adding 20–25 μl of DEPC H_2O and resuspend the pellet. Store the RNA at −20 °C.

3.5 DNase Treatment of RNA Samples Prior to RT-PCR

1. Quantify your RNA using the nanodrop or any other sensitive quantification tools.
2. Set up the DNAse digestion reaction as follows: RNA in water or TE buffer (use 5 μg RNA) in case you lose RNA during the procedure. RQ1 RNase-free DNase 10× reaction buffer 1 μl. RQ1 RNase-free DNase 1 μl (*see* **Note 3**).
3. Add nuclease-free water to a final volume of 10 μl. Incubate at 37 °C for 1 h. Add 1 μl of RQ1 DNase stop solution to terminate the reaction. Incubate at 65 °C for 10 min to inactivate the DNase. Add all of the treated RNA to the RT-PCR reaction.

3.6 RT-PCR First-Strand cDNA Synthesis

1. Use 1 μg (1000 ng) of total RNA in sterile RNase-free microcentrifuge. Anneal primers as recommended by the manufacturer (Table 3) (*see* **Note 4**).
2. Heat tube to 70 °C for 5 min, cool quickly on ice for 5 min.
3. Add components to annealed primer/template in the order shown in Table 4.
4. Fill up with Sigma water to 50 μl (50 μl PCR reaction volume).
5. Perform cDNA synthesis as shown in Table 5.

Table 3
Annealing of primers

Reagent	Final concentration	Volume per tube	Mix (x__)
Hexamer/random primer (500 μg/mL)	0.5 μg/ul	2.5 μl	__μl
RNAsin (40 U/μl)	40U/50 μl	1 μl	__μl
Total volume	_____	4 μl	__μl

Table 4
Reverse transcription components

Reagent	Final concentration	Volume per tube	Mix (x__)
M-MLV RT reaction buffer	5×	10 μl	__μl
dNTPs (10 mM)	0.5 mM	2.5 μl	__μl
M-MLV RT (h-) 200 U/μl	200 U	1 μl	__μl
Total volume	_____	_____	_____

Table 5
cDNA synthesis

PCR step	Temperature (°C)	Time	Cycle
Initial incubation	37	90 min	1
Inactivation	70	15 min	1
Refrigeration	4	Forever	–

Table 6
PCR reaction setup

Reagent	Final concentration	Volume per tube	Mix (x__)
PCR master mix Promega (2×)	1×	25 µl	__µl
Forward primer (20 µM)	1 µM	2.5 µl	__µl
Reverse primer (20 µM)	1 µM	2.5 µl	__µl
H_2O	_____	__µl	__µl
Total	–	__µl	__µl

3.7 PCR Reaction (Alternative Splicing)

1. Set up the PCR reactions as in Table 6 (*see* **Notes 5 and 6**).
2. Add the PCR Master Mix last and mix well before starting the PCR programs (Table 7). Transcript-specific primers may need optimization of PCR conditions.
3. Use 5–10 µl of cDNA as template.

3.7.1 Negative Controls

1. Add H_2O (Sigma) instead of cDNA.
2. Add H_2O (Sigma) instead of reverse and forward primers.

3.7.2 VEGF Controls

Known DNA samples and the experimental cDNA (Table 8) were used.

3.7.3 HnRNPA2 PCR (EXON 2) Control Experiments

The experimental cDNA (Table 8) was used.

3.7.4 MKNK2 PCR (EXON 13a and 13b) Control Experiments

The experimental cDNA (Table 8) was used.

3.8 Agarose Gel Electrophoresis

Weigh out 2 g of agarose gel (*see* **Note 7**). Dissolve in 100 ml 1× TBE by heating on low to medium in a microwave (2 % agarose gel for ease of separation of splice variants). Cool it down to about

Table 7
PCR amplification for VEGF controls

PCR step	Temperature (°C)	Time	Cycle
Initial denaturation	95	2 min	1
Denaturation	95	1 min	30
Annealing	55	1 min	
Extension	72	1 min	
Final extension	72	5 min	1
Refrigeration	4	Hold	–

Table 7b
PCR amplification for MKNK2 controls

PCR step	Temperature (°C)	Time	Cycle
Initial denaturation	95	2 min	1
Denaturation	95	1 min	30
Annealing	60	1 min	
Extension	72	1 min	
Final extension	72	5 min	1
Refrigeration	4	Hold	–

Table 7c
PCR amplification for HNRNPA2/B1 controls (*see* Note 8)

PCR step	Temperature (°C)	Time	Cycle
Initial denaturation	95	2 min	1
Denaturation	95	1 min	30
Annealing	55	1 min	
Extension	72	1 min	
Final extension	72	5 min	1
Refrigeration	4	Hold	–

Table 8
DNA templates for experiments and controls

Reagent	Final concentration	Volume per tube
Template tubes after RT-PCR first-strand synthesis	–	10 µl
VEGF165 in pcDNA3 (200 ng/µl)	200 ng	1 + 9 µl Sigma H_2O (10 µl)
VEGF165b in pcDNA3 (200 ng/µl)	200 ng	1 + 9 µl Sigma H_2O (10 µl)

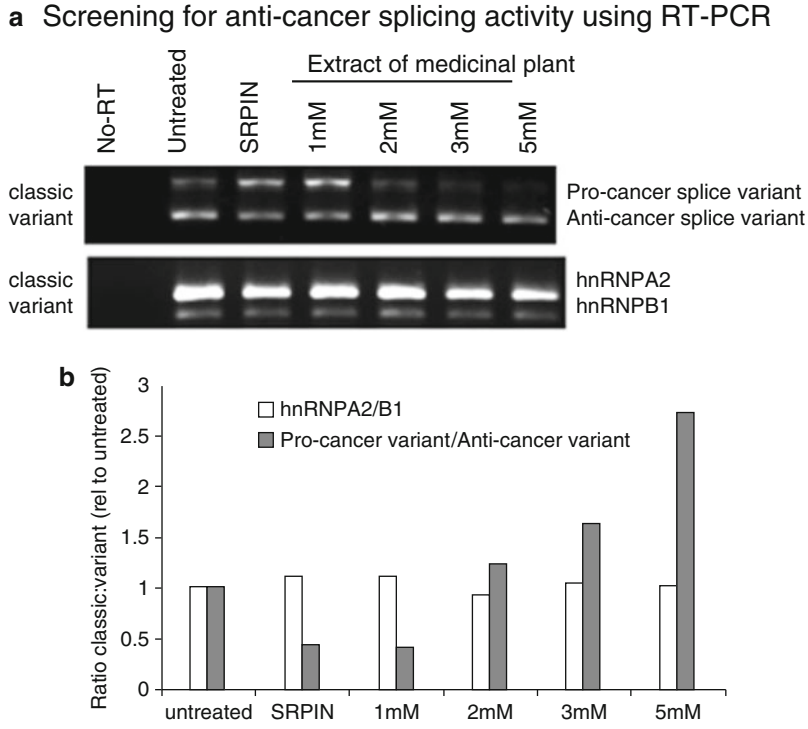

Fig. 1 There is a dose–response on gene splice variants. Cells were treated with a medicinal plant extract for 24 h, followed by mRNA extraction and RT-PCR. The dose–response is clearly visible after treatment with the plant extract when the anticancer splice variant becomes clearly evident. There is no dose–response on HnRNPA2 splice variants—no effect of the herbal extract to the HnRNPA2 splicing factor (**a**). (**b**) clearly shows the increase in ratio of the classic: variant in reference to untreated cells

50 °C and add 5 µl of 100 mg/ml ethidium bromide and pour the gel into a tray. When the gel has set, immerse the gel to a running buffer (1× TBE). Load samples in a loading dye including a lane of an appropriate molecular weight marker. Run at a voltage of 100 V for 10 min and then at 70 V until the dye front is ¾ way down the gel. Stop the gel and view it using the Gel Doc Image analyzer and capture the image for analysis (Fig. 1).

4 Notes

1. Tissue culture: Make sure that when you seed cells for treatment with herbal extract, the concentration of the cells in the wells are equivalent. Keep an autoclaved stock solution of 20× PBS to dilute it to 1× whenever needed.
2. RNA extraction: You can use the Tri Reagent (Sigma T9424) or the Trizol Reagent (Invitrogen 15596-018) for RNA extraction using exactly the same RNA extraction protocol.
3. DNase treatment: RQ1 RNase-free DNase 10× reaction buffer, RQ1 RNase-free DNase, and RQ1 DNase stop solution are all obtainable from Promega.
4. RT-reaction/first-strand cDNA synthesis: Random/Hexamer/OligodT: use the Promega C1181-20 μg. RNAsin, M-MLV Reaction buffer, and M-MLV RT (H-) are obtainable from Promega. dNTPs (10 mM) are from Fermentas R0191.
5. PCR reaction: PCR Master Mix: you can use the Promega or the Roche FastStart Universal SYBR Green Master Mix.
6. Oligos: Use Invitrogen Primers if possible. Tm for both primers should be as close as possible, i.e., 50 %.
7. Agarose Gel electrophoresis: Use the Bioline Molecular grade agarose powder.
8. hnRNPA2 RT-PCR control: This should be done for all treatments with herbal extracts.
9. Always include 10 μM SRPIN 340 treatment when doing herbal extracts treatment as a control experiment.

Acknowledgement

The British Royal Society, the South African Medical Research Council, the Oppenheimer Trust, and the National Research Foundation of South Africa supported this work.

References

1. Puckee T, Mkhize M, Zama M et al (2002) African traditional healers: what health care professionals need to know. Int J Rehabil Res 25:247–251
2. Pajares MJ (2007) Alternative splicing: an emerging topic in molecular and clinical oncology. Lancet Oncol 8:349–357
3. Venables JP (2004) Aberrant and alternative splicing in cancer. Cancer Res 64:7647–7654
4. Faustino NA, Cooper TA (2003) Pre-mRNA splicing and human disease. Genes Dev 17: 419–437
5. Garcia-Blanco MA, Baranik AP, Lasda EL (2004) Alternative splicing in disease and therapy. Nat Biotechnol 22:535–546
6. Pagani F, Baralle FE (2004) Genomic variants in exons and introns: identifying the splicing spoilers. Nat Rev Genet 5:389–396

7. Hoimila R, Fouquet C, Cadranet J et al (2003) Splice mutations on the p53 gene case report and review of the literature. Hum Mutat 21: 100–102
8. Hu CK, Madore SJ, Moldover B et al (2001) Predicying splice variant from DNA chip expression data. Genome Res 11:1237–1245
9. Black DL (2003) Mechanisms of alternative pre-messenger RNA splicing. Annu Rev Biochem 72:291–336
10. Colapietro P, Gervasini C, Natassi F et al (2003) Exon 7 skipping and sequence alterations in exonic splice enhancers (ESEs) in a neurofibromatosis patient. Hum Genet 113:551–554

ERRATUM TO

South African Herbal Extracts as Potential Chemopreventive Agents: Screening for Anticancer Splicing Activity

Zodwa Dlamini, Zukile Mbita, and David O Bates

Sabrina Strano (ed.), *Cancer Chemoprevention: Methods and Protocols*, Methods in Molecular Biology, vol. 1379,
DOI 10.1007/978-1-4939-3191-0_18, © Springer Science+Business Media New York 2016

DOI 10.1007/978-1-4939-3191-0_19

In the chapter named **South African Herbal Extracts as Potential Chemopreventive Agents: Screening for Anticancer Splicing Activity**, the name of one of the contributing authors is incorrect. The correct name should read as **David O Bates**

The online version of the original chapter can be found at
http://dx.doi.org/10.1007/978-1-4939-3191-0_18

Index

A

Agarose gel electrophoresis....207–210
AlamarBlue 119, 121
Alternative splicing....31, 202, 207
Angiogenesis assay....107–114
Animals 79, 81, 84, 109, 110, 114, 118, 130, 134, 135, 160, 161
Antibody....71, 73, 74, 134, 152, 154, 155, 183, 190, 192
Antibody array....189–199
Apoptosis....21, 45
Autophagy....151–162

B

Bioanalyzer.... 14, 16, 17, 22, 25, 26, 33, 35, 39, 41, 47, 48, 51–52, 57, 65, 66
Biodegradable....1, 2, 126
Biological fluids....81
Biomarkers 14, 22, 83, 202
Biotinylated proteins 190
Bisulfite sequencing....71
Blood vessels....107–109
Boyden chamber....108
Breast cancer....13–18, 67, 90, 94, 182
Buffy coat 13–19

C

CAM assay. *See* Chorioallantoic membrane (CAM) assay
Cancer 1, 5, 13, 21–28, 31–43, 45–67, 69–75, 77, 78, 89, 99–104, 107, 118–128, 139, 140, 151–162, 165–179, 181, 189–199, 202
Cancer stem cells (CSCs).... 119, 130, 131, 134
Cell cycle 149, 159
Cell labeling 185
Cell proliferation 14, 21, 108, 183
Chemoprevention....21–28, 31–43, 45–67, 77–87, 89–96, 99–104, 122, 129–137, 151–162, 165–179, 189–199, 201–210
Chemoresistance....99, 131, 135–136, 139–149
Chip. *See* Chromatin Immunoprecipitation (ChIP)
Chorioallantoic membrane (CAM) assay....108–110, 112–114
Chromatin....69, 70
Chromatin immunoprecipitation (ChIP).... 25, 42, 51
Circulating tumor DNA....45–67
Clonogenic assay 141
Comet assay....99–104
Conditioned medium 134, 137, 144, 147
Confocal microscopy....154–158, 162, 185, 186
Coomassie staining....170, 171
CpG islands....70
CSCs. *See* Cancer stem cells (CSCs)

D

DNA damage 99, 100, 103
Drug delivery systems....1

E

Eggs.... 109, 112–114, 185
Encapsulation 2
Enzyme-linked immunosorbent assay (ELISA) 166, 190, 197
Epigenetic remodeling....69–75
Extracellular matrix (ECM) 118

F

FACS....132, 134, 141, 143, 145–146, 149
Fluorophore.... 166, 167, 169, 177, 178, 184
Fresh tissues....21–28
Fluorescence resonance energy transfer (FRET assay)....165–179

G

Gene expression....13, 16, 21, 22, 28, 40, 69, 70, 130

H

High-throughput analysis 13

I

Immunoprecipitation.... 31, 72, 73

Sabrina Strano (ed.), *Cancer Chemoprevention: Methods and Protocols*, Methods in Molecular Biology, vol. 1379,
DOI 10.1007/978-1-4939-3191-0, © Springer Science+Business Media New York 2016

L

Liquid chromatography mass spectrometry (LC-MS) 77–87
Liposomes 2

M

Matrigel 108, 109, 111–112, 132, 135, 182
Mesothelioma 22, 140, 141, 143, 144, 189
Messenger RNAs (mRNAs) 13, 14, 21, 22, 25, 32, 42, 125, 201, 202, 209
Metabolomics 77–87, 89–96
Methylated DNA immunoprecipitation (MeDIP) 69–75
Micelles 2
Micro array analysis 18, 192
Microparticles 2
MicroRNA profiling 13–18, 146
MicroRNAs (miRNAs) 13–18, 21–28
mRNAs
Messenger RNAs (mRNAs)

N

Nanoparticles 2, 119, 120, 122–125, 127, 128
Natural agents 189–199
Next-generation sequencing 31, 45, 46, 71
Noncoding RNAs 13, 21
Non-small-cell lung cancer cells (NSCLCs) 119, 120
Nuclear magnetic resonance (NMR) 89–96

P

Patient-derived xenograft (PDXs) 130
Phospho-protein 190, 197
Plasma-seq 46, 60, 67
Primary cultures 139, 140, 144, 147–149
Proteomics 78

R

Retinoic acid (RA) 17, 70
RNA immunoprecipitation sequencing (RIP-Seq) 31
RNA-sequencing (RNA-seq) 28, 31–43

S

Single strand breaks (SSB) 100
Spheroids 118–128

T

Three dimensional (3D) cultures 99, 118–122, 126, 127, 181, 182, 185, 187
Thymoma 22
Time-lapse imaging 181–188
Toxicity 1, 2

U

Ultra-performance liquid chromatography (UPLC) 80, 82

W

Western blotting 120